UNDERSTANDING THE MOLECULAR MECHANISM OF THE *FAT* SIGNALING PATHWAY IN *DROSOPHILA MELANOGASTER*

by

YONGQIANG FENG

A Dissertation submitted to the

Graduate School-New Brunswick

Rutgers, The State University of New Jersey

and

The Graduate School of Biomedical Sciences

University of Medicine and Dentistry of New Jersey

in partial fulfillment of the requirements

for the degree of

Doctor of Philosophy

Graduate Program in Cell and Developmental Biology

written under the direction of

Kenneth D. Irvine

and approved by

_____

_____

_____

_____

_____

New Brunswick, New Jersey

October, 2009

ABSTRACT OF THE DISSERTATION

UNDERSTANDING THE MOLECULAR MECHANISM OF THE *FAT* SIGNALING PATHWAY IN *DROSPHILA MELANOGASTER*

By YONGQIANG FENG

Dissertation Director: Kenneth D. Irvine

Fat is an atypical cadherin and regulates planar cell polarity (PCP) and imaginal disc growth. The Golgi kinase Four-jointed modulates the interaction of Fat and its potential ligand Dachsous and an unconvential myosin Dachs mediates nearly all Fat functions. The Hippo tumor suppressor pathway was demonstrated to regulate growth and cell death through the kinase Warts and transcription factor Yorkie. Genetically, the Hippo pathway is downstream of Fat, Dachs and the FERM-domain protein Expanded. The molecular basis was unknown how Fat interacts with Expanded and how Fat and Dachs regulate the Hippo pathway.

We found that Fat regulates Warts stability in a Dachs-dependent manner. Expanded and other tumor suppressors inluding Hippo, Mats and Salvador do not affect Warts levels, suggesting a distinct mechanism in regulating Warts. A casein kinase I δ/ε mutant, dco^3 also destabilizes Warts, and genetically is upstream of *dachs*. The regulation of Warts by Fat and Expanded via different mechanisms was further validated by the additive effects of *fat* and *expanded* on imaginal disc growth and development. Mutation of *fat* also influences Expanded stability or subcellular localization through Dachs, indicating a crosstalk between Fat pathway and Expanded.

The significance of Warts in Fat and Expanded functions was demonstrated by our observation that mutations in either *expanded* or *fat* were rescued to viability by overexpressing Warts, indicating that reported effects on endocytosis or other pathways are not essential. These rescue experiments also separate the transcriptional from the PCP branches of Fat signaling and reveal that Expanded does not directly affect PCP.

We found that Fat is subject to a constitutive proteolytic processing, such that most or all cell surface Fat comprises a heterodimer of stably associated N- and C-terminal fragments. The cytoplasmic domain of Fat is phosphorylated, which is promoted by Dachsous. Dco is required for Fat signaling, and is able to phosphorylate the Fat intracellular domain in cultured cells, and is required for normal Fat phosphorylation in vivo. dco^3 mutant affects Fat's influence on growth and gene expression, but not its influence on PCP, suggesting separated growth and PCP pathways from Fat.

Preface

I grew up in an age after "the Great Proletarian Cultural Revolution" (1966-1976) in China (http://en.wikipedia.org/wiki/Cultural_Revolution). In 1980s, science and engineering became the major focuses of education from middle schools to colleges in China. Young generations of people were enthusiastic about natural sciences and engineering, dreaming to change their lives and modernize our country. However, China is a developing country and the programs in teaching science and technology are also developing. I spent a long time in China struggling for my interest before I came here to get trained in biological research.

It was a long way from China to USA, the longest distance between any two spots on the earth. Graduate programs in US were therefore unsurprisingly different. It was a great time for me to be exposed to various aspects of current biological research by taking courses in biochemistry, molecular biology, genetics and developmental biology etc. I did my lab rotations with Ken, Michael Shen and Danny Reinberg, and eventually joined Ken's lab, hoping to study cell communication during animal normal development. Although I was familiar with molecular biology before entered the graduate program in Cell and Developmental Biology, I had no idea how to study cell signaling and gene expression regulation in vivo during animal development. I jointed this graduate program hoping to learn the ways to study normal processes of animal development so as to appreciate the abnormalities under pathological conditions.

I started to work on Notch signaling because at that time most people in the lab was focusing on it. My first projects Ken suggested to me were to look at o-linked glycosylation modification of Notch extracellular domain[1,2], and potential modification of

Slit (ref. [3]) by Fringe[4]. But my interest changed to a whole genome RNAi screening project a few weeks later, because as a new technology[5-8] it appeared to be a more efficient way to identify modulators of Notch signaling. I spent approximately two years on this project untill it was eventually closed because of no cell based assays for ligand-dependent Notch signaling.

Under Ken's directions, I picked up a new project in the Fat pathway[9,10], because there appeared to be a lot things unknown. In the next four years I have been focusing on this pathway and trying to understand the underlying molecular mechanisms during Fat signal transduction. It turned out to be a challenge, and of course also a good chance to learn different technologies in genetics, biochemistry and molecular biology, and more importantly to learn how to address developmental issues with these tools.

In this dissertation, I am trying to summarize the work I have done in the past six years as a graduate student. Most of of data in Chapter II, III and IV have been published or submitted, as acknowledged on the first page of each chapter [11-13]. Some of the results and observations that have not been published but might be helpful for future work in the field were also included and discussed in each chapter. The data in Chapter V are mainly recent progresses, although may not be complete and conclusive at this point. The implications and future directions of these observations were discussed. In the Appendix, a lot of room was assigned to primers and constructs, hoping they will be helpful for future work.

Acknowledgement

Lot of people helped me in the past seven years during my graduate study. First, I would like to thank Ken for his help, training, insights, patience, tolerance, and supports. I was greatly influenced by the way he looked at things around us, his unique perspectives and strategies to view and approach scientific issues. That was probably the best thing I ever got from the graduate study.

I want to thank Richard Padgett, Ruth Steward, Isaac Edery, Michael Matise and Gary Struhl for their suggestion and help for my research and career development in the future.

I am very grateful to the program recruitment committee members who offered me the position and waited for one year for me to get a student visa. I would like to thank Carolyn Ambrose for her kindly help in my application to the graduate program and during my graduate study. It was therefore a precious opportunity for me to systematically reach various aspects of biological research with particular training in developmental biology and genetics.

I would like to thank Cordelia for training me in confocal imaging and great help with my projects. It would be impossible for me to go smoothly with my research without the help and training from former and current lab members, in particular, Robert Major, Trudy Correia, Olga Dunaevsky, Liang Lei, Aiguo Xu, Yuhru Lin, and Shemeeakah Powell. I also want to thank Koen Venken (Bellen lab) for his kindly help with P[acman] technique, Helen McNeil, Zhi-chun Lai, Duo-Jia Pan, Bruce Hays, Jin Jiang for sharing precious reagents.

I would like to thank the graduate program of Molecular BioSciences for the first year graduate fellowship, the Developmental Studies Hybridoma Bank and the Bloomington

stock center for plasmids, antibodies and *Drosophila stocks*, Howard Hughes Medical Institute and the NIH for their support to Ken.

I grew up from an unprivileged family in the under-developed region of China. I was very interested in natural science, but to get trained in science took me a long way. Fortunately, with the rapid development of Chinese economy, younger people now have more opportunities to pursue their dreams[14]. I am particularly grateful to my mother and father, because they supported my education and my career as much as they could, though she would not be able to know what I have achieved today. I should thank and apologize to my younger brother, because he sacrificed his education for mine. I would like to thank my wife Kun for her unlimited support, encouragement and enthusiasm in my career. I also should apologize to my son for my insufficient care for him.

TABLE OF CONTENTS

Abstract……..…..ii

Preface……..iv

Acknowledgement…….……vi

Table of contents……..viii

List of Tables……xiii

List of Illustrations……....xiv

CHAPTER I 1

General Introduction 1

Table 1. Mammalian Fat, Expanded and Hippo signaling homologues and their functions..... 12

Summary of significant progresses in the thesis research 13

Figures..... 19

Figure 1. Patterning of wing imaginal disc. 19

Figure 2. Polarization of epithelia..... 21

Figure 3. Cadherin proteins in *Drosophila.* 23

Figure 4. Core components of the Hippo/Warts pathway. 24

CHAPTER II..... 25

Fat signaling regulates growth by influencing Warts stability 25

Introduction..... 27

Materials and Methods..... 29

Results..... 32

Discussion 38

Figures..... 41

Figure 1. Influence of the Fat pathway on Warts levels. 41

Figure 2. Coprecipitation of Dachs and Warts. 43

Figure 3. Tissue staining with Warts antisera. 44

Figure 4. Regulation of Warts conformation. 45

Figure 5. The Fat pathway model. 46

CHAPTER III 47

Fat and Expanded act in parallel to regulate growth through Warts..... 47

Summary 48

Introduction..... 49

Materials and Methods..... 51

Results..... 53

Discussion 61

Figures..... 66

Figure 1. Rescue of *fat* and *expanded* by Warts overexpression. 66

Figure 2. *fat* and *expanded* have additive effects on growth and eye development. 68

Figure 3. Influence of Fat signaling on Expanded. 70

Figure 4. Fat signals even when Expanded is overexpressed. 72

Figure 5. Schematic model of the Fat-Hippo signaling network. 74

CHAPTER IV..... 75

Processing and Phosphorylation of the Fat receptor..... 75

Summary 76

Introduction 77

Materials and Methods 79

Results 87

Discussion 103

Figures 107

Figure 1. Processing of Fat. 107

Figure 2. Dachsous-promoted phosphorylation of Fat 109

Figure 3. Disc overgrown (Dco)-mediated phosphorylation of Fat 111

Figure 4. Dominant negative activity of Dco^3 113

Figure 5. *dco*^{3} specifically affects the Fat tumor suppressor pathway 115

Figure 6. Mapping Dco phosphorylation sites in Fat 117

Figure 7. Assay functions of phosphorylation site mutants of Fat. 119

CHAPTER V 121

Ongoing projects. 121

1. Study the conservation of vertebrate Fat functions in *Drosophila*. 122

Summary 122

Introduction 122

Materials and methods 124

Results and discussion 125

2. Fat might influence the Epidermal Growth Factor Receptor signaling pathway 134

Summary 134

Introduction 134

Results and discussion 135

3. Subcellular localization of Fat protein. 140

Summary 140

Introduction 140

Results and discussion 141

4. Subcellular localization of Hippo and Warts in wing epithelia. 145

Summary 145

Introduction 145

Results and discussion 146

Figures 149

Figure 1. Analysis of *Drosophila* Fat function from protein evolution. 149

Figure 2. Human Fat intracellular domain hybrids transduce planar cell planarity signal in *Drosophila* 150

Figure 3. Overexpression of Fat induces ectopic vein. 152

Figure 4. Overexpression of Fat promotes dorsal cell fate in wing discs. 154

Figure 5. Fat protein is not polarized along proximal-distal axis in wing disc epithelia. 156

Figure 6. Imaging Hippo and Warts subcellular localization. 158

APPENDICES 160

1. Strategies to generate Fat intracellular domain truncates. 160

2. Primers to make Fat-ICD point mutants. 162

3. Summary of Fat-ICD mutants and Dco mediated gel mobility shift. 164

4. List of Fat-ICD point mutants. 165

5. Universal primers for attB-P[acman]. 166

6. Primers to clone *fat* genomic region from BAC DNA. 166

7. Primers to clone *fat* locus from BAC DNA. 167

8. Primers to modify *fat* locus by recombineering..... 167

9. Primers to generate human Fat-ICD and *Drosophila* Fat hybrids. 169

10. Generate Fat-ICD ST minus. 171

11. Primers to tag Hippo. 174

12. Primers to tag Warts. 176

13. Maps of *fat* genomic rescue constructs. 178

14. Multi-alighment of *Drosophila* Fat-ICD anf human Fat-ICDs. 179

15. Multi-alighment of Fat-ICDs from various species. 180

16. Protein motif prediction of *Drosophila* Fat-ICD. 184

REFERENCES..... 185

CURRICULUM VITA 198

LIST OF TABLES

Table 1. Mammalian Fat, Expanded and Hippo signaling homologues and their functions. 12

LIST OF ILLUSTRATIONS

CHAPTER I

Figure 1. Patterning of wing imaginal disc. 19

Figure 2. Polarization of epithelia..... 21

Figure 3. Cadherin proteins in *Drosophila.* 23

Figure 4. Core components of the Hippo/Warts pathway. 24

CHAPTER II

Figure 1. Influence of the Fat pathway on Warts levels. 41

Figure 2. Coprecipitation of Dachs and Warts. 43

Figure 3. Tissue staining with Warts antisera. 44

Figure 4. Regulation of Warts conformation. 45

Figure 5. The Fat pathway model. 46

CHAPTER III

Figure 1. Rescue of *fat* and *expanded* by Warts overexpression. 66

Figure 2. *fat* and *expanded* have additive effects on growth and eye development. 68

Figure 3. Influence of Fat signaling on Expanded. 70

Figure 4. Fat signals even when Expanded is overexpressed. 72

Figure 5. Schematic model of the Fat-Hippo signaling network. 74

CHAPTER IV

Figure 1. Processing of Fat. 107

Figure 2. Dachsous-promoted phosphorylation of Fat 109

Figure 3. Disc overgrown (Dco)-mediated phosphorylation of Fat..... 111

Figure 4. Dominant negative activity of Dco^3 113

Figure 5. *dco^3* specifically affects the Fat tumor suppressor pathway..... 115

Figure 6. Mapping Dco phosphorylation sites in Fat..... 117

Figure 7. Assay functions of phosphorylation site mutants of Fat. 119

CHAPTER V

Figure 1. Analysis of *Drosophila* Fat function from protein evolution..... 149

Figure 2. Human Fat intracellular domain hybrids transduce planar cell planarity signal in *Drosophila*..... 150

Figure 3. Overexpression of Fat induces ectopic vein..... 152

Figure 4. Overexpression of Fat promotes dorsal cell fate in wing discs..... 154

Figure 5. Fat protein is not polarized along proximal-distal axis in wing disc epithelia..... 156

Figure 6. Imaging Hippo and Warts subcellular localization. 158

CHAPTER I

General Introduction

Wing imaginal disc, a model organ.

Animal development is basically organized cell division and differentiation[15]. Understanding the underlying mechanisms is one of the major topics in developmental biology. *Drosophila melanogaster* (fruit fly) is an excellent model organism for studying animal development because of its relative simplicity and the availability of various genetic and biochemical tools[16-20]. Organization of animal body plan and gene expression patterning are two crucial aspects of animals development and has been extensively studied in *Drosophila*[15,20]. However, how organ size or developmental growth is regulated is not well known[21-25]. Imaginal discs are clusters of cells that mainly develop during larval stages and contribute to adult organs like wings, legs, head etc[26,27]. Accumulating evidence has shown that imaginal discs are extraordinary systems to address various biological questions, e.g. organogenesis, cell-cell communication, cell growth and death control, cell fate determination, regeneration, cell fate plasticity[26,28-32] and signal transduction[26,27,33-36]. Most of the analysis in this dissertation is therefore focusing on wing imaginal discs.

Wing discs contain two layers of epthelia, columnar and squamous peripodial epithelia[37-39]. Although the peripodial epithelium has been shown to be very important for imaginal disc morphogenesis and signal tranduction[37,40-43], most of our work was focused on columnar epithelia[27], the major part of disc proper. Growth and patterning of wing discs are largely determined by two extensively studied molecules, Decapentaplegic (Dpp) and Wingless (Wg), which also separate the wing disc into anterior/posterior and

dorsal/ventral domains (Figure 1). Expression of the segment polarity gene *engrailed* (*en*) in the posterior domain is inherited when the wing disc precursors are determined during embryonic development. En activates the expression of Hedgehog (Hh) in posterior domain, which is then diffused into anterior domain and activates Dpp and Patched (Ptc) expression at a short range along the A/P boundary. Dpp protein is secrected from this strip and diffused to the lateral regions of the wing discs and thus forms a Dpp gradient (Figure 1C). Cells at different positions on the wing disc receive different amounts of Dpp (position value) and activate specific target genes (Figure 1E). For instance, Vestigial (*vg*) is very sensitive to Dpp and is turned on in whole wing pouch, while *spalt* can only be activated with higher amounts of Dpp[44]. Dorsal/Ventral Wg is regulated by Notch signaling along the interface between the dorsal and ventral cells in the wing disc (for review, see ref. [45]). The transcription factor Apterous (AP) is expressed in dorsal cells and activates the expression of Fringe and Serrate. Fringe modifies Notch so that the Delta ligand from ventral part can only activate Notch on the dorsal cells, and Serrate on dorsal part only activates Notch on ventral side (Figure 1D)[45,46]. Wg is expressed and secreted as a morphogen and activites gene expression with different concentration dependence (Figure 1E).

Dpp and D/V Wg are presumably generated as gradients on the wing disc, establishing a coordination system, so that the cells in the wing disc will have different values for Dpp and Wg. Dpp and Wg further pattern the wing discs by regulating distinct gene expression, which eventually direct cells to achieve different functions and morphologies (Figure 1F and B). For instance, Four-jointed (Fj) is expressed in the wing pouch and Ds is expressed in the proximal region. These differently expressed genes regulate wing disc

patterning in distal-proximal axis. Wg is also expressed in the proximal region and contributes to the growth in notum region, however proximal it is not directly regulated by Notch signaling.

The columnar epithelia are polarized along the basal-apical and proximal-distal axes (Figure 2A), which play crucial roles during organogenesis[47-50]. Polarity in the basal-apical axis can be shown by the asymmetrical distribution of cell adhesion molecules and their cytoplasmic binding factors (Figure 2A). These include Crumbs/Stardust/Discs Lost complex, Bazooka/aPKC/Par-6 complex, E-cadherin/Catenin adhesion complex, and lethal Giant Larvae/Discs Large/Scribble complex. In the last two decades, polarization of epithelia along the basal-epical axis has been extensively studied[48,49,51]. Defects in the polarization of this axis have been shown involved in various advanced cancers, especially in tumor invasion[52-54].

Epithelia are also polarized along the distal-proximal axis (i.e. planar cell polarity, PCP) (Figures 1 and 2), which becomes more obvious in fly pupa or adults as shown by the orientation of bristles on wing or abdominal epidermis. Determination of PCP includes the generation of polarity cues (e.g. polarized extracellular signals), perception and transduction of the polarity cues into cells, and interpretation by intracellular machinery[55]. A variety of genes and pathways have been found involved in PCP formation, among which the Frizzled (Fz) pathway is well studied. In the classical Wnt signaling pathway, binding of the ligand to the Fz receptor activates Dishevelled (Dsh) which stabilizes β-catenin by inhibiting APC complex activity. Stabilized β-catenin therefore is translocated into nucleus to turn on gene expression. The non-canonical Wnt pathway does not require β-catenin dependent transcriptional regulation and transduces PCP signal through Dsh to

the PCP interpretation machinery (Figure 2B). In the non-canonical Wnt pathway, the Fz receptor and the cytoplasmic protein Dsh are preferentially enriched on distal side of the epithelia, while the membrane protein Van Gogh (Vang) and cytoplasmic protein Prickle (Pk) are accumulated on proximal membrane. Polarization of these proteins is probably mediated by an amplification circuit in which Fz promotes the accumulation of Dsh in cis and Vng on the adjacent membrane in trans. Pk binds to Vang and inhibits the enrichment of Dsh in cis (Figure 2C). Subtle polarity cues therefore are perceived by cells and propagated along the distal-proximal axis[55-57].

Besides this model, a few key issues are still waiting for answers. For instance, ligands for Fz are not clear and the biological functions of PCP in animal development and under pathlogical conditions still need investigation. Studies on the polarization of epithelia along the distal-proximal axis thus is one of the important topics in developmental biology[58,59].

Genes regulating growth and PCP signaling

Atypical Cadherin Fat and Dachsous:

Study of the gene *fat* has a long history. The first mutant of *fat* (*fat*^{1}) was described in 1923 with subtle defects in *Drosophila* body phenotypes[60]. More than half a century later, the growth regulation function was linked to the *fat* locus[61]. In the strong *fat* mutant alleles, wing discs show excessive growth, especially in proximal regions[61,62]. Fat was classified as an atypical Cadherin because its amino acid sequence was homologous to Cadherins (Figure 3)[63]. Cadherins belong to cell adhesion molecules and have been shown regulating cell adhesion, sorting and tissue morphogenesis during animal development[64]. In fruit fly, classical Cadherin is a type I transmembrane protein with a

single transmembrane domain. Its extracellular domain contains five Cadherin repeats and the C-terminal domain binds to β-Catenin and α-Catenin which are associated with the actin filaments (Figure 3). In the Wnt pathway, β-Catenin is stabilized and translocated into nucleus to activate target gene expression[65]. The linkage between Catenin and Cadherins indicates that cell adhesion molecule Cadherin plays a significant role in modulating Wnt signaling.

Fat is classified as an atypical Cadherin with more than five thousand amino acid residues (Figure 3). The extracellular domain of Fat contains 34 Cadherin repeats[63], presumably binding to other atypical Cadherins, e.g. Dachsous[66,67]. The intracellular domain of Fat was shown interacting with nuclear co-repressor Atrophin[68-70], and could partially rescue *fat* mutants[71]. Loss of function of Fat shows overgrowth phenotype in the wing imaginal discs, suggesting that normally Fat acts as a tumor suppressor. In wing discs, distal-proximal signaling has been shown to regulate proximal Wg expression[9]. Mutation of *fat* turns on proximal Wg expression in a cell autonomous manner[9], suggesting that Fat may work as a receptor in suppressing proximal Wg expression in the proximal region of the wing discs. However, the proximal Wg and overall growth regulation might be two different readouts of Fat signaling, because the proximal Wg has been shown only responsible for growth in the proximal region[9,72]. Mutation of *fat* also showed defects in the planar cell polarity (PCP), a polarization abnormality in the distal-proximal axis[73,74]. Growth and PCP phenotypes of *fat* mutants indicate that at least two distinct functions may be regulated by Fat[9]. Mutation of *fat* also was shown to influence cell affinity in the mosaic clones[9,10], however, the nature and biological functions of the Fat regulated cell affinity is unknown.

Dachsous (Ds) is also classified as a large atypical Cadherin with more than three thousand amino acid residues[66]. The extracellular domain of Ds has 27 Cadherin repeats. Loss of function mutation of *ds* resulted in similar phenotypes as *fat* mutants, i.e. overgrowth of the wing imaginal discs and PCP phenotype in adult epidermis, though much weaker[75]. As *ds* and *fat* share similar phenotypes in growth and PCP regulation, Ds and Fat can directly bind to each other in cultured cells, it is believed that Fat and Ds may act as the receptor and ligand[67]. Ds is expressed in a gradient at transcriptional level, preferentially in the proximal region (Figure 1F). Given the receptor and ligand relationship between Fat and Ds, slope of Ds gradient may regulate Fat activity in a special way. However, it was unknown how this works at cellular and molecular levels[25,76,77].

Four-jointed, Dachs and Disc Overgrown (Dco):

Four-jointed (Fj) was also identified as a regulator of the distal to proximal signaling as shown by short cross vein spacing phenotype in adult wings[78]. Fj is a type II transmembrane protein[79,80] and expressed in a gradient at transcriptional level which is complementary to Ds gradient[9,81,82]. Fj protein is localized in the Golgi apparatus and was recently shown to be a kinase phosphorylating the Cadherin repeats of Fat and Ds[83]. Because the mutation and overexpression of Fj can influence proximal Wg and Fat cellular localization non-autonomously, Fj may modulate the interactions between Ds and Fat[9,73,77,84], though the molecular mechanism is not clear. The phosphorylation modification of the Fat and Ds extracellular domains probably depends on the Fj concentration, because Fat signaling is regulated by the slope of Fj protein.

dachs was identified as a gene required for fly appendage growth[85,86], and was show as a unconventional myosin[10]. Mutation of *dachs* reduces the growth of wings and legs and completely suppresses *fat* mutant induced wing disc overgrowth and cell affinity difference, suggesting that Dachs mediates almost all Fat signaling[9]. As shown by the overexpression of a tagged protein, Dachs was mainly localized on the distal side of the apical membrane in the columnar cells of wing discs, although no transmembrane domain has been identified in Dachs. Polarized distribution of Dachs was influenced by Fat signaling as shown by manipulating Ds and Fj gradients [87], suggesting that it is critical for Fat signaling transduction. Recently the DHHC palmitoyltransferase *approximated* (*app*) was shown to regulate Dachs subcellular localization and activity[88]. Mutation of *app* suppresses the *fat* mutant phenotypes in PCP and excessive growth, and also enhances PCP phenotypes in the *dachs* mutants, suggesting a potential biochemical interaction between Dachs and App. Myosin family proteins have been shown involved in a variety of cellular functions[89-92], it is unknown whether and how the motor activity of Dachs acts in the Fat signaling.

Dco (Disc overgrown) was identified in a search for mutations with excessive growth in mosaic clones[93]. At molecular level, Dco is classified as a casein kinase I δ/ε, which has been linked to various pathways including Wnt and Hedgehog signaling[94]. In particular, Dco was recently implied in the PCP regulation by phosphorylating Dishevelled (Dsh)[95,96], and in the cell viability control by post-transcriptionally regulating caspase inhibitor DIAP1 level (ref. [97]). However, due to the pleiotropic nature of Dco, phenotypes observed in the loss of function or overexpression of Dco may be difficult to interpret.

Two point mutations at the conserved domains of Dco lead to a specific allele *dco*^{3} and results in overgrowth in the wing discs, while other mutants and the null allele of *dco* induce cell death or disc loss[93]. Given the complexity of Casein kinase I mediated signaling, it was not clear which and how the signaling pathways are influenced by *dco*^{3} mutant.

Ds and Fj gradients and Fat signaling.

The gradient model was forged from the famous cockroach limb graft experiments in 1960s[76], although the morphogen had not been identified. The steepness (gradient) of this unknown morphogen was presumably recognized by cells and induces cell growth and differentiation. A similar model was employed to interpret the phenotypes related to *ds*, *fj* and *fat*, because Ds and Fj are expressed in gradients in imaginal discs[25]. Null mutation of *fj* reduces wing size and leads to the distal-proximal defects (e.g. shorter cross vein spacing), PCP phenotypes (e.g. disturbed bristle orientation in adults epidermis), and leg segmentation defects[82,85,98]. Uniformly overexpression of Fj results in the similar phenotypes as *fj* mutants, which cannot be explained by classic modulators of signaling transduction, because overexpression and loss of function of the regulators are believed to cause opposite phenotypes, e.g. Notch signaling[99]. However, these data fit very well with a gradient model, where removal of Fj and uniform overexpression of Fj both change the slope of Fj gradient and thus resulting in similar phenotypes.

Ds is expressed in a complementary gradient to Fj. Null mutation of *ds* and uniform overexpression of Ds gave similar effects in the PCP, also consistent with the gradient model. However, the wings of *ds* mutants were significantly bigger than those of Ds overexpression[71]. Ds therefore can be called a tumor suppressor and acts via a different

mechanism in growth regulation. The gradient model has been validated in mosaic clones, where changes in Ds or Fj gradients, either mutation or overexpression, affected PCP signals[74,79,100-102] and increased cell growth and the signaling in the Hippo/Warts pathway on the edges of the clones[87,103]. Although gradient model explains quite successfully how Fj and Ds regulate Fat signaling, it was unknown how gradient information is exactly interpreted by cells[25,76].

Expanded and Merlin:

Expanded (Ex) and Merlin (Mer) are FERM (Four-point one, Ezrin, Radixin, Moesin) domain containing proteins which has been shown to link cytoplasmic proteins to the membrane[104,105]. Mutation of *ex* alone only showed moderate overgrowth in the wing discs[106] but double mutation of *ex* and *mer* dramatically induced excessive growth, suggesting that they are functionally redundant in *Drosophila*[107,108]. Mer and Ex are cytoplasmic proteins localized mainly in the apical membrane of wing columnar epithelia, and associated with membrane structures and actin filaments[107,109]. In human, mutation of Mer has been shown contributed to the neurofibromatosis type 2 (NF2) disease[105,108,110], indicating the functional conservation in growth regulation in metazoan. In mammalian system, small RhoGTPase was shown regulating Mer activity[111,112], and in *Drosophila*, Mer and Ex had been linked to the downstream Hippo/Warts signaling pathway[113], although the biochemical mechanism was not well understood.

Hippo/Warts/Yorkie signaling pathway:

The Hippo/Wart/Yorkie cascade was recently identified as the core components of the Hippo (Hpo) pathway regulating cell growth and apoptosis (for review [22]). Hpo and Warts (Wts) are Ser/Thr protein kinases, where Hpo phosphorylates Wts and promotes

Wts activity in phosphorylating Yorkie (Yki) and inhibiting its transcriptional activity (Figure 4) [22,114]. The kinase activity of Hpo and Wts are enhanced by the scaffold protein Salvador (Sav)[115] and Mats[116]. Yki is the transcription factor identified by yeast two hybridization screening with Wts as the bait[117]. In *Drosophila*, the overexpression of Yki mimics almost all phenotypes of the mutations of *wts*, *hpo*, *sav*, and *mats*, while the null allele mutation of *yki* induces cell death[117]. It has recently been shown that Wts phosphorylates Yki mainly at Ser168 and tethers it at cytoplasmic side via protein 14-3-3 binding thus inhibiting its ability to activate transcription[118-120]. Yki does not bind to DNA and the transcriptional regulation by Yki is mediated, at least partially, by the TEAD/TEF family protein Scalloped, a DNA-binding transcription factor [121-124].

Transcriptional targets of the Hpo/Wts pathway are quite diverse, including genes responsible for cell division (*cyclinA*, *cyclinB*, *cyclinE*), inhibitors of cell death (*DIAP1*), microRNA (*bantam*[125,126]), tissue specific targets (*wingless*, *serrate*) and feedback response (*fj*, *ex*) etc. Cell growth and death regulation are general and unique in the Hpo/Wts pathway, because promotion of cell division is coupled with the inhibition of cell death[127]. Similar to *Drosophila*, the oncogenic protein and transcriptional co-activator YAP (Yes-Associated Protein) is phosphorylated and inhibited by Lats[117,119,128-135]. In mammalian system, the Hpo pathway has also been shown to negatively regulate TAZ (transcriptional co-activator with PDZ-binding motif), another binding partner of transcription factor TEAD, and inhibit cell proliferation and epithelial-mesenchymal transition in cultured cells[136-138]. It will be interesting to determine the functional

difference between YAP and TAZ in target and tissue specificity, transcriptional activity etc.

Protein conservation and evolution.

Almost all proteins discussed above appear to be conserved in vertebrates (Table 1), except Dachs[139]. For instance, four members of Fat have been identified in mouse and human[140]. Knock out of *fat4* in mouse has been shown to be involved in PCP regulation[141] and loss of *fat1* enhances *fat4* phenotypes (unpublished observation from H. McNeil). Dachsous1 and Dachsous2 are the vertebrate homologs of *Drosophila* Ds[142] and Dachsous1 seems to regulate PCP in the similar way as Fat4 (unpublished observation from Yaopan Mao). In addition, Mer has been shown to be involved in the neurofibromatosis type 2 (NF2) disease[105,108,110], loss of the Wts homolog Lats1 in mice caused soft-tissue sarcomas[143,144], mutation of *mats* and *sav* were found in a few cancer cell lines[145,146]. Recently, YAP was shown to regulate organ size[119] and promote tumorigenesis[128,129].

Table 1. Mammalian Fat, Expanded and Hippo signaling homologues and their functions.

D. melanogaster gene	Mammalian gene	Expression/functions	Reference
fat	*fat1*	Cell migration, invovled in cancer	[147-149]
	fat2	Required for cancer cells migration	[150]
	fat3	Enriched in nervous system	[151]
	fat4 (*fatj*)	PCP regulation, tumorigenic in breast cancer and oral cancer	[140,141,152,153]
dachsous	*dachsous1*	Highly expressed in brain, kidney	[154]
	dachsous2	Highly expressed in brain	[155]
four-jointed	*fjx1*	Dendrite extension, gene amplification in cancer cell lines	[142,156,157]
disc overgrown, dco	CKIδ/ε	Multiple pathways	[94]
merlin (*mer*)	(NF2)	Tumor cuppressor	[158,159]
expanded (*ex*) *dachs*	FRMD6	Expressed in various tissues	[160]
hippo (*hpo*)	MST1/STK4	tumor suppressor	[161]
	MST2/STK3	tumor suppressor, chromosome alignment	[132,161-163]
salvador (*sav*)	WW45	tumor suppressor	[145,164]
warts (*wts*)	LATS1	Inhibits YAP, tumor suppressor	[131,134,143]
	LATS2	Tumor suppressor, cell division	[165-167]
mats (*mats*)	Mob1	Mutant in cancer cell lines	[146]
yorkie (*yki*)	YAP	Transcription coactivator , oncogenic	[117,128,129,131,132,134,135,168]
	TAZ/WWTR1	Transcription coactivator , oncogenic	[137,138]

CKI: Casein kinase I. FRMD6: FERM-domain-containing-6. Mats: mob as tumor suppressor. Mob1: Mps-one binder kinase activator-1. MST1/2: Mammalian sterile-20-like kinase type 1 and type 2. NF2: Neurofibromatosis type 2. LATS: Large tumor suppressor. YAP: Yes associated protein.

(These papers were also referenced: [169,170])

Summary of significant progresses in the thesis research

Genetic linkage from Fat to the Hippo/Warts pathway (by E. Cho[11])

Mutations of *fat*, *sav*, *mats*, *ex*, *wts* and *hpo* share similar phenotypes in excessive growth and cell affinity change. Genetic analysis of these genes had shown that the Hpo/Wts pathway is downstream of *ex* and *fat*. At transcriptional level, the Fat and Hpo/Wts pathways regulate the same set of genes' expression. Ectopic expression of Hpo leads to cell death and is epistatic to Fat and Ex. In the null allele of *yki*, cells are prone to die because of less amount of cyclinE and DIAP1. Mutant of *yki* is epistatic to all other mutations upstream of the pathway. All these data suggest that the Hpo/Wts pathway is downstream of Fat and Ex. However, the genetic analysis did not distinguish the relationship between Ex and Fat, because both of *fat* and *ex* cause similar phenotypes in growth.

Biochemical basis of the Wts regulation by Fat and Ex.

In order to understand the biochemical basis for the relationship between Fat and the downstream Hpo/Wts pathway, I examined the downstream protein cellular staining in the *fat* mutant mosaic clones. As the antibodies against Wts, Sav, Mats and Hpo did not work for tissues staining, epitope tagged proteins of Wts, Sav, Mats and Hpo were used for tissue staining. I found that in *fat* but not *ex*, *sav*, *mats* and *hpo* mutant clones, tagged Wts staining was specifically decreased, indicating unique mechanism in regulating Wts by Fat, because the documented regulation of Wts was phophorylation modifications[22,113,117,119]. Dachs mediates almost all Fat functions[9,10]. Double mutation of *dachs* and *fat* suppressed the effect on Wts, consistent with the model that Fat signaling goes through Dachs. In order to confirm this with endogenous Wts protein staining,

antiserum was generated against the N-terminal half of Wts protein and purified with the Wts affinity columns. Western blotting with the lysate from different genotypes of wing discs showed that Wts protein was diminished in the *fat* and dco^3 mutants. The influence of *fat* on Wts stability was suppressed by the additional mutation in *dachs*. Consistent with the observations from tissue staining, Wts protein level is regulated by Fat and Dco in a Dachs dependent manner. Mutation of *fat* did not show any effect on other proteins including Hpo, Mats and Sav. Co-immune precipitation of overexpressed Wts and Dachs in S2 cells further confirmed the biochemical interaction between Wts and Dachs[11].

In *Drosophila* S2 cells Ex has been shown increasing the Wts protein phosphorylation and therefore promoting its kinase activity in phosphorylating Yki, probably through Hpo[171]. However, it is unknown whether this observation also represents the mechanism in wing epithelia. Recently, Ex was found associate with Yki in S2 cells mediated by the partially redundant PPxY motifs of Ex and the WW domains of Yki[172]. In vivo, overexpressed Ex was shown to suppress the excessive growth phenotype of wts^{X1}mutant (this observation has not been confirmed)[172]. As wts^{X1} might be a hypomorphic allele[173] (personal communication with T. Xu), the functional significance of the binding between the overexpressed Ex and endogenous Yki in S2 cells still need further assessment[172,174].

Discrimination of the regulatory functions of Ex and Fat on Wts.

As discussed above, mutations of *ex* and *fat* showed similar phenotypes in growth regulation. However, *ex* and *fat* had different effects on Wts. Ex has been shown regulates the phophorylation level of Wts protein in S2 cells[113], it was therefore believed that Fat regulates Wts stability and Ex regulates Wts activity probably by phosphorylation[11,25,113], although Ex mediated Wts phosphorylation still need verification

in vivo. Observations from different labs, however, showed that the mutation of *fat* influenced the Ex protein stability or subcellular localization in the wing epithelia[175-177]. It was thus proposed that Fat regulates growth via Ex-Hpo-Wts cascade[22,23]. In this case, the Fat, Ex and Wts will form a single pathway to regulate growth, which is distinct from our observation that *fat* and *ex* mutants had different effects on Wts stability. In order to discriminate these two different models, I used simple genetic methods to measure the additive effects of *ex* and *fat*, and found that, the *ex fat* double mutant clones and homozygous animals both had stronger overgrowth phenotypes than the single mutations of *fat* or *ex*. Ectopic expression of Ex normally kills cells, however, in the *fat* mutant clones, the same amount of Ex protein did not lead to cell death. On the contrary, these clones were intermediates between the *fat* mutants and wild type cells, in terms of growth and target gene expression[12]. All these data strongly argue that Ex and Fat regulate growth in parallel pathways. The effect of *fat* mutation on the stability of Ex protein is subtle although transcripts of *ex* is increased in the *fat* mutant cells[113]. In *dachs* and *fat* double mutant clones, Ex protein was restored to normal level, suggesting that the *fat* effect on Ex requires Dachs protein. All these observations indicate a cross talk between Fat, Dachs and Expanded. Currently it is not clear how significant this cross talk is in Fat and Ex signaling.

Significance of Wts in Ex and Fat mediated growth control.

Although the additive effects of *fat* and *ex* suggest that they regulate growth through parallel pathways, it remain unclear how much the Hpo/Wts pathway contributes to them. This issue became more obvious when the influence of *ex* and *mer* on membrane proteins, e.g. Notch, EGFR, was observed and the endocytosis of multiple membrane proteins was

proposed as a way to explain *ex* and *mer* phenotypes[171]. Furthermore, membrane composition was also changed in *ex* and *fat* mutant cells[178]. In order to address this issue, I took advantage of the effect of *fat* mutation on the stability of Wts protein, expecting to saturate the degradation process by simply overexpressing Wts. Overexpression of Wts with stronger uniform tub-Gal4 driver indeed rescued the *fat* mutant animals to viability with normal wings, legs, eyes and body size, except some wing vein and PCP phenotypes[12]. Because the same amount of Wts in wild type background did not induce any growth phenotype, the rescue experiment demonstrates the significance and specificity of Wts in the Fat signaling. Surprisingly, the overexpression of Wts in *ex* mutants also rescues the animals to adults, but the rescue was only partial because the wings were enlarged. This different amount of rescue is consistent with the observation that *fat* and *ex* influence Wts in different ways. Degradation of Wts in the *fat* mutant may be more easily saturated by the overexpressed Wts, but the Wts activity loss in the *ex* mutants, as proposed by others[113], may not be fully compensated by overexpressing Wts.

Fat protein processing and post-translational modification by Dco.

In order to examine Fat protein in vivo by tissue staining and Western blotting, I generated antisera with the help of Shemeeakah Powell, following the protocol from H. McNeil[175]. At the same time, I fused Fat protein with small epitope tags at both N- and C-terminals in Bacterial Artificial Chromosome clone with recombineering technology (http://recombineering.ncifcrf.gov/). Transgenic animals were generated with φC31 mediated transgenesis[179,180]. With these constructs and transgenic animals, the Fat protein wass expressed at the levels close to the endogenous Fat protein[181]. I found that Fat undergoes post-translational cleavage with N- and C-terminals stably associated on cell

membrane. Although the cleavage was Ds or Fj independent, it could be a way to modulate Fat functions. The cleaved intracellular domain (ICD) was phosphorylated in Dco dependent manner, and seems highly correlated with Fat activity as indicated by manipulating Ds and Fj gradient levels. Dco^3 mutant specifically lost the ability to phosphorylate the Fat ICD in vivo and in cultured cells. As dco^3 mutation influences Wts protein stability, overexpression of Wts also rescued dco^3 mutant phenotype[11,181]. In cultured cells, the mobility shift of the Fat ICD was mapped to three Ser sites. Triple mutation of these three sites significantly removed the Dco dependent mobility shift of the Fat ICD in cultured cells and in wing discs, however, it fully rescued *fat* mutants, suggesting that the three Ser sites are not essential for Fat function. More efforts are still be needed to identify the biologically significant phosphorylation sites.

Separate PCP and growth signal from Fat.

As discussed above, Fat regulates both PCP and growth signals probably through two different pathways[9,10,25,76]. When Wts was overexpressed to rescue the *fat* and *ex* mutants, the PCP phenotypes were still obvious in the rescued *fat* mutant animals but not in the rescued *ex* mutants, even though the rescue in the latter was less successfull[12]. This suggests that the Wts only mediates growth signals from Fat and a distinct PCP pathway is mediated through a different mechanism and might requires Atrophin[69]. In dco^3 clones, no significant PCP phenotypes were observed, although the clones undergo excessive growth[181]. As the *dachs* and *fat* double mutation showed subtle PCP phenotypes, the distinct PCP pathway may branches at or before Dachs. Wts mediated transcription may also contribute a permissive signal to PCP determination, because PCP phenotype in the *fat* mutants appears stronger than that from the Wts rescued *fat* mutant animals[10,71].

Subcellular localization of Wts and Hpo.

In the Hpo/Wts signaling cascade, Yki has been shown localized in both cytoplasmic and nuclear regions, depending on Wts kinase activity[119,120]. In fly, Fat and tagged Wts are mainly localized on apical membrane[11,171]. However, in vertebrates, Wts homolog Lats was found associated with CDC2 [143,144], localized in centrosomes or nuclear[182], and thus being proposed to regulate the progression of mitosis[182]. Unfortunately, endogenous Wts cannot be readily examined with Wts antisera. Hpo cellular localization is also not clear, because the ectopic expression of Hpo induces cell death and antisera does not work well for tissue staining. In order to address these problems, small epitope tags were fused to *hpo* or *wts* in the BAC DNA clones that cover the *hpo* and *wts* loci. The cellular localization of tagged Hpo and Wts were thereafter examined by anti-tag staining in transgenic animals.

Figures

Figure 1. Patterning of wing imaginal disc.

A). Illustration of anterior/posterior and dorsal/ventral domains. B). Fate map of adult wing. Distal part is colored green and proximal part blue. Yellow line separates anterior and posterior domains and red lines show the regions secreting Wg. C) Signaling cascade regulating of *Decapentaplegic* (*Dpp*) expression: Segment polarity gene *Engrailed* (*En*) is expressed in posterior domain and activates *Hedgehog* (*Hh*) expression. Hh antivates Dpp expression in anterior domain in a short range. D) Signaling cascade regulating D/V Wingless (WG) expression is mediated by Notch signaling (see text). E) Different targets are activated by different concentration of Dpp and Wg gradients, although growth speed is relatively uniform on wing pouch (not shown here)[183]. F) Genes expressing in distal (green) and proximal (blue) regions of the wing disc. Modified from ref [9,44,46,184].

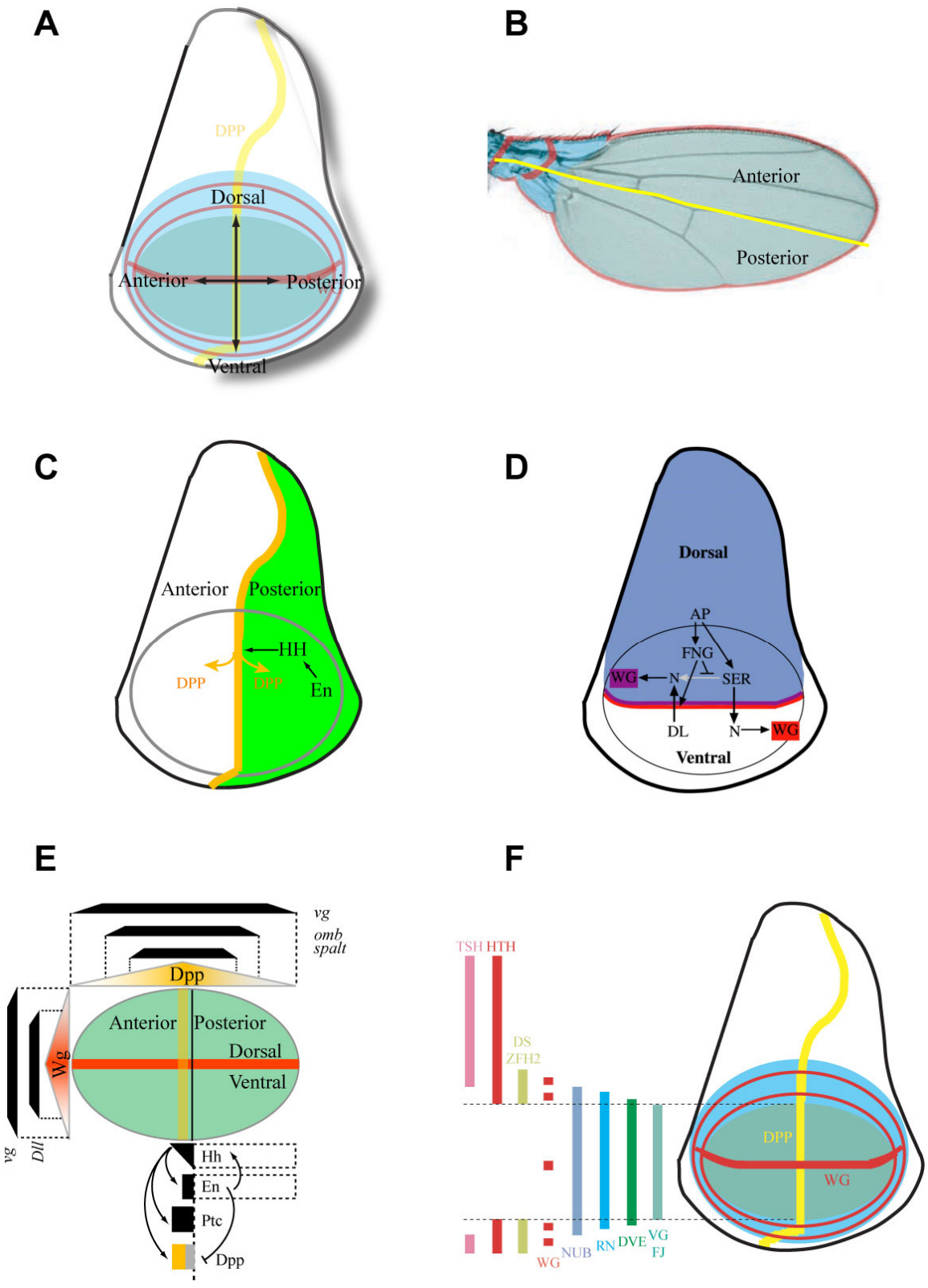
A
DPP
Dorsal
Anterior
Posterior
WG
Ventral
B
Anterior
Posterior
C
Anterior
Posterior
HH
DPP
DPP
En
D
Dorsal
AP
FNG
WG
N
SER
DL
N
WG
Ventral
E
vg
omb
spalt
Dpp
Anterior
Posterior
Dorsal
Ventral
Wg
vg
Dll
Hh
En
Ptc
Dpp
F
TSH HTH
DS
ZFH2
DPP
WG
WG
NUB
RN
DVE
VG
FJ

Figure 1

Figure 2. Polarization of epithelia.

(A). Apical-basal polarization of epithelia. Apical side of epithelia is adjacent to extracellular matrix and nuclear is positioned on the basal side.Epithelia are tightly connected to each other via marginal zone, zonula adherens and gap junctions. Cytoplasmic membrane copositions on different domains are shown. (B). Simplified Wnt pathway. β-catenin mediates the transcriptional output of the classical Wnt pathway and a non-canonical signal from Dishevelled (Dsh) is interpreted by the planar cell polarity (PCP) machinery. (C). In the non-canonical Wnt pathway, the Frizzled (Fz) receptor and cytoplasmic protein Dsh are preferentially enriched on the distal side of epithelia, while the membrane protein Van Gogh (Vang) and cytoplasmic protein Prickle (Pk) are accumulated on the proximal membrane. Polarization of these proteins is probably mediated by an amplification circuit in which Fz promotes the accumulation of Dsh in cis and Vang on the adjacent membrane in trans. Pk binds to Vang and inhibits the enrichment of Dsh in cis. (A) Modified from ref. [49]. (C) Modified from ref [55,57].

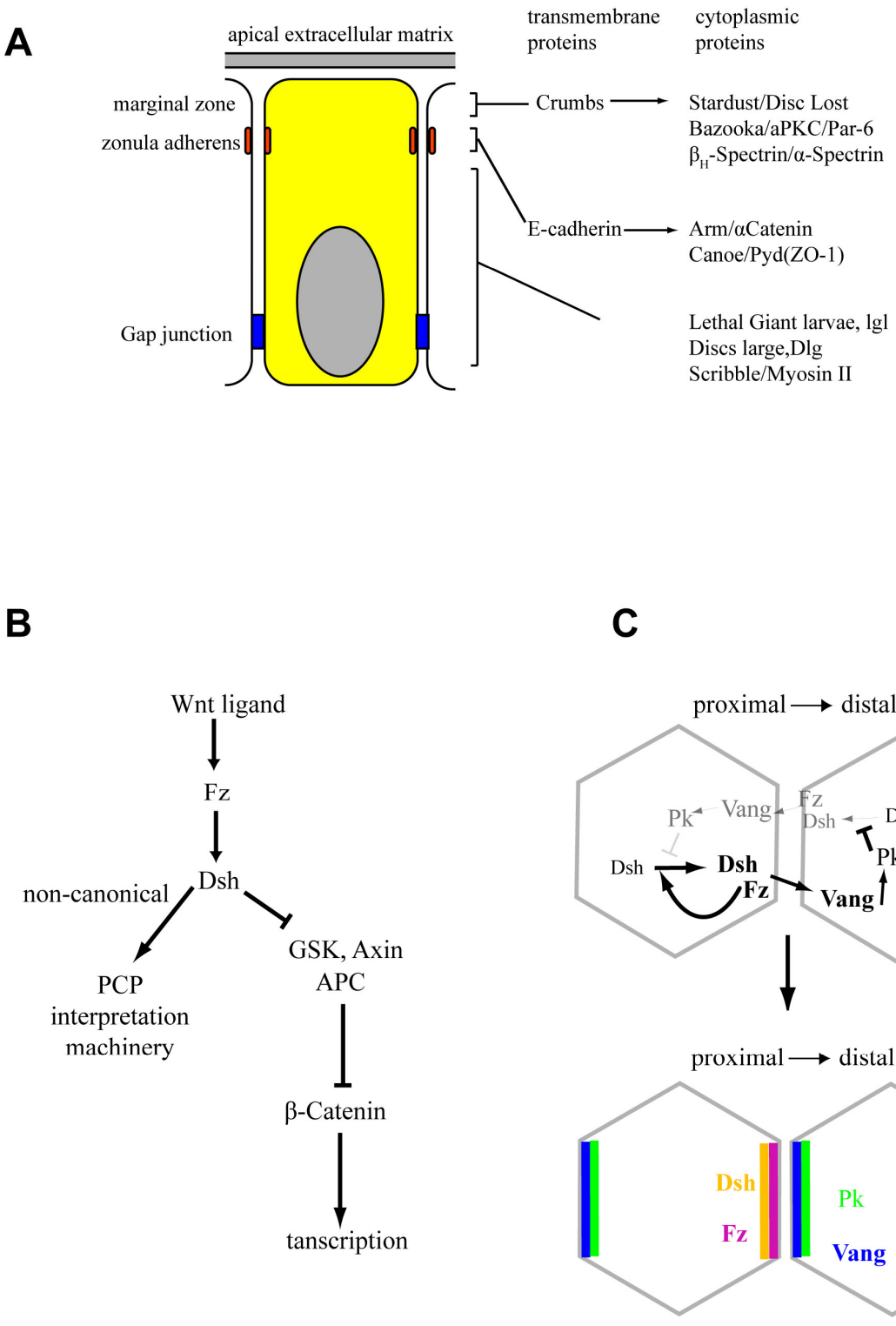
A
apical extracellular matrix
transmembrane proteins
cytoplasmic proteins
marginal zone
zonula adherens
Gap junction
Crumbs
Stardust/Disc Lost
Bazooka/aPKC/Par-6
βH-Spectrin/α-Spectrin
E-cadherin
Arm/αCatenin
Canoe/Pyd(ZO-1)
Lethal Giant larvae, lgl
Discs large,Dlg
Scribble/Myosin II
B
Wnt ligand
Fz
Dsh
non-canonical
PCP interpretation machinery
GSK, Axin APC
β-Catenin
tanscription
C
proximal → distal
Pk
Vang
Fz
Dsh
Dsh
Dsh
Fz
Pk
Vang
proximal → distal
Dsh
Fz
Pk
Vang

Figure 2

Figure 3. Cadherin proteins in *Drosophila.*

(Adapted from reference [64,185]).

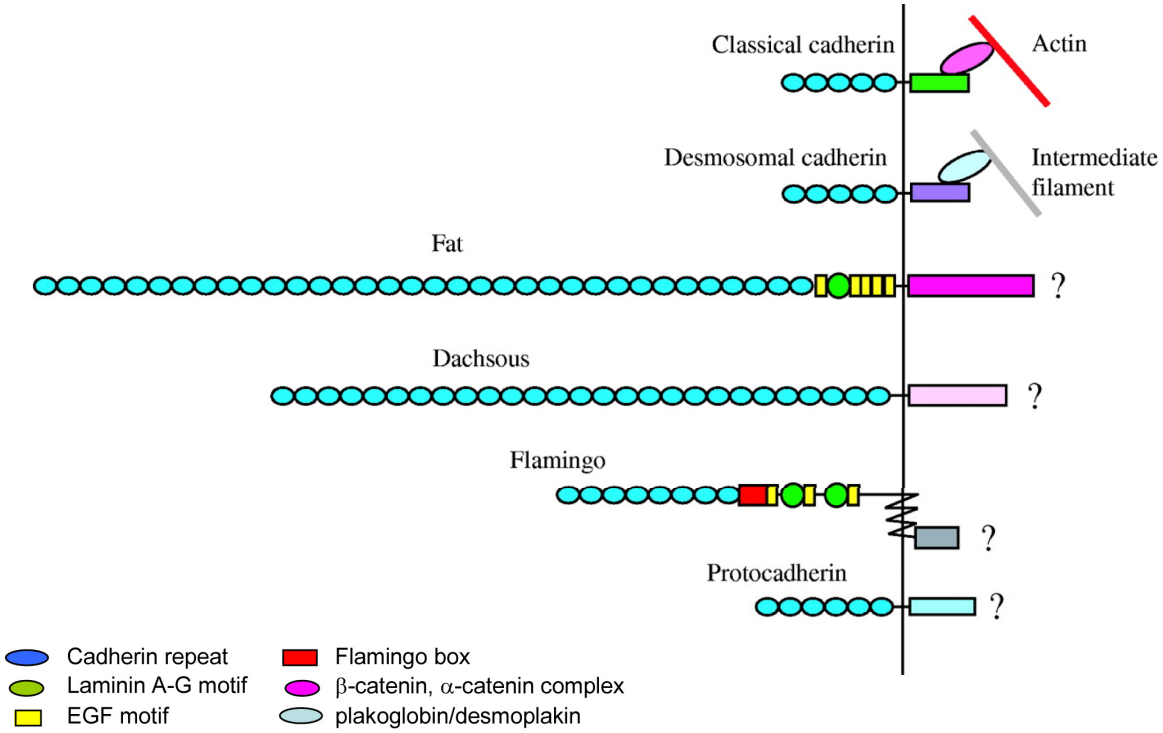

Figure 3

Figure 4. Core components of the Hippo/Warts pathway.

Kinase activity of Wts is enhanced by the phosphorylation or other modifications from Hpo, Mats and Sav. Wts inhibits Yki function by phosphorylation. Ex may activate Hpo or directly inhibits Yki fuction[186].

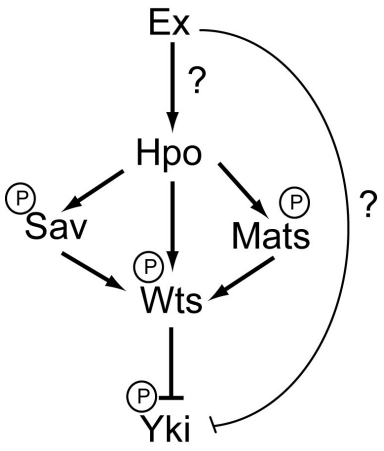

Figure 4

(Modified from ref. [25,169])

CHAPTER II

Fat signaling regulates growth by influencing Warts stability

Yongqiang Feng, Eunjoo Cho, Cordelia Rauskolb and Kenneth D. Irvine

The major part of this chapter was published in *Nat Genet* 38, 1142-1150 (2006).

Summary

Fat, Dco, Dachs, Fj, Ds, Ex and Merlin have been genetically linked to the downstream Hippo/Warts/Yorkie pathway[11,113], besides the potential regulation of Wts activity from Ex and Mer[113], the biochemical basis of these interactions was unknown. When Myc:Wts was uniformly expressed in wing discs with exogenous *tubulin-Gal4* driver, mutation of *fat*, not *ex*, *sav*, *mats* and *hpo*, specifically influenced the Myc staining. Double mutation of *fat* and *dachs* restored the staining to normal level, suggesting that Dachs is required. In order to detect endogenous Wts level change in the *fat* and dco^3 mutants, antisera against Wts was generated and purified with affinity columns. In the Western blotting with wing disc lysate, Wts protein level was dramatically decreased in the *fat* and dco^3 mutants and did not change in the *ex* mutants. Dco^3 has been shown upstream of Dachs[11], therefore its effect on Wts stability presumably is also Dachs dependent. Consistent with the tissue staining, *dachs* mutation also suppressed the *fat* influence on Wts levels in Western blotting. In *Drosophila* cultured cells, when tagged Dachs and Warts were cotransfected, immune precipitation of Dachs could pull down Wts, suggesting that they may form a complex in vivo, which may mediate the degradation of Wts in a similar manner as the adenomatous polyposis coli (APC) during the Wnt signal transduction[187,188]. The activity of Dachs/Wts complex is negatively regulated by the signals from Fat and Dco. In addition, because *ex* mutant does not influence the Wts level, Ex may regulate Wts through a different mechanism[113].

Introduction

Besides an excellent model system to study animal development[20], *Drosophila* has also been shown as an insect model to investigate a variety of vertebrate diseases, e.g. cancers[189-191]. With the rapid development in mosaic technologies[16,192], screening for genes regulating cell growth or cell death in imaginal discs has led to the identification of various oncogenes and tumor suppressor genes[22]. For instance, Wts was identified as a tumor suppressor in regulating cell growth in imaginal discs[173,193]. A few proteins interacting with Wts have recently been identified and delineated as the Hpo/Wts/Yki pathway[22]. The FERM domain proteins Ex and Mer are homologous to the vertebrate tumor suppressor Mer and partially redundant in growth regulation in *Drosophila*[194,195]. However, the relationship between these tumor suppressors and oncogenes and the molecular basis of their influence on growth were poorly understood[11,22,25].

As discussed above, *fat*, *ds*, *fj* and *dachs* mutants have been shown influencing the distal-proximal signaling, imaginal disc growth and planar cell polarity (PCP)[25]. In order to understand the downstream signaling mechanism of the Fat mediated growth, PCP and distal-proximal regulation, candidate genes that showed similar phenotypes were analyzed by E. Cho[11,25], which led to the identification of the Ex/Mer and the Hpo/Wts pathway that interact with Fat signaling. The Hpo/Wts/Yki cascade was found downstream of Fat, Ds, Fj, Dco, Dachs and Ex/Mer by classical genetic epistasis analysis. The Ex/Mer, Hpo/Wts/Yki (including Mats and Sav) and Fat pathways regulate the same set of target genes, suggesting that all these genes act through the same pathway instead of converge on the different aspects of growth regulation[11,25]. Besides these genetic interactions and the shared transcriptional targets, relationship between Fat and Ex/Mer

and the biochemical basis of the genetic interactions among Fat, Ex/Mer and the Hpo/Wts pathway was unknown.

To approach this problem, the protein cellular localization and levels in the Hpo/Wts pathways were examined in the mutations of *fat*, *ex*, *sav*, *hpo*, *mats* etc. We found that mutations of *fat*, dco^3 and *dachs* specifically influenced Wts protein levels in vivo post-transcriptionally, while the mutations of *ex*, *sav*, *mats* and *hpo* did not. In cultured S2 cells, Dachs co-immunoprecipitates with Wts. All these observations suggest a unique regulatory mechanism between Fat and Wts.

Materials and Methods

D. melanogaster genetics.

Mutant clones were created using FLP-FRT–mediated recombination, with the following stocks:

y w; d^{GC13}FRT40A/CyO-GFP, y w; fat^{8}FRT40A/CyO-GFP, y w; $fat^{G\text{-}rv}$FRT40A/L14, y w; $d^{GC13}fat^{8}$FRT40A/CyO-GFP, ywhs-$flp^{[122]}$;M(2)25AUbi-GFP FRT40A/CyO, w; ex^{e1}FRT40A/ CyO-GFP, FRT42D $hpo^{42\text{-}47}$/CyO, FRT82Bwts^{X1}/TM6b, FRT82B sav^{3}/TM3Sb, w; FRT82B $mats^{e235}$/TM6b.

To examine expression of Wts or Sav in mutant clones:

hs-flp[122]; *arm-lacZ FRT40A/CyO;UAS-Myc-Wts.1*, *y w hs-$flp^{[122]}$*; *arm-lacZ FRT40A/CyO;UAS-HA:sav.6/TM2, y w*; *fat^{8} FRT40A/CyO-GFP*; *tub-Gal4/TM3, y w; d^{GC13} fat^{8}FRT40A/CyO-GFP; tub-Gal4/TM3, y w; ex^{e1}FRT40A/CyO-GFP; tub-Gal4/TM3, y w hs-$flp^{[122]}$;UAS-Myc:Wts.2/CyO; FRT82B Ubi-GFP, tub-Gal4/CyO-GFP; FRT82B sav^{3}/TM6b and tub-Gal4/CyO-GFP; FRT82B $mats^{e235}$/TM6b*.

Histology.

Imaginal discs were fixed and stained as described previously[9], using as primary antibodies goat anti–β-gal (1:1,000, Biogenesis), mouse anti-Myc (9E10, 1:800, Babco), mouse anti-HA (16B12, 1:800, Covance) and mouse anti-Flag (M2, 1:800, Sigma). *In situ* hybridization to *ex* was conducted as described previously[196], using RNA probes derived from transcription of a 1,020-bp PCR product. For generation of a template for in vitro transcription to make an *ex* probe for in situ hybridization, primers

5’-tgtaa tacga ctcac tatag ggcga (T7 promoter) ATG CGA GCA TTT TGC ACC GTC AGC-3’ and 5’-ggatt taggt gacac tatag aatac (SP6 promoter) GGA AGA GCT GTT GGT AGA CTC TCC-3’ were used.

Immunoprecipitation.

D. melanogaster S2 cells were cultured with Schneider's *Drosophila* Medium (Invitrogen) supplemented with 10% FBS (Sigma). Transfection was conducted in *D. melanogaster* serum-free medium (Invitrogen) with Cellfectin (Invitrogen) according to the manufacturer's protocol. Plasmids used were pAct-GFP:V5-His (constructed by excising the green fluorescent protein (GFP) coding region from pMT/Bip/V5 His/GFP (Invitrogen) by *Kpn*I and *Xba*I digestion and then ligating it into pAC5.1/V5His (Invitrogen)); pUAS-myc:Wts (J. Jiang); pUAS-d:V5 (ref. [10]) and pAW-Gal4 (S. Blair). Cells were harvested 48–72 h after transfection and induction, washed once with cold PBS and lysed with freshly prepared RIPA buffer (50 mM Tris-HCl, pH 8.0; 150 mM NaCl; 1% NP-40; 0.5% sodium deoxycholate; 0.1% SDS; 1 mM EDTA; 1 mM DTT and 10% glycerol, supplemented with protease inhibitor cocktail (Roche) and phosphatase inhibitor cocktail (CalBiochem)). Anti-V5 beads (Sigma) were mixed with 500 μg cell lysate and incubated for 4 h at 4 °C. Beads were then washed with RIPA buffer six times.

Wts antibody preparation.

I amplified the region of Wts N-terminal to residue 635 by PCR (primers 5’-gga att cca tgc atc cag cgg gcg aaa aaa gg-3’ and 5’-gaa agc ggc cgc tca ctc ctt gga gat ctt ctt gcg ctc-3’ were used.) and cloned it into pGEX-6p-3 (Amersham Biosciences) through *Eco*RI and *Not*I sites. GST-Wts fusion protein was expressed in BL21(DE3) (Invitrogen) by IPTG induction and was purified with glutathione Sepharose 4B (Amersham

Biosciences). Rabbits were immunized by Cocalico Biologicals. Antibodies against Wts were purified with GST-Wts affinity columns (AminoLink Plus) according to the manufacturer's instructions (Pierce).

Protein blotting.

Wing discs were collected from wild-type (*Oregon-R*), $dco^{3}/TM6b$, $ex^{e1}/CyoGFP$ and ft^{Grv}/Cyo wandering third instar larvae, and wing discs were collected from dco^{3}, ex^{e1}, ft^{Grv}, ft^{Grv}/ft^{8} and $d^{GC13}ft^{8}$ larvae when their heterozygous siblings became wandering third instar. Larvae were collected and dissected in Ringer's solution, and wing discs were separated with forceps and lysed with RIPA buffer. Lysate was cleared by centrifugation at 14,000 g at 4 °C for 10 min, total protein was quantified using a BCA Kit (Pierce) and equal amounts were loaded in each lane of SDS polyacrylamide gels. Protein blotting was conducted according to standard protocols. Blots were stripped using Restore Western Blot Stripping Buffer (Pierce) between antibodies. Primary antibodies used for blotting included rabbit anti-Wts (1:5,000), guinea pig anti-Wts (1:2,000, Pan), rabbit anti-Merlin (1:4,000), guinea pig anti-Sav (1:2,000, Halder), guinea pig anti-Hpo (1:2,000, Halder), mouse anti-dMats (1:2,000, Lai), mouse anti-actin (JLA20, 1:15,000, Calbiochem), mouse anti-Engrailed (1:1,000, DSHB), mouse anti-Myc 9E10 (1:200) and mouse anti-V5-HRP (1:40,000, Invitrogen).

Results

Mutation of *fat* influences Warts staining in vivo.

Studies on the distal-proximal signaling led to the identification of the Fat signaling pathway[9]. Genetic epistasis experiments were performed by E. Cho and C. Rauskolb[11]. They found a cascade for the Fat mediated growth regulation, in which *dco* is upstream of *fat*, *fat* is upstream of *dachs*, *dachs* is upstream of *Mer* and *ex*, and *Mer* and *ex* act upstream of *wts*. However, genetic epistasis did not shed light on the biochemical basis for these interactions. In order to understand the molecular mechanism of these genetic interactions, proteins in the Hpo/Wts/Yki pathway were examined when upstream pathway components were mutated.

Wts was one of the key proteins examined in this experiment. Although it has been discovered for more than ten years [173,193], antisera against Wts only works for Western blotting and not for in vivo staining[115]. To address this issue, UAS-Myc:Wts was uniformly expressed under the exogenous promoter *tubulin-Gal4*. Overexpression of Myc:Wts did not induce significant growth phenotype (Chapter III, Figure 1*E*), however it rescued the wts^{X1} mutant, suggesting that it was functional and Wts protein was made in inactive form. Overexpressed Wts was distributed throughout the region from the basal to apical sides of columnar epithelia, except nucleus, and appeared to accumulate more on both apical and basal regions, especially when Wts was expressed at a higher level (Figure 3c and d). In *fat* mutant mosaic clones, the staining on membrane was significantly decreased (Figure 1*a*), but did not completely disappear. As the tagged Wts was driven by the exogenous promoter tubulin-Gal4, this effect indicates a post-

transcriptional regulation, probably post-translational. In order to show whether this effect was specific to *fat* mutation, the same staining was done for *sav*, *hpo*, *mats* and *ex* mutant clones, however, none of these mutants showed any effect on Myc:Wts staining (Figure 1*c-f*). To test whether *fat* mutation influences protein translation, HA tagged Sav was uniformaly expressed in the same way as Myc:Wts, and was also examined in *fat* mutant clones under similar conditions, but no effect was observed (Figure 1*g*), suggesting that *fat* mutation did not influence protein translation in general, and the influence of *fat* mutation on Myc:Wts staining most likely indicates a post-translational modification of Wts. Consistent with the observations that mutation of *dachs* suppressed all Fat mediated growth regulation[9,10], double mutation of *fat* and *dachs* restored Myc:Wts staining to normal level (Figure 1*b*). The influence of *fat* mutation on Wts therefore requires Dachs. As most of the regulatory mechanisms of Wts published to date only involve phosphorylation modifications[117], *fat* mutation induced Wts stability decrease is thus a unique mechanism of Wts regulation. Fat therefore appears to act in parallel with Ex, Hpo, Mats and Sav in regulating Wts.

Wts levels are influenced by *fat*, *dco*^{3} and *dachs* in vivo.

As shown above, *fat* mutants influenced Myc:Wts staining in wing discs, which may be caused by a changes in Wts conformation, stability or subcellular distribution. In order to distinguish these different possibilities, endogenous Wts should be blotted at denatured conditions, e.g. Western blotting, so that total amount of Wts could be measured. To generate antisera to Wts, two approaches were tested. First, the Wts amino acid sequence was analyzed with specific algorythm and potential peptide sequences were selected for chemical synthesis (Sigma).These peptides were then used as immunogens to induce

antisera in chicken or rabbits. Two peptides located on both ends of Wts were synthesized to generate antisera, but with no success (data not shown). In another approach, Wts antigens were prepared in bacteria as recombinant fusion proteins with Glutathione S-transferase (GST). Both the N- and C- terminal halves of Wts were cloned and expressed in *E. coli* as GST fusion proteins and were purified with Glutathione columns and used to immunize rabbits. The antisea was further purified with a GST affinity column as negative selection and a GST Wts affinity column as positive selection. The affinity purified antisera against Wts N terminal half worked well for both overexpressed Wts and endogenous Wts protein in Western blotting (data not shown), and also recognized overexpressed Wts in tissue staining (Figure 3). Endogenous Wts was blotted with the antisera in the wing disc lysates from various genotypes. Consistent with Myc:Wts staining in the wing discs, the Western blotting also showed less amount of Wts protein in the *fat* mutants, which was restored to normal level in the *dachs* and *fat* double mutants (Figure 1*h*). Other proteins like Hpo, Mats and Mer were not changed in any of these genotypes. In addition, the dco^3 mutants also influenced the Wts level. Because *dachs* is downstream of Fat and Dco, and *dachs* mutation suppressed almost all *fat* overgrowth phenotypes[11], Dco may regulate the Wts stability in a similar manner as Fat.

Dachs co-immune-precipitates with Wts in cultured *Drosophila* cells.

Although the Wts protein stability was regulated by Fat and Dco in a Dachs dependent manner, it remained unclear whether there was any direct biochemical interactions between these proteins. Protein binding assay is one of the few ways to test direct interactions between proteins. To test whether Dachs can bind to Wts in vitro, Dachs and

Wts were cotransfected into cultured *Drosophila* S2 cells. Without crosslinking, immune precipitation of Dachs pulled down Wts (Figure 2), suggesting that Dachs formed a stable complex with Wts. However, coexpression of Dachs with Wts in S2 cells did not induce Wts degradation, even though no Fat or Ds could be detected in S2 cells (data not shown). Dachs therefore is not a protease that can directly cleave Wts, and additional proteins are presumably required to mediate Wts degradation. Binding of Dachs and Wts indicates a direct biochemical interaction and confirms with the observation that both Dachs and Wts were localized to apical membrane (Figure 1 and ref. [10]). Regulation of protein stability or degradation is a widely used and crucial way to modulate signal transduction[197,198]. Similar to the canonical Wnt signaling where APC complex mediates β-Catenin degradation in the absence of Wnt signaling[65,187], the stability of Wts is regulated by upstream signaling from Fat and Dco in a Dachs dependent manner. In S2 cells, Fat binds to Wts but does not bind to Dachs (data not shown) and in wing discs Fat negatively regulates the Dachs subcellular localization[10], suggesting that other molecules may mediate the biochemical interaction between Fat and Dachs/Wts complex.

Regulation of Wts conformation in a transcription dependent manner (unpublished observations)

Although Myc:Wts was localized on cytoplasmic membrane(Figure 1, Z section not shown), subcellular localization of the endogenous Wts was unknown. In transfected S2 cells, Myc:Wts could be detected preferentially in cytoplasmic regions, by anti Myc or anti Wts staining (Figure 3*a*). When overexpressed in wing epithelia, Myc:Wts could be specifically detected on cell membrane (mostly on apical side) with anti Myc or anti Wts staining (Figure 3*b*). However, the endogenous Wts could not be readily detected (Figure

4) even though around one thousand Wts molecules are expressed in each epithelium (based on unpublished estimation).

When the endogenous Wts was stained in the *fat* mutant cells, surprisingly, enhanced signal was observed autonomously inside the mutant clones (Figure 4*a*) which was opposite to the effects shown above by tissue staining and Western blotting (Figure 1*a*, *h*). In order to determine the specificity of this effect, the same staining was performed for other mutations, e.g. *sav* (Figure 4*c*), *mats* (data not shown), *ex mer* (Figure 4*f*), *hpo* (Figure 4*d*), and for the overexpression clones of Ex (Figure 4*g*) and Yki (Figure 4*h*). Similar to the effect found in *fat* mutant clones (Figure 4*a*), increased staining in the cytoplasmic side of the cells was also observed in the *sav*, *mats*, *hpo*, *ex mer* mutant clones and Yki overexpression clones (Figure 4*c*-*h*). Because overexpression of Ex will lead to cell death, Ex ectopic clones were induced with the overexpressiong of a viral apoptosis inhibitor P35[199]. In the Ex+P35 clones, Wts staining was subtly decreased cell autonomously and enhanced non-autonomously in the adjacent cells (Figure 4*g*). As the mutations of *sav*, *mats*, *hpo*, *ex mer* and overexpression of Yki all showed increased transcriptional activity of the Hpo/Wts signaling, and the overexpression of Ex decreased the Hpo/Wts signaling, enhanced Wts staining seems correlated very well with the activity of Hpo signaling. The non-autonomous effect on Wts staining in the ectopic Ex clones may suggest a signaling to the adjacent cells that somehow decreases the Hpo pathway activity. Surprisingly, enhanced Wts staining was also seen in the wts^{X1} mutant clones (Figure 4*e*). As wts^{X1} may be a hypomorphic allele (personal communication with T Xu), it is consistent with above observations that increased staining of Wts is correlated with the transcriptional activity of Hpo/Wts signaling.

The enhanced Wts staining in *fat* mutants was restored to normal in *fat dachs* double mutants (Figure 4*b*), further confirmed the significance of Dachs in the Fat signaling pathway. Because Wts total protein was normal in the *ex* mutants and less in the *fat* mutants (Figure 1*h*), the enhanced Wts staining in the *ex* or *fat* clones was not caused by increased Wts protein quantity. Instead, Wts protein confirmation may be influenced by certain transcriptional targets of Yki, which determines the accessibility of Wts antibodies (Figure 5). This population of Wts appears to be localized across apical-basal axis (Figure 4*a*, *c*, *d* and *e*) without preference on apical membrane. If Wts is mainly localized on apical membrane at endogenous level, the Wts with this conformation might indicate a special function, e.g. a more acive form, which could act as a negative feedback to decrease the transcriptional activity of Yki.

Discussion

In the efforts to understand the biochemical basis between the Fat, Ex signaling and the Hpo/Wts cascade, Wts, Hpo, Mats and Sav proteins were examined by tissue staining and/or western blotting. I found that the Wts protein level was regulated post-transcriptionally by Fat, Dco and Dachs. In the *fat* mutant clones and homozygote wing discs, the Wts protein level was significantly decreased. This effect was suppressed by additional mutation in *dachs*, consistent with the observation that the *dachs* mutation suppressed nearly all Fat functions[9,10]. In the homozygote dco^3 mutants, two point mutations in the conserved domains of casein kinase I δ/ε [93], the endogenous Wts protein was also less than wild type discs. Because *dachs* genetically is epistatic to dco^3 (ref. [11]), effect of dco^3 on the Wts level may act in the same manner as *fat*. The stability regulation of Wts by *fat*, dco^3 and *dachs* but not by other proteins including *ex*, *sav*, *hpo* and *mats* suggests that the Fat signaling to Wts is distinct from other regulators of Wts[22,25]. Fat therefore acts in parallel with other proteins, e.g. Ex, Hpo, in regulating Wts via different mechanisms.

Although Wts level was regulated post-transcriptionaly by Fat, Dco and Dachs, because Myc:Wts was driven by exogenous *tub-Gal4*, it was not clear whether these observations indicate direct biochemical interactions. To answer this question, protein-protein binding was tested in *Drosophila* cultured S2 cells by coIP experiments. For instance, Dachs binds to Wts and Hpo, Sav and Wts binds to the Fat intracellular domain (Fat-ICD), but Dachs does not bind to Fat-ICD. Because the co-IP experiments were based on the overexpression of proteins in cultured cells, detected protein-protein bindings might not

happen in vivo when proteins are expressed at lower levels, post-translationally modified, or localized at distinct subcellular regions. Therefore, the interactions detected with co-IP experiments need to be interpreted cautiously and verified by other experiments.

The complex of Wts and Dachs may indicate a way how the Wts stability is regulated. The working model is that Dachs is a significant component required for Wts degradation and can be inhibited by functional Fat-ICD and Dco (Figure 5). The inhibition probably is indirect, because Fat-ICD sub-cellular localization was not overlapping with Dachs and Fat inhibits the apical membrane localization of Dachs[10]. An unknown mechanism may mediate the inhibitory function of Fat-ICD to Dachs. Given the polarized distribution of Dachs protein on the apical membrane[10], the inhibitory function of Fat-ICD may also be polarized. The significance of Dachs polarization in the Fat mediated growth regulation is not clear, although it was highly correlated with the Ds and Fj gradient mediated growth regulation[87]. This question can be approached from a few ways. For instance, Dachs can be artificially targeted to various sub-cellular domains to establish the relationship between the sub-cellular localization and function of Dachs. Alternatively, regions required for the Dachs polarization or membrane tethering, e.g. through App[88], can be mapped in vivo so that different versions of Dachs protein can be generated and tested in vivo. Another way is to search for factors required for Dachs polarization. This can be approached with mosaic random mutagenesis or RNAi screening. Finally, the Wts protein sub-cellular localization could be an indication of how much the polarization of Dachs contribute Wts stability. It will be interesting to examine Wts protein subcellular

localization to show whether it is also polarized. This issue can be approached with the tagged Wts expressed under endogenous promoter and enhancers (Chapter V).

Although the effects of *fat*, *dco*^{3} and *dachs* on Wts levels were confirmed by both tissue staining and western blotting in vivo, staining of the endogenous Wts in the mutant clones was increased whenever transcriptional activity of the Hpo/Wts pathway was increased. Enhanced staining therefore may not indicate increased Wts level, but rather suggests an unknown mechanism in modulating Wts protein conformation. One possible explanation is that the N- terminal of Wts is normally inaccessible to antisera during tissue staining. In the mutant clones of *fat*, *ex mer*, *sav*, *mats*, *hippo*, *wts*^{X1} and ectopic expression clones of Yki, Wts protein undergoes a conformation change which leads to the binding of antisera. This conformation change could be the dissociation of Wts with its binding factors or a simple structure switch, so that epitopes are exposed. This change appears to be mediated by certain unknown transcriptional targets of Yki, becaue the overexpression of Yki showed the same effect on Wts staining. It will be very interesting in the future to characterize the nature of this conformation alteration, identify the transcriptional targets, and address the biological significance of Wts conformation change during the Hpo/Wts signaling.

Figures

Figure 1. Influence of the Fat pathway on Warts levels.

(a–e) Wing imaginal discs containing clones of cells (marked by absence of GFP or β-gal (green)) mutant for fat^{8} (a,g), $dachs^{GC13}fat^{8}$ (b), ex^{e1} (c), $mats^{e235}$ (d), sav^{3} (e) or hpo^{42-47} (f) and stained for expression of Myc:Wts (red, a–f) or HA:Sav (red, g) under *UAS* and *tub-Gal4* control. (h) Protein blot probed with anti-Wts sera, then serially stripped and reprobed with anti-FatICD, anti-Hpo, anti-Sav, anti-Mer, anti-Mats and anti-actin. Each lane comprises total cell lysate from (1) wild-type, (2) dco^{3}/+, (3) dco^{3}, (4) ex^{e1}/+, (5) ex^{e1}, (6) $ft^{G\text{-}rv}$/+, (7) $fat^{G\text{-}rv}$, (8) $fat^{8}/fat^{G\text{-}rv}$ and (9) $d^{GC13}fat^{8}$.

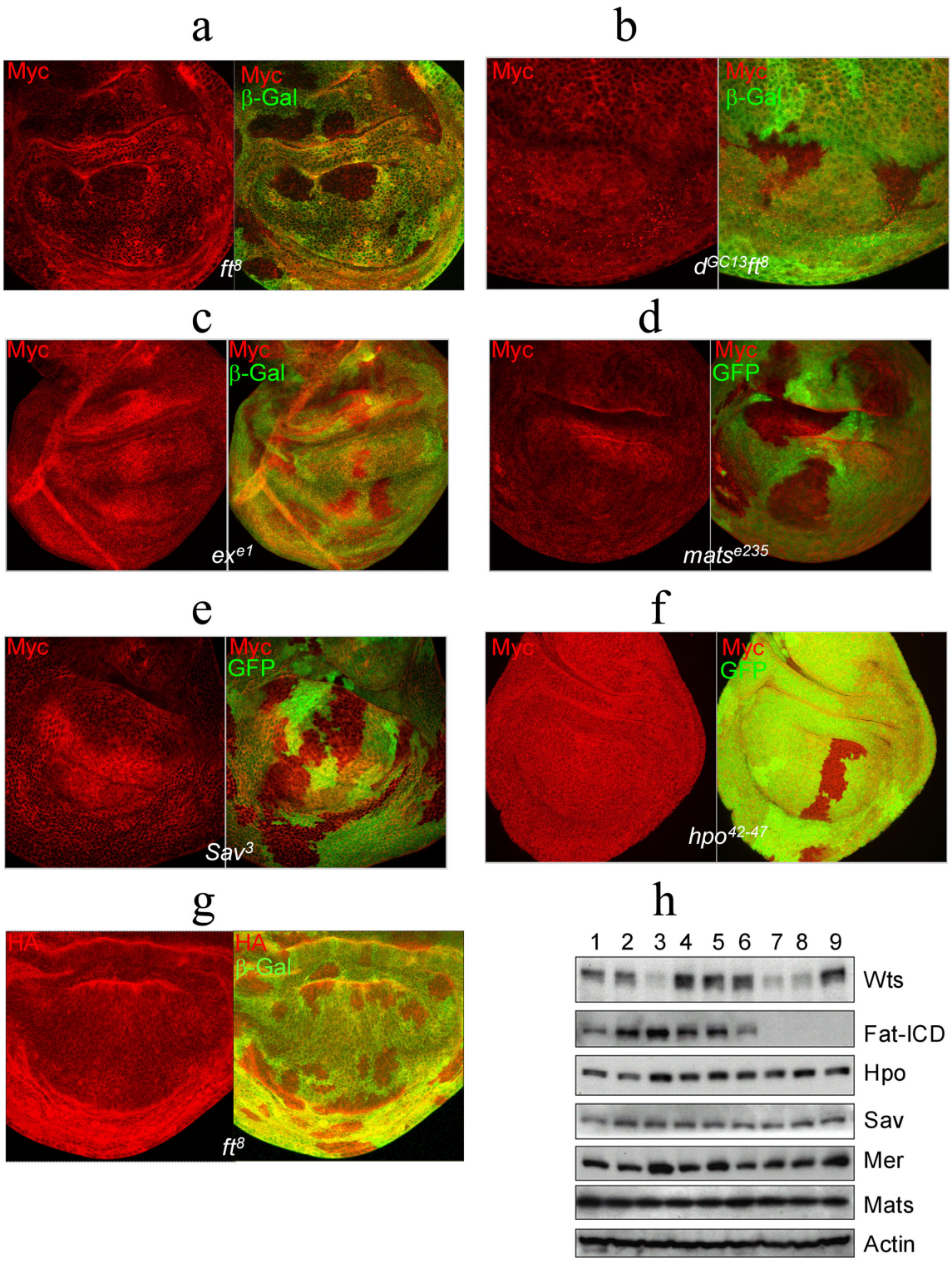
a
Myc
Myc
β-Gal
ft8
b
Myc
Myc
β-Gal
dGC13ft8
c
Myc
Myc
β-Gal
exe1
d
Myc
Myc
GFP
matse235
e
Myc
Myc
GFP
Sav3
f
Myc
Myc
GFP
hpo42-47
g
HA
HA
β-Gal
ft8
h
1 2 3 4 5 6 7 8 9
Wts
Fat-ICD
Hpo
Sav
Mer
Mats
Actin

Figure 1

Figure 2. Coprecipitation of Dachs and Warts.

Protein blots on lysates of S2 cells and on material precipitated from S2 cell lysates with anti-V5 beads. Lanes labeled 1 show material from cells transfected to express Myc:Wts and Dachs:V5. Lanes labeled 2 show material from cells transfected to express Myc:Wts and GFP:V5. GFP and Dachs bands (anti-V5) are from the same blot but were cropped because of their distinct mobilities. Blot was probed with anti-Myc and then serially stripped and reprobed with anti-V5, anti-Engrailed and anti-actin.

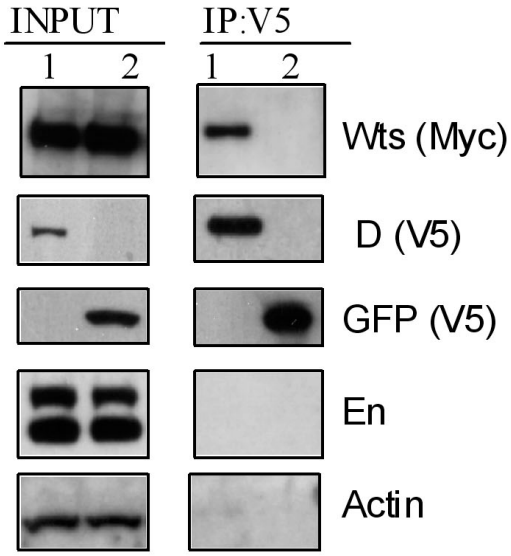

Figure 2

Figure 3. Tissue staining with Warts antisera.

(a) S2 cells was co-transfected with Actin-Gal4, UAS-Myc:Wts, Actin-GFP, and stained with Myc antibody or Warts antisera. (b) Wing discs expressing Myc:wts and GFP were stained with Myc antibody and Warts antisera. (c, d). Cellular localization of Myc:Wts was shown by anti-Myc staining (expressed by tub-Gal4 UAS-Myc:Wts) with Z-sections in (c' and d'). Myc:Wts was expressed at a higher level in (c). Arrows and arrow heads indicate apical and basal membranes, respectively. The section in (c) shows peripodial epithelia and apical region of columnar epithelia. The section in (d) shows a region between apical and basal of columnar epithelia.

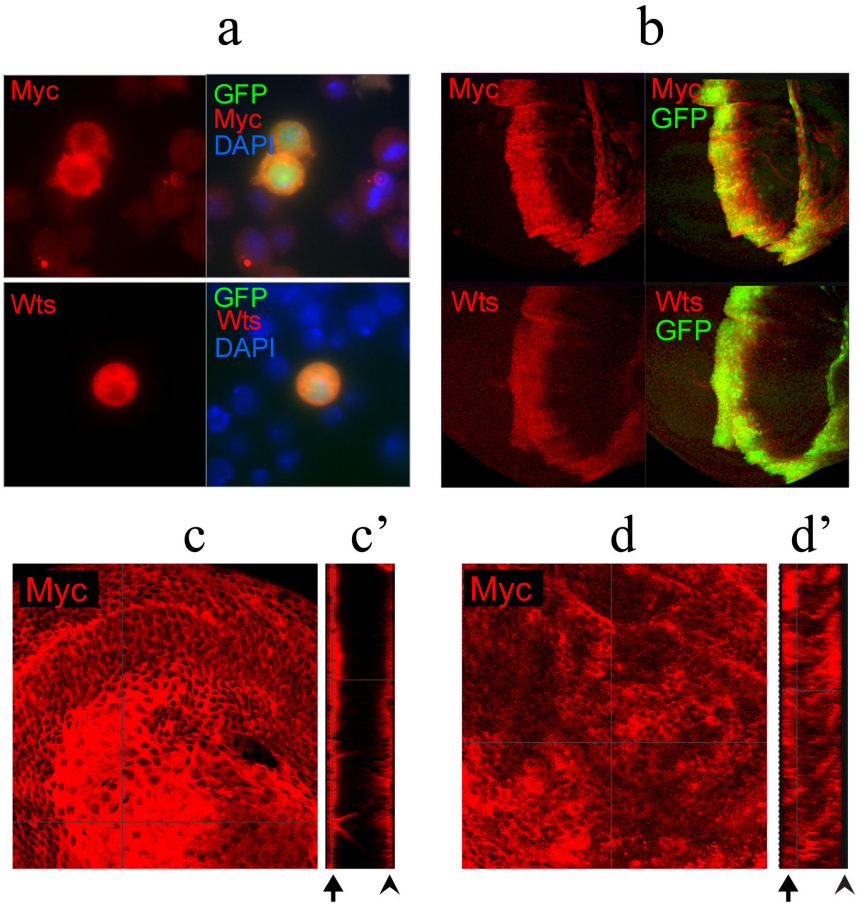

Figure 3

Figure 4. Regulation of Warts conformation.

Anti Wts staining in wing imaginal discs containing ft^{8} (a), $d^{GC13}ft^{8}$ minute (b), sav^{3} (c), hpo^{42-43} (d), wts^{XI} (e), $ex^{e1}Mer^{4}$ (f), *UAS-ex UAS-p35* (g), *UAS-yorkie* (h) clones. Z sections are coupled to show the distribution of Wts in apical-basal axis.

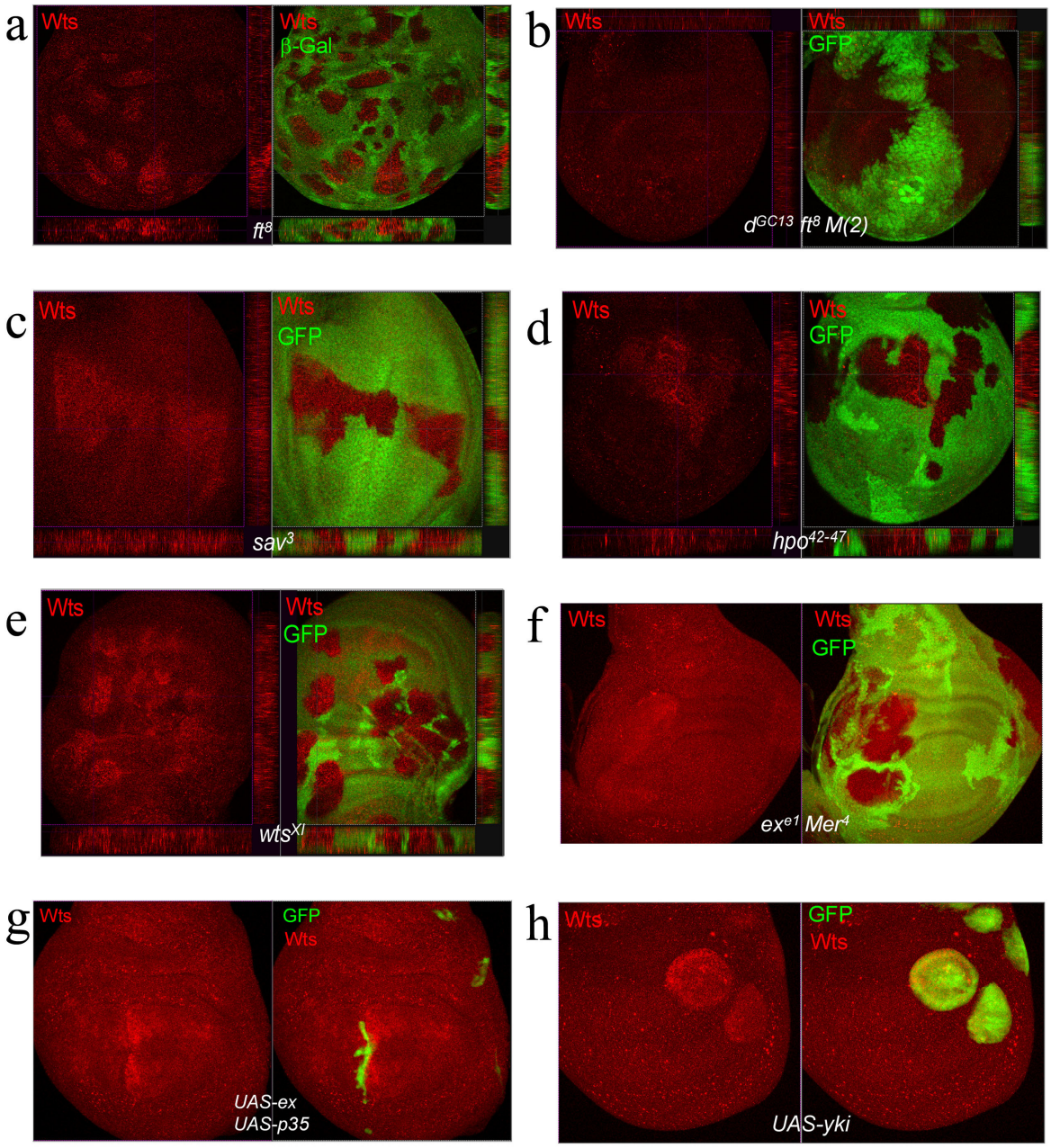

Figure 4

Figure 5. The Fat pathway model.

Dachs forms complex with Wts and mediates its degradation in the absence of upstream signals from Fat and Dco. The degradation is suppressed by signals from Fat and Dco via an unknown mechanism. Active Wts phosphorylates Yki and tethers it in cytoplasmic domain. Un-phosphorylated Yki is translocated into nuclear to activate target gene expression, some of which may form a feedback to regulate Wts conformation.

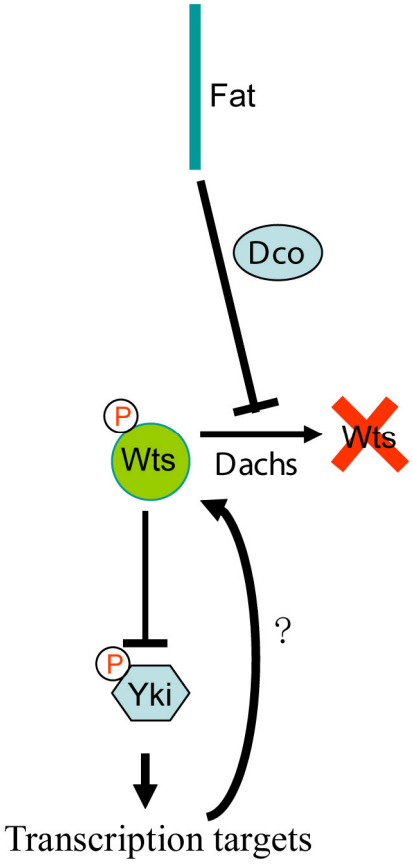

Figure 5

CHAPTER III

Fat and Expanded act in parallel to regulate growth through Warts

Yongqiang Feng and Kenneth D. Irvine

Most of this chapter was published in *Proc Natl Acad Sci USA* 104, 20362-20367 (2007).

Summary

Fat and Expanded have been implicated in regulating the activity of the Warts tumor suppressor[11,175-177]. However, the nature of the links between Fat, Expanded and Warts, and the significance of these links to growth control are controversial[11,171,175-178]. We found that *expanded* and *fat* mutations have additive effects on imaginal disc growth. Mutation of *fat* causes partial loss of Expanded protein from the membrane. However, mutation of *fat* promotes growth even when Expanded is over-expressed and accumulates at its normal location. These observations argue against recent proposals that Fat acts as a receptor for the Hippo signaling pathway, and instead support the proposal that Fat and Expanded act in parallel to regulate Warts through distinct mechanisms. We also found that mutations in either *expanded* or *fat* can be partially rescued by Warts over-expression. This indicates that, not withstanding reported effects of Fat and Expanded on other signaling pathways, their influence on Warts is their most essential function. When growth phenotype of *fat* mutation is rescued by Warts overexpression, planar cell polarity (PCP) phenotype is still similar to *fat* mutant animals. However, for *expanded* mutants, though the growth phenotype is partially rescued by overexpressed Warts, PCP is completely normal. These observations suggest that Warts only mediates growth signal from Fat, an unknown signaling cascade may contribute to Fat mediated PCP regulation.

Introduction

We and a few other groups recently linked Fat pathway to the Hpo/Wts cascade[11,175-177]. Based on the influence of Wts protein stability, we proposed that Fat regulates Wts protein levels in a Dachs dependent manner, which is distinct from the mechanisms shown for Ex, Sav, Hpo and Mats[11,113,117]. Other groups found that in the *fat* mutant clones Ex protein stability or sub-cellular localization is influenced[175-177]. In *Drosophila* cultured S2 cells the Fat intracellular domain (Fat-ICD) promotes Wts phosphorylation[176]. An alternative model was therefore proposed that Fat regulates Wts activity by modulating Ex stability or sub-cellular localization. In addition to these proposed models, mutation of *ex* and *mer* was shown influencing endocytosis of membrane proteins including Notch and EGF receptor[171], therefore potentially affecting multiple pathways.

There are a few critical issues that need to be addressed in order to provide further insights to understand the interactions among Fat, Ex and the Hpo pathway. First, it is not clear whether Ex and Fat act in a single pathway or parallel pathways. To address this problem, growth speed of *fat*, *ex* and *fat ex* double mutation was measured in both mosaic clones and homozygote animals. I found that double mutation of *fat ex* grows significantly faster than single mutation of *fat* or *ex*. Additive effect of this and other experiments argues that Ex and Fat act in parallel in regulating cell growth. Second, contribution of the Hpo/Wts pathway to the *fat* and *ex* mutant phenotypes needs to be evaluated. Taking the advantages of the effect of *fat* mutation on Wts protein stability[11], higher levels of Wts was overexpressed in *fat* or *ex* mutants in order to saturate the degradation process and discriminate the difference between *fat* and *ex*. Overexpression

of Wts in wild type background did not give growth phenotype, however, it fully rescued the growth phenotypes of *fat* mutation and partially rescued the growth phenotypes of *ex* mutation. Wts therefore is the critical target of both Fat and Ex. Different degrees of rescue may suggest that the effects of *ex* and *fat* on Wts are most likely distinct, as the degradation of Wts in *fat* mutants can be easily saturated by expressing more Wts but the its activity loss in *ex* mutants cannot be fully compensated.

When the growth phenotype of *fat* mutation is rescued by Wts overexpression, the planar cell polarity (PCP) phenotype is still similar to the *fat* mutant animals. However, even though the growth phenotype was partially rescued by the overexpressed Wts, PCP was completely normal in the *ex* mutant animals. These observations suggest that Wts only mediates the growth signal from Fat and an unknown signaling cascade, e.g. via Atrophin[69], may contribute to the Fat mediated PCP regulation. The PCP signal and growth signal may branch at Dachs, because *dachs* mutation completely suppressed the overgrowth phenotype and most of PCP phenotype in *fat* mutants[10].

Materials and Methods

Drosophila Stocks and Crosses.

For examination of Myc:Wts expression, *yw; UAS-Myc:Wts.2/CyO* and *yw; UAS-Myc:Wts.1/TM6b* were crossed to *ptc-Gal4 UAS-GFP*.

Negatively marked clones were generated by crossing *yw; ft^{8} FRT40A/CyO-GFP*, *yw; ft^{Grv} FRT40A/CyO-GFP*, or *yw; d^{GC13} ft^{8} FRT40A/CyO-GFP* to *yw hs-FLP; Ubi-GFP FRT40A/CyO* or *yw hs-FLP;M(2) Ubi-GFP FRT40A/CyO*, and *yw; dco^{3} FRT82B/TM6b* to *yw hs-FLP; Ubi-GFP FRT82B/CyO.*

Positively marked (MARCM) clones were generated by crossing *w; ex^{e1} FRT40A/CyO-GFP*, *yw; ex^{e1} ft^{8} FRT40A/CyO-GFP*, *yw; ex^{e1} ft^{Grv} FRT40A/CyO-GFP*, *yw; ft^{8} FRT40A/CyO-GFP*, *yw; ft^{Grv} FRT40A/CyO-GFP*, *yw; UAS-ex/TM6b*, or *yw; ft^{8} FRT40A/CyO-GFP; UAS-ex/TM6b* to *yw hs-FLP tub-Gal4 UAS-GFP; FRT40A tub-Gal80*.

For Wts rescue experiments, we crossed *fat^{8} UAS-Myc:Wts.2/CyO* to *$ft^{G\text{-}rv}$ tub-Gal4[LL7]/TM6b*, *UAS-Myc:Wts.2* to *tub-Gal4[LL7]/TM6b*, and *ex^{e1} UAS-Myc:Wts.2/CyO* to ex^{e1}/CyO; *tub-Gal4[LL7]/TM6b.*

Histology and Imaging.

Discs were fixed and stained as described previously[9] using mouse anti-Wg (1:800, 4D4; Developmental Studies Hybridoma Bank), guinea pig anti-Ex (1:5,000, R. Fehon, University of Chicago, Chicago), rat anti-E-cadherin (1:40, DCAD2; Developmental

Studies Hybridoma Bank), mouse anti-Myc (9E10, 1:800; Babco), rat anti-ELAV (Developmental Studies Hybridoma Bank), and rat anti-Fat. Fluorescent stains were captured on a Leica TCS SP5. For horizontal sections, maximum projection using Leica software was used to allow visualization of staining in different focal planes. This method takes the brightest pixel at any given *xy* position in each of a series of *z* sections being projected. For adult tissues, combineZM (http://www.hadleyweb.pwp.blueyonder.co.uk/CZM/combinezm.htm) was used to allow visualization of features in different focal planes within a single image.

Size Measurements.

To measure clone sizes, embryos were collected from corresponding crosses for 12 h. Forty-eight hours later, larvae were heat-shocked at 36°C for 10 min, and an additional 72 h later animals were dissected and fixed. Clone sizes were measured by tracing in NIH Image J. Samples from different genotypes were collected and analyzed in parallel.

To compare disk sizes, embryos were collected from corresponding stocks or crosses for 8 h and animals were dissected and fixed at appropriate stages as mentioned in the text.

Results

fat and *ex* mutants can be partially rescued by Wts overexpression.

Although we and other groups have shown fat and ex act through Wts to regulate growth and target gene expression[11,175-177], two other models have been proposed to explain the *fat* and *ex* phenotypes. One model argues that Ex and Mer regulate growth by modulating the EGFR, Notch, Hedgehog, Wg and Fat signaling pathways, because the double mutation of *ex mer* influences the endocytosis of these membrane proteins[171]. Another group found that *fat* and *ex* influence membrane sterol composition and argued that Fat modulates multiple pathways[178].

Taking advantage of the observation that Fat signaling influences Wts stability[11], I reasoned that it might be possible to saturate this mechanism by overexpressing Wts, though overexpression of Wts did not preclude observation of the influence of Fat signaling on Wts protein levels in prior experiments[11]. This amount of Wts may not be sufficient to saturate the mechanism of Wts degradation. However, higher amount of Wts expressed from different UAS-Myc:Wts transgenic animals was enough to rescue *fat* mutant animals to adults (Figure 1B, F, I, L). Because the same amount of Wts in wild type background only induces subtle wing vein phenotype (Figure 1E), the rescue experiment suggests Wts is the critical target for Fat signaling.

Ex has been proposed to regulate growth and gene expression by influencing Wts phosphorylation through Hpo[113]. Although overexpression of Wts in wild type animals did not show significant growth phenotype in adult wings, wing discs at late third instar larval stage appear smaller than wild type discs (data not shown), suggesting that

overepressed Wts has subtle gain of function. As *ex* growth phenotype is milder than *wts* mutant[106,173,193], Wts activity is only partially lost in *ex* mutant. Overexpression of Wts can therefore compensate some activity loss in *ex* mutant and might at least partially rescue *ex* mutants. Indeed, *ex*-null mutant animals could be partially rescued to adults by overexpression of Wts (Figure 1C). The rescue is incomplete, i.e. the wing discs and adult wings of these animals are enlarged (Figure 1C, G, J, M), but, aside from this, and mild wing vein phenotypes, these Wts-rescued *ex* mutants appear normal (Figure 1C). They differ most obviously from Wts-rescued *fat* mutants in their enlarged wings and in the absence of any visible PCP phenotype (Figure 1B, F, I, L), which suggests that previously reported influences of *ex* on PCP reflect the influence of Ex on Wts-dependent transcription[195].

Separate growth and PCP signaling from the Fat pathway.

Although Wts-rescued *fat* mutants are similar to wild-type animals in terms of the overall size and most aspects of their morphology, the most dramatic phenotype is a PCP phenotype, evident in the misalignment of hairs and bristles on adult wings and abdominal epidermis (Figure 1I, L)[200]. In the abdomen, this PCP phenotype was similar to that of unrescued *fat* mutants[10,201]. However, in the wing, the PCP phenotype is weaker than unrescued *fat* mutants and similar to the PCP phenotype of *fat* mutants that have been partially rescued by overexpression of the *fat* intracellular domain (FatICD)[71]. These observations are consistent with studies that have implied the existence of two distinct branches of Fat signaling, one affecting transcription via the Wts/Yorkie pathway and one regulating PCP[10,69], probably through Atrophin[69]. In addition, Wts and Fat-ICD rescue experiments suggest transcriptional activity of Fat signaling also play a role in

PCP determination, at least in wings[10,71]. Wts-rescued *fat* mutants also show abnormal legs (fused segments), smaller wings, and wing vein phenotypes. When the cross veins are visible, the spacing between them is reduced, which is a classic Fat pathway phenotype[10,71].

***fat* and *ex* acts in parallel in regulating Wts.**

As previously shown, *fat* mutant destabilizes Wts protein, Fat signaling therefore may regulate growth by influencing Wts protein levels[11]. However, others reported an effect of Fat on Ex levels or membrane localization and proposed this as a basis for Fat signaling[175-177]. Analysis of double mutant animals provides a test of whether *fat* and *ex* act in a single linear pathway or in parallel pathways, because, if Fat signaled solely through Ex, then *ex fat* double mutants would be expected to be identical to *fat* or *ex* single mutants. Indeed, a critical piece of evidence in favor of the hypothesis that Fat signals through Ex was the claim that *ex* mutants, *fat* mutants, and *ex fat* double mutants have identical phenotypes[175-177]. However, this claim was based on analysis of a single phenotype, the number of interommatidial cells in pupal eyes, which is normally reduced by Hippo pathway-dependent apoptosis[202]. One report did acknowledge that *ex fat* double mutants have stronger overgrowth phenotypes in the head[176], but this phenotype was not well characterized, and its significance was discounted.

In one assay, the relative areas of mutant clones were measured. For these experiments we used a null allele of *ex*, ex^{e1}, and two different alleles of *fat*, fat^{8} and fat^{Grv}. Both of these encode proteins that are truncated in the extracellular domains[71] and lack detectable expression using antibodies directed against the intracellular domain (data not shown). Clones of cells mutant for *fat* or *ex* are larger than control clones in both wing and eye

discs (Figure 2A, B). *ex fat* double mutant clones were larger than single mutant clones (Figure 2A, B)[10,203]. This indicates that *fat* and *ex* have additive effects on growth, consistent with the hypothesis that they act in parallel pathways. Unexpectedly, fat^{Grv} clones were larger than fat^{8} clones. The reason for this difference is not clear, but, because there was a correspondingly greater enhancement of growth in both *ex fat* double mutant combinations, it does not affect the conclusion that *fat* and *ex* have additive effects. As an alternative growth assay, we examined the relative size of the entire wing disk in animals transheterozygous for *ex* fat^{Grv} and *ex* fat^{8} and compared it to the respective single mutants. This confirmed that *fat* and *ex* have additive effects, because double mutants have larger discs (Figure Figure 2C-E). Many *Drosophila* tumor suppressors delay pupariation, and the additive influence of *fat* and *ex* mutants on disk growth was especially pronounced during this extended larval period. The additive effects of *ex* and *fat* mutants on growth confirm that at least some Fat signaling occurs independent of *ex*.

Although mutation of *ex* results in overgrowth, the developing eye is actually reduced in size[204]. This reduction in the eye field is visible in wandering third-instar larvae stained with a pan-neural antibody, anti-ELAV (Figure 2F-I). *fat* mutants appear to have a modest loss of eye development (Figure 2G). *fat ex* double mutants have a strong additive phenotype, because in most cases (28 of 30 discs) they completely failed to initiate eye development, as monitored by ELAV expression (Figure 2I). The compound eye of *Drosophila* is composed of ~800 ommatidia and each ommatidium contains a cluster of photoreceptor cells surrounded by support cells and pigment cells. Ommatidia are precisely aligned during eye disc development though the molecular mechanism is

unknown[205,206]. In *ex* and *fat* single mutant clones spacing between ommatidia is increased (Figure 2 *J-L*), both autonomously and in the adjacent cells. *ex fat* double mutant can further enhance the spacing (Figure 2*M*) between ommatidia. Similar to the homozygote eye discs of *ex fat* double mutant, *ex fat* double mutant clones also inhibit neuronal cell differentiation. Broader spacing between ommatidia may be due to the overgrowth in *fat*, *ex* and *ex fat* mutants, or non-autonomous patterning defects. Neuronal differentiation defects in *ex fat* double mutant could be the results of certain mis-regulated expression of transcriptional target genes. In summary, *fat* and *ex* mutations are additive not only for growth, but also for other phenotypes.

Influence of Fat signaling on Ex localization.

Central to the hypothesis that Fat signals through Ex was the observation that mutation of *fat* causes a decrease in the levels of Ex at the apical membrane. There are, however, discrepancies among prior reports in terms of the strength of this effect, ranging from a modest decrease[175] to virtually complete loss[176,177]. We have assessed the influence of Fat on Ex by carefully examining Ex protein staining in *fat* mutant clones throughout the third instar larva, examining both fat^{8} and $fat^{G\text{-}rv}$ clones, in both wing and eye imaginal discs, and throughout the apical-to-basal axis of these discs. We do see in most instances some decrease in the levels of Ex membrane staining within *fat* mutant clones, although in no case is Ex staining completely lost (Figure 3*A*). Confirmation of the specificity of Ex staining in these experiments was provided by examining *ex* mutant clones, in which loss of Ex is readily detectable (data not shown).

In addition to reducing Ex levels at the membrane, *fat* clones are sometimes associated with a shift in distribution of Ex staining to a more basal focal plane, especially at late

third instar. In single horizontal sections, this can give the impression of a substantial loss of Ex staining (data not shown), which might have contributed to prior reports of almost complete loss of Ex staining. However, in vertical sections (Figure 3*B*) or more basal horizontal sections (Figure 3*A*) it is clear that Ex staining is shifted basally rather than lost. To visualize Ex staining in different focal planes within a single horizontal image, we used maximum projection, which reveals a modest decrease in Ex staining (Figure 3*A'*). Although the basal shift could be a consequence of a specific relocalization of Ex in response to loss of Fat, it could also derive from altered cell shape. To investigate this, *fat* mutant clones were stained for E-cadherin, which normally localizes near Ex in the subapical membrane. E-cadherin levels often appear slightly elevated within *fat* mutant clones[207]. E-cadherin staining was also shifted basally, in what appears to be a consequence of a change in cell shape rather than a specific effect on the subcellular localization of Ex or E-cadherin (Figure 3*B*).

Previously, we described a pathway in which signaling downstream of Fat is mediated by its antagonism of the unconventional myosin Dachs [9-11]. We also identified another *Drosophila* tumor suppressor, *dco* [393], as a kinase that acts genetically upstream of *dachs* within the Fat pathway[11]. To investigate how the influence of Fat on Ex relates to this branch of Fat signaling, we analyzed their influence on Ex. Ex staining appears slightly reduced in dco^3 clones (Figure 3*D*). The influence of *dco* on Ex is weaker than that of *fat*, but it also has weaker effects on the expression of downstream target genes[11]. The influence of Fat on growth, cell affinity, and gene expression depends completely on *dachs*[9,10]. The reduction in Ex levels observed in *fat* mutant clones is similarly *dachs*-

dependent, because in *fat dachs* double mutant clones Ex staining was indistinguishable from that in surrounding wild-type cells (Figure 3*C*).

Fat signaling can occur independent of effects on Ex levels.

The results described above confirm prior observations that Fat can influence Ex levels at the membrane but do not address the significance of decreased Ex staining to the regulation of growth and gene expression. Thus, to further investigate the relationship between Ex levels and Fat signaling, we examined the influence of *fat* on Ex overexpression. When the MARCM method[208] was used to overexpress Ex within *fat* mutant cells, high-level Ex staining was readily detected and appeared at its normal subapical location (Figure 4*A*-*B*). Thus, although Fat can modulate Ex membrane localization, it is not required for it.

The observation of elevated Ex staining within these clones provided an opportunity to further explore the relationship between *fat* and *ex*. Prior studies have indicated that Ex overexpression appears to mimic Ex gain of function, resulting in a Wts-dependent induction of apoptosis and repression of downstream targets of Hippo signaling[11,113,195]. Consequently, Ex-expressing clones are greatly reduced in size and number (Figure 4*C*-*D*)[11,178]. Conversely, *fat* mutant clones overgrow compared with wild-type clones. Clones of cells mutant for *fat* and overexpressing Ex exhibited an intermediate phenotype (Figure 4*C*-*D*). These clones are slightly overgrown compared with wild-type control clones and substantially overgrown compared with Ex-expressing clones (Figure 4*C*-*D*). The observation that mutation of *fat* dramatically enhances the growth of Ex-expressing clones, even though Ex staining remains strong at the subapical membrane, clearly argues against models in which Fat signals primarily through modulation of Ex levels or

localization. By contrast, it is consistent with the hypothesis that *fat* and *ex* act in parallel to regulate growth. As a further test, we examined the expression of downstream target of Wts and Yorkie activity. Wg expression in the proximal wing is up-regulated by mutation of *fat* or by mutation of any of the tumor suppressors in the Hippo pathway (Figure 4*E*)[9,11]. Conversely, overexpression of Ex represses Wg expression in the proximal wing[11]. Clones of cells mutant for *fat* and overexpressing Ex exhibit an elevation of Wg expression (Figure 4*F*), further demonstrating that Fat signaling can occur independent of an effect on Ex levels or localization.

Discussion

Fat and Ex act through Wts.

The observation that *fat* and *ex* mutants are rescued to viability simply by overexpressing Wts (Figure 1) provides a powerful argument that regulation of Wts is their most critical function and against the hypothesis that the influence of Fat and Ex on growth stems from combinatorial effects on many pathways, due to influences on endocytosis or membrane composition[171,178]. Instead, reported effects of *ex* on other pathways or processes are likely mediated downstream of Wts. Indeed, whereas an increase in Fat protein staining in *Mer ex* double mutants was interpreted as supporting a general influence of Mer and Ex on endocytosis[171], we have observed a similar effect on Fat staining in clones of cells mutant for *wts* or overexpressing Yorkie (C. Rauskolb and K.I., unpublished observations), which implies that the influence of *Mer* and *ex* on Fat is actually mediated through their influence on transcription. Although the incomplete rescue of *ex* mutants might be taken as evidence that Ex regulates growth in part independent of Wts, it is also possible that it is simply not possible to generate wild-type levels of active Wts in *ex* mutants by overexpression.

Parallel action of Fat and Ex.

The nature of the processes that regulate the Hippo pathway has been a major question in the field, hence the critical importance of the claim that Fat acts as the Hippo receptor. This claim was based largely on three observations. First, it was reported that mutation of *fat* leads to a substantial loss of Ex protein from its normal subapical location. In fact, however, Ex levels are only partially reduced (Figure 3). Moreover, even when Ex levels

are artificially elevated, Fat has strong effects, because mutation of *fat* completely reverses the consequences of Ex overexpression and even leads to some elevation of growth and downstream gene expression (Figure 4). This indicates that Fat can regulate Wts independent of any effects on Ex levels or localization. This result contradicts that of Tyler and Baker[178] but we confirmed both the overexpression of Ex (Fig. 4) and the absence of Fat (data not shown) by antibody staining and quantified the effects of >400 clones in two different discs using two different *fat* alleles. Others have claimed that mosaic loss of *fat* had no effect on Ex overexpression phenotypes during late eye development[176,177], but close examination of their figures suggests that an intermediate phenotype is actually observed, which would be consistent with our results.

A second argument that Fat acts through Ex to regulate Hippo signaling was provided by the claim that *ex fat* double mutants exhibit the same phenotype as *fat* or *ex* single mutants[175-177]. Although this may be the case in terms of their influence on the number of interommatidial cells, it is not true for other *fat* and *ex* phenotypes (Figure 2). Instead, analysis of *ex fat* double mutants, together with Ex overexpression in *fat* mutants, confirms that Fat and Ex can act in parallel. We note that our results do not exclude the possibility that Fat can also act through Ex, whether through its effect on Ex levels or an effect on Ex activity, but they do clearly indicate that at least some Fat signaling occurs independent of Ex.

A third argument was a reported influence of Fat on Wts and Hpo phosphorylation[175,176]. However, this effect has been observed only in experiments in which an intracellular fragment of Fat is expressed at high levels within cultured cells. It could not be observed when full-length Fat was expressed, and it has not been observed *in vivo*. Because *fat* can

affect Ex staining in discs (Figure 3)[175-177], it is plausible that high-level expression of the Fat intracellular domain might influence Ex in cultured cells and thereby influence Hippo signaling. However, the relevance of this mechanism to normal Fat and Hippo signaling *in vivo* remains to be determined. By contrast, an influence of *fat* on Wts protein levels has been reported *in vivo* using simple loss-of-function mutations for *fat* and examining endogenous Wts protein[11]. Moreover, the observation that genetically *fat* can act independent of *ex* clearly supports the conclusion that effects of Fat that are independent of Ex, such as its influence on Wts levels, are important.

What then is the functional significance of the influence of Fat on Ex? One possibility is that Fat signals both through an effect on Wts levels (independent of Ex) and through an effect on Wts activity (via Ex). A dual pathway mechanism like this could ensure a robust response to Fat signaling. Resolving whether Fat normally signals through Ex will require reagents for monitoring Wts activity *in vivo*, which do not yet exist. This dual pathway hypothesis also raises the interesting possibility that the respective contributions of these pathways to Fat signaling could vary in different developmental contexts.

An alternative explanation for the effect of Fat on Ex is suggested by the realization that the discernible effect of *fat* on Ex protein staining underestimates the actual effect, because *ex* transcription is up-regulated within *fat* mutant clones[11,175,176]. Mutations in components of the Hippo pathway (e.g., *wts*) elevate both *ex* mRNA levels and Ex protein staining[113]. These observations suggest that a negative influence of Fat signaling on Ex protein accumulation might act as a homeostatic mechanism, maintaining low amounts of Ex at the subapical membrane despite increases in *ex* mRNA. This could, for

example, facilitate the continued regulation of Hippo signaling through Ex independent of Fat.

The Fat–Hpo signaling network.

Currently we can describe at least three signal transduction processes downstream of Fat: an influence on Wts levels, an influence on Ex levels, and an influence on PCP (Figure 5). The influence of Fat on PCP is separable from its influences on transcription, because overexpression of Wts only partially rescues *fat* PCP phenotypes (Figure 5) and mutation of *dachs* only partially suppresses *fat* PCP phenotypes[10]. However, the persistence of a some PCP phenotype in *fat dachs* double mutants, together with the polarized distribution of Dachs protein[10], raises the possibility that Dachs, along with Atrophin[69], might have an input into PCP (Figure 5).

Although we have found that the influence of Fat on both Wts and Ex requires Dachs, these processes are distinct because *wts* mutation does not decrease Ex levels[113,175,176] and *ex* does not influence Wts levels[11]. Instead, our results imply that two parallel pathways converge on a common target, Wts, but regulate it in distinct ways, with Hippo signaling influencing Wts activity[22,202] and Fat signaling influencing Wts levels[11] (Figure 5). Although our results show that these pathways can act in parallel, it is clear that they intersect at multiple points, forming what might be better described as a Fat–Hippo signaling network (Figure 5). Points of intersection include regulation of Wts, regulation of Ex, and transcriptional feedback regulation of network components including *four-jointed* and *ex*. A fuller understanding of the relationship between these pathways awaits the identification of additional regulatory inputs into Ex and Mer activity and of reagents to monitor Wts and Yorkie activity *in vivo*.

Because Wts rescued *fat* mutants show weaker PCP phenotypes (Figure 1*I*, *L*) than *fat* mutants[10,71], there appears a transcriptional input into PCP determination, which is probably permissive due to the assumption that uniform overexpression of Wts keeps Yki equally active along proximal-distal axis. Instead, the PCP pathway of Fat may be instructive for PCP formation, because of the observation that overexpression of Fat-ICD[71] and Wts (Figure 1*I*, *L*) only partially restored PCP phenotype in *fat* mutants.

Figures

Figure 1. Rescue of *fat* and *expanded* by Warts overexpression.

Null mutations in *fat* or *ex* are lethal but can be rescued to viability by overexpression of Wts. (*A–C*) Adult flies of wild type (*A*), *fat^{8} UAS-Myc:Wts.2/$ft^{G\text{-}rv}$*; *tub-Gal4* (*B*), and *ex^{e1} UAS-Myc:Wts.2/ex^{e1}*; *tub-Gal4* (*C*). (*D–G*) Adult wings from wild type (*D*), *UAS-Myc:Wts.2/tub-Gal4* (*E*), *fat^{8} UAS-Myc:Wts.2/$ft^{G\text{-}rv}$*; *tub-Gal4* (*F*), and *ex^{e1} UAS-Myc:Wts.2/ex^{e1}*; *tub-Gal4* (*G*). The arrows point to extra vein material. (*H–J*) Portion of abdomens from wild type (*H*), *fat^{8} UAS-Myc:Wts.2/$ft^{G\text{-}rv}$*; *tub-Gal4* (*I*), and *ex^{e1} UAS-Myc:Wts.2/ex^{e1}*; *tub-Gal4* (*J*). In *H* and *J* all hairs and bristles point posteriorly (down); in *I* bristles and hairs are misoriented and swirling patterns of hairs are visible. *(K-M*) Close-up images of wings from wild type (*K*), *fat^{8} UAS-Myc:Wts.2/$ft^{G\text{-}rv}$ tub-Gal4* (*L*), and *ex^{e1} UAS-Myc:Wts.2/tub-Gal4* (*M*). In *K* and *M* hairs and bristles point distally (right), and in *L* some hairs in the proximal wing are misoriented. This is most evident between the first and second wing veins (arrows).

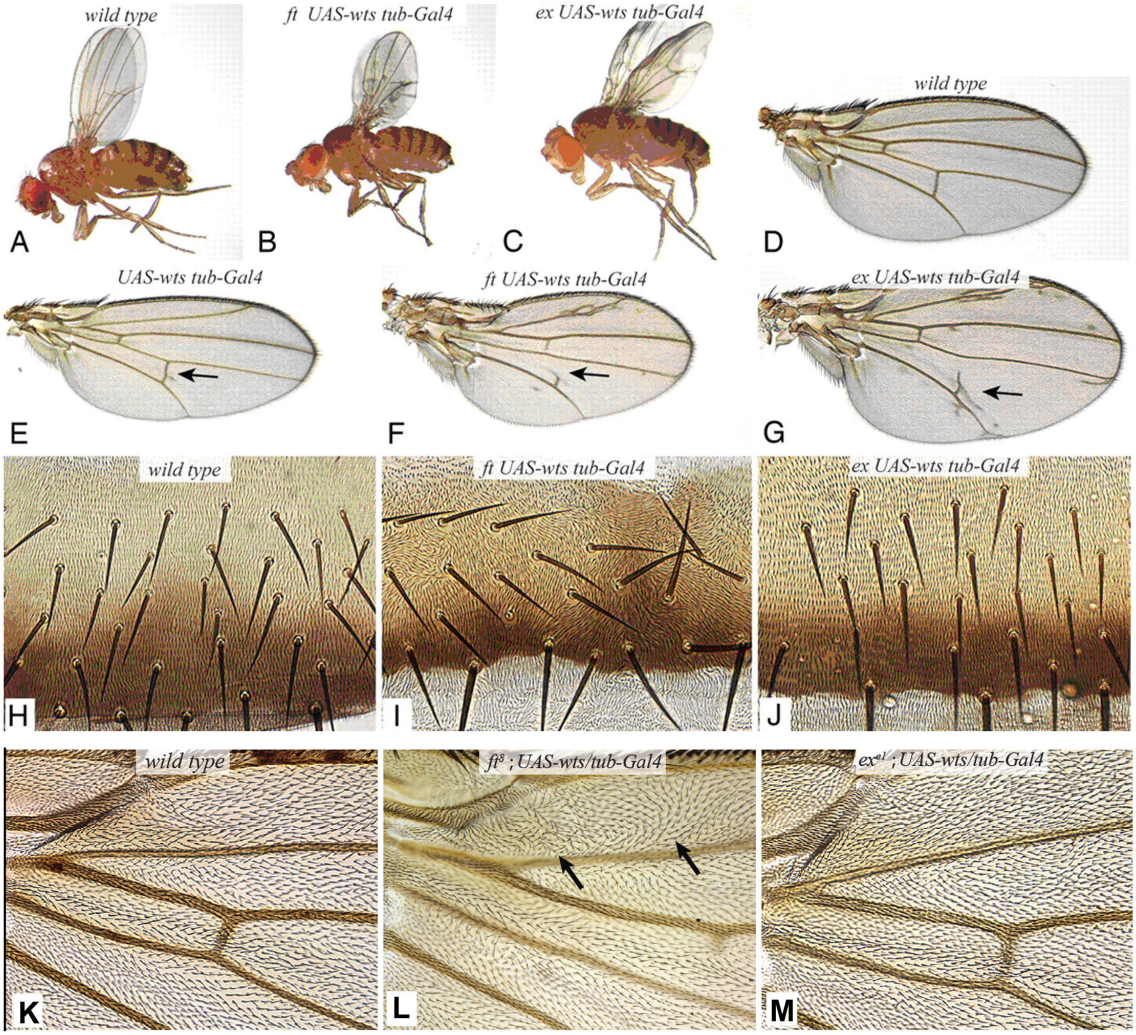
wild type
ft UAS-wts tub-Gal4
ex UAS-wts tub-Gal4
wild type
A
B
C
D
UAS-wts tub-Gal4
ft UAS-wts tub-Gal4
ex UAS-wts tub-Gal4
E
F
G
wild type
ft UAS-wts tub-Gal4
ex UAS-wts tub-Gal4
H
I
J
wild type
ft[8] ; UAS-wts/tub-Gal4
ex[e1] ; UAS-wts/tub-Gal4
K
L
M

Figure 1

Figure 2. *fat* and *expanded* have additive effects on growth and eye development.

(*A* and *B*) The average sizes (in arbitrary units) of GFP-expressing clones of the indicated genotypes were measured. Error bars show SEM. For wild-type (+), *n* (number of clones measured) = 166 for wings and 95 for eyes; for ex^{e1} *n* = 132 for wings and 154 for eyes; for ft^{8} *n* = 114 for wings and 152 for eyes; for $ft^{G\text{-}rv}$ *n* = 133 for wings and 133 for eyes; for ex^{e1} ft^{8} *n* = 46 for wings and 70 for eyes; for ex^{e1} $ft^{G\text{-}rv}$ *n* = 184 for wings and 169 for eyes. The increased size of *ex fat* double mutant clones compared with single mutant clones is significant in all cases ($P < 0.01$). (*C–E*) Representative wing imaginal discs of the indicated genotypes are shown from larvae dissected 7 days after egg laying. (*F–I*) Eye imaginal discs of the indicated genotypes from wandering third-instar larvae stained for ELAV. Arrows point to posterior regions of the eye disk that lack ELAV staining in mutants. All discs are shown at the same magnification. (*J-M*) Eye discs carrying MARCM clones of ex^{e1} (*J*), ft^{8} (*K*), $ft^{G\text{-}rv}$ (*L*), ex^{e1} $ft^{G\text{-}rv}$ (*M*) were stained for ELAV..

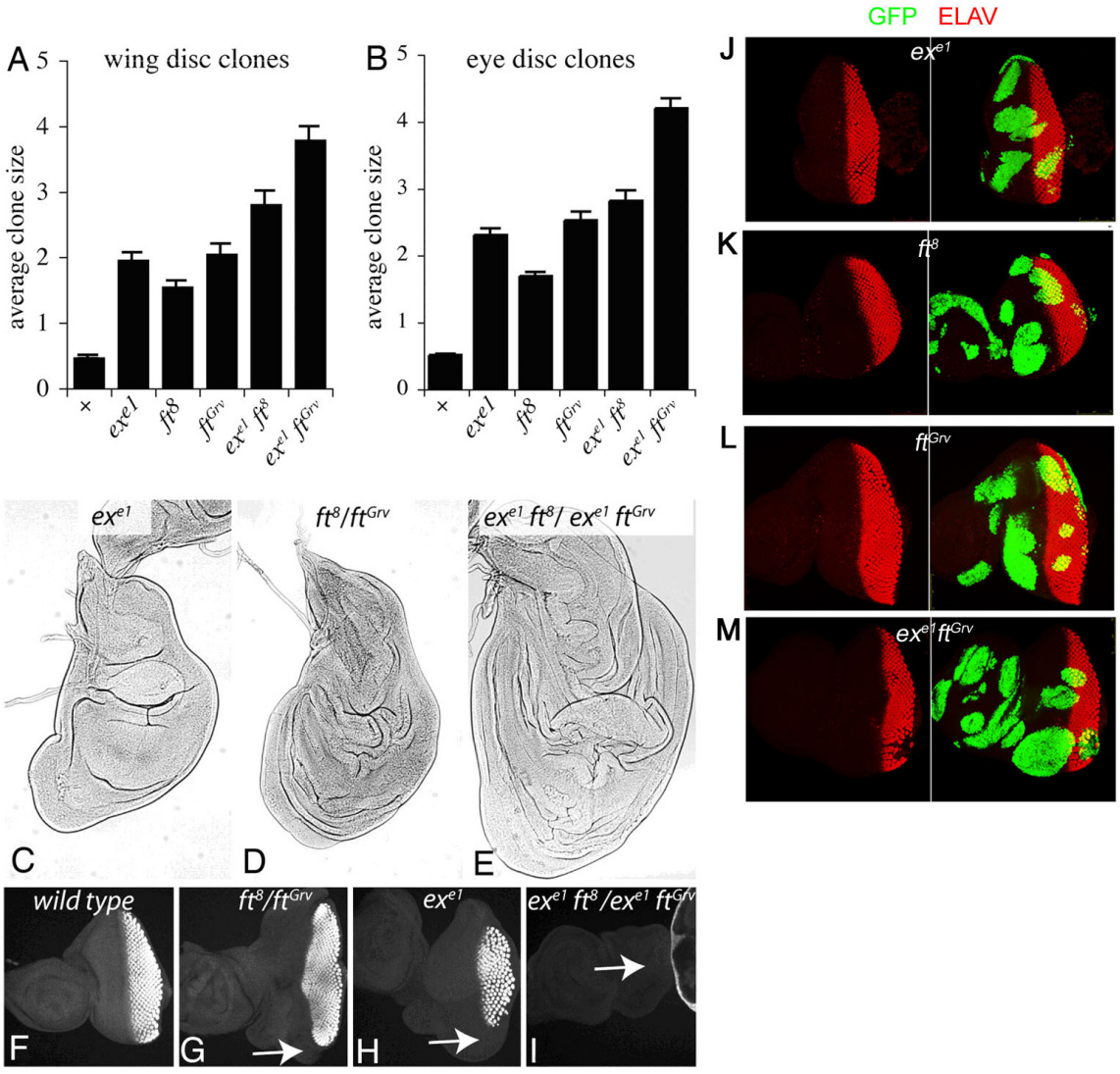
A
wing disc clones
average clone size
0
1
2
3
4
5
×
exe1
ft8
ftGrv
exe1 ft8
exe1 ftGrv
B
eye disc clones
average clone size
C
exe1
D
ft8/ftGrv
E
exe1 ft8/ exe1 ftGrv
F
wild type
G
ft8/ftGrv
H
exe1
I
exe1 ft8/exe1 ftGrv
GFP ELAV
J
exe1
K
ft8
L
ftGrv
M
exe1 ftGrv

Figure 2

Figure 3. Influence of Fat signaling on Expanded.

Shown are wing imaginal discs stained for Expanded (red) and E-cadherin (green). (*A* and *C*) Projections through horizontal sections. (*B* and *D*) Vertical sections. *A′–D′* and *A″–D″* show individual channels of the image. Mutant clones (outlined by dashes) were marked by the absence of GFP (blue). GFP staining does not overlap Expanded and E-cadherin and is shown from more basal focal planes in the horizontal images. Endogenous Expanded staining is lower along the dorsal–ventral boundary (D-V, yellow arrows) and anterior–posterior boundary (A-P, green arrows). (*A* and *B*) fat^{8} mutant clones. Ex staining is decreased. E-cadherin staining sometimes appears increased (20). (*C* and *D*) d^{GC13} fat^{8} mutant clones. No consistent difference in Ex staining between wild-type and mutant tissue was observed. (*E* and *F*) dco^{3} mutant clones. Expanded staining is sometimes decreased, but the effect is less evident than for *fat*.

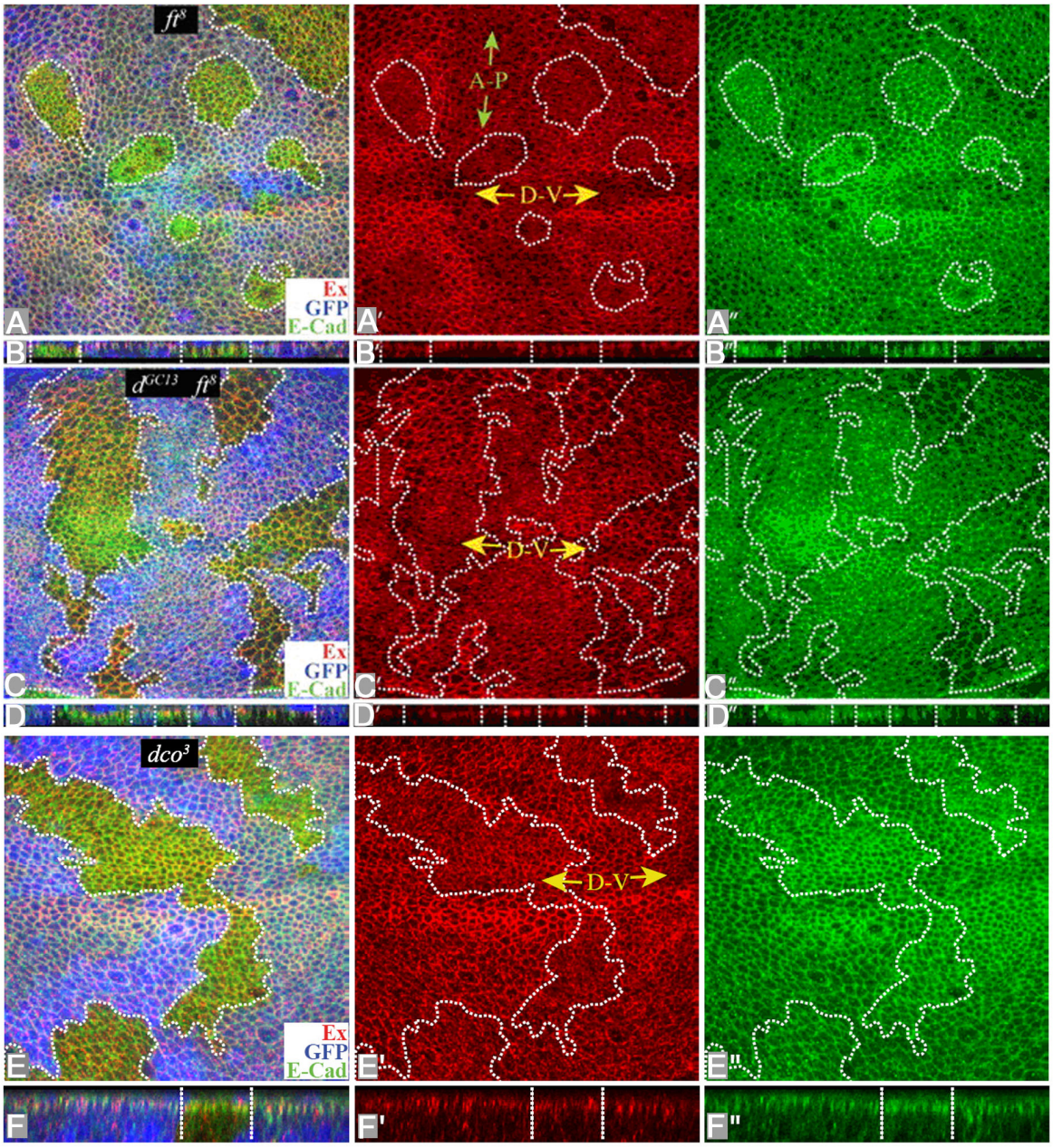
ft8
A-P
D-V
Ex
GFP
E-Cad
A
A′
A″
B
B′
B″
dGC13 ft8
D-V
Ex
GFP
E-Cad
C
C′
C″
D
D′
D″
dco3
D-V
Ex
GFP
E-Cad
E
E′
E″
F
F′
F″

Figure 3

Figure 4. Fat signals even when Expanded is overexpressed.

(*A* and *B*) Portions of wing imaginal discs stained for Expanded (red) and E-cadherin (green). *A* shows horizontal sections, and *B* shows vertical sections. MARCM clones mutant for fat^{8} and overexpressing Expanded were marked by the presence of GFP (blue). Expanded staining was captured with intensity settings different from those in Fig. 3 to illustrate the difference in expression levels between endogenous Expanded (barely visible) and ectopic Expanded (bright red); the localization of ectopic Expanded appears normal. (*C* and *D*) The average sizes of GFP-expressing clones of the indicated genotypes. Error bars show SEM. For wild-type, n = 166 for wings and 95 for eyes; for fat^{8} n = 114 for wings and 152 for eyes; for *UAS-expanded* n = 61 for wings and 82 for eyes; for ft^{8} *UAS-expanded* n = 68 for wings and 102 for eyes. (*E* and *F*) Wing imaginal discs stained for WG (magenta) and containing clones (arrows, marked by GFP, green) mutant for fat^{8} (*E*) or mutant for fat^{8} and overexpressing Ex (*F*).

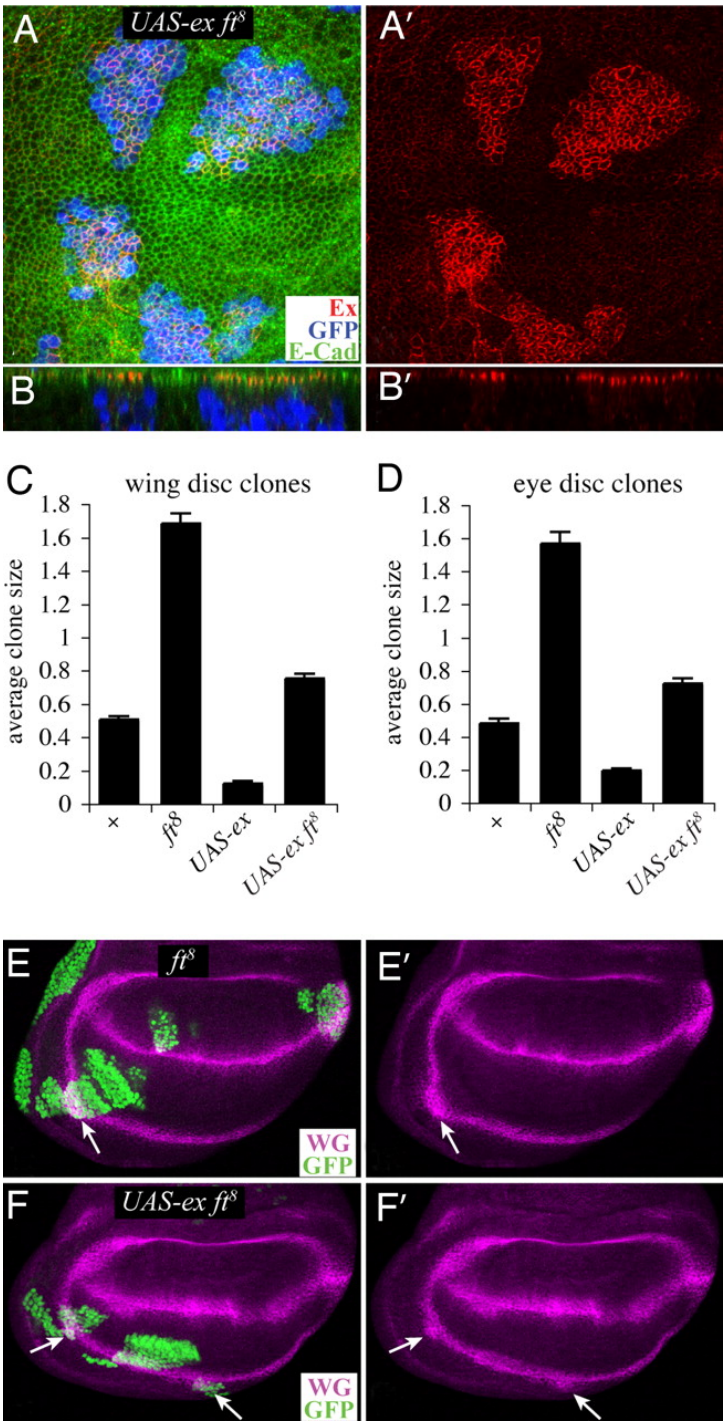
A
UAS-ex ft8
Ex
GFP
E-Cad
A′
B
B′
C
wing disc clones
average clone size
1.8
1.6
1.4
1.2
1
0.8
0.6
0.4
0.2
0
+
ft8
UAS-ex
UAS-ex ft8
D
eye disc clones
average clone size
1.8
1.6
1.4
1.2
1
0.8
0.6
0.4
0.2
0
+
ft8
UAS-ex
UAS-ex ft8
E
ft8
WG
GFP
E′
F
UAS-ex ft8
WG
GFP
F′

Figure 4

Figure 5. Schematic model of the Fat-Hippo signaling network.

Different branches are color-coded. Red identifies components assigned to the Fat tumor suppressor signaling pathway, blue identifies components assigned to the Hippo signaling pathway, and purple identifies components that function in both pathways to affect transcription (see text for details). Fat and Hippo signaling regulate transcription, and a number of downstream target genes have been identified. Fat signaling also influences PCP through transcriptional dependent (black) and independent pathways (green). Conformation of Wts may be regulated by certain transcriptional targets (yellow arrow).

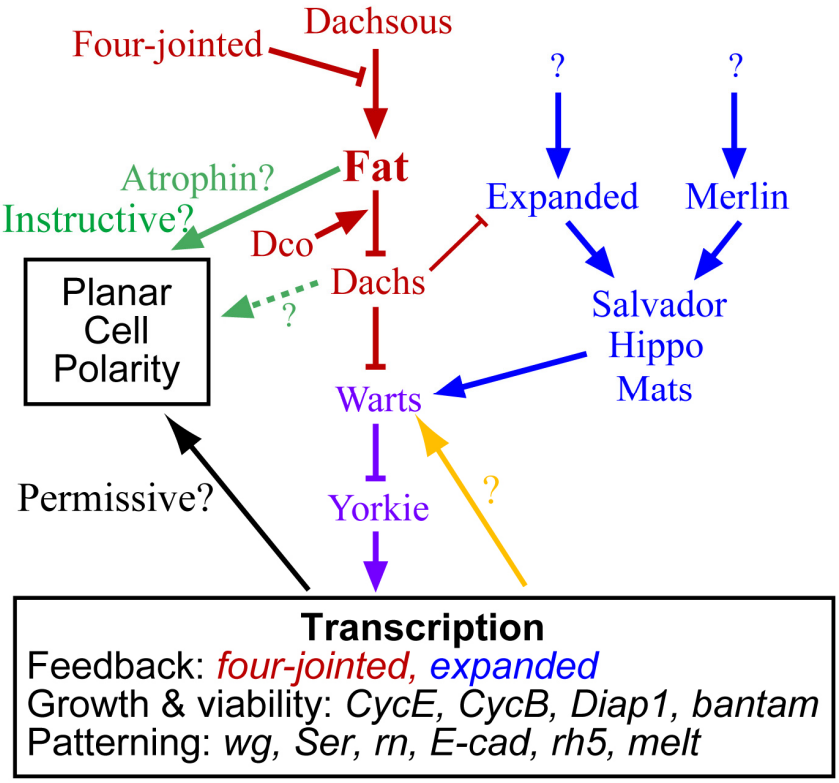

Figure 5

CHAPTER IV

Processing and Phosphorylation of the Fat receptor

Yongqiang Feng and Kenneth D. Irvine

Most of this chapter was re-submitted to *PNAS.*

Summary

The *Drosophila* tumor suppressors *fat* and *discs overgrown* (*dco*) function within an intercellular signaling pathway that controls growth and polarity. *fat* encodes a transmembrane receptor, but post-translational regulation of Fat has not been described. We found that Fat is subject to a constitutive proteolytic processing, such that most or all cell surface Fat comprises a heterodimer of stably associated N- and C-terminal fragments. The cytoplasmic domain of Fat is phosphorylated, and this phosphorylation is promoted by the Fat ligand Dachsous. *dco* encodes a kinase that influences Fat signaling, and Dco is able to promote the phosphorylation of the Fat intracellular domain in cultured cells and in vivo. Three amino acid residues in the Fat intracellular domain required for Dco phosphorylation and mobility shift were identified. Mutation of these three Sers in *fat* genomic rescue construct removes most of the mobility shift in wing discs, but does not lose any activity in rescuing *fat* mutant, suggesting the Dco dependent mobility shift of Fat intracellular domain is not essential for Fat function. Evaluation of *dco* mutants indicates that they affect Fat's influence on growth and gene expression, but not its influence on planar cell polarity. Our observations identify processing and phosphorylation as post-translational modifications of Fat, correlate the phosphorylation of Fat with its activation by Dachsous in the Fat-Warts pathway, and enhance our understanding of the requirement for Dco in Fat signaling.

Introduction

Studies in *Drosophila* have identified several genes that function to regulate the growth of developing tissues, and linked them into two interconnected signaling pathways, the Fat and Warts/Hippo pathways[25]. Homologues of these genes exist in mammals, and they have been implicated in growth control and tumorigenesis in a wide range of organs (Chapter I, Table 1). Fat is an atypical cadherin that acts as a receptor for intercellular signaling pathways that influence gene expression and planar cell polarity (PCP)[25]. Wts is made in an inactive form, and upstream components of the Wts/Hpo pathway activate Wts.

Fat acts in parallel to this Hpo-dependent regulation of Wts activity, influencing the levels of Wts protein through the unconventional myosin Dachs, but may also act through Hpo signaling via an effect on Expanded to influence Wts activation. Activated Wts phosphorylates and thereby inactivates a transcriptional co-activator protein, Yorkie. When upstream tumor suppressors are mutant, expression of downstream genes that promote growth and inhibit apoptosis becomes elevated. Fat influences PCP via a distinct pathway or process[25]. The separation of Fat PCP and tumor suppressor pathways is illustrated most clearly by the observation that the overgrowth phenotype of *fat* mutants, but not the PCP phenotypes, can be rescued by Wts over-expression[12]. Since Fat itself, and upstream regulators of Fat (Ds, Fj) influence both PCP and growth, distinct PCP and transcriptional pathways must branch at or below Fat.

discs overgrown (*dco*) encodes the *Drosophila* homologue of Casein Kinase I δ and ε (CKIδ/ε), and was identified as a *Drosophila* tumor suppressor based on the overgrowth phenotype of a particular recessive allele, dco^3 (ref. [93]). Dco also participates in other processes, including circadian rhythyms[209], apoptosis[97], Hedgehog signaling[210,211], and Wnt signaling[95,96]. *dco* was genetically linked to Fat signaling based on the observations that dco^3 mutant clones influence the expression of Fat pathway target genes, that the overgrowth and transcriptional phenotypes of dco^3 are suppressed by mutation of *dachs*, and that dco^3 influences Wts protein levels in imaginal discs[11]. These last two features of dco^3 are shared by *fat*, but not by components of the Hippo pathway, linking *dco* specifically to the Fat pathway, but the biochemical basis for this link is unknown.

Materials and Methods

Histology and imaging

Imaginal discs were fixed and stained as described previously[9], using mouse anti-Wg (1:800, 4D4, Developmental Studies Hybridoma Bank (DSHB)), rat anti-DE-Cadherin (1:40, DCAD2, DSHB), rabbit anti-Gal4 (1:400, pre-absorbed, Santa Cruz Biotechnology), mouse anti-Myc (9E10, 1:800, Babco), mouse anti-V5 (1:400 preabsorbed, Invitrogen) and rat anti-Fat (1:1600). Fluorescent stains were captured on a Leica TCS SP5 confocal microscope. For horizontal sections, maximum projection through multiple sections was employed to allow visualization of staining in different focal planes.

For adult tissues, combineZM software was used to allow visualization of features in different focal planes within a single image.

Western blotting

Western blotting was performed as described previously[11], using rabbit anti-Wts (1:5000, pre-absorbed), rabbit anti GFP (1:1000, Invitrogen), rat anti-Fat-ICD (1:25,000, pre-absorbed), guinea pig anti-Period (1:10,000, I. Edery), rat anti-Ds-ICD (1:3000, Simon), rat anti-Fj (1:3000, Strutt), mouse anti-Actin JLA20 (1:15000, Calbiochem), mouse anti-V5-HRP (1:40000, Invitrogen), goat anti-mouse-HRP (10ng/ml, Pierce), goat anti-rabbit-HRP (10ng/ml, Pierce), donkey anti-rat-HRP (1:40000, Jackson Immunology), donkey anti-guinea pig-HRP (1:40000, Jackson Immunology). All protein samples were resolved by electrophoresis through 4-15% gradient SDS polyacrylamide gel (BioRad). Chemiluminescent detection was performed with SuperSignal West Femto maximum

Sensitivity Substrate (Pierce), and blots stripped by Restore Western Blot Stripping Buffer (Pierce) between antibody blotting. Fluorescent detection was performed on a LiCor Odyssey, using goat anti-mouse IRdye680 (1:10,000, LiCor) and sheep anti-rat IRdye800 (1:10,000, Rockland) secondary antibodies.

For line scanning, blots were scanned and digitized. Ten vertical lines were drawn through each lane, and the intensity values at every pixel were calculated using NIH Image J. The average intensity values were then plotted versus position using Microsoft Excel.

IP experiment (including live IP):

Antibody coupled beads (anti-FLAG gel from Sigma) were mixed with cell lysate and incubate for 4 hours at 4°C. The beads were then spinned down and washed with RIPA buffer for 6 times. SDS-PAGE loading buffer was added and heated at 100°C for 10 minutes before electrophoresis[11]. To pull down extracellular domain of Fat protein, *pUAST-V5:ft* construct was transfected into S2 cells. 36 hours after transfection, cells were collected by centrifugation and washed with cold PBS twice. Then cells were resuspended with PBS plus 2% BSA and incubated at 4°C with anti V5 antibody (Invitrogen) for 30 minutes. Then cells were collected and washed with cold PBS twice before lyse with complete RIPA buffer. The lysate was clarified by centrifugation and the supernatant was incubated with protein G agarose (Amersham Pharmacia) at 4°C for 4 hours. The agarose was then washed with RIPA according to normal IP protocol.

Cell culture and transfection

Culturing, transfection and lysis of *Drosophila* S2 cells was performed as described previously[11]. pUAS-ft:FVH or pUAST-V5:fat, constructs were co-transfected into S2

cells with pAct-Gal4, pMT-dco:V5, pMT-dco3:V5 or vector control. Dco:V5 and Dco^3:V5 were induced with Cu2+ for 36 hours. pAct-Per was co-transfected into S2 cells with pMT-dco or pMT-dco^3.

In vitro kinase assay:

Fat intracellular domain, including wild type and mutants, were expressed in S2 cells and then pulled down by anti-FLAG-beads (Sigma). Protein was eluted with FLAG peptide (Sigma) and concentrated with Microcon YM30 (Millipore). 200μM ATP was used as the final concentration in the reaction of Fat-ICD and CKI according the manufacture's protocol (New England Biolabs). The reaction was stopped 1 hour after incubating at 30°C by adding SDS loading buffer and heating at 100 °C for 10 minutes.

Phosphatase treatment:

Calf intestinal phosphatase (CIP) treatment of phosphorylated Fat-ICD from cell cultures: Fat-ICD and Dco were co-expressed in S2 cells and pulled down by FLAG beads. CIP treatment was performed on beads by incubating at 37°C for 1 hour in NEBuffer 3. SDS-loading buffer was added and heated at 100 °C for 10 minutes before electrophoresis. For CIP treatment of wing disc extracts, the lysate was mixed with SDS loading buffer and incubated at 100°C for 5 minutes. After cooled down, the mixture was desalted and the buffer was changed to weak detergent buffer (10mM HEPES pH7.5, 100mM KCl, 1mM EDTA, 10% Glycerol, 0.1% Triton X-100, 5mM DTT) by ultrafiltrating through Microcon YM30 (Millipore). CIP treatment was performed in NEBuffer 3 by incubating at 37°C for 1 hour. SDS-loading buffered was added and heated before electrophoresis (New England Biolabs).

Mutagenesis:

Mutagenesis was conducted with QuikChange Multi Site-Directed Mutagenesis Kit (Stratagene). All constructs were confirmed by sequencing.

Anti *Drosophila* Fat antisera:

GST fusion protein of Fat intracellular domain was expressed in *E. coli* and isolated to immunize rat by Cocalico Biologicals according to Helen McNeill[175]. GST-Fat-intracellular domain fusion construct (from Helen McNeill) was transformed into E. coli BL21 DE3 cells and induced with IPTG. Bacteria were then collected and lysed by sonication in buffer 20mM Tris-HCl pH8.0 supplemented with 1mM EDTA and protease inhibitor cocktail (Roche). Inclusion body was separated from soluble part by centrifugation and resuspended with 20mM Tris-HCl pH8.0 plus 0.5% triton X-100. After centrifugation, the pellet was washed with PBS and used for immunization. After preabsorbed with embryos, 1:1600 dilution was used for tissue staining and 1:25,000 used for western blotting.

Fly stocks:

yw; ft^{8} FRT40A/CyO-GFP, yw; ft^{Grv} FRT40A/CyO-GFP, yw; FRT82B dco^{3} /TM6b, yw; FRT42D, fj^{d1}/CyO, yw; ds^{36D} FRT40A/L14, yw; Df(2L)ED94/CyoGFP, yw; Df(2L)ED94 fj^{d1}/CyoGFP, yw; ds^{36D} fj^{d1}/CyOGFP, yw; tub-Gal4/CyOGFP (flip-out of yw; tub>CD2>Gal4/CyO), yw; tub-Gal4[LL7]/TM6b,

yw; UAS-Myc:Wts.2/CyO, yw; UAS-Myc:Wts.1/TM6b, yw hs-FLP tub-Gal4 UAS-GFP; UAS-y+/CyO; FRT82B tub-Gal80, yw; ft^{8} FRT40A UAS-ft(II)/L14 (yw; UAS-ft(II) from Blair*), yw; UAS-d:V5[50.5]/CyoGFP; FRT82B dco^{3} /TM6b, yw; UAS-d:V5[50.5]/CyoGFP; FRT82B/TM6b, yw; UAS-fj[6a.2]/CyoGFP, yw; UAS-fj[146.3]/TM6b, yw; GS-ds/CyOGFP, yw; UAS-ds[III]/TM6b, yw; UAS-fj[146.3] UAS-*

ds[III]/TM6b, yw; GS-ds/CyOGFP; FRT82B dco^3 /TM6b, yw; UAS-dcoKD/CyO; MKRS/TM2 (kinase domain, Jiang)*, yw; UAS-CKIαKD/CyO; MKRS/TM2* (kinase domain, Jiang)*, yw; UAS-dcoKD/CyOGFP; FRT82B dco^3 /TM6b, yw; UAS-CKIαKD/CyOGFP; FRT82B dco^3 /TM6b, yw; en-Gal4 UAS-GFP[T-2]/CyO, yw; ptc-gal4 UAS-GFP, yw; ft^{Grv} en-Gal4/Cyo, yw; tub-Gal4/CyoGFP; FRT82B dco^3 /TM6b, yw; tub-Gal4[LL7] dco^3/TM6b yw; ; UAS-Myc:Wts.2/CyOGFP; FRT82B dco^3 /TM6b, yw; UAS-dbt/CyO, yw; Sp/CyO; UAS-dbt7.2Flag* (Jiang)*, yw; tub-Gal80^{ts}/CyOGFP; tub-Gal4 UAS-dcr2/TM6b* (Kucuk).

Plasmids and constructs:

pAW-Gal4[67], *pAct-GFP:V5:His*[11], *pMT-dco:V5:His*[212], *pMT-dco^{AR}:V5:his*[212], *pAct-Per*[212], *pMK-CKIα:HA*[213], *pMK-CKIα:HA* kinase negative[213], *pUAS-ft*[67].

pMT-dco^3:V5:His: Primers dbt-R4C (5'-GGA ATT C (EcoRI) AC CAT GGA GCT GTG CGT GGG TAA CAA ATA TCG-3') and dbt-E74K (5'-CAT AAT CTG GTG CGG CAG CAA GGG CGA CTA CAA TGT GAT G-3') were used to change R4C and E74K on *pMT-dco:V5:His* by site directed mutagenesis with QuikChange Multi Site-Directed Mutagenesis Kit (Stratagene). The result was confirmed by sequencing the whole insert.

pUAS-dco^3:V5:His: To clone *dco^3* into *pUAST*, *dco^3* was amplified by PCR with primer dbt-R4C (above) and V5-His-XhoI-3 (5'-AAC TCG AG (XhoI) T CAA TGG TGA TGG TGA TGA TGA CCG GTA CG-3'), restricted by EcoRI and XhoI and ligated to the same digested pUAST. The insert was confirmed by sequencing. Transgenic flies were generated by standard protocols.

pMT-dco:HA: To make dco:HA, wilt type dco was amplified with primers dcoF_EcoRI (5'-G GAATTC AAC ATG GAG CTG CGC GTG GGT AAC AAA-3') and

dcoR_HA_XhoI (5'-AA *CTCGAG* tcactatcctgcatagtccgggacgtcatagggatagcccgcTTT GGC GTT CCC CAC GCC ACC GCC-3'), restricted by EcoRI and XhoI and ligated to the same digested pMT-WB (Aiguo Xu). The insert was confirmed by sequencing.

pUAS-ft:GFP: The stop codon of ft on *pUAS-ft* was first removed by replacing the 4.5kb region at the 3' end with the PCR product amplified by primer ft-Bsu-5 (5'-GAC CCA CAT TCA CAC CTG AGG GTC-3') and UAS-ft-MT-R (5'-GAT CCT CTA GAG GTA CCT CCC ACG TAC TCC TCT GGA GC-3') through restriction sites Bsu36I and KpnI. GFP coding region was flanked by KpnI site at both ends by PCR amplification of GFP gene with primer KpnI_EGFP_5 (5'-AAG GTA CC(KpnI) A TGG TGA GCA AGG GCG AGG AGC-3') and KpnI_EGFP_3 (5'-AAG GTA CC(KpnI) T TAC TTG TAC AGC TCG TCC ATG CCG AG-3') and then digested with KpnI and ligated to restricted pUAS-ft (codon removed). The correct construct was confirmed by sequencing. Transgenic flies were generated by standard protocols.

pUAS-ft:FVH (stands for FLAG:V5:His tandem tags): FLAG:V5:His tandem tags was flanked by KpnI sites at both ends by PCR amplification of pAC5.1/V5 His-A (Invitrogen) with primer KpnI_FlagV5His_5 (5'-AAG GTA CC(KpnI) ***G^{214} ACT ACA AGG ACG ACG ACG ACA AGG GT*** (***FLAG***) A AGC CTA TCC CTA ACC C-3') and KpnI_FlagV5His_3 (5'-AAG GTA CC(KpnI) C CTT AGA AGG CAC AGT CGA GGC-3') and then digested with KpnI and ligated to restricted pUAS-ft (codon removed).

Genomic rescue construct of V5:ft and pUAST-V5:ft:

Bacterial artificial chromosome clone BACR11D14 was purchased from BACPAC Resources Center (http://bacpac.chori.org/). To introduce V5 tag after the signal peptide, recombineering technology was employed (http://recombineering.ncifcrf.gov/). Briefly,

galK gene was inserted after fat signal peptide coding sequence by amplifying galK with primers galK_fatsignal_F (5'-cgt ggc cga agt tac gcc acc acc tat gaa caa tat gcc gcc ttt ccg cga aga aga agc CCT GTT GAC AAT TAA TCA TCG GCA-3') and galK_fatsignal_R (5'-gaa atc ggc act ggt gtc cac cgc acg gga ttg cat ctc acc cga tgg cga gga tga tga TCA GCA CTG TCC TGC TCC TT-3') (red letters for amplification of galK gene). After positive selection the galK gene was replaced with V5 tag donor (5'GGT AAG CCT ATC CCT AAC CCT CTC CTC GGT CTC GAT TCT ACG CGT ACC GGT-3') via recombination and a negative selection for galK minus. V5 donor was made by PCR with primers, Ft357up_F (5'-cgctttagcgcctcatatttcaccg-3'), FtslV5_R (5'- gcg tag aat cga gac cga gga gag ggt tag gga tag gct tac cgc ttc ttc ttc gcg gaa agg cgg ca-3'), FtV5cad_F (5'-cct ctc ctc ggt ctc gat tct acg cgt acc ggt tca tca tcc tcg cca tcg ggt gag a-3') and Ft718_R (5'-ctagatgcagatacgaggtgtctccac-3').

To make the genomic rescue construct of V5:ft, genomic region between and including Rpl40 and CG3714 was subcloned by recombination into attB-P[acman]-ApR[180]. Primers used for making subcloning donor include Rpl40LA_F (5'-aaa ggcgcgcc ctcggagaggccaactaattgcag-3'), Rpl40LA_R (5'- cct ggatcc ccttggaggtggagccttctgacacc-3'), CG3714RA_F (5'- agg ggatcc aggtgggtgtaatcatttgatttggc-3') and CG3714RA_R (5'-acc ttaattaa caacacttaagtactagaaaaatattaaagacata-3').

Primer for cloning galK into phosphorylation regions of Fat ICD: Forward: galK_phosFat_F: 5'-gag ttc cca gca gcc gcg cat tct cac ttt gca cga cat ttc cgg aaa gcc gct gca aag CCT GTT GAC AAT TAA TCA TCG GCA-3'. Reverser: galK_phosFat_R:5'-ggc ggt caa gcc catg gaa gtt tgc tgc gcc tgc tgc tgt ggc act ccg ggc ttt tgc ctT CAG CAC TGT CCT GCT CCT T-3'.

To make the *pUAST-V5:ft* construct, the V5:fat genomic region was cubcloned into attB-P[acman]-ApR and restriction sites NotI and KpnI were introduced into 5' end and 3' end respectively. Primers used to make the subcloning donor are ftex1_LA_Nt_As_F (aaa ggc gcg ccg cgg ccg cat gga gag gct act gct cct gtt ttt cc), ftex1_LA_Bm_R (ctc gga tcc att tcc agc cac gat ctc ata ctg), ftex8_RA_Bm_F (aat gga tcc gag gcg cct cga gtg tcg agc agc g) and ftex8_RA_Kp_Pc_R (acc tta att aag gta ccc aac ata tat tac acg tac tcc tct gg). V5:fat was then released with NotI and KpnI and ligated into *pUAST-attB*[179].

The constructs were verified by restriction fingerprinting and sequencing. Transgenic flies was generated via ϕC31 mediated transgenesis into attP2 (68A4)[179,180,215,216].

Information of pUAS-ft intracellular domain truncates and point mutations are available upon request.

Results

Proteolytic processing of Fat

Activation of transmembrane receptors often involves post-translational modifications, such as phosphorylation or cleavage. To investigate potential modifications, Fat was examined by Western blotting. In lysates of wing discs, an antisera raised against the Fat intracellular domain (anti-Fat ICD) detected a prominent band with a mobility of approximately 95 kd (Ft-95), and a faint band with a mobility corresponding to a much larger polypeptide (Ft-565)(Figure. 1*C*). *fat* is predicted to encode a 5147 amino acid protein, with a calculated mass of 565 kD. Thus, Ft-95 is too small to correspond to full length Fat. Nonetheless, examination of lysates from *fat* mutant discs confirmed that both Ft-95 and Ft-565 are *fat*-dependent (Figure 1*C*).

To investigate this apparent cleavage of Fat, a C-terminally tagged Fat protein (Fat:FVH) was created (Figure 1*A*). When Fat:FVH was transfected into cultured *Drosophila* S2 cells, a band with a high apparent molecular weight, consistent with full length Fat, was observed (Figure1*D*). However, most Fat was detected in lower molecular weight bands. One correlates with the 95 kd fragment of endogenous Fat (after accounting for the C-terminal tags), but the other appears smaller, around 70 kd (Ft-70)(Figure 1*D*). Although Ft-70 was not detected when endogenous Fat was examined in imaginal discs, it could be detected in discs when Fat:FVH was over-expressed from UAS transgenes (not shown). Expression of Fat:FVH under *tub-Gal4* control also confirmed that Fat:FVH is functional, as it rescued *fat* mutant animals. The detection of Ft-95 and Ft-70 with C-terminal epitope tags supports the conclusion that Fat is proteolytically processed. Based on their mobility, the cleavage leading to Ft-95 occurs in or near the two extracellular laminin G-

like domains, whereas the cleavage leading to Ft-70 occurs near the transmembrane domain (Figure 1*A*). A Fat construct that excludes the cadherin and EGF domains but includes most of the laminin G domain region (Fat-STI:FVH, Figure 1*A*) appears to be processed to the same cleavage products as is full length Fat, whereas a smaller Fat construct that also lacks the laminin G domains (Fat-STI-4:FVH) yields a single major band, suggesting that it is not processed (Figure 1*F*).

To further characterize Fat processing, an N-terminally tagged Fat (V5:Fat) was constructed (Figure 1*A*). Examination of V5:Fat by Western blotting lysates of S2 cells identified two bands of high apparent molecular weight, and did not detect Ft-70 or Ft-95 (Figure. 1*D*). Although the resolving power of the gel and the lack of suitable markers precluded precise determination of the size of these large bands, their mobility is consistent with the expected detection of both full length Fat (Ft-565) and an ~470 kd N-terminal product of proteolytic processing in the Laminin G domain region (Ft-470). Double staining V5:Fat with anti-Fat ICD and anti-V5 supported the conclusion that slowest mobility isoform is full length Fat, whereas Ft-470 lacks the Fat ICD (Figure 1*D*). To characterize cleavage of V5:Fat in vivo at endogenous expression levels, the V5 tag was incorporated into a fat^{+} genomic clone (Figure 1*B*), and then phiC31-mediated recombination was used to insert this into the *Drosophila* genome[180]. This genomic $V5{:}fat^{+}$ construct fully rescued *fat* mutants. Western blotting lysates of imaginal discs revealed that Ft-470 is more abundant than Ft-565 (Figure 1*E*). Because these proteins are similar in size, this differential detection is unlikely to be due to differences in blotting transfer efficiency. Hence, we conclude that the majority of Fat protein in vivo is processed.

To investigate the nature of Fat displayed on the cell surface, biochemical experiments were performed on cultured cells. S2 cells expressing V5:Fat were incubated with anti-V5 in the absence of detergent, and then cell surface Fat bound by anti-V5 antibodies was immunoprecipitated. As a control, we expressed Fat:FVH, which includes a cytoplasmic V5 tag that should not be accessible in intact cells. Western blotting of the immunoprecipitated material with anti-Fat ICD antibodies confirmed that cell surface V5:Fat is processed (Figure 1*G*). In addition, these experiments demonstrate that Ft-470 and Ft-95 remain stably associated after processing. By contrast, Ft-70 was not detected, indicating that it is not associated with Ft-470. Because co-immunoprecipitation of Ft-470 and Ft-95 could be observed under reducing conditions, the association between them does not require disulfide bonds.

Since Fat processing can occur in S2 cells, which do not express detectable levels of Ds and grow as isolated cells, and processing can occur on a truncated Fat polypeptide that lacks the cadherin and EGF domains (Fat-STI:FVH), it appears that Fat processing is part of its normal maturation, rather than a regulated event. In this regard, it appears analogous to the S1 cleavage that is involved in maturation of the Notch receptor[217], or to the apparent processing of the Starry night/Flamingo cadherin[218].

Ds-dependent phosphorylation of Fat

Under optimal conditions, Ft-95 from wing discs runs as doublet, with a prominent lower band, a weaker upper band, and a faint smear in between (Figure 2*A*). Treatment of lysates with calf intestinal alkaline phosphatase (CIP) resulted in a single sharp band around 95 kd, with a mobility similar to the fastest of the 95 kd mobility isoforms in untreated samples (Figure 2*B*). Thus, a fraction of Ft-95 in vivo is phosphorylated. Since

Ft-95 is too C-terminal to include the cadherin domains (Figure 1*A*), the phosphorylation detected presumably reflects a phosphorylation of the intracellular domain, rather than Fj-mediated phosphorylation of cadherin domains[83]. To investigate the relationship between Ft-95 phosphorylation and Fat signaling, Fat was examined in lysates of wing imaginal discs in which its putative ligand, *ds*, was either mutant or over-expressed. Proteolytic processing of Fat was not Ds-dependent, as Ft-95 was observed at similar levels in all cases. Mutation of *ds* results in enlarged wings and wing discs, and lower levels of Wts protein, a phenotype similar to, though weaker than, that of *fat* (Figure 2*A*, *G*)[71]. Western blotting of Fat from *ds* mutant wing discs revealed that levels of the faster mobility Ft-95 band are elevated, whereas the slower mobility band (Ft-95-P) is reduced (Figure 2*A*). Over-expression of Ds causes a reduction in wing size (Figure 2*K*)[87,219]. Strikingly, over-expression of Ds increased the relative amount of Ft-95-P (Figure 2*A*). These observations imply that the presence or absence of Ds modulates Fat phosphorylation. This was confirmed by the observation that phosphatase treatment of lysates from Ds-expressing discs collapsed the Ft-95 doublets into a single band (Figure 2*B*). The visual impression that the presence of the slower mobility (Ft-95-P) isoform(s) was promoted by Ds was confirmed by quantitative line scanning of Western blots (Figure 2*D*).

Both mutation of *fj* and *fj* over-expression are associated with modest reductions in wing and leg size (Figure 2*J*, *K*). Western blotting of disc lysates revealed that over-expression of *fj* was associated with an increase in the relative amount of phosphorylated Fat, and when co-expressed with *ds*, the increase in phosphorylated Fat appeared even greater, consistent with the reductions in wing size (Figure 2*A*, *L*). Mutation of *fj* had only subtle affects (Figure 2*A*, *H*).

Altogether, these observations identify a correlation between the presence of the Fat ligand Ds, the level of signaling through Fat to regulate Warts levels and wing growth, and the phosphorylation of the Fat cytoplasmic domain. Thus, they suggest that activation of Fat by its ligand Ds is associated with Fat phosphorylation. We can infer from the relative levels of different mobility isoforms that in the absence of Ds over-expression, a majority of Fat is in a hypophosphorylated form, whereas over-expression of Ds promotes the production of a hyperphosphorylated form. This identification of a post-translational modification of Fat that is promoted by Ds is consistent with the hypothesis that Fat and Ds act as receptor and ligand in a signal transduction pathway, and identifies a molecular process that appears correlated with Fat activation. Constructs that lack most of the extracellular domain, and presumably can't interact with Ds, can rescue *fat* mutants[71]. However, this rescue is only partial, and has only been observed when intracellular domain constructs are over-expressed. One possibility is that interaction with ligand triggers clustering of Fat, and that over-expression of the intracellular domain allows ligand-independent clustering. This would be analogous to other signaling pathways (e.g. TGF-ß, Receptor tyrosine kinase), in which ligand-mediated clustering promotes phosphorylation of the cytoplasmic domain of the receptor by bringing kinases and their substrates together, and for which the requirement for ligand can sometimes be bypassed by receptor over-expression.

Dco-mediated phosphorylation of the Fat intracellular domain.

In considering kinases that might contribute to the Ds-promoted phosphorylation of Fat, the CKIδ/ε family member Dco was a logical candidate. Genetic epistasis tests positioned *dco* within the Fat pathway, upstream of *dachs*[11]. At the same time, *dco*^{3} exerts cell-

autonomous affects on the expression of Fat target genes, which implies that it acts within receiving cells[11]. These observations suggested Dachs or Fat as potential substrates. Initial assessment of the ability of Dco to phosphorylate them was conducted by assaying for mobility shifts in S2 cells. Dco had no effect on Dachs (not shown). By contrast, when Dco was co-transfected together with Fat, a shift in the mobility of the C-terminal cleavage products was observed (Figure 3*A*). A Dco-dependent mobility shift was also observed for both the Fat-STI:FVH and Fat-STI-4:FVH constructs (Figure 3*D*). Confirmation that this mobility shift was due to phosphorylation of Fat was provided by the observation that it could be reversed by phosphatase (Figure 3*B*). Over-expression of Dco (not shown) or Dco kinase domain (Dco-KD)[210] under tub-Gal4 control could also increase phosphorylation of endogenous Fat in vivo (Figure 3*E*, *F*).

If phosphorylation of Fat by Dco were relevant to the participation of Dco in Fat signaling, then the dco^3 mutation, which causes loss of Fat signaling, should impair Fat phosphorylation. Sequencing of dco^3 identified two distinct amino acid substitutions[93]; these were introduced into a Dco:V5 expression construct. Dco^3:V5 resulted in much less shift in the mobility of Fat in S2 cells than did wild-type Dco:V5 (Figure 3). Thus, the same amino acid changes that cause overgrowth in vivo impair Dco-dependent phosphorylation of Fat in cultured cells. To investigate whether endogenous phosphorylation of Fat could also be influenced by mutation of *dco*, we examined the mobility of Fat in lysates from dco^3 mutant wing discs. Unphosphorylated Fat (Ft-95) appeared slightly elevated, and a distinct Ft-95-P band was no longer visible, but rather a faint smear was detected (Figures 2,3). This change in Fat mobility was confirmed by line scanning (Figure 2*E*). Thus, dco^3 reduces levels of phosphorylated Fat in vivo. Consistent

with this, overexpression of Dco-KD in *dco*^{3} mutant restored hyper-phosphorylated Ft-95 (Figure 3*E*, *F*) and rescued animals to viability (data not shown and Figure 3*G*).

To explore the relationship between the Ds-promoted phosphorylation of Fat, and the Dco-dependent phosphorylation of Fat, the mobility of Fat isolated from discs simultaneously over-expressing Ds and mutant for *dco*^{3} was examined. Direct examination of Western blots, as well as line scanning, revealed that Fat mobility in these lysates was similar to that in *dco*^{3} mutants (Figure 2*C*, *E*). Thus, Ds-mediated phosphorylation can be influenced by Dco. *dco*^{3} mutant clones have no obvious effect on Fat protein staining in wing imaginal discs (data not shown), suggesting that they do not affect its overall levels or distribution. Nor did *dco*^{3} noticeably affect processing of Fat.

The simplest explanation for Dco-promoted Fat phosphorylation in cultured cells, and for *dco*-dependent effects on Fat signaling and Fat phosphorylation in vivo, would be that Dco directly phosphorylates Fat. A purified mammalian homologue of Dco, CKIδ (ref. [220]), phosphorylated the Fat intracellular domain in vitro, but with reduced specificity, as even greater mobility shifts than those observed in vivo could be induced (data not shown). CKI's are Ser/Thr kinases, and the 538 aa Fat ICD includes 109 Ser or Thr residues. Three different kinase site prediction programs (see Methods) individually predict 7, 15, or 36 CKI sites, and cumulatively identify 46 potential CKI sites. The variation in predictions emphasizes the limited accuracy of kinase site prediction programs. We also note that distinct CKI sites could act redundantly, and that among the many potential CKI sites within the Fat ICD, phosphorylation sites responsible for the evident mobility shift on SDS-PAGE gels could be distinct from sites responsible for the influence of *ds* or *dco*^{3} on Fat activity. Thus, the identification of specific

phosphorylation sites within the Fat ICD that are required for its biological activity will ultimately be essential for confirming the importance of Dco- and Ds-promoted phosphorylation to Fat signaling.

Dco^3 is antimorphic and specifically deficient in Fat phosphorylation

In contrast to the overgrowth associated with *dco^3* mutants, *dco* null mutants lack discs, and *dco* null mutant clones grow poorly[93]. This could reflect the participation of *dco* in other processes. However, targets of Fat signaling, including Wingless (WG) in the proximal wing, and Diap1, are upregulated in *dco^3* mutant clones[11]. but not in *dco* null (*dco^{le88}*) mutant clones (E. Cho and KI, unpublished observations)[97]. The apparent absence of *fat* phenotypes in *dco* null alleles suggests that *dco^3* is an unusual allele.

dco is also known as *double time*, because viable alleles were independently isolated as circadian rhythm mutants[209]. This circadian phenotype reflects a role for Dco in phosphorylating, and thereby promoting the turnover, of the circadian protein Period[212,221]. This activity of Dco can be reproduced in S2 cells. Notably, Dco^3:V5 was as effective as wild-type Dco:V5 at promoting Period turnover in S2 cells, whereas a circadian rhythm mutant isoform, Dco$^{Dbt\text{-}AR}$, was less effective (Figure 4*A*). Thus, *dco^3* is impaired in promoting Fat phosphorylation, but active on another substrate.

Analysis of the Dco-Period interaction revealed that Dco and Period can be stably associated, as assayed by their ability to be co-precipitated from cultured cells[209,212]. Similarly, Dco and the Fat-ICD can be co-precipitated, and this association was not impaired by the Dco^3 mutations (Figure 4*B*). Since Dco^3 can associate with Fat, but doesn't efficiently phosphorylate it, Dco^3 might act as an antimorphic (dominant negative) protein by competing with wild-type kinase. Indeed, although *dco^3* is recessive at

endogenous expression levels, when *dco*^{3} was over-expressed, aspects of the *dco*^{3} phenotype, including wing overgrowth (Figure 4*C*) and the induction of a Fat pathway target gene (Figure 4*E*, *E*') could be reproduced. By contrast, over-expression of wild-type forms of Dco only shows subtle growth suppression (Figure 3*G*) and weak influence on *Diap1* transcription (data not shown)[95-97,209-211], despite influencing the mobility of Fat in SDS-PAGE gels (Figure 3*E*, *F*). This observation suggests that Dco sites that influence Fat mobility shift in SDS-PAGE gels are not well coincident with Dco sites that influence Fat signaling.

In addition to having a CKIδ/ε homologue, *Drosophila* also have a CKIα homologue, and in some contexts they can act partially redundantly[94]. A partial shift in Fat ICD mobility could be detected when CKIα was expressed in S2 cells or in wing discs (Figure 3*D*-*F*). Thus, CKIα can promote phosphorylation of Fat, although apparently to a lesser degree than Dco. This observation, together with the *dco*^{3} phenotypes observed when Dco^{3} is over-expressed, and the observation that although *dco*^{3} is defective in Fat phosphorylation, *dco* null mutant cells do not appear to be impaired for Fat signaling, suggest that *dco*^{3} might act as an antimorphic, or dominant negative, mutation, failing to effectively phosphorylate Fat and at the same time interfering with an ability of CKIα to phosphorylate Fat. By contrast, we hypothesize that in *dco* null mutant cells, CKIα or other kinases could phosphorylate Fat without interference. However, we were unable to achieve rescue of *dco*^{3} with a UAS-CKIα transgene (data not shown), although overexpression of CKIα in wild type background subtly inhibits *Diap1* transcription and adult wing growth (Figure 3*G* and data not shown), and in *dco*^{3} mutants restores Fat phosphorylation (Figure 3*E*, *F*). By contrast, we

could rescue *dco*^{3} with a UAS-Dco transgene (Figure 3*G*). In the presence of Dco^{3} binding, the amount of overexpressed CKIα might not be sufficient to phosphorylate the functional significant sites on Fat-ICD, although can still phosphorylate other sites that contribute to Fat mobility shift. It is therefore plausible that in *dco* null allele, CKIα may be able to access and phosphorylate these sites and activate Fat receptor.

dco^{3} specifically affects the Fat-Warts pathway

Dco also participates in other pathways and processes. To determine whether the tumor suppressor phenotype of *dco*^{3} can be accounted for solely by its influence on Fat signaling, we took advantage of the observation that over-expression of Wts under the control of a heterologous promoter *(tub-Gal4 UAS-Myc:Wts*) could rescue the lethality and tumor suppressor phenotype of *fat* mutants[12]. The lethality and overgrowth phenotypes of *dco*^{3} were also rescued by Wts over-expression *(tub-Gal4 UAS-Myc:Wts*), resulting in animals that, aside from some mild wing vein phenotypes, are indistinguishable from wild-type animals over-expressing Wts (data not shown). Since they are rescued simply by elevating Wts expression, *dco*^{3} mutant animals are specifically defective in Fat signaling; other essential processes that Dco participates in are not impaired.

dco^{3} does not affect the Fat polarity pathway

Although Wts over-expression rescued the overgrowth and lethality of *fat* mutants, these animals have obvious PCP phenotypes in multiple tissues, consistent with the conclusion that Wts functions specifically in a Fat tumor suppressor pathway, and not in a Fat PCP pathway[12]. (Figure 5*G*, *I*). By contrast, Wts-rescued *dco*^{3} mutants appear to have normal PCP (Figure 5*J*). The absence of an obvious PCP phenotype also indicates that the

influence of Dco and CKIα on PCP through phosphorylation of Dishevelled[95,96] is not affected by *dco*^{3}.

To confirm the lack of influence of *dco*^{3} on PCP, we also examined *dco*^{3} mutant clones. *fat* mutant clones in the abdomen exhibit obvious disruptions in the normal posterior orientation of hairs and bristles[10,74], but *dco*^{3} mutant clones had no effect (Figure 5*K*). In addition to affecting the canonical PCP pathway, studies of the relationship between Fat and its downstream effector Dachs revealed a novel form of PCP, in which Fat signaling causes a polarized distribution of Dachs, which can be visualized by mosaic expression of a tagged form of Dachs, Dachs:V5[10,87]. In the developing wing, Dachs:V5 is present on distal cell membranes, but not on proximal cell membranes. In clones of cells mutant for *fat*, Dachs:V5 is equally distributed on proximal and distal membranes (Figure 5D, by C. Rauskolb). In clones of cells mutants for *dco*^{3}, Dachs:V5 localization is still polarized (Figure 5*E*). Thus, the regulation of Dachs localization by Fat does not appear to be affected by *dco*^{3}, although a weak effect on Dachs localization would have been difficult for us to detect. The apparent absence of Dachs relocalization in *dco*^{3} clones is difficult to reconcile with the hypothesis that the influence of Fat on Warts depends on its ability to polarize Dachs[25,87], and further studies will be required to resolve this.

Mapping Dco phosphorylation sites in Fat.

In order to map Dco phosphorylation sites in Fat, we took advantage of the fact that *wild type* Dco but not Dco^{3} phosphorylates Fat-ICD in *Drosophila* S2 cells, which can be readily visualized by mobility shift in SDS-PAGE (Figure 3). The intracellular domain of Fat is predicted to be 538 amino acids, and we began mapping phosphorylation sites by examining the mobility of Fat-STI:FVH constructs containing deletions of parts of the

intracellular domain (Figure 6*A*). The smallest fragment that was visibly shifted by co-expression with Dco in this assay included amino acids 172 through 415 of the intracellular domain (ft-STI-11:FVH) (Figure 6*A*). None of a series of constructs encompassing further deletions of this region were visibly affected by Dco (Figure 6A), suggesting either that recognition by Dco, or the ability to detect a mobility shift, was lost when this region was further truncated. Thus, we turned to site-specific mutagenesis of potential phosphorylation sites.

The 244 amino acid region from 172 to 415 of the intracellular domain includes 66 potential sites of phosphorylation (ie Ser, Thr or Tyr residues). To determine which of these were subject to Dco-dependent phosphorylation, we constructed a series of 20 different Fat-STI- 4:FVH constructs (P1 to P20) in which clusters of potential phosphorylation sites, collectively encompassing all 66 sites, were changed to Ala (Appendix). Eighteen of these constructs were clearly shifted by co-expression with Dco (Appendix), while the mobility shift of two constructs, P14, and P15, was impaired (Figure 6*B*). These constructs encompass 10 Ser residues (Figure 6E and Appendix). To further refine the mapping of Dco-dependent phosphorylation sites, these 10 Ser were changed to Ala alone and in combinations within 13 additional constructs (P21 to P33) (Figure 6*E*, Appendix). This led to the determination that three Ser residues in the middle of the Fat ICD (Ser4891, Ser4895, Ser4898) contribute to the Dco dependent mobility shift, whereas other Ser's have no significant affect (Figure 6*B*, Appendix). When any of these three are individually mutated to Ala (P25, P26, P27), the mobility shift is reduced, and when all three are changed to Ala (P32) the mobility shift is eliminated (Figure 6*B*). These three Ser's are conserved among insect Fat proteins (Figure 6*E*). Only one is

clearly conserved in alignments of Fat with its closest mammalian homologue, Fat4, although an overall Ser-rich character of this region is conserved (Figure 6*E*).

Mutation of Ser to Asp can sometimes act as a phosphomimetic, because it introduces an equivalent negative charge. Thus we made a series of constructs in which Ser residues in and around the three critical Ser were changed to Asp (Appendix). Single amino acid changes did not have much affect, but mutation of multiple Ser residues in this region (P14D, P15D and P32D) was sufficient to effect a mobility shift (Figure 6*B*). However, the mobility shift induced by Ser to Asp mutations was not as great as that effected by Dco-mediated phosphorylation, suggesting that it only partially mimics phosphorylation. It was also unaffected by CIP treatment (Figure 6*C*), which argues that it is not dependent upon stimulation of phosphorylation at additional sites, but rather reflects a conformational change elicted by the introduction of a negative charge in this region.

To investigate whether these three Ser residues can be directly phosphorylated by CKI, we employed an in vitro kinase assay. As has been found previously[222], we were unable to purify active Dco from S2 cells, even though a recent report showed that labile Dco could be purified from insect Sf9 cells[223]. Thus, we employed a commercially available mammalian homologue. In vitro kinase assays with mammalian CKIδ resulted in shifts in the mobility of Fat-STI-4:FVH (Figure 6*D*) although in contrast to the discrete mobility shift observed in cultured cells, the bands appeared more smeared, and at higher enzyme and ATP concentrations, mobility shifts which exceed that observed in vivo could be detected. Nonetheless, the CKIδ-mediated mobility shift of Fat was reduced by mutation of sites required for the Dco-mediated mobility shift in S2 cells (Figure 6D), which argues that these Ser residues can be directly phosphorylated by CKIδ.

Assay Dco Phosphorylation sites in Fat activity in vivo.

If the Dco-dependent phosphorylation sites identified above contribute to Fat signaling in vivo, then expression of a Fat isoform that cannot be phosphorylated at these sites would be expected to have reduced activity. As the large size of Fat hinders both genetic engineering and transformation, we took advantage of the observation that over-expression of a truncated Fat protein lacking the Cadherin and EGF domains can provide partial rescue of *fat* phenotypes[71]. Wild-type and mutant versions of Fat-STI:FVH were introduced into flies under UAS-Gal4 control. As insertions at different chromosomal locations are associated with different levels of transgene expression, we employed phiC31-mediated recombination to insert these truncated Fat expressing transgenes at exactly the same chromosomal location[215], such that the relative expression levels of wild-type and mutant forms of Fat-STI:FVH should be identical (Figure 1*A*).

The activity of different Fat proteins was then compared by assaying their ability to rescue *fat* mutants. *fat* mutant wing discs are overgrown compared to wild-type discs (Figure 7*A, B*). To control for potential variations in age or culture conditions, rescue was assayed by expressing Fat proteins under *en-Gal4* control in the posterior half of the disc, and then measuring the relative sizes of the anterior (A) and posterior (P) compartments of the developing wing pouch marked by proximal WG. In wild-type animals the P/A ratio was 1.05 (Fig. 7*A, F*). In *fat* mutant animals, the P/A size ratio was 1.08, as both compartments overgrow equally (Figure 7*B, F*). When full length Fat is expressed from a UAS transgene in P cells, the P/A ratio was approximately 0.34 (Figure 7*C, F*), reflecting the rescue and consequently reduced growth of the P compartment. Truncated Fat (Fat-STI:FVH) has reduced rescuing activity compared to full length Fat, as its expression in

P cells resulted in an P/A ratio of 0.74 (Figure *7D, F*), even though it is expressed at levels well above endogenous Fat (not shown). The reduced activity of Fat-STI:FVH presumably reflects the normal role of the extracellular domain in interacting with Ds and thereby promoting the phosphorylation of the intracellular domain. Nonetheless, over-expression of the intracellular domain evidently bypasses, at least partially, the normal requirement for interaction with ligand. When the triple Ala substitution mutant, Fat-STI-P32:FVH (Figure 6*E*), was expressed under *en-Gal4* control, the degree of rescue of *fat* was lower, as evidenced by the P/A ratio of 0.94 (Figure 7*E, F*). Thus, the 3 Ser residues mutated in this isoform appear to contribute to Fat activity in vivo.

Because wild type Ft-STI only partially rescues *fat* mutant phenotypes in vivo (Figure 7*F*), the phosphorylation mutants therefore should be assayed in the full length *fat* construct and at Fat endogenous level. The coding sequence of *fat* is more than 15kb which limits the mutagenesis and current PCR and restriction enzyme based cloning strategies. In addition, the Gal4-UAS system always give much higher expression than endogenous genes[224], which in a lot of cases may result in gain of function of the gene, e.g. Notch, Ex, Hpo, Yki and Fat (unpublished observations). To address this issue, it is better to express *fat* at or close to its endogenous level. Manipulation of *fat* locus is the best way to achieve this goal[225], however, *fat* locus was somehow resistant to gene targeting (unpublished observations), besides it is time-consuming. An alternative way is to manipulate *fat* locus in BAC genomic DNA clones in bacteria *E coli* with recombineering technology and then inject into *Drosophila* to generate transgenic animals via phiC31-mediated recombination[180]. As the *Drosophila* genome is relatively

compacted[226-228] and cis-elements are usually closer to the genes, a BAC clone will be possible to cover all these regulatory sequences[180]. If the BAC contains all the cis-elements required for proper expression of *fat*, Fat protein can be expressed in the same pattern and level as its endogenous counterpart. As an example, the Fat expressed from the *V5:fat* transgenic animals was close to the endogenous Fat (Figure 1*E*) without any growth phenotype even when the transgene was homozygous, suggesting that the copy number variation of *fat* locus between 1 to 4 does not influence Fat signaling. V5:Ft fully rescued *fat* mutant phenotypes, indicating that the BAC clone faithfully represents the regulatory elements for *fat*.

Mutant versions of P15, P15D, P32 and P32D were introduced into the BAC genomic clones by recombineering technology and *fat* locus was subcloned into attB-P[acman][180] system to generate transgenic flies with the same attP landing site as that for *V5:ft*. The functions of the *fat* mutants were then assayed by the extent to rescue the *fat* mutant phenotypes. Surprsingly, all four different Fat phosphorylation site mutants fully rescued *fat* null mutants to viability with no difference to wild type flies and the V5:Fat rescued *fat* mutants (data not shown). In order to show whether the phosphorylation sites contributing to the Fat mobility shift in S2 cells are the same as those responsible for the mobility shift in wing discs, the wing discs from the rescued *fat* mutant larva were separated and lysed for Western blotting with Fat-ICD antisera. Consistant with the results from S2 cell, triple mutation P32 removes most of the mobility shift in wing discs (Figure 7*G, H*). These results indicate that phosphorylation mediated mobility shift is not directly related to Fat functions in vivo.

The discrepancy between the mutant *fat* genomic rescue constructs and *UAS-fat-ICD*s in rescuing *fat* mutation may suggest a few models. One model is that Fat-ICD is the key target for Dco^3 but the three Ser sites identified by the mobility shift are not essential for Fat functions. The difference between the triple-Ser mutant and wild type Fat-ICD may be an artifact. The biological significant sites may not contribute to Fat-ICD mobility shift as shown by Western blotting. Another possibility is that the three Ser sites might be redundant with other sites in Dco dependent phosphorylation, which may be shown when Fat is sensitized, e.g. in partially functional Fat-ICD. Redundancy of these phosphorylation sites might be responsible for other functions of Fat, e.g. robustness of Fat signaling under certain developmental or environmental contexts, which cannot be assayed at current conditions. Lastly but less likely, Fat-ICD is not the key target of Dco^3, and other unknown protein(s), genetically located between Fat and Dachs, might be mainly influenced by Dco^3.

Discussion

Phosphorylation and Fat signaling pathways

The atypical cadherin Fat is a transmembrane receptor for pathways that control PCP and growth. We have identified two post-translational modifications of Fat. First, Fat is proteolytically processed, resulting in the production of stably-associated N- and C-terminal polypeptides. The functional significance of this processing is not known, but its discovery is a necessary precursor to further experiments aimed at this question. Processing appears to be constitutive rather than regulated. Nonetheless, processing may facilitate subsequent events that regulate Fat.

We also identified a phosphorylation of the Fat cytoplasmic domain. This phosphorylation is promoted by the Fat ligand Ds, is influenced by the Fat pathway kinase Dco, and correlates with Fat pathway activity in *ds* or *dco*^{3} mutant animals, or when Ds or Fj are over-expressed. These observations suggest that phosphorylation of Fat is a key step in Fat receptor activation. However, when Dco was over-expressed, a mobility shift of the Fat ICD was detected and only subtle suppression of growth and DIAP-1 transcription was observed (data not shown). Thus the phosphorylation-dependent mobility shift of Fat is a general marker of the extent of Fat phosphorylation, but not a precise marker of phosphorylation at a site required for Fat activity. Our favored interpretation for this uncoupling is that there are multiple Dco sites within the Fat ICD, sites that can contribute to a Dco-mediated mobility shift are not completely congruent with sites required for the influence of Fat on Warts, and that a site or sites required for the influence of Fat on Warts is only efficiently phosphorylated when Fat is engaged by Ds. The sites phosphorylated by Dco and contributed to the mobility shift appear not essential for Fat function, although may contribute to its function at certain physiological or environmental conditions. This scenario was recently shown in yeast, where deletion of around 80% of yeast genes did not generate obvious phenotypes in rich medium[229]. However, the functions of almost all the genes could be demonstrated under certain chemical stresses. It is thus possible that the phosphorylation sites in Ft-ICD may be functionally redundant. Although it also remains possible that the biologically relevant target of Dco is not Fat, the observation that *dco*^{3} can be completely rescued by Warts over-expression, together with the epistasis of *dachs* to *dco*^{3}, indicates that the tumor

suppressor phenotype of *dco*^{3} is due to an impairment of Fat-Warts signaling, which occurs at or upstream of the action of Dachs.

Three Ser sites were identified as the Dco phosphorylation sites contributing to the mobility shift of Fat-ICD in cell cultures and in wing discs. These sites were mutated in UAS-Fat-ICD constructs and the transgene was assayed for its ability to rescue the *fat* mutant phenotypes. There appeared a subtle difference between the wild type Fat-ICD and the mutant Fat-ICD. In order to fully test the significance of these phosphorylation sites in Fat functions, triple mutation of these three Ser sites was introduced into the *fat* genomic rescue construct. The triple mutant Fat was expressed at a level close to the endogenous Fat (Figure 7G) and fully rescued *fat* mutants to viability. Because the triple mutant showed diminished hyper-phosphorylation form of FatICD (Figure 7H) in wing disc lysate, these three Dco phosphorylation sites appear not essential for normal Fat functions. The subtle activity loss of the triple mutation in UAS-Fat-ICD construct (Figure 7A-F) might indicate a marginal contribution in Fat function, which can only be shown when the Fat function or level is sensitized (e.g. partially functional UAS-Fat-ICD). It is also possible that the subtle functional different observed in mutant UAS-Fat-ICD was an artifact. To address this issue will need more knowledge about Fat functions during animal development, especially the robustness of Fat signaling under various environmental and genomic contexts.

Mapping Dco phosphorylation sites in Fat.

Unbiased ways like mass spectrum has been employed to identify Fat-ICD phosphorylation in *Drosophila* embryos and a few sites have been described[230]. However,

as Fat function has not been shown during embryonic development[231,232], phosphorylation sites identified in embryonic lysate may not be important for imaginal disc development. The mobility shift of Fat-ICD is not always coincident with Fat function in wing discs, the functional significant sites modified by Dco therefore are probably Ds dependent. The Fat-ICD mobility shift manifested in S2 cell thus unlikely covers these functional sites. In the future, it will be a better choice to identify Fat-ICD phosphorylation sites in wing discs lysate, given that enough Fat-ICD protein can be isolated or purified for mass spectrum. Density dependent differential centrifugation could be an more efficient way to isolate imaginal discs at large scale[233]. As an alternative way to identify phosphorylated protein, PhosTag reagent (www.phos-tag.com) has been synthesized to detect various phosphorylation events[120,234-236]. Although hyper-phosphorylated Fat-ICD could not be well separated by Phos-tag SDS-PAGE (data not shown), it may be enriched with Phos-tag chromatography for mass spectrometry analysis[236].

Figures

Figure 1. Processing of Fat.

Western blots of Fat and Fat constructs, the approximate positions of markers, and inferred identity of Fat bands, are indicated. A) *UAS-fat* constructs. B) Genomic rescue construct of *fat*. C) Lysates of *wild type* and $fat^{G\text{-}rv}$ wing discs. D) Lysates of S2 cells expressing V5:Fat or Fat:FVH. V5 and Fat were detected simultaneously by immunofluorescense, and are shown together in the left panel and separately in the right panels. E) Lysates of *wild type*, $fat^{G\text{-}rv}$, and $fat^{G\text{-}rv}/fat^{8}$ *attB-P[acmanV5:fat+]* wing discs. F) Lysates of S2 cells expressing Fat:FVH, or truncated isoforms. G). Left two panels show lysates of S2 cells expressing V5:Fat or Fat:FVH, right two panels show material immunoprecipitated after anti-V5 beads were incubated with intact cells.

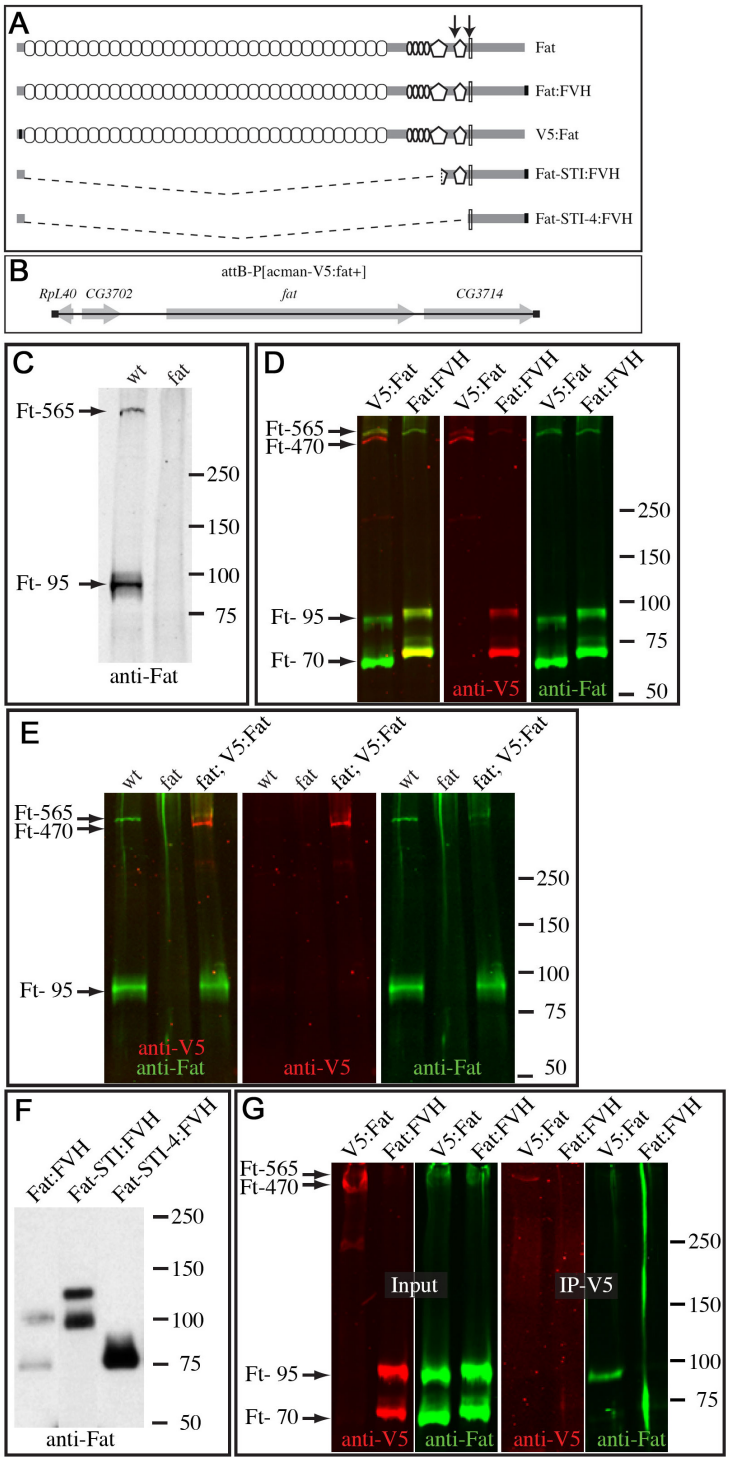
A
Fat
Fat:FVH
V5:Fat
Fat-STI:FVH
Fat-STI-4:FVH
B
attB-P[acman-V5:fat+]
RpL40
CG3702
fat
CG3714
C
wt
fat
Ft-565
Ft- 95
250
150
100
75
anti-Fat
D
V5:Fat
Fat:FVH
Ft-565
Ft-470
Ft- 95
Ft- 70
anti-V5
anti-Fat
250
150
100
75
50
E
wt
fat
fat; V5:Fat
Ft-565
Ft-470
Ft- 95
anti-V5
anti-Fat
250
150
100
75
50
F
Fat:FVH
Fat-STI:FVH
Fat-STI-4:FVH
250
150
100
75
50
anti-Fat
G
V5:Fat
Fat:FVH
Ft-565
Ft-470
Input
IP-V5
Ft- 95
Ft- 70
anti-V5
anti-Fat
250
150
100
75

Figure 1

Figure 2. Dachsous-promoted phosphorylation of Fat

Western blots of lysates of wing discs from ds36D/Df(2L) ds, fjd1, fjd1 ds36D/fjd1 Df(2L) ds, tub-Gal4 UAS-ds, tub-Gal4 UAS-fj, tub-Gal4 UAS-ds UAS-fj, wild-type, dco3, ftG-rv, as indicated. A) Ft-95 mobility in different genotypes; Wts levels indicate relative Fat activity and Act (Actin) is a loading control. B) Comparison of lysates treated with CIP versus untreated lysates. C) Lysates from wing discs of the indicated genotypes shows that dco3 reverses the promotion of Ft-95 phosphorylation by ds. E, F) Line scanning traces generated from A and C of Fat protein in lysates of different genotypes. Relative intensity traces across bands from ten traces were averaged. Adult wings from F) fjD1 ds36D/ fjD1 Df ds, G) ds36D/Df ds, H) fjD1, I) wild type (Oregon-R), J) tub-Gal4 UAS-fj, K) tub-Ga4 UAS-ds, and L) tub-Gal4 UAS-ds UAS-fj.

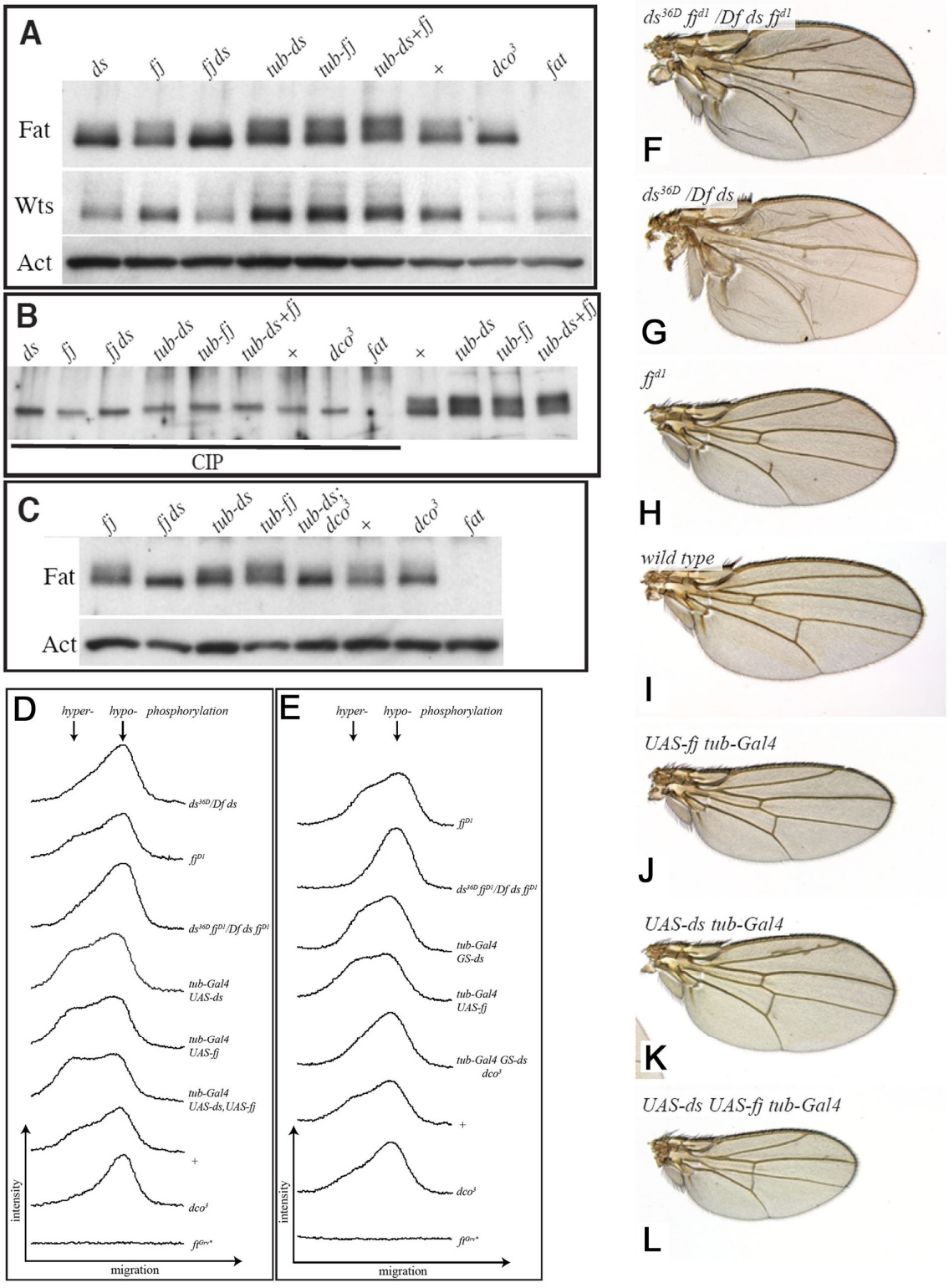
A
ds
fj
fj ds
tub-ds
tub-fj
tub-ds+fj
+
dco3
fat
Fat
Wts
Act
B
CIP
C
tub-ds;
dco3
D
hyper-
hypo-
phosphorylation
ds36D/Df ds
fjD1
ds36D fjD1/Df ds fjD1
tub-Gal4
UAS-ds
UAS-fj
UAS-ds,UAS-fj
intensity
migration
E
tub-Gal4
GS-ds
tub-Gal4 GS-ds
dco3
ftGrv*
F
ds36D fjd1 /Df ds fjd1
G
ds36D /Df ds
fjd1
H
wild type
I
UAS-fj tub-Gal4
J
UAS-ds tub-Gal4
K
UAS-ds UAS-fj tub-Gal4
L

Figure 2

Figure 3. Disc overgrown (Dco)-mediated phosphorylation of Fat.

Western blot of Fat, and Fat constructs (detected using anti-FLAG). Where indicated, Fat constructs were co-transfected with Dco or CKI constructs, or treated with phosphatase (CIP). A) Fat:FVH in S2 cells. B) Fat-STI-4:FVH in S2 cells. C) *wild type (+)*, dco^3, and $fat^{G\text{-}rv}$ wing disc lysates. D) Fat-STI:FVH and Fat-STI-4:FVH in S2 cells. E) *wild type* (+), dco^3, *tub-Gal4 UAS-CKIα* dco^3, *tub-Gal4 UAS-dco kinase domain* (*dcoKD*) dco^3, *tub-Gal4 UAS-CKIα*, *tub-Gal4 UAS-dcoKD*. F) Quantitative line scanning of blot in (E). Hyper- and hypo-phosphorylation forms, marked by arrows, indicate slower and faster mobility bands, respectively. Adult wing size of *wild type* (+), *tub-Gal4 UAS-CKIα*, *tub-Gal4 UAS-dcoKD* and *tub-Gal4 UAS-dcoKD* rescued dco^3 mutants. Females in all genotypes have bigger wings than males ($p<0.01$) and wild type animals from the same sex have bigger wings than other three genotypes ($p<0.05$).

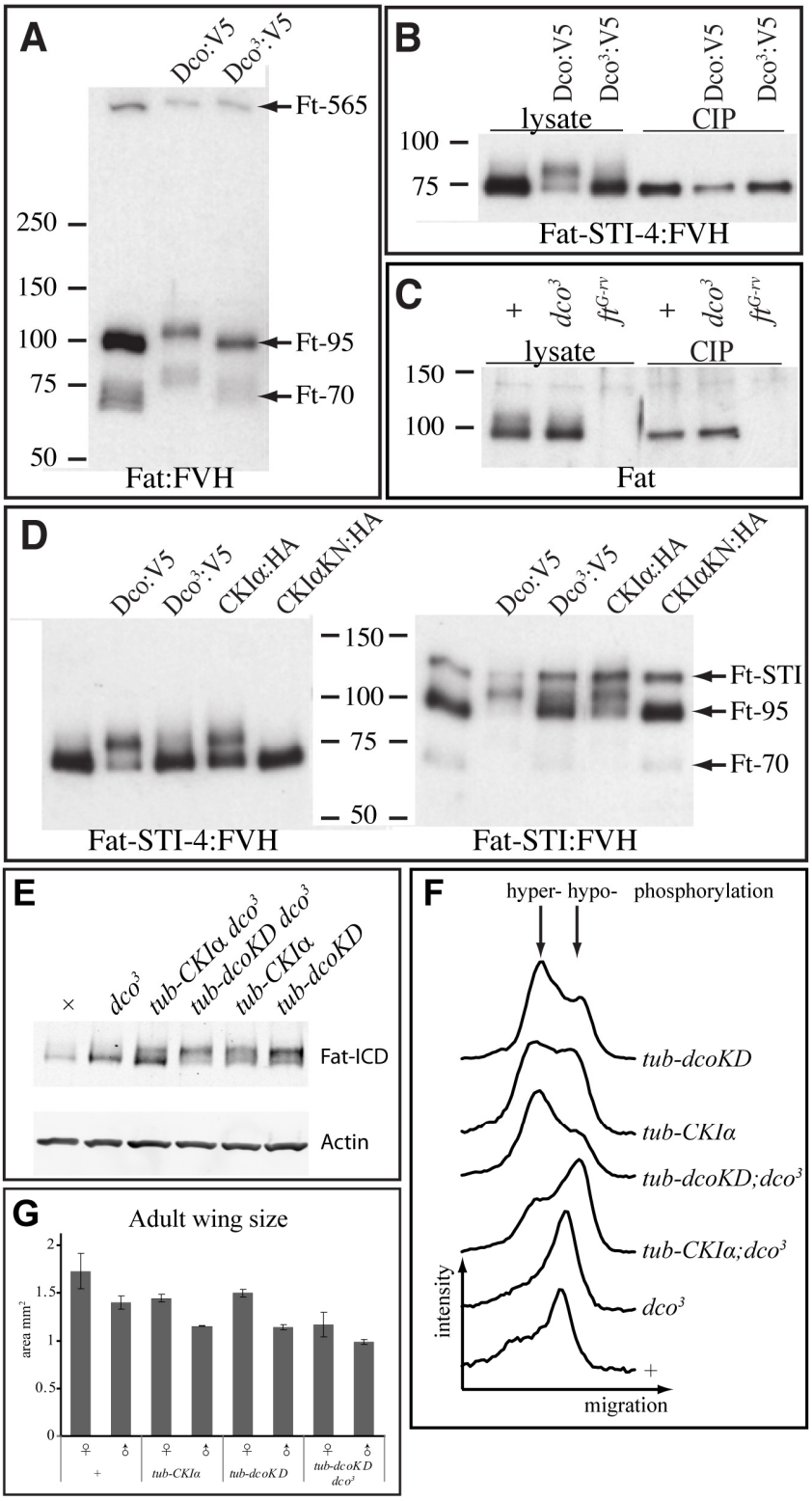
A
Dco:V5
Dco3:V5
Ft-565
250
150
100
75
50
Ft-95
Ft-70
Fat:FVH
B
Dco:V5
Dco3:V5
lysate
CIP
100
75
Fat-STI-4:FVH
C
+
dco3
ftG-rv
lysate
CIP
150
100
Fat
D
Dco:V5
Dco3:V5
CKIα:HA
CKIαKN:HA
150
100
75
50
Ft-STI
Ft-95
Ft-70
Fat-STI-4:FVH
Fat-STI:FVH
E
dco3
tub-CKIα dco3
tub-dcoKD dco3
tub-CKIα
tub-dcoKD
Fat-ICD
Actin
F
hyper-
hypo-
phosphorylation
tub-dcoKD
tub-CKIα
tub-dcoKD;dco3
tub-CKIα;dco3
dco3
+
intensity
migration
G
Adult wing size
area mm2
2
1.5
1
0.5
0
♀
♂
+
tub-CKIα
tub-dcoKD
tub-dcoKD dco3

Figure 3

Figure 4. Dominant negative activity of Dco^3

A) Dco-dependent destabilization of Per. Upper panel. Western blot of Per in lysates of transfected S2 cells shows that Dco and Dco_3 promote Per degradation. Lower panel. Western blot of Dco:V5 shows that similar amounts of each isoform were expressed; GFP:V5 is a transfection and loading control. B) Western blots (anti-V5) on S2 cells co-transfected with plasmids expressing (lane 1) Dco:V5, (2) Dco_3:V5, (3)Dco:V5 + Fat-STI-4:FVH, (4) Dco_3:V5 + Fat-STI-4:FVH, (5) Fat-STI-4:FVH. Upper panel shows blot of lysates (input); lower panel shows blot of material precipitated with anti-FLAG beads. C) Adult wing showing that overexpression of *dco*^{3} under *en-Gal4* control induces overgrowth of the posterior compartment. D) wild-type wing. E) Wing imaginal disc expressing of *dco*$_3$ under *en-Gal4*. The posterior compartme nt (marked by GFP, green) is enlarged and WG expression (red) is broadened.

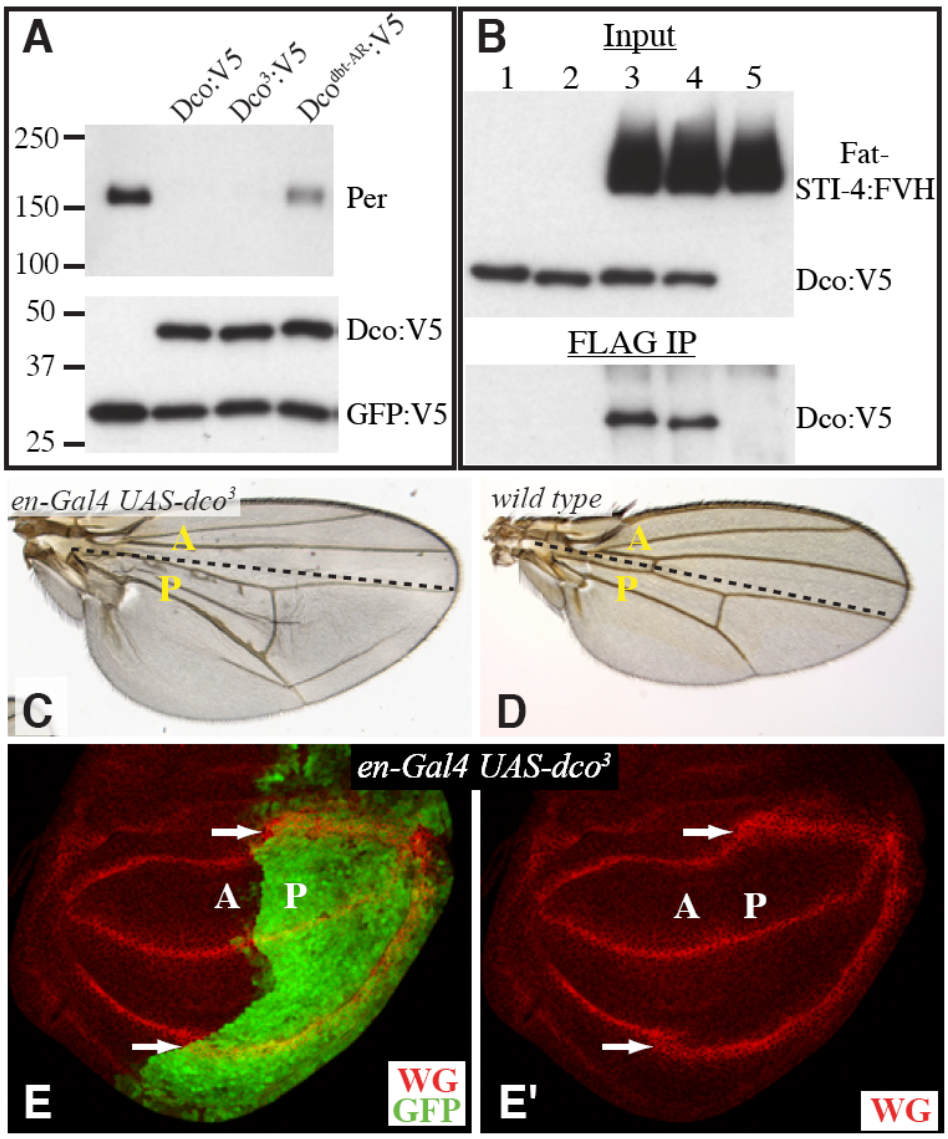
A
Dco:V5
Dco³:V5
Dco^dbt-AR:V5
250
150
100
50
37
25
Per
Dco:V5
GFP:V5
B
Input
1 2 3 4 5
Fat-
STI-4:FVH
Dco:V5
FLAG IP
Dco:V5
en-Gal4 UAS-dco³
A
P
C
wild type
A
P
D
en-Gal4 UAS-dco³
A P
WG
GFP
E
A P
WG
E'

Figure 4

Figure 5. *dco*^{3} specifically affects the Fat tumor suppressor pathway.

A) Wild-type fly. B) *dco*^{3} fly rescued by over-expression of *wts*. C-E) Clones of cells expressing Dachs:V5 (white); in D and E the MARCM technique was used to make these clones mutant for *fat*^{8} (D) or *dco*^{3} (E). Arrows point to clone edges with accumulation of Dachs:V5, arrowheads point to clone edges where Dachs:V5 is low. F-H) Wings from *wild type* (F), *ft*^{8}/*ft*$^{G\text{-}rv}$ rescued by over-expression of Wts (G), and *dco*^{3} rescued by over-expression of Wts (H). Arrowheads point to the crossveins, arrow points to extra vein material. Crossvein spacing is rescued for *dco*^{3}, but not for *fat*. I-K) Portions of adult abdomens from *ft*^{8}/*ft*$^{G\text{-}rv}$ rescued by over-expression of Wts (I), *dco*^{3} rescued by over-expression of Wts (J), an animal with *dco*^{3} mutant clones, marked by *y*+ (dark patches). A PCP phenotype is observed in I, but not in J or K.

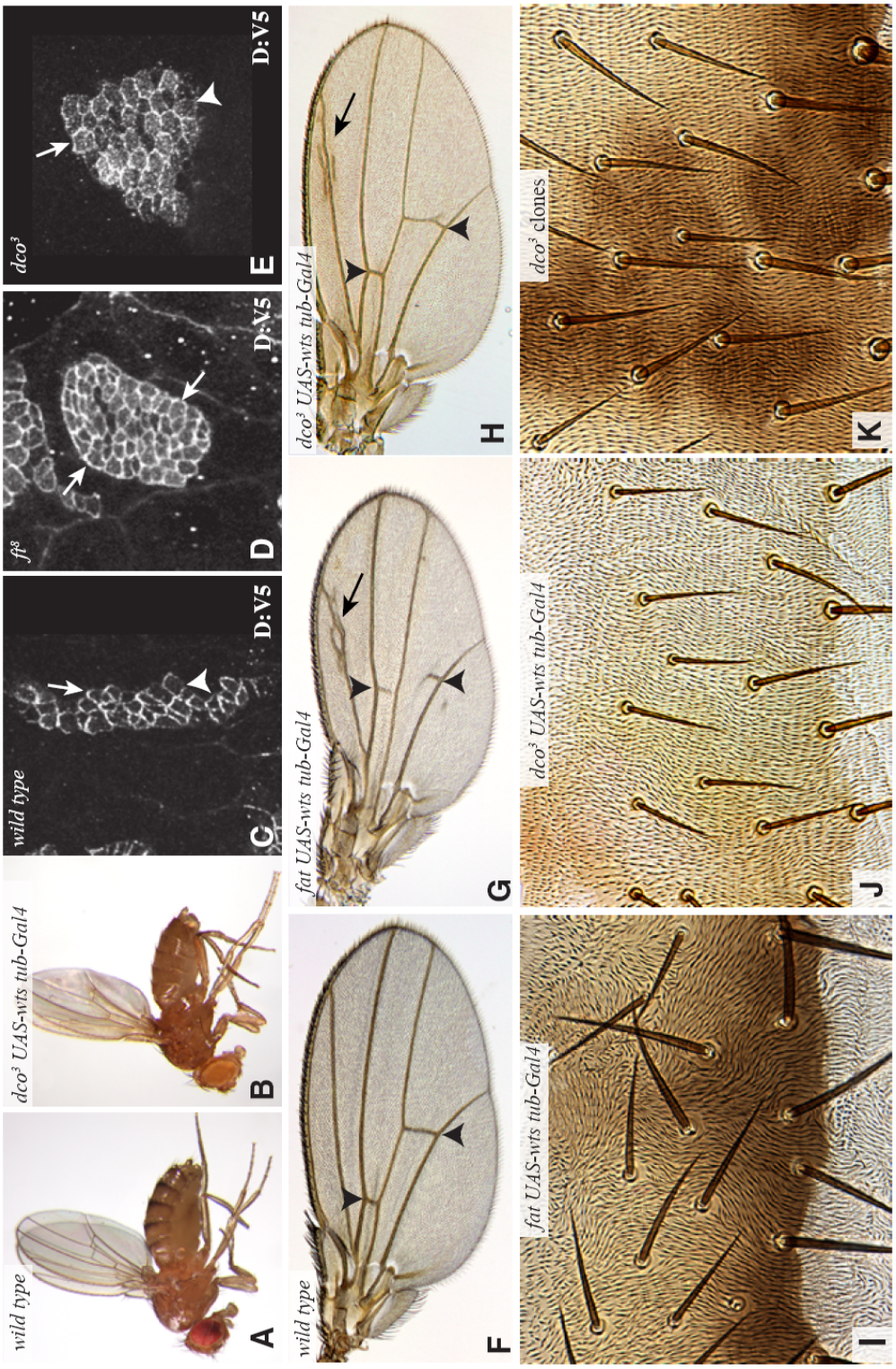
wild type
A
dco³ UAS-wts tub-Gal4
B
wild type
C
D:V5
ft⁸
D
D:V5
dco³
E
D:V5
wild type
F
fat UAS-wts tub-Gal4
G
dco³ UAS-wts tub-Gal4
H
fat UAS-wts tub-Gal4
I
dco³ UAS-wts tub-Gal4
J
dco³ clones
K

Figure 5

Figure 6. Mapping Dco phosphorylation sites in Fat

A) Fat intracellular domain truncations employed are indicated, dashed boxes indicate region deleted in each construct. Portions of a blot of lysates of S2 cells expressing these constructs and Dco or Dco3 are shown, presence of a detectable mobility shift is indcated by "+." B,C Show Western blots on S2 cells expressing Fat-STI-4:FVH and point mutant derivatives, together with Dco or Dco^3, as indicated. B) Mobility shift assay on point mutants. The amino acids mutated in each construct are indicated in panel 5D, a D indicates a Ser to Asp mutation, in other cases Ser to Ala mutations were employed. Additional mutations are shown in Supplementary Figures S3 and S4. C) The mobility shift induced by Ser to Asp mutations is not reversed by CIP treatment. D) Western blot on products of a kinase assay with CKIδ shows that purified Fat-STI-4:FVH can be directly phosphorylated by CKIδ in vitro, with the extent of phosphorylation is proportional to the amount of enzyme; for comparison protein phosphorylated in vivo was run on the same gel. The S to A triple mutant Fat-STI-4-P32:FVH is still a substrate for CKIδ, but the degree of phosphorylation, as assayed by mobility shift, is reduced. E) Alignment of a portion of the Fat intracellular domain with corresponding regions of other insect Fat proteins, and vertebrate Fat4 proteins. Yellow indicates amino acids conserved among all six species, blue indicate amino acids conserved only among insect Fat proteins, and green indicates amino acids conserved only among vertebrate Fat4 proteins. The three amino acids critical for the Dco-mediated mobility shift are underlined. The amino acids mutated in selected point mutations are indicated above.

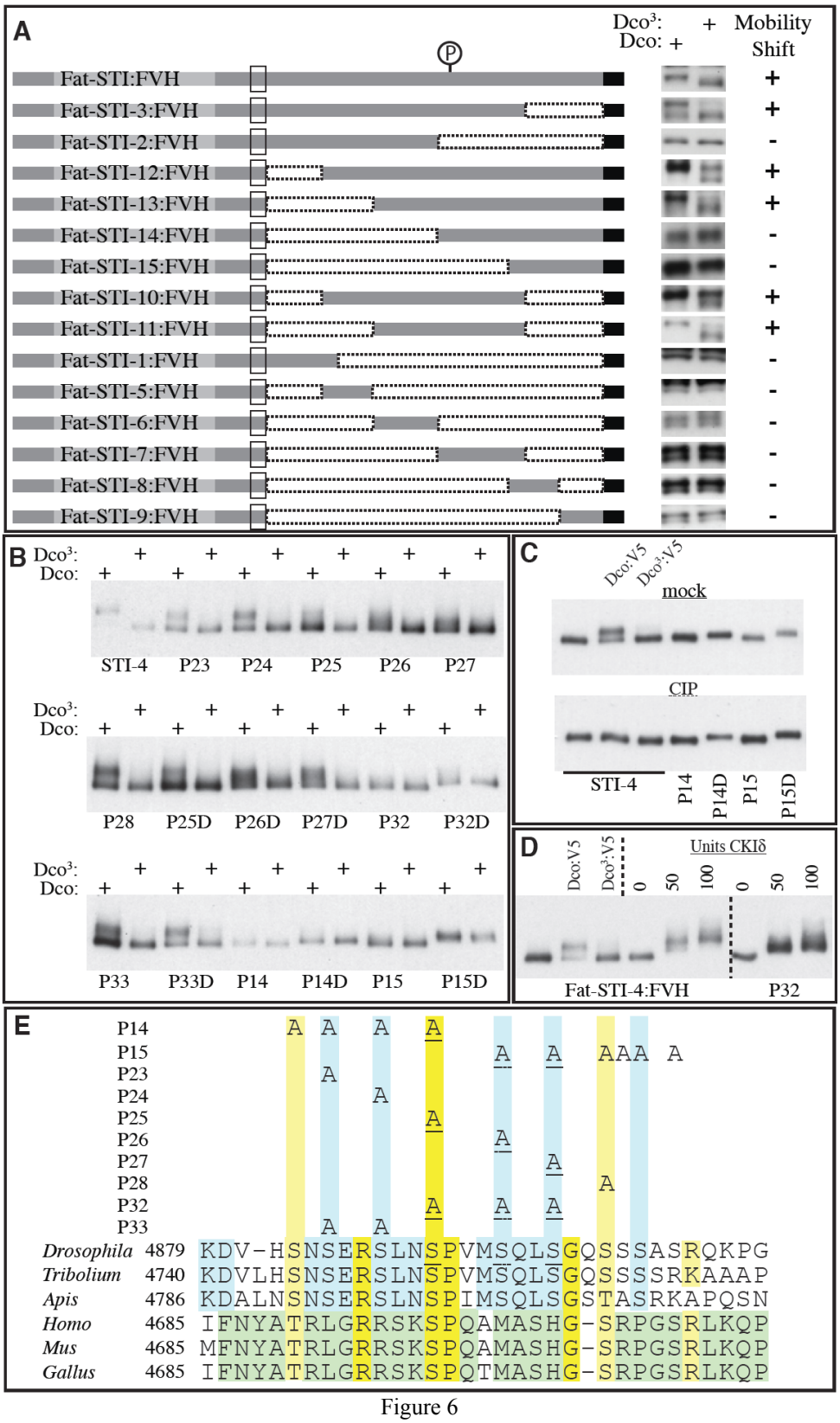
A
Dco³: +
Dco: +
Mobility Shift
P
Fat-STI:FVH +
Fat-STI-3:FVH +
Fat-STI-2:FVH -
Fat-STI-12:FVH +
Fat-STI-13:FVH +
Fat-STI-14:FVH -
Fat-STI-15:FVH -
Fat-STI-10:FVH +
Fat-STI-11:FVH +
Fat-STI-1:FVH -
Fat-STI-5:FVH -
Fat-STI-6:FVH -
Fat-STI-7:FVH -
Fat-STI-8:FVH -
Fat-STI-9:FVH -
B
Dco³: + + + + + + +
Dco: + + + + + + +
STI-4 P23 P24 P25 P26 P27
Dco³: + + + + + + +
Dco: + + + + + + +
P28 P25D P26D P27D P32 P32D
Dco³: + + + + + + +
Dco: + + + + + + +
P33 P33D P14 P14D P15 P15D
C
Dco:V5
Dco³:V5
mock
CIP
STI-4 P14 P14D P15 P15D
D
Dco:V5
Dco³:V5
Units CKIδ
0 50 100 0 50 100
Fat-STI-4:FVH P32
E
P14 A A A A
P15 A A AAA A
P23 A
P24 A
P25 A
P26 A
P27 A
P28 A
P32 A A A
P33 A A
Drosophila 4879 KDV-HSNSERSLNSPVMSQLSGQSSSASRQKPG
Tribolium 4740 KDVLHSNSERSLNSPVMSQLSGQSSSSRKAAAP
Apis 4786 KDALNSNSERSLNSPIMSQLSGSTASRKAPQSN
Homo 4685 IFNYATRLGRRSKSPQAMASHG-SRPGSRLKQP
Mus 4685 MFNYATRLGRRSKSPQAMASHG-SRPGSRLKQP
Gallus 4685 IFNYATRLGRRSKSPQTMASHG-SRPGSRLKQP

Figure 6

Figure 7. Assay functions of phosphorylation site mutants of Fat.

(*A-F*) Phosphorylation site mutants were introduced in UAS-ft-STI:FVH construct and assyed by en-Gal4 in ft mutant background. Show imaginal discs of the indicated genotypes stained for expression of WG (red), and a marker of posterior cells (blue, as indicated). F) Histogram of the relative area of P and A compartments in wing discs of the indicated genotypes. The wing pouch was measured, defined for these experiments as the area inside the inner ring of WG expression. Error bars show standard error; more than 15 discs were measured for each genotype. (*G-H*) Phosphorylation site mutants were introduced in *ft* genomic rescue construct and assyed by en-Gal4 in ft mutant background. *ft* mutant was fully rescued by both *wild type* and *P32* triple mutant. Lysate of *wild type*, dco^3 and rescued wing discs was blotted with Fat antisera (*G*), line scanning was performed to show distribution of hypo- and hyper phosphorylation forms of FatICD (*H*).

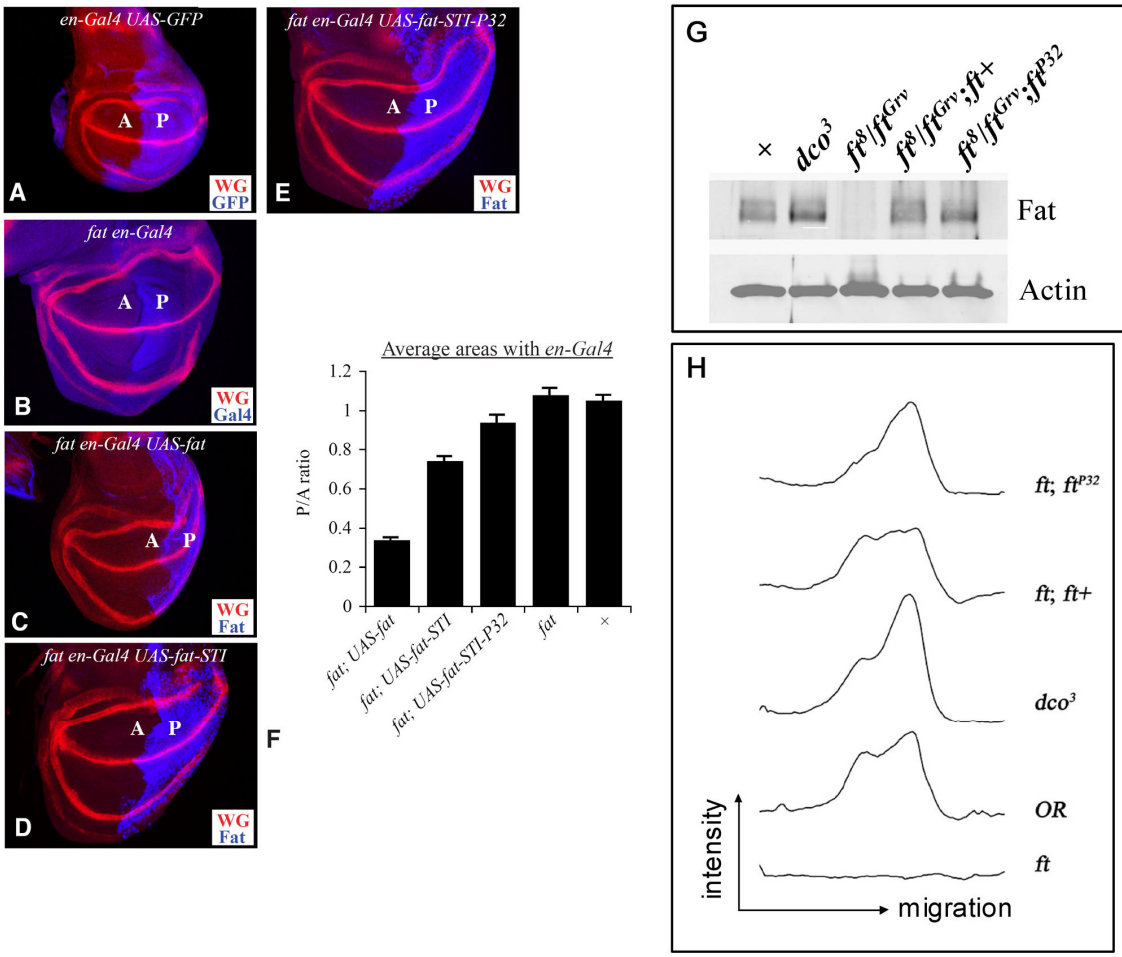
en-Gal4 UAS-GFP
A P
A
WG
GFP
fat en-Gal4 UAS-fat-STI-P32
A P
E
WG
Fat
fat en-Gal4
A P
B
WG
Gal4
fat en-Gal4 UAS-fat
A P
C
WG
Fat
fat en-Gal4 UAS-fat-STI
A P
D
WG
Fat
F
Average areas with en-Gal4
P/A ratio
1.2
1
0.8
0.6
0.4
0.2
0
fat; UAS-fat
fat; UAS-fat-STI
fat; UAS-fat-STI-P32
fat
×
G
×
dco3
ft8/ftGrv
ft8/ftGrv;ft+
ft8/ftGrv;ftP32
Fat
Actin
H
ft; ftP32
ft; ft+
dco3
OR
ft
intensity
migration

Figure 7

CHAPTER V

Ongoing projects.

1. Study the conservation of vertebrate Fat functions in *Drosophila*.

2. Fat might influence the Epidermal Growth Factor Receptor signaling pathway.

3. Subcellular localization of Fat protein.

4. Subcellular localization of Hippo and Warts in wing epithelia.

Yongqiang Feng and Kenneth D. Irvine

1. Study the conservation of vertebrate Fat functions in *Drosophila*.

Summary

Drosophila Fat has been shown to regulate both PCP and growth via different pathways[9-13,71,177,237]. In vertebrates, four Fat genes have been identified and Fat4 was considered as the vertebrate homolog of *Drosophila Fat*[140]. Fat4 recently was shown to be involved in PCP regulation[141], and a tumorigenic function was linked to it in the breast and oral cancers[152,153]. In order to study the functional conservation of Fat proteins during metazoan evolution, *Drosophila* Fat-ICD region was replaced by four human Fat-ICDs individually in the *fat* genomic rescue construct[13]. These fusion proteins were then used to study the functional conservation of Fat-ICDs in *Drosophila*. All four fusion proteins did not show growth regulation function as measured by rescuing the *fat* mutant phenotypes. To assay the PCP functions of these hybrids, all four Fat transgenes were introduced into *fat* mutants where the overgrowth phenotype was rescued by the overexpression of Wts[12]. Among all four hybrid molecules, only Fat4 rescued most of the PCP phenotypes in adult wings and abdomens of *fat* mutants when growth phenotype was suppressed by excessive Wts. These observations suggest that human Fat4-ICD conserves the PCP function of *Drosophila* Fat-ICD and probably acts via similar molecular mechanism.

Introduction

Fat was first identified in *Drosophila* and involved in growth and planar cell polarity (PCP) regulation[63,237]. In vertebrates, four Fats have been identified based on amino acid sequence similarity[140], however none of these Fat proteins to date has been shown to directly regulate growth, although a few Fats have been implied in tumorigenesis[140,150,153].

Drosophila Fat was recently linked to the downstream Hpo/Wts/Yki cascade in modulating cell growth and apoptosis[11,175-177], more experiments are therefore needed to show whether growth regulation and the signaling pathway are also conserved in vertebrates. In mouse, Merlin and the Hpo/Wts/Yki pathway have been shown to play important roles in growth regulation, organ size control, and tumorigenesis or metastasis[128,129,131,132,134,168,170,247,248]. If Fat proteins are upstream of the Hpo/Wts/Yki cascade in vertebrates, phenotypes in organ size and growth regulation should be observed in loss-of-function mutation of *fat* genes. In addition to growth regulation, *Drosophila* Fat also polarizes epithelial cells via an unknown PCP pathway, vertebrate Fat proteins may hereby regulate PCP via a similar mechanism as *Drosophila* Fat. This prediction was recently confirmed by the observations that knocking out of *fat4* in mouse caused PCP phenotypes in inner ear and kidney[141]. In mouse Fat1 and Fat3 are mainly expressed in epithelia while Fat4 in mesenchymal cells[142], which suggests tissue specificity and functional redundancy between certain Fats. More experiments are necessary in order to know which of the four Fats are PCP regulators and which are involved in growth regulation, if any. This analysis in mouse will become very difficult when some of Fats are functionally redundant, a common issue in vertebrates, because double or triple gene knockout technically is a challenge. A simpler way to address this problem is to assay vertebrate Fats' functions individually in *Drosophila*, if their functions are conserved during metazoan development. As Fat-ICD appears to be indispensable for all Fat functions in *Drosophila*[13,71], analysis of vertebrate Fat-ICDs' functions in *Drosophila* could be a shortcut to study Fat functional conservation. Assaying the functions of all vertebrate Fat-ICDs in *Drosophila* will also avoid the issues

in manipulating and expressing full length vertebrate *fat* genes and the binding specificity of extracellular domain with Ds.

Materials and methods

Fly stocks:

yw; *ft*^{8}/*CyOGFP*, *yw*; *ft*^{Grv}/*CyOGFP*, *yw*; *ft*^{Grv}/*CyOGFP*; *tub-Gal4*$^{[LL7]}$/*TM6b*, *yw*; *ft*^{8} *UAS-myc:Wts*/*CyOGFP*; *attB-ft*^{1}/*TM6b*, *yw;ft*^{8}*UAS-myc:Wts/CyOGFP; attB-ft*^{2}/*TM6b*, *yw; ft*^{8}*UAS-myc:Wts/ CyOGFP; attB-ft*^{3}/*TM6b, yw;ft*^{8}*UAS-myc:Wts/CyOGFP; attB-ft*^{4}/*TM6b*.

yw; *FRT42D hpo*^{KC202}/*CyO*; *attB-Flag:Hpo*/*TM6b*, *yw*; *FRT42D hpo*^{KC202}/*CyO*; *attB-Flag*:*Hpo*:*V5*/*TM6b*, *yw*; *FRT42D hpo*$^{42-47}$/*CyO*.

yw attB-myc:wts; *FRT82B wts*^{X1}/*TM6b*, *yw attB-myc:wts*:*V5*; *FRT82B wts*^{X1}/*TM6b*, yw; *FRT82B wts*^{P2}/*TM6b*.

Plasmids and Constructs

UAS-ft:GFP, Ft genomic rescue constructs (see Appendix 6-9).

All human *fat* genes contain multiple exons and introns and intracellular domains are coded by single exons that were used to amplify *fat*-ICD. Following the recombineering technique (http://recombineering.ncifcrf.gov/), *Drosophila ft*-ICD region in the genomic construct was replaced by *galactose kinase* (*galK*) via positive selection and then the *galk* was recombined with PCR fragments of four *fat*-ICDs by negative selection[269]. All constructs were then amplified by copy induction in order to enhance DNA yield[246] and the supercoiled DNA was then purified with exonuclease to remove nicked plasmid DNA (Qiagen). This DNA was then injected with integrase mRNA into attP landing sites on 3L(62A)[215].

Wts genomic rescue constructs (see Appendix 12)

Hpo genomic rescue constructs (see Appendix 11)

Histology and imaging

Imaginal discs were fixed and stained as described previously[9], using mouse anti-Wg (1:800, 4D4, Developmental Studies Hybridoma Bank (DSHB)), rat anti-DE-Cadherin (1:40, DCAD2, DSHB), rat anti dLMP (1:100, S. Cohen[270]), mouse anti FLAG M2(1:400, Sigma), mouse anti-Myc (9E10, 1:800, Babco), mouse anti-V5 (1:400 preabsorbed, Invitrogen) and rat anti-Fat (1:1600). Fluorescent stains were captured on a Leica TCS SP5 confocal microscope. For horizontal sections, maximum projection through multiple sections was employed to allow visualization of staining in different focal planes.

For adult tissues, combineZM software was used to allow visualization of features in different focal planes within a single image.

Results and discussion

Construction of *Drosophila fat* and human *fat* intracellular domain hybrids in genomic rescue constructs.

Drosophila Fat intracellular domain (ICD) is similar to other insects' Fat-ICD in amino acid sequence, and homologous to Fat4-ICD in vertebrates (Figure 1*A*). Conservation of Fat-ICD functions during evolution might be a way to study *Drosophila* Fat functions. In order to study functional conservation of vertebrate *fat* genes, human *fat-ICD*s are cloned from human genomic DNA (data not shown) to replace *Drosophila Fat-ICD* in a *fat* genomic rescue construct (Chapter IV). These *Drosophila* and human *fat*-ICD hybrids

will avoid the issue of introducing human Dachsous to ensure the binding between Dachsous and Fat. However, these hybrids will bind to *Drosophila* Dachsous in the same way as noral *Drosophila* Fat, given that the expression, folding and stability of them will be the same as *Drosophila* Fat. This experiment will test how and to what degree the human Fat-ICD will be able to transduce *Drosophila* Fat signals to the downstream cascades, regulating growth and/or planar cell polarity (PCP).

Animals carrying *Drosophila fat* genomic rescue constructs expressed Fat protein at a level similar to or the same as endogenous Fat and fully rescued *fat* mutant phenotypes with adults indistinguishable from their wild type siblings (Chapter IV). This 53kb genomic rescue construct covers *fat* locus and therefore is an excellent target plasmid to readily manipulate *fat* locus in vitro or in *E. coli* in the similar way as gene targeting in vivo[271,272]. Facilitated by phiC31 integrase-mediated tansgenesis in *Drosophila*, the supercoiled form of this construct can be efficiently integrated into fly genome: around 5% of the injected embryos had transformed offspring (data not shown)[179,215,216,246]. Traditional P-element mediated transgenesis is low in efficiency, especially for large DNA constructs, and the insertion sites are distributed in fly genome[273], which may influence gene expression level by the so called "position effects"[274]. The phiC31 system, on the contrary, can insert different constructs, assuming carrying different alleles of a gene, into the same landing site on fly genome so that position effects will be the same for all constructs and the biological functions of these alleles are therefore comparable.

The overall transformation efficiency for all constructs is around 5%, much lower than smaller constructs[179]. Low efficiency for larger constructs is probably caused by DNA nicking and shearing during manipulation and micro-injection. As DNA fragments in

mega-base length have been successfully injected into cells in the form of satellite microchromosomes[275,276] when DNA fiber was compacted during interphase, increasing DNA packing to decrease chances of nicking or shearing may be a way to enhance transformation efficiency for even larger DNA in the future. There are a few ways to compact DNA. The simplest way is to wind DNA on histones to form nucleosome structures, but may be difficult to perform it in vitro. In this case, compacting DNA constructs could be done in eukaryotic cells like yeast where nucleosomes can be formed and isolated easily. Small DNA binding compounds could be another way to compact DNA, which have been widely used in gene therapy and/or DNA delivery[277]. Although the structures are distinct, these compounds usually have common positively charged amines on their surface which nonspecifically absorbs the phosphate groups of DNA. DNA molecules are thus coated onto the surface of these organic polymers and are resistant to nucleases. In vivo the DNA molecules will gradually dissociate with the polymers to perform their functions. I have recently tested a few of these polymers with *fat* genomic rescue constructs, i.e. polyethyleneimine (PEI)[278], silicon nanoparticles[279]. However, once DNA formed complexes with these polymers it would precipitate in the solution and could not be injected into fly embryos (data not shown). In the future, the degree of compacted DNA needs to be optimized in order to keep sufficient solubility.

Assay growth and PCP functions of human *fat*-ICD hybrids in *Drosophila*.

All four human *fat* hybrids (Figure 1*B*) were injected into *attP2* landing site on the left arm of chromosome three at *68A4*. The transgenic flies were then combined with a *fat* mutant allele (ft^8) located on the left arm of the second chromosome (Figure 1*C*). As discussed before, mutation of *fat* results in wing disc overgrowth. These hybrid *fat*

proteins were first assayed for their growth regulation function in *fat* mutant background (Figure 1*C*) . None of the four *fat* fusion proteins rescued *fat* mutant to adults. Dissection of the third instar larva showed that all wing discs from these genotypes were excessively grown and indistinguishable from the wing discs of *fat* mutants. Measuring wing discs from larva at exactly the same stages is critical in identifying subtle growth difference, it is therefore very difficult to measure subtle difference of growth control in these *fat* mutants, because they delay larval development. It appears that all four human Fat-ICDs do not contain growth regulation function as *Drosophila* Fat, which is consistent with the observations that *fat4* and *fat1* knockout mice did not show overgrowth phenotypes (ref.[141,280] and information form H. McNeil). It is likely that PCP function was maintained when *fat* was diversified to four different genes during evolution and the growth regulation function of Fat could be either lost or distributed to other cell adhesion molecules. Four vertebrate Fats are expressed in specific tissues/organs[140,142,151] and thus may function in a tissue/organ specific manner. Systematically examining the functions of all four *fat* genes in vertebrates will undoubtedly provide more information about *fat* gene evolution.

In addition, although vertebrate Fats were classified as the homolog of *Drosophila* Fat (Figure 1*A*), it is unknown whether vertebrate Fats will act in a similar way as *Drosophila* Fat in regulating PCP. Addressing this issue will not only tell whether the mechanisms discovered in *Drosophila* will be similar to the one in vertebrates, but also provide a way to study *Drosophila* Fat signaling, e.g. identifying the conserved regions for PCP signaling. To approach this problem, I took the advantage of the observation that overexpression of Wts rescued growth phenotypes of *fat* mutants[12]. By suppressing

overgrowth phenotypes of *fat* mutants with Wts, it will be possible to assay whether human Fat-ICD hybrids will recue the PCP phenotypes in fly (Figure 1*C*). Previously I have shown that in these Wts rescued *fat* mutants, PCP phenotypes were still obvious (Figure 3*G*, *H*) though were not as strong as *fat* mutants[10,12,71]. Human Fat-ICD hybrids were thus introduced into these Wts rescued *fat* mutants to test their ability to restore the PCP phenotypes (Figure 1*C*).

To date animals mutant for *fat*, overexpression of Wts and carrying human *fat2*, *fat3* and *fat4* hybrids have survived to adults with *fat4* as the most successful one. Although Fat1 rescue experiment still needs careful analysis, it might be possible that it made the Wts rescued *fat* mutants even unhealthy by an different mechanism. Because these mutant larva were less healthy than their wild type siblings, unsuccessful recovery might suggest that they could not compete quite well with their wild type siblings. Another possibility is that eclosion of the mutant pupa may be less successful. In the future, mutant larva should be separated from the wild type animals and fed with nutritious food.

In terms of animal size, leg length and segmentation (now shown) and wing cross vein spacing, human Fat4 hybrid restored most of the phenotypes in Wts rescued *fat* mutanta (Figure 2*Q*-*T*). Orientation of bristles on wings and abdominal epidermis of these animals were largely normal, suggesting that human Fat4-ICD can efficiently transduce Ds and Fj gradient information from Fat extracellular domain to the downstream PCP pathway. The obvious phenotypes observed in these animals are shorter cross vein spacing (albeit broader than Wts rescued *fat* mutants), vein loss, ectopic vein material, positioning of wings from animal body (normally wings will be folded on the back of animals at rest). These phenotypes might not be caused by incomplete growth rescue by Wts, because Wts

rescued *expanded* mutants do not have these phenotypes, even though the rescue for *expanded* was less sufficient than for *fat* (Chapter III)[12]. It is most likely that insufficient PCP signaling or unknown functions of *Drosophila* Fat may cause these phenotypes. Both Wts and Wts Fat4-ICD rescued *fat* mutant females laid eggs with normal polarity and appendage (data not shown), but these eggs did not hatch to larva. Although Merlin and the Hpo/Wts/Yki pathway have been shown to be involved in the differentiation of the follicular epithelium during *Drosophila* oogenesis[232,267,281,282], Fat appears dispensable for it. The failure to give offspring in these Wts and Ft4-ICD rescued *fat* mutants might indicate some defects in their reproduction systems, either inablility to produce normal eggs or sperm, or inability to allow the eggs and sperms to form normal embryos. In the future, it will be interesting to clarify this issue.

In Fat2-ICD and Wts rescued *fat* mutants (Figure 2*I-L*), ectopic or loss of veins were observed and cross vein spacing was not restored (Figure 2*J*), although the legs were slighty shorter and leg segmentation was similar to wild type (data not shown). When the cuticles in wings and abdomens were examined, PCP was slightly abnormal and weaker than Wts rescued *fat* mutants (Figure 2*L*), suggesting that human Fat2-ICD may be able to restore all leg segmentation signals and part of PCP signals. In Fat3-ICD and Wts rescued *fat* mutants (Figure 2*M-P*), cross vein spacing appeared similar to Fat2-ICD+Wts rescued *fat* animals, however, legs from those animals were obviously shorter and in some case, a few tarsal segments were fused, a sensitive indicator of proximal-distal signaling defects [283-285]. PCP on wings and abdomens in these animals still showed subtle defects.

It is not clear whether leg length and segmentation or cross-vein spacing, are regulated by the same PCP pathway, because whenever PCP signaling is influenced by Fat signaling cross vein spacing and leg lenth/segmentation will be affected, however, when PCP is restored, as shown by Fat2-ICD and Fat4-ICD, cross-vein spacing or leg length/ segmentation are not restored to wild type. These could be caused by different sensitivities of PCP and proximal-distal phenotypes, i.e. cross vein spacing and leg length/segmentation, to the Fat signaling. As previously discussed, PCP signals from Fat pathway requires both transcriptional activity and an unique PCP cascade. However, leg length and segmentation, and cross vein spacing may not require transcriptional regulation. Different sensitivity of PCP and proximal-distal phenotypes in these human Fat-ICD+Wts rescued *fat* mutants, assuming they act in similar pathways, may suggest that interpreting the gradient readout from FatICD is performed by distinct machinery, one for bristle orientation[286,287] (runs earlier than but appears parallel to the Frizzled pathway[76,288]) and one for cell-cell movement/ spindle orientation during cell division[289,290]. Identification of the biochemical linkage between Fat-ICD and different machinery will provide valuable information in understanding how Fat signals.

A few more experiments need to be done before a convincing conclusion can be made. First, protein stainings need to be performed for all Fat-ICD hybrids in order to show that these proteins are correctly expressed, folded and localized on the correct subcellular domains. Second, ICD deleted version of *Drosophila* Fat (FatΔICD) should be tested in Wts rescued *fat* mutants to show whether there is any PCP restoration. Overexpression of *UAS-fatΔICD* has been shown as a dominant negative form of Fat[71], however,

FatΔICD:Cherry at endogenous level did not shown any phenotype (data not shown). It is possible that Fat can signal Ds or other proteins when FatΔICD is overexpressed.

Dissect *Drosophila* Fat-ICD function from amino acid sequence and functional conservation in vertebrates (directions for future work).

The rescue experiment of human Fat-ICDs + Wts in *fat* mutant animals also provides a way to reevaluate the significance of polarized distribution of Dachs protein in Fat signaling[10,87]. Because Dachs is required for almost all Fat functions, the assymetrical distribution of Dacha protein in wing epithelia has been proposed as an indicator of how Fat interprets Ds and Fj gradients in regulating growth and PCP[10,25,87]. However, as shown and discussed before, Dco specifically phosphorylates Fat-ICD and genetically acts upstream of *dachs*[9-11,13]. In *dco*^{3} mutant, phosphorylation of Fat-ICD was dramatically decreased both in cultured cells and in wing discs. In wing and abdominal epidermis *dco*^{3} mutant clones did not show any PCP pehntypes[13], although it induces wing dics overgrowth[93] and destabilizes Wts protein[11]. Surprisingly, *doc*^{3} mutation does not influence the proximal-distal polarization of Dachs on the apical membrane[13], indicating that the loss of a significant amount of growth signals from Fat does not affect Dachs asymmetrical distribution on membrane. Albeit the key evidence is missing to show Fat as the functional target of Dco, it is still possible to clarify whether the polarization of Dachs is required for either growth regulation or PCP signaling, by taking the advantage of human Fat4-ICD restoring transcriptional independent PCP signaling and overexpression of Wts rescuing transcriptional phenotypes of *fat* mutants[12]. This can be done by only introducing heat shock promoted Flipase and a "flip-out"[291] transgene of *dachs*, e.g. actin promoter driven P_{actin}*-FRT-yellow-FRT-dachs*.

Because human Fat4 was considered as the vertebrate homolog of *Drosophila* Fat (Figure 1*A*), the conserved regions (Appendix 15) may indicate conserved functions, i.e. PCP signaling. A few small segments/motifs appear to be highly conserved from insects to vertebrates, clearly indicating a positive evolutionary selection[292]. The constraints of these segments/motifs may suggest their functional significance for animal development. The regions conserved between *Drosophila* Fat-ICD and human Fat4-ICD can therefore be mutated or deleted in *Drosophila* Fat-ICD in the genomic rescue construct and tested in vivo by their functions in PCP regulation, growth regulation or Dachs protein localization.

Although human Fat2-ICD and Fat3-ICD also partially restored the PCP phenotypes in Wts rescued *fat* mutants, protein strcture conservation (as have been shown in other protein families, e.g. GTPase superfamily[293]) of these proteins may contribute to the their functions in fly, but these regions in Fat2-ICD and Fat3-ICD might be less conserved and therefore less functional (Appendix 14). To address this issue will need the structure information of Fat2-ICD and Fat3-ICD that are not currently available.

2. Fat might influence the Epidermal Growth Factor Receptor signaling pathway.

Summary

Overexpression of Fat in ventral cells of the wing discs induced dorsal cell fate and ectopic dorsal/ventral Wingless (WG) around the clones. Two different lines of UAS-fat, one for untagged Fat [71] and one for UAS-fat:GFP (constructed in this work), showed similar phenotypes. In adult wings, overexpression of Fat resulted in ectopic vein formation and the loss function of *fat* led to vein loss. Because the Epidermal Growth Factor Receptor (EGFR) signaling pathway promotes dorsal cell fate in the third instar wing discs[238-240] and regulates vein formation[68] in the pupa wing, and Atrophin[68], a negative regulator of EGFR signaling, can bind to Fat intracellular domain[69], Fat might promote EGFR signaling by inhibiting Atrophin function. However, as the *fat* mutation did not significantly influence D/V Wg expression, Fat may not modulate EGFR signaling significantly during normal wing development, although it might play crucial roles under other developmental contexts.

Introduction

As we have shown and discussed previously, Fat signaling regulates various target genes through the Hpo/Wts/Yki pathway (Chapter II, III and IV), e.g. proteins involved in cell death and growth regulation (Cyclin E, DIAP1[249-251]), microRNA mediated gene silencing (bantam[126,252-254]), genes regulating other pathways (Wingless, Serrate[11], Dally and Dally-like[255], E-Cadherin[207]). Fat also has an input to PCP determination via a different cascade, as implied from the Wts rescued *fat* and *ex* mutants (Chapter III).

Understanding the direct interactions between Fat signaling with other pathways will provide more information in elucidating the biological functions of Fat. During the manipulation of *fat* mutation and Fat overexpression, a few lines of evidence suggested a direct interaction of Fat signaling with the EGFR pathway. More experiments are necessary to confirm this hypothesis by identifying the biochemical basis, and the biological significance should be determined under different developmental contexts.

Results and discussion

In order to visualize Fat protein on apical membrane in wing epithelia, Fat was tagged on C-terminal with EGFP (enhanced green fluorescent protein)[294] and expressed in various ways. First, C-terminal tagged Fat was put under the control of traditional UAS promoter[291]. When uniformly expressed with *tub-Gal4* drive both wild type[67] and Fat:GFP rescued *fat* mutants (Figure 3*E* and data not shown), suggesting that the Fat:GFP was functional. These animals were largely normal, except for narrower cross vein spacing, ectopic vein material, very subtle, if any, PCP phenotype on wings or abdomen (Figure 3*E*, *F* and data not shown). These phenotypes might be the results of gain of function of Fat, because it was similar to *fj* mutants and overexpression of Ds or Fj (Chapter IV, Figure 2). Surprisingly, without Gal4 driver, *UAS-fat:GFP* transgene also rescued *fat* mutants (Figure 3*G*, *H*), because Fat:GFP was expressed at very low level (data not shown). These rescued animals appear normal, except for shorter cross vein spacing, partial loss of cross vein material and PCP henotype, indicating that Fat level was not enough to restore all Fat functions.

These observation are consistent with the knowledge that Fat signaling regulates distal-proximal patterning (as indicated by cross vein spacing) and PCP[9,25], because both loss of Fat function (Figure 3*G*) and gain of Fat activity (Figure 3*C*) produced similar effects in cross vein spacing. However, gain of function and loss of function of Fat showed opposite effects on vein formation (compare Figure 3*C*, *E* and *G*), more Fat activity inducing ectopic vein formation and loss of Fat resulting in vein loss. Changes in Ds and Fj gradients also showed ectopic or loss of vein by influencing the Fat activity (Chapter IV, Figure 2). As discussed in Chapter III, Fat regulates growth mainly through the Hpo/Wts/Yki pathway, and regulate PCP through permissive transcriptional targets and an unknown PCP branch. Fat might also regulate vein formation through these pathways. In Chapter III, I showed that overexpressiong of Wts partially rescued growth phenotypes of *ex* mutants. In these rescued animals, the PCP, leg length and segmentation, and cross vein spacing were mostly indistinguishable from wild type flies, except vein phenotypes, i.e. vein loss in posterior domain and ectopic vein in anterior domain (Chapter III, Figure 1). These vein phenotypes in the Wts rescued *ex* mutants were similar to the Wts rescued *fat* mutants. Because transcriptional activity of Yki in these mutants was believed to be largely restored to normal situation by Wts, vein formation is probably regulated by Fat and Ex through a transcriptional independent pathway. It is also possible, though less likely that vein formation is mediated by certain transcriptional targets of the Hpo/Wts pathway, but is not fully restored to normal in Wts rescued *fat* and *ex* mutants.

When traditional ectopic clones of UAS-*fat* (data not shown) or *UAS-fat:GFP* was generated[17] in wing discs, dorsal/ventral (D/V) Wingless (Wg) was influenced. Wg was induced on the dorsal side of ventral clones and adult wings were notched, a classical

Notch phenotype (Figure 4*A*, *B*, *D*). Although clones were not marked on the adult wings (Figure 4*D*), ectopic vein was obviously formed on the wings carring Fat overexpressing clones, which was consistent with the phenotypes observed when Fat:GFP was uniformally expressed with *tub-Gal4* (Figure 3*C*). D/V Wg was turned on by Notch signaling along the D/V boundary where Notch signaling is enhanced via Fringe induced ligand sensitivity[4,295,296]. Serrate from dorsal cell cells activates Notch on the ventral cells and Delta from ventral cells activates Fringe modified Notch on the dorsal cells, thus cells on D/V boundary have highest Notch signaling which activates Wg expression[4,46,295]. Because ectopic Wg was only induced in ventral clones of UAS-Fat which mimics Serrate or Fringe ectopic clones[4], overexpression of Fat might turn on the transcription of Serrate or Fringe, or might simply promote dorsal cell fate. Staining of dorsal cell marker dLMO[240,270,297,298] showed that Fat ectopic clones in ventral domain induced dLMO expression (Figure 4*C*), thus overexpression of Fat in ventral domain switched cells to dorsal cell fate. Serrate and Fringe were presumably induced in these ectopic dorsal cells, new D/V boundary and Wg were therefore generated once these cells were surrounded by ventral cells (Chapter I, Figure 1D). Theoretically, Wg will be induced in both contacting dorsal and ventral cells all around the ectopic Fat clones whenever dorsal cells and ventral cells meet. However, Wg was only induced in normal ventral cells outside of Fat ectopic clones (Figure 4*A*, *B*), suggesting that these clones might express Serrate which activated Notch on the surrounding ventral cells, but Fringe might not be expressed in the clones so that Delta on the surrounding ventral cells could not activate Notch inside of the clones. On the other hand, Wg was induced at higher levels in the cells closer to normal D/V boundary (Figure 4*A*, *B*), which could be caused by gradient expression of

Serrate in Fat ectopic clones. Careful examination of Fringe and Serrate expression in Fat overexpressing clones will be helpful in the future to address this issue.

How overexpression of Fat changes ventral cell fate is not clear. One possible explanation is that Fat-ICD binds to Atrophin[69] and excessive Fat-ICD may titrate out or inhibit Atrophin's function as a nuclear corepressor[70]. Because Atrophin negatively regulates epidermal growth factor receptor (EGFR) signaling in *Drosphila* [68] and EGFR has been shown to promote dorsal cell fate in wing discs by inducing Apterous expression[238,239,299] and inhibiting Delta expression[68], overexpression of Fat in ventral cells may promote dorsal cell fate by inhibiting Atrophin[70] and increasing EGFR signaling. In adult wing, activation of EGFR signaling has been shown to promote vein cell fate[300] and induces ectopic vein, while loss of EGFR signaling resulted in vein loss[68]. Overexpression of Fat therefore will increase EGFR signaling and induce vein formation, and mutation of *fat* will decrease EGFR signaling and inhibit vein formation.

However, how nuclear protein Atrophin was tethered or inhibited by membrane protein Fat is unknown. We previously showed that Serrate was turned on in *fat* mutant clones in leg discs via the Hpo/Wts pathway[11]. The influence of ectopic Fat on D/V Wg may not be mediated by the Hpo/Wts pathway, because manipulation of its activity in both directions did not affect D/V Wg (data not shown). The interaction of Fat with EGFR signaling may be a new function of Fat signaling. Besides dorsal cell fate determination and wing vein formation, EGFR signaling have been involved in various developmental processes[301], e.g. adult midgut progenitors (ancestors of intestinal stem cells)[302], R3/R4 determination in eye[265], cell alignment and intercalation in tracheal placode[303], and even in *Drosophila*

sleep[304]. Understanding the input of Fat signaling in EGFR pathway will also provide valuable information to dissect Fat functions.

3. Subcellular localization of Fat protein.

Summary

Interpretation of Ds and Fj gradients at molecular level is critical in understanding the mechanism of Fat signaling transduction[76]. Mutation of *dachs* suppresses all the growth phenotype and most of PCP phenotype of *fat* mutants[9,10], indicating that Dachs mediates almost all Fat signals. As Dachs protein is polarized in wing disc epithelia along distal-proximal axis[10] and is influenced by Fj and Ds gradients[87], the interpretation of Ds and Fj gradients by Fat is proposed to work in a similar way as the non-canonical Wnt pathway[87,183]. However, it was unknown whether Fat protein is also polarized as Frizzled[241] or Flamingo[242] in the wing disc epithelia. To visualized Fat protein subcellular localization, epitope tag V5 was inserted into Fat N-terminal after the signal peptide and Flag was fused to Fat C-terminal in the *fat* genomic rescue constructs. When total Fat protein level was kept uniform in wing discs, the mosaic clones of V5:Fat did not show polarized distribution in wing epithelia. Because the Dachs polarization requires Fat and is influenced by Fj and Ds gradients[10,87], the uniform distribution of V5:Fat might suggest a significant functional asymmetry for Fat in individual epithelium. Future experiments will be needed to show which of Fat functions, growth or PCP regulation, is asymmetrical along the proximal-distal axis and is mediated by Dachs polarization.

Introduction

Gradient concept has been widely used to explain various problems in developmental biology[256], e.g. establishment of animal body plans during embryos genesis[257], patterning

and growth regulation of *Drosophila* wings [258], axon projections in visual system[259,260], however, how it works at molecular level is not fully understood. Various models have been proposed to explain how gradient information is interpreted at cellular level (for review see ref. [261]). For instance, the perception of Dpp and Wg gradients requires cell autonomous transcriptional activity induced by their signals transduction[183,262], while in the non-canonical Wnt signaling pathway, Wnt gradient information was interpreted at cell surface without transcriptional contribution[241,263-266]. Shallow gradient slope of the potential ligand(s) is amplified by a lateral signaling across adjacent cells, which leads to the polarized distribution of various proteins in the pathway including receptor Frizzled[266]. Dachs is downstream of *fat* and mediates almost all functions of Fat [10,87]. Ectopic clones of tagged Dachs has been shown asymmetrically distributed on the apical membrane in wing epithelia and was influenced by the Ds and Fj gradients[10,87]. It appears that perception of the Ds and Fj gradients is probably performed by a similar mechanism as the non-canonical Wnt pathway. In order to show whether Fat receptor itself is also asymmetrically localized on cell membrane as Dachs, Fat protein was tagged and examined with various techniques.

Results and discussion

Interpretation of morphogen gradients has been shown to be involved in various mechanisms[183,256,261]. How Fat interprets Ds and Fj gradients is a key to understanding Fat signaling. Dachs was shown to be downstream of Fat and to mediate almost all Fat functions[9-11]. Dachs protein is asymmetrically localized on the distal side of epithelial membranes in the wing pouch and is influenced by Ds and Fj gradients[10,87]. Because

Dachs was uniformly distributed on cell membranes when Fat was removed (Chapter IV), polarization of Dachs suggests asymmetrical signal input from Fat. Fat therefore might be polarized in a way similar to Frizzled receptor during non-canonical Wnt signaling[241,263,266,305,306].

To show Fat protein subcellular localization in wing epithlia, Fat was tagged in both UAS constructs[307] and genomic rescue constructs (Chapter IV). With the traditional "flip-out" technique, ectopic clones of UAS-Fat:GFP were induced. Beside the above Wg phenotypes, Fat:GFP fusion protein was localized on the apical membrane of wing epithelia, without obvious asymmetrical distribution along proximal-distal axis. In order to test whether the Fat signaling is transduced in the normal way when Fat was overexpressed, tagged Dachs was coexpressed in Fat:GFP clones. It appeared that Dachs was still polarized even when Fat:GFP was overexpressed (data not shown), suggesting that Fat signaling is asymmetrical even though Fat itself is uniformly distributed on apical membrane. To further validate this observation, UAS-Fat:GFP was examined without Gal4 driver because of its leaky expression which partially rescued *fat* mutants (Figure 3*G*), even though this amount of Fat:GFP was barely seen under fluorescence microscope. The faint GFP signal was uniformly distributed on apical membrane, consistent with overexpressed Fat:GFP.

To visualize Fat subcellular distribution without influencing Fat signaling activity, Fat should be labled at its endogenous level in mosaic clones. *V5:fat* genomic rescue transgene (Chapter IV) was therefore combined with *FRT* to generate mosaic clones on wing pouch (Figure 5*A*)[16]. The background cells carried one copy of *V5:fat* and mosaic clones had either two copies of *V5:Fat* or no *fat* transgene. On the edges of V5:Fat minus

cells, only the membrane of V5:Fat plus cells could be visualized by anti-V5 staining (Figure 5*B* and *C*). The amount of V5 staining was relatively uniform along proximal-distal axis when more than 20 clones were examined. Because the total amount of Fat protein was not even on the edges of the clones, which might influence Fat signaling activity, Dachs protein should be co-expressed simultaneously to monitor whether Fat signaling is still polarized.

In order to visualize Fat protein in mosaic clones at its endogenous level and with uniform expression of total Fat on wing discs, N- and C-terminals of Fat were tagged in *fat* genomic rescue constructs. Both tagged Fat and wild type Fat were positioned in trans on the same chromosome arm so that mosaic clones generated by FRT technique[16] will not change total Fat level on wing discs (Figure 5*D*). These clones were induced with traditional Flipase/FRT technique and Fat protein was visualized by anti-tag staining. In wild type discs, tagged Fat was localized on apical membranes and overall expression level of Fat was uniform on wing pouch as indicated by Fat-ICD staining (Figure 5*E*, *E'*). Inside of V5:Fat clones, more signal was observed because of contributions from two adjacent cells. Anti-V5 staining showed that V5:Fat level was relatively uniform around the edges of V5:Fat minus cells. These clones were examined for V5:Fat and the C-terminal has not been well studied becaue V5:Fat:Cherry and V5:Fat:Flag were not readily visualized by fluorescence or anti-Flag staining. As shown in Chapter IV, Fat is cleaved after translation, and the extracellullar and intracellular parts are associated as heterodimers. It is not clear whether N- and C-terminals of Fat are complexed in 1:1 ratio and whether this ratio is influenced by upstream signaling at cellular level, although Fat-

ICD is uniformly distributed. Futher efforts should be taken to show whether Fat C-terminal distribution on apical membrane is similar as Fat N-terminal.

Uniform distribution of Fat at a cellular level, however, does not exclude the possibility that signals from Fat-ICD are significantly asymmetrical in the proximal-distal axis (Figure 5*F*), because polarization of Dachs requires Fat and is influenced by Ds and Fj[10,87]. In this model, gradient information of Ds and Fj in the proximal-distal axis is somehow amplified, which leads to the dramatic polarization of Fat activity, i.e. conformation change and/or phosphorylation of Fat-ICD. However, to directly visualize Fat-ICD activity in the wing pouch requires more knowledge of Fat activity and reagents for imaging. In another model, signals from Fat-ICD may be only slightly asymmetrical and an unknown mechanism therefore is proposed to amplify this subtle difference, probably in a similar manner as in the non-canonical Wnt pathway (Chapter I, Figure 1B and C) [57,241,266], to enrich Dachs on distal side of epithelia (Figure 5*G*).

Interpretation of gradient information in Dpp and Wg pathways has been shown to require transcriptional activity of their signal transduction[183,262]. Although it is less likely that polarization of Dachs on apical membranes requires transcriptional activity of Fat-Wts-Yki signaling, further experiments will be possible to clarify this issue. It is totally unknown how this amplification mechanism works during Fat signaling, however, dissection of Dachs functions[9-11] and its biochemical interaction with App[88] might be able to provide more insights.

4. Subcellular localization of Hippo and Warts in wing epithelia.

Summary

Because Wts [243] and Hpo [244,245] have been implicated in different functions, subcellular localization of Wts and Hpo therefore need careful examinations at their endogenous levels. To approach this goal, epitope tags were inserted into the C- and N-terminals of Wts and Hpo in their genomic rescue constructs, and transgenic flies were generated with phiC31 integrase mediated transgenesis[179,215,246]. The tagged Wts and Hpo fully rescued the *wts* and *hpo* mutants, respectively, therefore can be used to visualize Wts and Hpo subcellular localization.

Introduction

The transcriptional coactivator Yki was shown to translocate between cytoplasmic domain and nucleus during signal transduction from Wts[119,120]. However, the subcellular location where Wts phosphorylates Yki is not clear. In imaginal disc epithelia, the upstream regulators of the Hpo/Wts pathway, Fat[10,69], Ex[12,171,194,203] and Mer[109,194,267]are localized on the cytoplasmic membrane. The Hpo was also shown to regulate dendrite development in peripheral sensory neurons, probably independent of Yki [244,245]. Work in other tissues showed that YAP is required for maintaining proper neural progenitor cell [130] or germline cell [268] numbers. How the Hpo/Wts signaling is transduced in neurons and neural progenitor cells is one of the major goals of this project.

On the other hand, examination of the subcellular localization of Wts will be an approach to address whether polarized signals from Fat-ICD, indicated by asymmetrical subcellular

distribution of Dachs on the distal-proximal axis[10,87], is responsible for growth regulation which appears to be mediated by Wts stability (Chapter II, III and IV)[11,12].

To address these issues, small epitope tags or fluorescence protein were fused to Hpo and Wts on either ends in their genomic rescue constructs. The fluorescence fusion proteins are expected to be self-telling without antibody staining, given that they are as functional as their wild type counterparts. One advantage of smaller epitope tags is their minimum interruption on normal protein folding, and thus most likely generating proteins with normal functions. Smaller tags also provide more flexibility to visualize proteins with different methods so as to meet various experimental requirements.

Results and discussion

To visualize Hpo and Wts subcellular localization, tags were inserted into N- and C-terminals of Hpo and Wts in their genomic rescue constructs (Figure 6*A*, *B*). All Hpo constructs were injected into flies with phiC31 integrase-mediated transgenesis [179,215,216,246] to generate transgenic animals. All fusion proteins of Hpo were fully functional because they completely rescued *hpo* mutant animals to adults without any visible phenotypes. Traditional Gal4-UAS system usually expresses Hpo at higher levels that lead to cell death and thus precluding imaging overexpressed Hpo protein at subcellular domains[11,249-251,308]. These genomic constructs, however, will presumably express tagged Hpo at endogenous levels (need to be confirmed by Western blotting) and therefore can be used for visualizing Hpo localization or for further modifications, e.g. studying Hpo phosphorylation. In S2 cells, Hpo appeared to be exclusively localized in cytoplasmic domain (Figure 6*C*). In wing epithelia, both N- and C-terminal tagged Hpo

were uniformly expressed and localized, preferentially, on the apical regions (Figure 6*D*, *D*'), consistent with the proposed function and localization in mediating Ex and Mer signaling[113,204]. Hpo:Cherry fusion protein was unable to be visualized in wing discs, probably because of its low expression level, or inefficient photon productivity, though Cherry has been shown as an excellent fluorescence protein with extended photostability[294,309]. Similar issues also occured to Fat:Cherry. In the future, other fluorescent proteins with higher brightness and reasonable photostability, e.g tdTomato (tandem dimer), EGFP (weak dimer), or mCitrine (monomer)[294], will be fused with Wts, Hpo or Fat.

Immediate experiments with these tagged Hpo will include examination of its subcellular localization in *fat* and *ex* mutant mosaic clones, localization of Hpo in non-epithelial cells (e.g. neurons, neural progenitor cells and germline stem cells), co-localization of Hpo and other proteins like Ex, Fat and Mer. Although Hpo localization and its alterations in certain genetic conditions will indicate its functional relevance, these experiments will not address how Hpo is regulated by Ex or Fat. Identification of the underlying molecular basis will be the key to shed light on the Hpo/Wts signaling. In the future, when enough tagged Hpo can be isolated from imaginal disc lysate (e.g. isolate imaginal discs at large scale with differential centrifugation [233]), post-translational modifications of Hpo could be studied with mass spectrum as has been done in *Drosophila* embryos[310].

N- and C-terminal of Wts were tagged with Myc and V5 respectively (Figure 6*B*) in its genomic rescue constructs and transgenic animals were generated with phiC31 integrase-mediated transgenesis [179,215,216,246]. Myc:Wts and Myc:Wts:V5 transgenes fully rescued *wts* mutants wts^{X1}/wts^{P2} to adults with normal morphologies. In transfected S2 cells, Wts

was exclusively localized in cytoplasmic domain (e.g. Myc staining in Figure 6*E*). However, staining with antibodies to the epitope tag Myc and V5 did not show good signals in wing discs, which resembles the Wts antisera staining (Chapter II), suggesting that both ends of Wts probably are inaccessible to antibody. The N- and C-terminals of Wts might be buried inside of Wts 3D structure, or Wts itself is coated by other proteins, e.g. Hpo, Sav, Mats, Ex, Dachs. To address this issue, Wts can be fused to a fluorescent protein so that the fusion protein will be readily visualized by fluorescent imaging. Wts:Cherry construct was generated for this purpose, but, unfortunately, so far the construct has not been inserted into chromosomes. More efforts are being taken to inject Wts:Cherry construct and in the future other fluorescent proteins with better brightness will be fused to Wts[294,309,311].

More experiments can be done with this new versions of tagged Wts transgens. Here are a few examples. First, Wts stability/level can be re-evaluated with tagged Wts at endogenous level and in tissue staining. Second, it will be possible to test whether Wts is also asymmetrically stabilized, because Dachs mediates almost all Fat functions[9-11], is required for Wts degradation[11] and is polarized in proximal-distal axis[10,87]. If Wts is polarized in the same way as Dachs, it will be a proof of the model that asymmetrical Fat signaling regulated growth via Wts/Yki pathway[10,25,87].

Figures

Figure 1. Analysis of *Drosophila* Fat function from protein evolution.

Phylogram tree of Fat intracellular domains from insect Fat and vertebrate Fat4, and phylogram tree of *Drosophila* Fat and four human Fat intracellular domains (A). Constructs of *Drosophila* Fat and human Fat intracellular domain hybrids (B). Strategies to assay functions of human hybrid Fats in *Drosophila* (C).

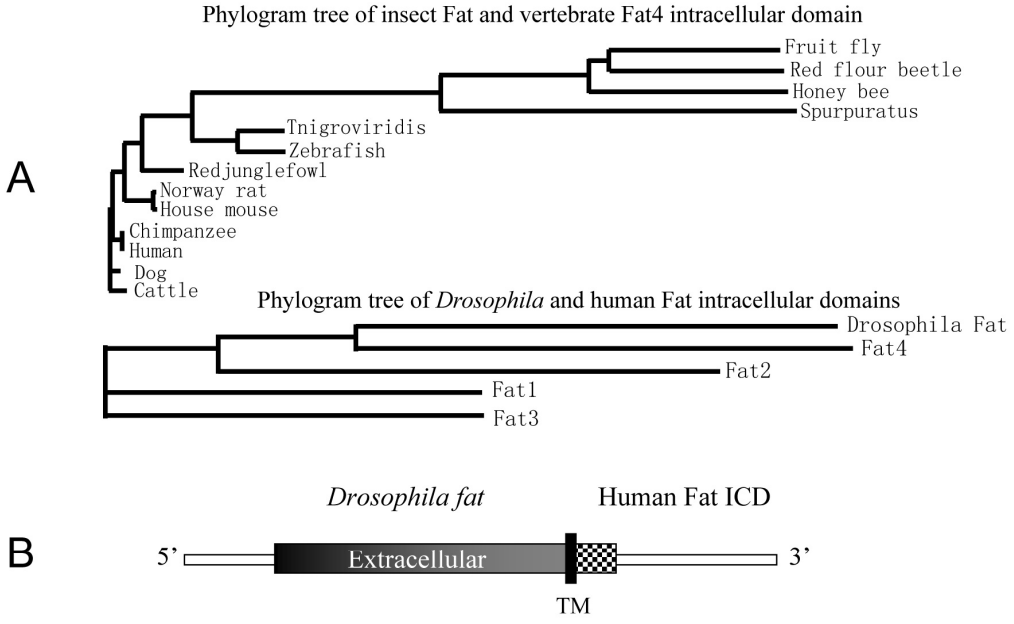

C

Growth regulation assay: $\frac{ft^{8}}{ft^{Grv}};\frac{human.fatICD.hybrid}{+}$

PCP assay: $\frac{UAS-Mycwtsft^{8}}{ft^{Grv}};\frac{human.fatICD.hybrid}{tub-Gal4}$

Figure 1

Figure 2. Human Fat intracellular domain hybrids transduce planar cell planarity signal in *Drosophila*.

Female adults (A, E, I, M, Q), wings (B, F, J, N, R), wing PCP (C, G, K, O, S) and PCP on abdominal epidermis (D, H, L, P, T) were aligned for wild type (A-D), Wts rescued *fat* mutants (E-H), Wts and human Fat2 (n>5, I-L), Fat3 (n=3, M-P) and Fat4 (n>10, Q-T) hybrids rescued *fat* mutants. *UAS-Myc:Wts* was overexpressed with *tub-Gal4* driver. Ectopic and vein loss were observed in all *fat* mutants even though Wts was overexpressed in (F, J, N, R). Cross vein spacing was shorter in all *fat* mutants(B, F, J, N, R), although was partially rescued by human Fat4 hybrid (R). Wing PCP phenotype was stronger in Wts rescued *fat* mutants (G) and weaker in Wts and human Fat ICDs rescued *fat* mutants (K, O, S). PCP phenotype was stronger in Wts rescued *fat* mutants (H), but dramatically weaker in Wts and human Fat2 and Fat3 ICDs rescued *fat* mutants, and largely normal in Wts and human Fat4 ICD rescued *fat* mutants. Pictures in the same column were taken with the same magnification.

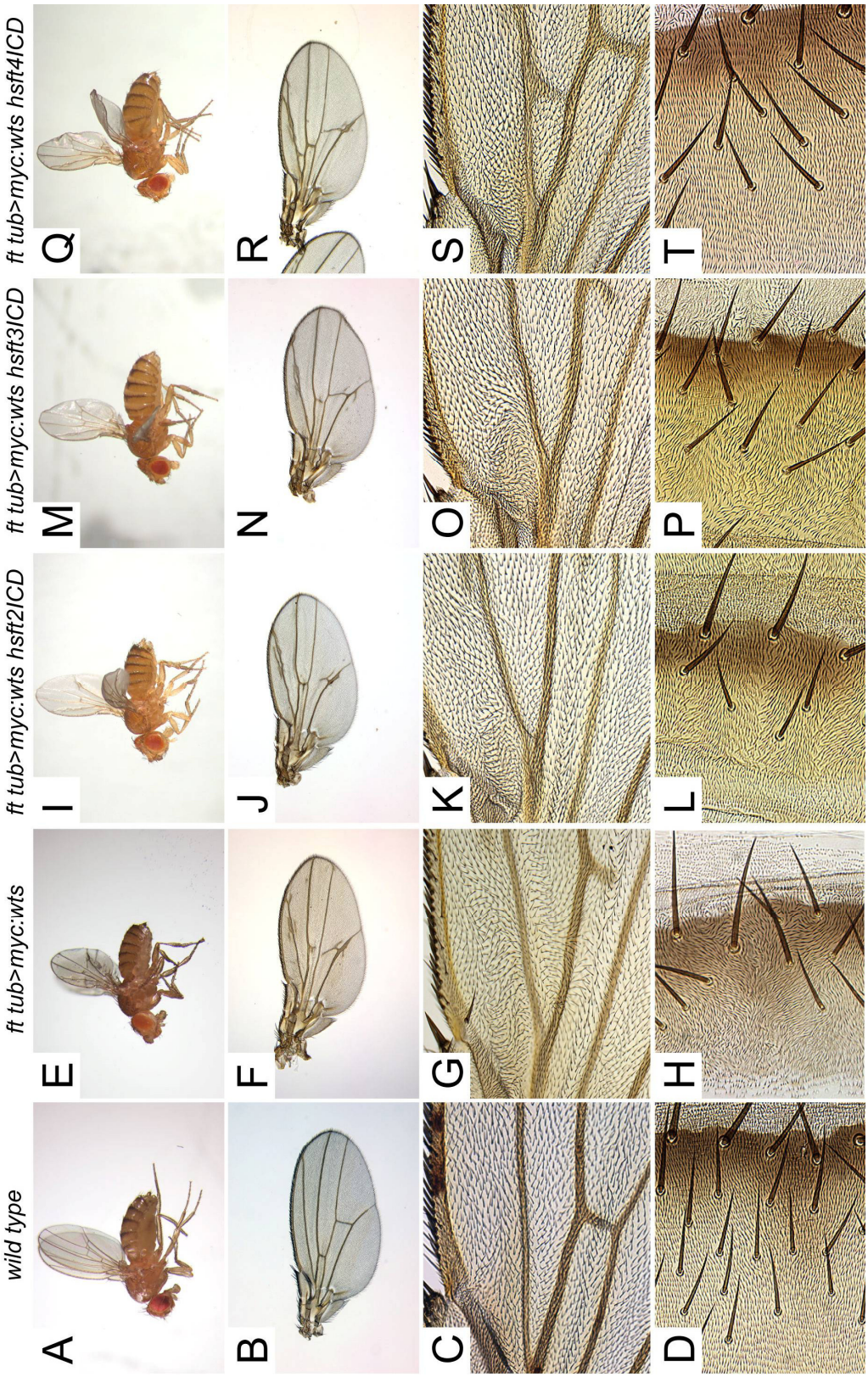
wild type
ft tub>myc:wts
ft tub>myc:wts hsft2ICD
ft tub>myc:wts hsft3ICD
ft tub>myc:wts hsft4ICD
A
B
C
D
E
F
G
H
I
J
K
L
M
N
O
P
Q
R
S
T

Figure 2

Figure 3. Overexpression of Fat induces ectopic vein.

Wings from wild type (A, B), *tub-Gal4 UAS-fat:GFP* (C, D), fat^{Grv}/fat^{8} *tub-Gal4UAS-fat:GFP*(E, F), fat^{Grv}/fat^{8} *UAS-fat:GFP*(G, H) are aligned to show wing size, cross vein spacing (A, C, E, G), and PCP (B, D, F, H). Cross vein spacing was significantly narrower when Fat:GFP was overexpressed in wild type background (C) or in *fat* mutants (E) where ectopic vein was also induced. Without *tub-Gal4*, *UAS-fat:GFP* rescued *fat* mutants, however the cross vein spacing was narrower and cross vein material was partially lost (G). PCP in the wings from *tub-Gal4 UAS-fat:GFP* (D) and fat^{Grv}/fat^{8} *UAS-fat:GFP* (F) was normal. Obvious PCP phenotype was observed in wings from *tub-Gal4*, *UAS-fat:GFP* (H).

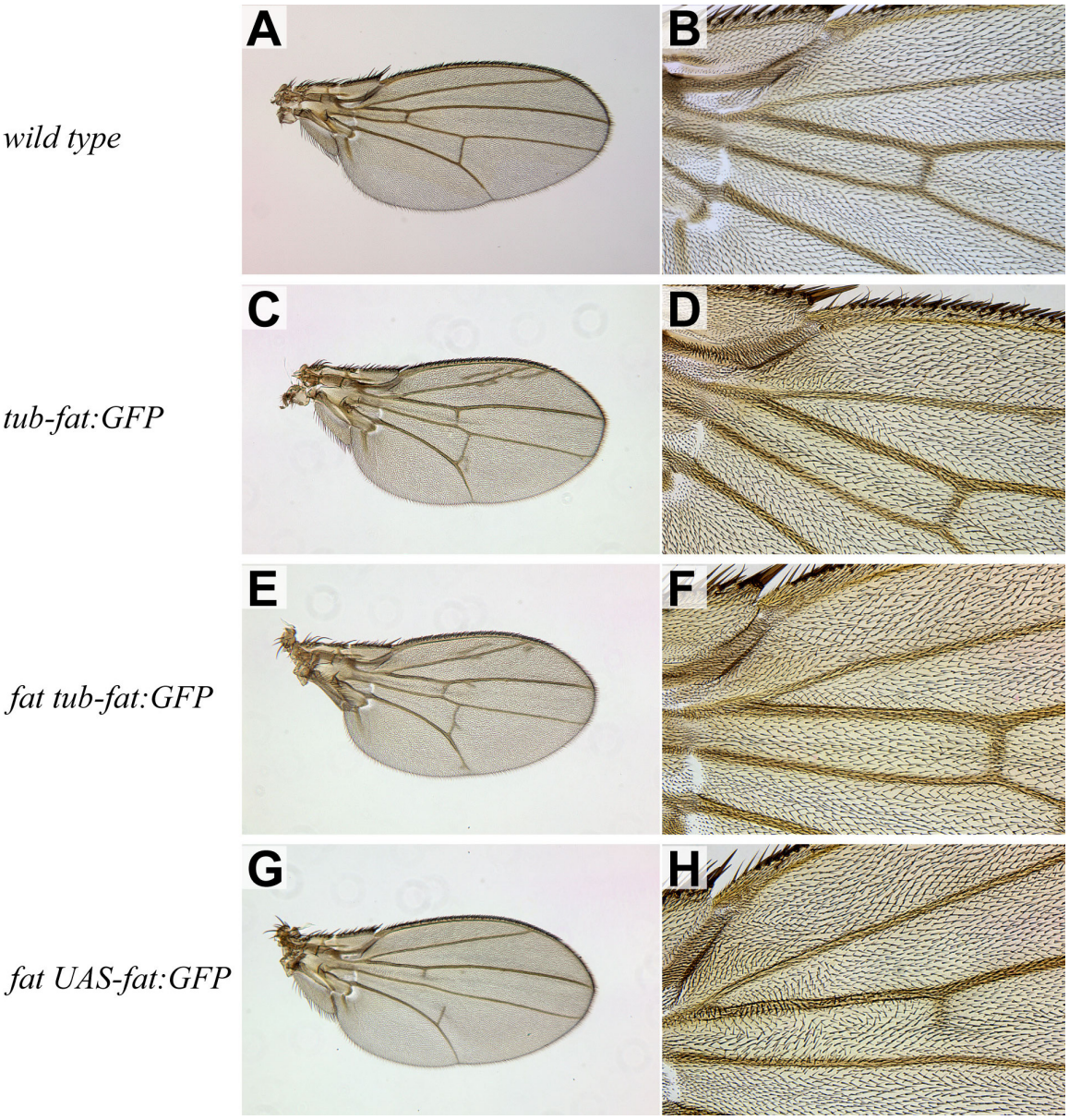

Figure 3

Figure 4. Overexpression of Fat promotes dorsal cell fate in wing discs.

Ectopic clones of UAS-Fat:GFP in the ventral side of wing pouch induce dLMO autonomously (C-C") and induce Wingless on the dorsal side of the clones (A-A", B-B"). Clones of ectopic Fat:GFP violated dorsal/ventral compartment boundary (B-B") and induced Notched wing phenotype (D). All wing discs are positioned dorsal up and ventral down. Ectopic vein material was also formed in these wings (D). Overexpression of Fat might promote EGFR signaling by suppressing Atrophin, an inhibitor of EGFR signaling, thus leading to the expression of Apterous in ventral cells. Apterous turns on dorsal cell markers dLMO, Serrate and Fringe and thus leading to the transition of ventral cells to dorsal cells.

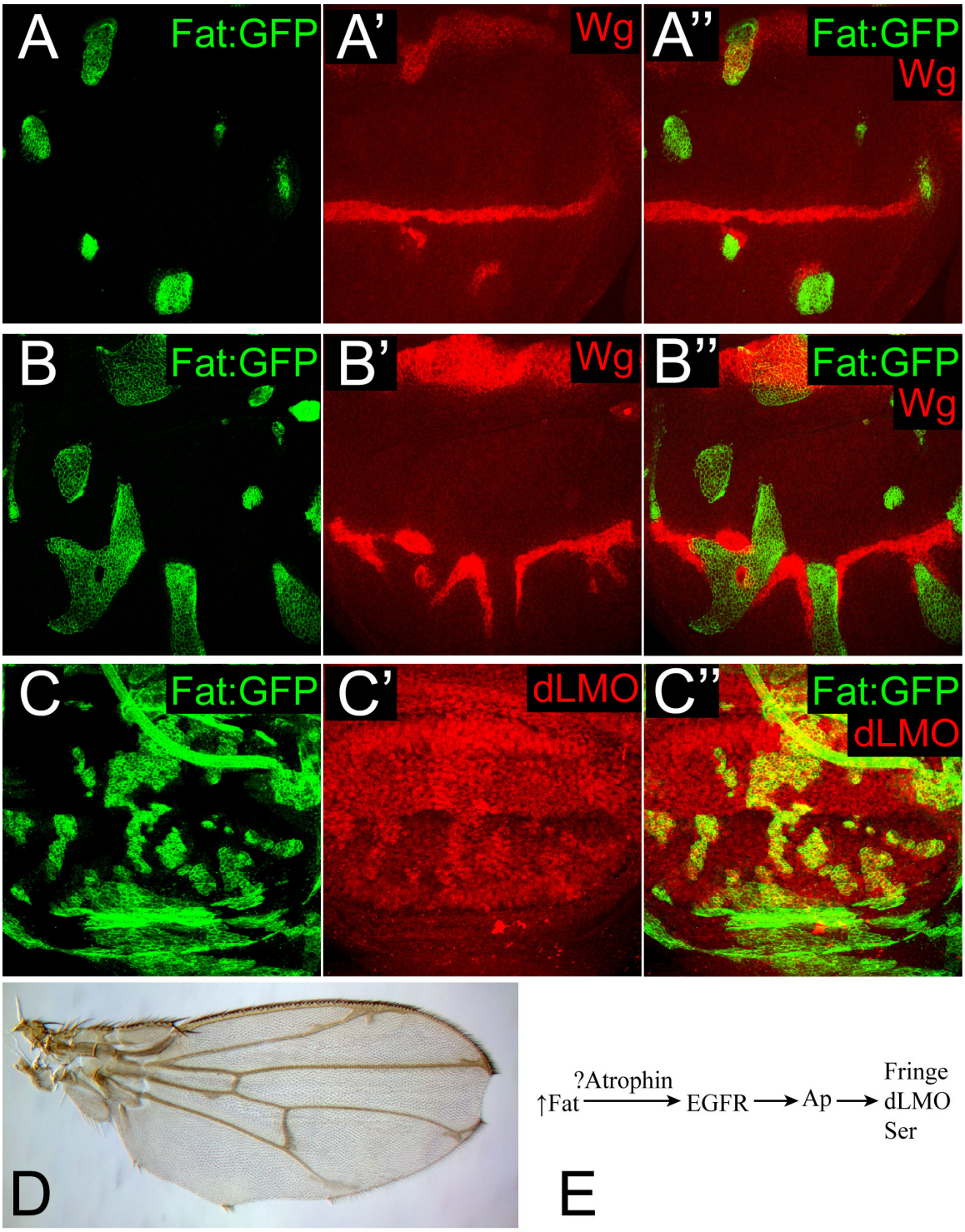
A
Fat:GFP
A'
Wg
A''
Fat:GFP
Wg
B
Fat:GFP
B'
Wg
B''
Fat:GFP
Wg
C
Fat:GFP
C'
dLMO
C''
Fat:GFP
dLMO
D
?Atrophin
↑Fat
EGFR
Ap
Fringe
dLMO
Ser
E

Figure 4

Figure 5. Fat protein is not polarized along proximal-distal axis in wing disc epithelia. Mosaic clones of N-terminal tagged *V5:fat* (*A*-*C*) or both N- and C-terminal tagged *V5*:*fat*:*Cherry* (*D* and *E*) were generated in wing discs by FLP/*FRT* system. *fat* genomic rescue constructs were inserted on 3L (left arm of chromosome 3) and combined with *FRT80* located on proximal side of 3L. Wild type *fat* locus (2L) was not shown in (A and D). In (*A*-*C*), *V5*:*fat* was put in trans with normal chromosome so that mosaic clones have either no or two copies of. *V5*:*fat*. In (*D* and *E*), *V5*:*fat*:*Cherry* was in trans with an un-tagged wild type *fat* so that mosaic clones will carry either two copies of *V5*:*fat*:*Cherry* or two copies of un-tagged *fat*. Tagged Fat was visualized by anti-V5 staining and no obvious difference in distribution on proximal and distal sides along the edges of un-tagged *fat* clones (indicated by arrows and arrowheads). When clones were induced in (*D* and *E*) , total Fat was uniform across wing pouch as shown by anti Fat intracellular staining (*E*'). One model is that the difference of Fat activity on the membrane of an epithelium along proximal-distal axis is somehow amplified so that Fat activity, not total Fat protein, is significantly polarized (shown by thickness of arrows in *F*), which promotes the accumulation or stability of Dachs on distal side of the cell. Alternatively, the activity of Fat is subtly different on the proximal and distal sides of an epithelium which is amplified for Dachs distribution by a different mechanism, e.g. exclusive distribution of unknown factors on the proximal or distal sides (*G*).

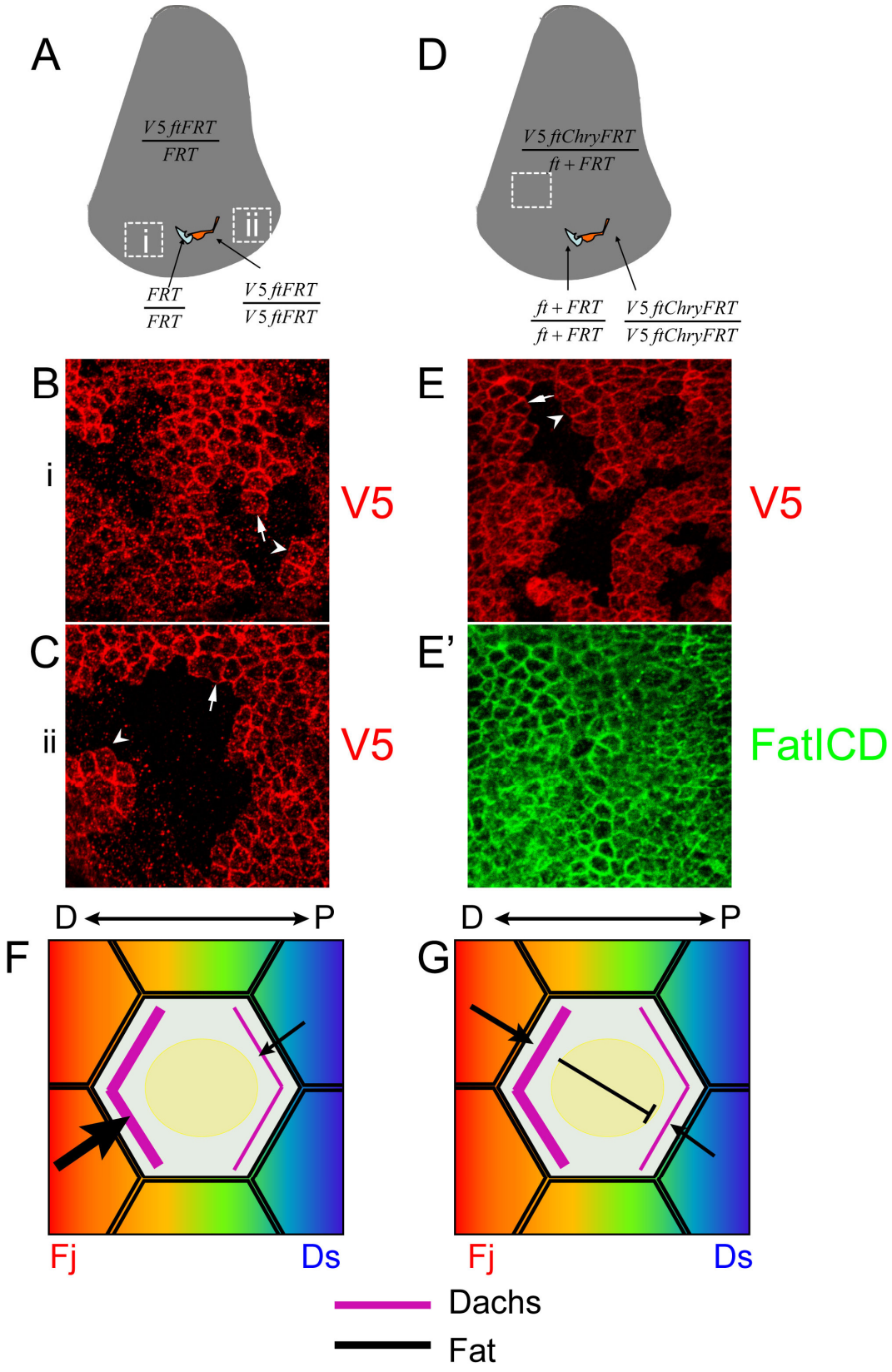
A
V5 ftFRT / FRT
i
ii
FRT / FRT
V5 ftFRT / V5 ftFRT
D
V5 ftChryFRT / ft + FRT
ft + FRT / ft + FRT
V5 ftChryFRT / V5 ftChryFRT
B
i
V5
E
V5
C
ii
V5
E'
FatICD
D
P
F
Fj
Ds
D
P
G
Fj
Ds
Dachs
Fat

Figure 5

Figure 6. Imaging Hippo and Warts subcellular localization.

Schematic illustration of tagged *hpo* (*A*) and *wts* (*B*) constructs are shown in lines (introns and non-coding regions) and boxes (exons). S2 cells transfected with Flag:hpo:V5 (*C*) and Myc:wts:V5 (*E*) were stained with anti Flag and anti Myc respectively. Both Wts and Hpo are exclusively localized in cytoplasmic region. In transgenic flies the tagged Hpo is mainly localized to sub-apical cell membrane in wing discs (*D* and its magnified region in D'), shown on the Z-section (*D*).

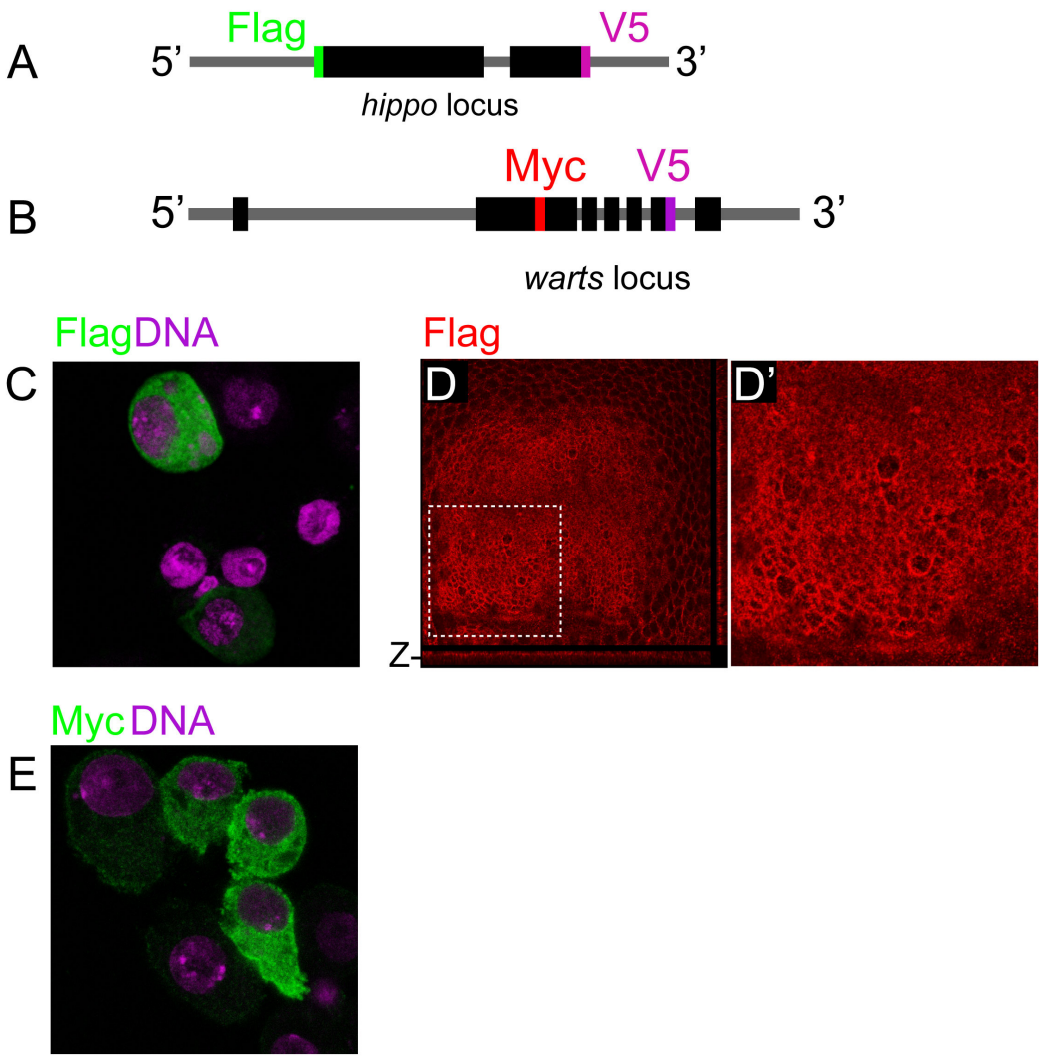
A
Flag
V5
5'
3'
hippo locus
B
Myc
V5
5'
3'
warts locus
FlagDNA
C
Flag
D
D'
Z
MycDNA
E

Figure 6

APPENDICES

1. Strategies to generate Fat intracellular domain truncates.

Construct	PCR template	Primers for 5' fragment		Primers for middle fragment		Primers for 3' fragment	
ft-STI	ft:FVH	ft_SPL_NotI5	ft_SPL_SOE3			ft_L2_SOE5	ft_FVH_XbaI3
ft-STI-1	ft-STI	ft_SPL_NotI5	STI_1_SOE			FVH_SOE5	ft_FVH_XbaI3
ft-STI-2	ft-STI	ft_SPL_NotI5	STI_2_SOE			FVH_SOE5	ft_FVH_XbaI3
ft-STI-3	ft-STI	ft_SPL_NotI5	STI_3_SOE			FVH_SOE5	ft_FVH_XbaI3
ft-STI-4	ft:FVH	ft_SPL_NotI5	STI_4_SOE			TM_SOE	ft_FVH_XbaI3
ft-STI-5	ft-STI	ft_SPL_NotI5	ft_TM3	STI_5_SOE_A	STI_5_SOE_B	FVH_SOE5	ft_FVH_XbaI3
ft-STI-6	ft-STI	ft_SPL_NotI5	ft_TM3	STI_6_SOE_A	STI_2_SOE	FVH_SOE5	ft_FVH_XbaI3
ft-STI-7	ft-STI	ft_SPL_NotI5	ft_TM3	STI_7_SOE_A	STI_3_SOE	FVH_SOE5	ft_FVH_XbaI3
ft-STI-8	ft-STI	ft_SPL_NotI5	ft_TM3	STI_8_SOE_A	STI_8_SOE_B	FVH_SOE5	ft_FVH_XbaI3
ft-STI-9	ft-STI	ft_SPL_NotI5	ft_TM3			STI_9_SOE	ft_FVH_XbaI3
ft-STI-10	ft-STI	ft_SPL_NotI5	ft_TM3	STI_5_SOE_A	STI_3_SOE	FVH_SOE5	ft_FVH_XbaI3
ft-STI-11	ft-STI	ft_SPL_NotI5	ft_TM3	STI_6_SOE_A	STI_3_SOE	FVH_SOE5	ft_FVH_XbaI3
ft-STI-12	ft-STI	ft_SPL_NotI5	ft_TM3			STI_5_SOE_A	ft_FVH_XbaI3
ft-STI-13	ft-STI	ft_SPL_NotI5	ft_TM3			STI_6_SOE_A	ft_FVH_XbaI3
ft-STI-14	ft-STI	ft_SPL_NotI5	ft_TM3			STI_7_SOE_A	ft_FVH_XbaI3
ft-STI-15	ft-STI	ft_SPL_NotI5	ft_TM3			STI_8_SOE_A	ft_FVH_XbaI3

ftSPL_NotI5: 5'-TCT GCG GCC GCA TGG AGA GGC TAC TGC TCC-3'

ftSPL_SOE3: 5'-TGA AGT TGA GAG TGC TTC TTC TTC GCG GAA AGG CGG CAT-3'

ftL2_SOE5: 5'CCG CGA AGA AGA AGC ACT CTC AAC TTC AAC AAA CAG CCC CTG-3

ftFVH_XbaI3: 5'-GG TCT AGA GAT CA GCG GGT TTA AAC TCA ATG GTG-3'

FVH_SOE5: 5'-ACC GAC TAC AAG GAC GAC GAC GAC AAG-3'

(Overlapping sequence: 5'-CGT CGT CGT CCT TGT AGT CGG TAC C-3')

STI-1-SOE: 5'- CGT CGT CGT CCT TGT AGT CGG TAC C AAG CGG CGG AAT GGG CAG GTG ATG-3'

STI-2-SOE: 5'- CGT CGT CGT CCT TGT AGT CGG TAC C TTC GCT GTT GCT GTG AAC GTC CTT-3'

STI-3-SOE: 5'- CGT CGT CGT CCT TGT AGT CGG TAC C CTC ACC ACC GCT TAG TGC TCT GGA-3'

STI-4-SOE: 5'-CTT CTT CGC GGA AAG GCG GCA TAT-3'

TM-SOE: 5'-GCC GCC TTT CCG CGA AGA AGA GCC GAT CCT CTC AGC ATT GGC TTC-3'

ft-TM3: 5'-CGA TAG ATA ACA TAG GAG CCC AGT-5'

(Overlapping sequence: 5'-GGG CTC CTA TGT TAT CTA TCG ATT C-3')

STI5-SOE-A: 5'- GGG CTC CTA TGT TAT CTA TCG ATT C CAG CAA CGT CCC CAG CGA CCC GAT-'3

STI6-SOE-A: 5’- GGG CTC CTA TGT TAT CTA TCG ATT C AGT GTT CCA CCT GTT TCC GCC TAC-3’

STI7-SOE-A: 5’- GGG CTC CTA TGT TAT CTA TCG ATT C CAC AGC AAC AGC GAA CGC AGT CTG-3’

STI8-SOE-A: 5’- GGG CTC CTA TGT TAT CTA TCG ATT C AAC AGT CTC AGT GGC GAC GGC AAG-3’

STI9-SOE: 5’- GGG CTC CTA TGT TAT CTA TCG ATT C AAT GGA GCC GCA TCC CCA TCG GCC-3’

(Overlapping sequence: 5’-CGT CGT CGT CCT TGT AGT CGG TAC C-3’)

STI5-SOE-B: 5’- CGT CGT CGT CCT TGT AGT CGG TAC C GGC CTT GTA TTT GCG TAG GCC AGC-3’

STI8-SOE-B: 5’- CGT CGT CGT CCT TGT AGT CGG TAC C ATT GGC CTT GCG GTA GAT ACC GCT C-3’

2. Primers to make Fat-ICD point mutants.

Primers for site directed mutagenesis in Fat intracellular domain.

Construct name	Amino acid change	Primer
C1	S4753A, S4754A, S4758A	5’ -C TAC GAC CTC GAG AAC GCC GCC GCC ATT GCT CCG GCC GAC ATT GAT ATA GTC TAT C-3’
C2	Y4766A	5’-GAC ATT GAT ATA GTC TAT CAT GCC AAG GGC TAT CGT GAG GCT G-3’
T1	S4796A, S4798A	5’-CG CAT CAC AAG CAT CAG AAC GCT GGC GCT CAG CAG CAG CAG CAG CAG-3’
T2	T4825A,S4826A, S4828A, T4830A	5’-GC CAA CCG CCA CCG CCG CCC GCC GCT GCA GCC CGC GCC CAT CAG AGC ACT CCA CTG-3’
T3	T4924A	5’-CAG CAA ACT TCC ATG GGC TTG GCC GCC GAG GAG ATT GAG AGA-3’
T4	S4939A, S4942A, T4943A	5’-AAT GGC AGA CCA CGA ACT TGT GCC CTA ATC GCC GCC CTG GAT GCC GTC TCC TCC-3’
T5	S4948A, S4949A, S4950A, S4951A	5’-ATC TCC ACC CTG GAT GCC GTC GCC GCC GCC GCT GAG GCG CCT CGA GTG TCG -3’
T6	S4973A, S4974A, T4975A, S4976A, 4977A	5’-GGT GGA GAT GTG GAT GCC CAT GCT GCG GCT GCC GCG GAC GAA AGC GGC AAC GAC-3’
T7	S4984A, T4986A, S4988A	5’-ACG GAC GAA AGC GGC AAC GAC GCC TTC GCG TGC GCG GAG ATC GAG TAC GAC AAT AAC-3’
T8	Y4992A	5’-TTC ACG TGC TCG GAG ATC GAG GCC GAC AAT AAC AGT CTC AGT GGC-3’
T9	S4781A, S4786A, Y4788A, T4789A	5’-GGC CTA CGC AAA TAC AAG GCC GCT GTT CCA CCT GTT GCC GCC GCC GCG CAT CAC AAG CAT CAG AAC TCT G-3’
T10	T4808A, T4813A	5’-CAG CAG CAG CAG CAC CGC CAC GCA GCT CCC TTT GTG GCC CGG AAC CAA GGT GGC CAA CCG-5’
T11	S4833A, T4834A	5’-AGT GCA TCC CGC ACC CAT CAG GCC GCT CCA CTG GCC CGA CTC TCG CCC-3’
T12	S4840A, S4842A, S4843A, S4846A, S4847A	5’-AGC ACT CCA CTG GCC CGA CTC GCG CCC GCC GCG GAG TTG GCT GCC CAG CAG CCG CGC ATT CTC ACT-3’
T13	T4870A, T4871A, S4872A, S4873A, S4874A	5’-CTG CAA AGT GCC CTG CTG GCC GCG GCC GCC GCT GCC GGT GGC GTT GGC AAG GAC GTT-3’
T14	S4883A, S4885A, S4888A, S4891A	5’-GGC GTT GGC AAG GAC GTT CAC GCC AAC GCC GAA CGC GCT CTG AAC GCC CCG GTT ATG TCG CAG CTG TCC-3’
T15	S4895A, S4898A, S4901A, S4902A, S4903A, S4905A	5’-AGT CTG AAC AGC CCG GTT ATG GCG CAG CTG GCC GGC CAA GCT GCC GCT GCC GCC AGG CAA AAG CCC GGA GTG CCA-3’
T16	T4919A, S4920A	5’-CCA CAG CAG CAG GCG CAG CAA GCT GCC ATG GGC TTG ACC GCC GAG GAG-3’
T17	S4957A, S4958A, S4959A, S4964A	5’-AGC AGT GAG GCG CCT CGA GTG GCG GCC GCC GCT CTG CAT ATG GCG CTG GGT GGA GAT GTG GAT GCC-3’
T18	S4996A, S4998A	5’-GAG ATC GAG TAC GAC AAT AAC GCT CTC GCT GGC GAC GGC AAG TAT TCC ACC-3’

T19	S5004A, T5005A, S5006A, S5008A	5’-CTC AGT GGC GAC GGC AAG TAT GCC GCC GCC AAG GCT CTC CTC GAT GGA CGC AGT CCC-3’
T20	S5014A, S5017A, S5021A	5’-AAG AGT CTC CTC GAT GGA CGC GCT CCC GTG GCC AGA GCA CTA GCC GGT GGT GAG ACG AGC AGA AAT-3’
T14D	S4883D, S4885D, S4888D, S4891D	5’-GGC GTT GGC AAG GAC GTT CAC GAC AAC GAC GAA CGC GAT CTG AAC GAC CCG GTT ATG TCG CAG CTG TCC-3’
T15D	S4895D, S4898D, S4901D, S4902D, S4903D, 4905D	5’-AGT CTG AAC AGC CCG GTT ATG GAC CAG CTG GAC GGC CAA GAT GAC GAT GCC GAC AGG CAA AAG CCC GGA GTG CCA-3’
T21	S4883A, S4885A, S4891A	5’-GTT CAC GCC AAC GCC GAA CGC AGT CTG AAC GCC CCG GTT ATG TCG-3’
T22	S4883A	5’-GGC GTT GGC AAG GAC GTT CAC GCC AAC AGC GAA CGC AGT CTG AAC-3’
T23	S4885A	5’-GGC AAG GAC GTT CAC AGC AAC GCC GAA CGC AGT CTG AAC AGC CCG-3’
T24	S4888A	5’-GTT CAC AGC AAC AGC GAA CGC GCT CTG AAC AGC CCG GTT ATG TCG-3’
T25	S4891A	5’-AGC AAC AGC GAA CGC AGT CTG AAC GCC CCG GTT ATG TCG CAG CTG TCC-3’
T26	S4895A	5’-AGT CTG AAC AGC CCG GTT ATG GCG CAG CTG TCC GGC CAA AGT TCC-3’
T27	S4898A	5’-AGC CCG GTT ATG TCG CAG CTG GCC GGC CAA AGT TCC AGT GCC AGC-3’
T28	S4901A	5’-GTT ATG TCG CAG CTG TCC GGC CAA GCT TCC AGT GCC AGC AGG CAA AAG-3’
T29	S4902A	5’-TCG CAG CTG TCC GGC CAA AGT GCC AGT GCC AGC AGG CAA AAG CCC-3’
T30	S4903A	5’-CAG CTG TCC GGC CAA AGT TCC GCT GCC AGC AGG CAA AAG CCC GGA-3’
T31	S4905A	5’-TCC GGC CAA AGT TCC AGT GCC GCC AGG CAA AAG CCC GGA GTG CCA-3’
T25D	S4891D	5’-AGC AAC AGC GAA CGC AGT CTG AAC GAC CCG GTT ATG TCG CAG CTG TCC-3’
T26D	S4895D	5’-AGT CTG AAC AGC CCG GTT ATG GAC CAG CTG TCC GGC CAA AGT TCC-3’
T27D	S4898D	5’-AGC CCG GTT ATG TCG CAG CTG GAC GGC CAA AGT TCC AGT GCC AGC-3’
T32	S4891A, S4895A, S4898A	5’-AGC AAC AGC GAA CGC AGT CTG AAC GCC CCG GTT ATG GCG CAG CTG GCC GGC CAA AGT TCC AGT GCC AGC-3’
T32D	S4891D, S4895D, S4898D	5’-AGC AAC AGC GAA CGC AGT CTG AAC GAC CCG GTT ATG GAC CAG CTG GAC GGC CAA AGT TCC AGT GCC AGC-3’
T33	S4885A, S4888A	5’-GGC AAG GAC GTT CAC AGC AAC GCC GAA CGC GCT CTG AAC AGC CCG GTT ATG TCG-3’
T33D	S4885D, S4888D	5’-GGC AAG GAC GTT CAC AGC AAC GAC GAA CGC GAT CTG AAC AGC CCG GTT ATG TCG-3’

3. Summary of Fat-ICD mutants and Dco mediated gel mobility shift.

Construct name	Amino acid change	Phosphorylation Dco*
C1	S4753A, S4754A, S4758A	+
C2	Y4766A	+
T1	S4796A, S4798A	+
T2	T4825A,S4826A, S4828A, T4830A	+
T3	T4924A	+
T4	S4939A, S4942A, T4943A	+
T5	S4948A, S4949A, S4950A, S4951A	+
T6	S4973A, S4974A, T4975A, S4976A, 4977A	+
T7	S4984A, T4986A, S4988A	+
T8	Y4992A	+
T9	S4781A, S4786A, Y4788A, T4789A	+
T10	T4808A, T4813A	+
T11	S4833A, T4834A	+
T12	S4840A, S4842A, S4843A, S4846A, S4847A	+
T13	T4870A, T4871A, S4872A, S4873A, S4874A	+
T14	S4883A, S4885A, S4888A, S4891A	-
T15	S4895A, S4898A, S4901A, S4902A, S4903A, S4905A	-
T16	T4919A, S4920A	+
T17	S4957A, S4958A, S4959A, S4964A	+
T18	S4996A, S4998A	+
T19	S5004A, T5005A, S5006A, S5008A	+
T20	S5014A, S5017A, S5021A	+
T14D	S4883D, S4885D, S4888D, S4891D	-
T15D	S4895D, S4898D, S4901D, S4902D, S4903D, 4905D	-
T21	S4883A, S4885A, S4891A	
T22	S4883A	
T23	S4885A	
T24	S4888A	
T25	S4891A	
T26	S4895A	
T27	S4898A	
T28	S4901A	
T29	S4902A	
T30	S4903A	
T31	S4905A	
T25D	S4891D	
T26D	S4895D	
T27D	S4898D	
T32	S4891A, S4895A, S4898A	-
T32D	S4891D, S4895D, S4898D	-
T33	S4885A, S4888A	-
T33D	S4885D, S4888D	-

*Phosphorylation is indicated by electrophoresis mobility shift.

4. List of Fat-ICD point mutants.

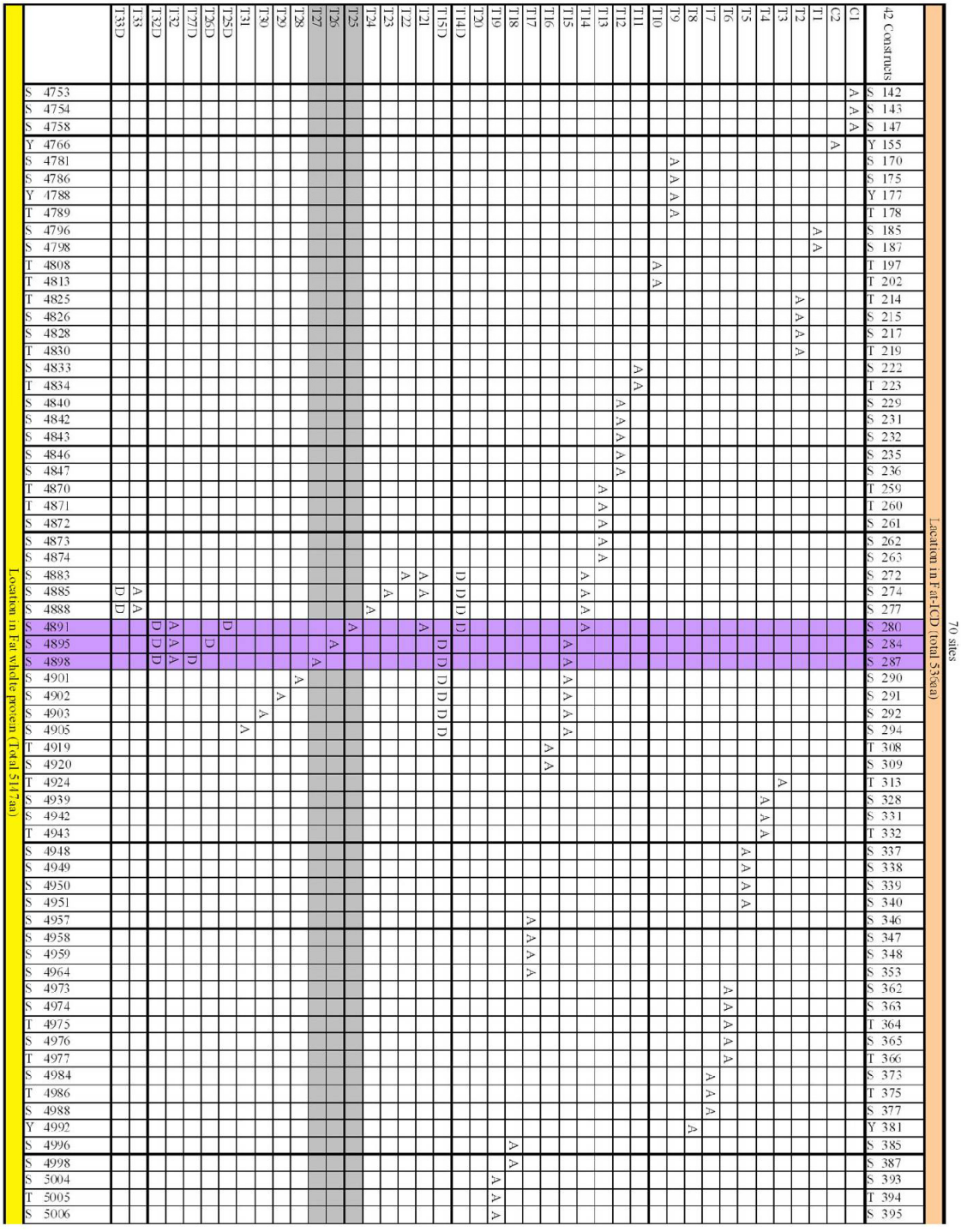

5. Universal primers for attB-P[acman].

Primers for attB_P[acman]_ApR and transgenesis[180]:

MCS-F TTTAAACCTCGAGCGGTCCGTTATC

MCS-R CTAAAGGGAACAAAAGCTGGGTAC

attP-F CTTCACGTTTTCCCAGGTCAGAAG

attP-R GTCGCGCTCGCGCGACTGACGGTC

attB-F GTCGACGATGTAGGTCACGGTC

attB-R TCGACATGCCCGCCGTGACCGTC

6. Primers to clone *fat* genomic region from BAC DNA.

Primers to generate ft exon1_LA and ft exon8_RA

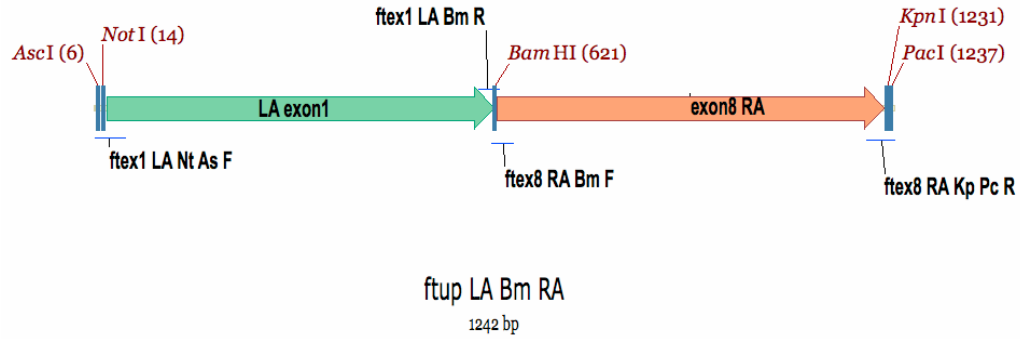

ftex1_LA_Nt_As_F: aaaggcgcgccgcggccgcatggagaggctactgctcctgtttttcc

ftex1_LA_Bm_R: ctcggatccatttccagccacgatctcatactg

ftex8_RA_Bm_F: aatggatccgaggcgcctcgagtgtcgagcagcg

ftex8_RA_Kp_Pc_R: accttaattaaggtacccaacatatattacacgtactcctctgg

7. Primers to clone *fat* locus from BAC DNA.

Primers to generate Rpl40LA and CG3714RA

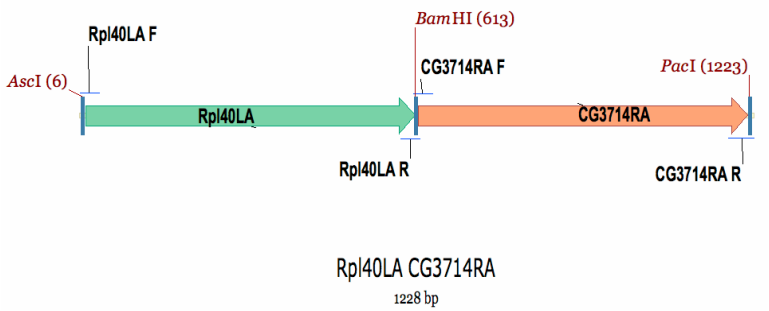

Rpl40LA_F: 5'-aaa ggcgcgcc ctcggagaggccaactaattgcag-3'

Rpl40LA_R: 5'- cct ggatcc ccttggaggtggagccttctgacacc-3'

CG3714RA_F: 5'- agg ggatcc aggtgggtgtaatcatttgatttggc-3'

CG3714RA_R: 5'- acc ttaattaa caacacttaagtactagaaaaatattaaagacata-3'

Primers for checking pattB-Pacman-Rp40-CG3714

Rpl14checkR: cagatcttcgtgaaaaccctcacc

CG3714checkF: cgatcacaagcgcacgctcaacccg

8. Primers to modify *fat* locus by recombineering.

To generate bigger Phos-Fat-galK fragment:

Phos-FatLA_R: tgcagcggctttccggaaatgtcgtgc

Phos-FatRA_F: gaaggcaaaagcccggagtgccacagc

Primers to generate C-term tagger Fat

Without stop codon TAA:

Fat_Cterm_galkF: 5’-gtg gtg tcc acg cta cga atg cca tca tcg aat gga ccg gcg gct cca gag gag tac gtg CCT GTT GAC AAT TAA TCA TCG GCA-3’

Fat_Cterm_galkR: 5’-tgg ggc tca gac ttt agg aac act tta act ttc gtt gaa gag cat aca caa cat ata tta TCA GCA CTG TCC TGC TCC TT-3’

Primers for checking 510bp

Fat_C_checkF: 5’-gccgcatccccatcggccaccacc-3’

Fat_C_checkR: 5’-tccgacatatgcacgattctacac-3’

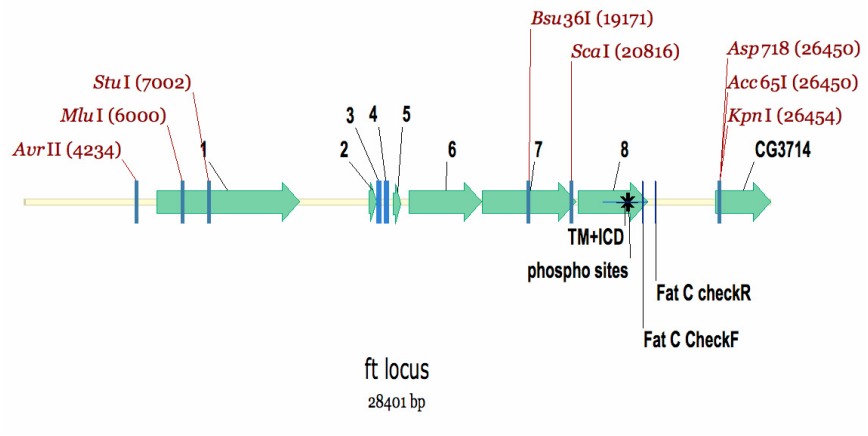

To generate fat C-term mCherry (fat:Chry)

GGA/TCC: Gly linker

Fat_Cterm_chryR: (reverse strand; use with primers from upstream)

5’- tatcctcctcgcccttgctcaccat TCC TCC TCC TCC cacgtactcctctggagccgccggt -3’

Fat_Cterm_chryF: (sense strand; use with downstream reverse primers)

5’- cggcatggacgagctgtacaagtaa tatatgttgtgtatgctcttcaacg-3’

Fat_Cterm_downsR: (reverse strand; use with Fat_Cterm_cherryF)

5’- ccgacatatgcacgattctacactttg-3’

Downstream fragment size: 299bp.

To generate fat-C-term FLAG (fat:FLAG): homologous region 60bp; use with upstreram primer; template for PCR ft:FVH. 266bp.

Fat_Cterm_F: 5'- gcatccccatcggccaccaccctcggctgg-3'

Fat_Cterm_FLAG_R: 5'-aa ttg ggg ctc aga ctt tag gaa cac ttt aac ttt cgt tga aga gca tac aca aca tat aTT A acc cttg tcgtcgtcgtccttgtag-3'

Primer for cloning galK to exchange ft-ST minus region

galK: 1231bp

Forward: galK_ftSTminusF: 5'-cac gcc agt tcc gtg gac atg ggt tcc gag tac ccg gaa cac tac gac ctc gag aac gcc CCT GTT GAC AAT TAA TCA TCG GCA-3'

Reverser: galK_ftSTminusR: 5'- cgg cgg aat ggg cgg tgt ctt gac cac agt tgt cgg tgg att tct gct cgt ctc acc acc TCA GCA CTG TCC TGC TCC TT-3'

ftSTm_checkF: 5'- gccagttccgtggacatgggttcc-3'

ftSTm_checkR: 5'- cggaatgggcggtgtcttgaccac-3'

921bp for ft-STm

1345bp for ft-STmgalK

9. Primers to generate human Fat-ICD and *Drosophila* Fat hybrids.

Primers to insert galK into fly *fat* ICD reion.

galK: 1231bp

Forward: galK_ICD_F: 5'-att gtc ttc ttc gtc att ctg gtg gtg gct ata ctg ggc tcc tat gtt atc tat cga ttc CCT GTT GAC AAT TAA TCA TCG GCA-3'

Reverser: galK_ICD_R: 5'-tgg ggc tca gac ttt agg aac act tta act ttc gtt gaa gag cat aca caa cat ata tta TCA GCA CTG TCC TGC TCC TT-3'

FtICDminus_chkF: 5'- ggttgcctggccaatgtgacggtg-3'

FtICDminus_chkR: 5'- tccgacatatgcacgattctacac-3'

1765bp for ICD-galk.

2142bp for ICD wt.

To generate fusion protein of human Fat-ICD with Drosophila Fat (signal peptide plus transmembrane domain) in pUAST plasmid.

ft1: PCR 1164bp/ 388aa

hsft1_SOE5: 5'- ggg ctc cta tgt tat cta tcg att c tgc cgt aag atg att agt cgg aaa-3'

hsft1_FLAGXhoI3: 5'-AAA CTC GAG *TCA* ACC CTT GTC GTC GTC GTC CTT GTA GTC gac ttc cgt gtg ctg ctg gga atc-3'

ft2: PCR 846bp/282aa

hsft2_SOE5:5'- ggg ctc cta tgt tat cta tcg att c ttc tac tgc cgc cgt tgc aag tct-3'

hsft2_FLAGXhoI3: 5'-AAA CTC GAG *TCA* ACC CTT GTC GTC GTC GTC CTT GTA GTC gaa cat gac ctc ctc aca gct gcc-3'

ft3: PCR 1152bp/384aa

hsft3_SOE5:5'-ggg ctc cta tgt tat cta tcg att c ttc cgc aag aag gtc ttc cgc aag-3'

hsft3_FLAGXhoI3:5'-AAA CTC GAG *TCA* ACC CTT GTC GTC GTC GTC CTT GTA GTC cac ttg agt ctg atg ctg agt ctc-3'

ft4: PCR 1368bp/456aa

hsft4_SOE5:5’- ggg ctc cta tgt tat cta tcg att c AAC CAG TGC AGG GGG AAG AAG GCC-3’

hsft4_FLAGXhoI3:5’-AAA CTC GAG *TCA* ACC CTT GTC GTC GTC GTC CTT GTA GTC CAC ATA CTG TTC TGC TTC CCC ATC-3’

Nest PCR primers for ft-4: 1569bp

Ft4ICD5: 5’-agg acc tgt gag atg gtg gtg gcc-3’

Ft4ICD3: 5’-tca cac ata ctg ttc tgc ttc ccc-3’

Mutagenesis primers:

Ft1_432C: 5’-tcc tgc tct gac gtg tca gcc Tgc tgc gaa gtg gag tcc gag gtc-3’

Ft2_131P: 5’-agc tcc tgc aac aac ctc aac caa cCg gaa ccc agc aag gcc tct gtt-3’

Ft3_200S: 5’-gcc ccc aac ctc ccc gcc gtg Tca ccc tgc cgc tcc gac tgc gac-3’

Generate fusion proteins of human Fat-ICD with Drosophila Fat (ECD plus transmembrane domain) in genomic rescue construct

TM_F: 5’-ctcagcattggcttcaccctggtc-3’

TM_R: 5’-cgatagataacataggagcccagt-3’

FLAGft_dwn_F: 5’- GAC TAC AAG GAC GAC GAC GAC AAG GGT TGA ta ata tat gtt gtg tat gct ctt caa cg-3’

FLAG_R: 5’- *TCA* ACC CTT GTC GTC GTC GTC CTT GTA GTC-3’

10. Generate Fat-ICD ST minus.

Fat_ICD_F: 5’-attgtcttcttcgtcattctggtggtggctatactgggctcctatgttatctatcgattc-3’

Fat_ICD_R: 5’-tggggctcagactttaggaacactttaactttcgttgaagagcatacacaacatatatta *TCA* ACC CTT GTC GTC GTC GTC CTT GTA GTC -3’

Template: pUAST-attB-ft-STI4-STminus

Oligos to synthesize fatSTI_ST_minus

Forward oligos:

Fat_STminus_1: 5’-gccgccattgctccggccgacattgatatagtctatcattacaagggcta-3’

Fat_STminus_2: 5’- tcgtgaggctgctggcctacgcaaatacaaggccgccgttccacctgttg-3’

Fat_STminus_3: 5’- ccgcctacgcccatcacaagcatcagaacgccggcgcccagcagcagcag-3’

Fat_STminus_4: 5’- cagcagcaccgccacgccgctccctttgtggcccggaaccaaggtggcca-3’

Fat_STminus_5: 5’- accgccaccgccgcccgccgccgcagcccgcgcccatcaggccgccccac-3’

Fat_STminus_6: 5’- tggcccgactcgcccccgccgccgagttggccgcccagcagccgcgcatt-3’

Fat_STminus_7: 5’- ctcgccttgcacgacattgccggaaagccgctgcaagccgccctgctggc-3’

Fat_STminus_8: 5’- cgccgccgccgccgccggtggcgttggcaaggacgttcacgccaacgccg-3’

Fat_STminus_9: 5’- aacgcgccctgaacgccccggttatggcccagctggccggccaagccgcc-3’

Fat_STminus_10:5’- gccgccgccaggcaaaagcccggagtgccacagcagcaggcgcagcaagc-3’

Fat_STminus_11:5’- cgccatgggcttggccgccgaggagattgagagattgaatggcagaccac-3’

Fat_STminus_12:5’- gagcctgtgccctaatcgccgccctggatgccgtcgccgccgccgccgag-3’

Fat_STminus_13:5’- gcgcctcgagtggccgccgccgctctgcatatggccctgggtggagatgt-3’

Fat_STminus_14:5’- ggatgcccatgccgccgccgccgccgacgaagccggcaacgacgccttcg-3’

Fat_STminus_15:5’- cctgcgccgagatcgagtacgacaataacgccctcgccgg-3’

Fat_STminus_16:5’- cgacggcaagtatgccgccgccaaggccctcctcgatgga-3’

Fat_STminus_17:5’- cgcgcccccgtggccagagcactagccA-3’

Reverse Oligos:

Fat_STminus_18:5’- ggctagtgctctggccacgggggcgcgtccatcgaggagggccttgg-3’

Fat_STminus_19:5’- cggcggcatacttgccgtcgccggcgagggcgttattgtc-3’

Fat_STminus_20:5’- gtactcgatctcggcgcaggcgaaggcgtcgttgccggct-3’

Fat_STminus_21:5’- tcgtcggcggcggcggcggcatgggcatccacatctccacccagggccat-3’

Fat_STminus_22:5’- atgcagagcggcggcggccactcgaggcgcctcggcggcggcggcgacgg-3’

Fat_STminus_23:5’- catccagggcggcgattagggcacaggctcgtggtctgccattcaatctc-3’

Fat_STminus_24:5’- tcaatctcctcggcggccaagcccatggcggcttgctgcgcctgctgctg-3’

Fat_STminus_25:5’- tggcactccgggcttttgcctggcggcggcggcggcttggccggccagct-3’

Fat_STminus_26:5’- gggccataaccggggcgttcagggcgcgttcggcgttggcgtgaacgtcc-3’

Fat_STminus_27:5’- ttgccaacgccaccggcggcggcggcggcggccagcagggcggcttgcag-3’

Fat_STminus_28:5’- cggctttccggcaatgtcgtgcaaggcgagaatgcgcggctgctgggcgg-3’

Fat_STminus_29:5’- ccaactcggcggcgggggcgagtcgggccagtggggcggcctgatgggcg-3’

Fat_STminus_30:5’- cgggctgcggcggcgggcggcggtggcggttggccaccttggttccgggc-3’

Fat_STminus_31:5’- cacaaagggagcggcgtggcggtgctgctgctgctgctgggcgccgg-3’

Fat_STminus_32:5’- cgttctgatgcttgtgatgggcgtaggcggcaacaggtggaacggcggcc-3’

Fat_STminus_33:5’- ttgtatttgcgtaggccagcagcctcacgatagcccttgtaatgatagac-3’

Fat_STminus_34:5’- tatatcaatgtcggccggagcaatggcggcA-3’

fatICD_ST_minus: (55 Ser and 17 Thr→Ala GCC)

```
GCC GCC att gct ccg GCC gac att gat ata gtc tat cat tac aag ggc tat cgt
gag gct gct ggc cta cgc aaa tac aag gcc GCC gtt cca cct gtt GCC gcc tac
GCC cat cac aag cat cag aac GCC ggc GCC cag cag cag cag cag cag cac cgc
cac GCC gct ccc ttt gtg GCC cgg aac caa ggt ggc caa ccg cca ccg ccg ccc
GCC GCC gca GCC cgc GCC cat cag GCC GCC cca ctg gcc cga ctc GCC ccc GCC
GCC gag ttg GCC GCC cag cag ccg cgc att ctc GCC ttg cac gac att GCC gga
aag ccg ctg caa GCC gcc ctg ctg gcc GCC GCC GCC GCC GCC ggt ggc gtt ggc
aag gac gtt cac GCC aac GCC gaa cgc GCC ctg aac GCC ccg gtt atg GCC cag
ctg GCC ggc caa GCC GCC GCC gcc GCC agg caa aag ccc gga gtg cca cag cag
cag gcg cag caa GCC GCC atg ggc ttg GCC gcc gag gag att gag aga ttg aat
ggc aga cca cga GCC tgt GCC cta atc GCC GCC ctg gat gcc gtc GCC GCC GCC
GCC gag gcg cct cga gtg GCC GCC GCC gct ctg cat atg GCC ctg ggt gga gat
```

```
gtg gat gcc cat GCC GCC GCC GCC GCC gac gaa GCC ggc aac gac GCC ttc GCC
tgc GCC gag atc gag tac gac aat aac GCC ctc GCC ggc gac ggc aag tat GCC
GCC GCC aag GCC ctc ctc gat gga cgc GCC ccc gtg GCC aga gca cta GCC
```

11. Primers to tag Hippo.

Primer for cloning galK into N-terminal of Hpo (before ATG):

Forward: galK_hpoNterm_F: 5'-tgt cgc tgt gaa tag cca att atc tgt gtt ttc tcg tgc taa atc aga aaa ttt ttc gca CCT GTT GAC AAT TAA TCA TCG GCA-3'

Reverser: galK_hpoNterm_R: 5'-gga gga gga tat gtt ggg cga ttt cat atc tac aac gct ggt cac ctc tgg ctc aga cat TCA GCA CTG TCC TGC TCC TT-3'

Primer for cloning galK into C-terminal of Hpo (before TAG):

Forward: galK_hpoCterm_F: 5'-acg cca tga atg caa agc gca aac gcc agc aga aca tca ata ata atc tga tta aga taC CTG TTG ACA ATT AAT CAT CGG CA-3'

Reverser: galK_hpoCterm_R: 5'- att gag tga gtt gag att tca taa tca gtt gtc ttg cga aat tgt gag ttg ctt tac cta TCA GCA CTG TCC TGC TCC TT-3'

Primer to amlify hpo (coding region): genomic DNA 2572bp

Hpo_F: 5'-atgtctgagccagaggtgaccagc-3'

Hpo_R:5'-ctatatcttaatcagattattattgatg-3'

Checking primers

542bp (wt)

Hpo_Nterm_chkF: 5'-tcgtcataaatctaatcaatagcc-3'

Hpo_Nterm_chkR: 5'-cttttccggcggctgcagaagcgac-3'

331bp(wt)

Hpo_Cterm_chkF: 5'-ccagcggctgtgcaacatcgatca-3'

Hpo_Cterm_chkR: 5'- gattgattttagacccttccaccagg-3'

To generate Pacman-hpo-donor

hpo_domor_LA_F: 5’-atcgatggcgcgccgcgactagcatccccaccaggatg-3’

hpo_donor_LA_R: 5’-cgtaaggatccaaccaaatacgcccccatttgcagacgc-3’

hpo_donor_RA_F: 5’-ggttggatccttacggataaataaagtattccgtgaattt-3’

hpo_donor_RA_R: 5’-ggccttaattaagatgcgctgcaccagttggccctg-3’

LA check with MCS_F: 735+36bp

Hpo_LACheck_R: 5’- ggcgagaagatacacccggtgataccgc-3’

RA check with MCS_R: 668+57bp

Hpo_RACheck_F: 5’- ggtcaaactgctccggcaggtcatcc-3’

To make Pacman-FLAGhpo

HpoN_FLAG_R: 5’-atcgtcatcgtccttgtaatccattgcgaaaaattttctgatttagcacg-3’

HpoN_FLAG_F: 5’- cgcaatggattacaaggacgatgacgataaggc-3’

To make hpo:chry

HpoC_chry_R: 5’-atcctcctcgcccttgctcaccattcctcctcctcctatcttaatcagattattattgatgttctgctggcg-3’

HpoC_chry_F: 5’- ggcatggacgagctgtacaagtaataggtaaagcaactcacaatttcgcaagacaactg-3’

To make hpo:V5

HpoC_V5R: 5’-

aatcgagaccgaggagagggttagggataggcttacctcctcctcctcctatcttaatcagattattattgatgttctgc-3’

HpoC_V5F: 5’- cctaaccctctcctcggtctcgattctacgcgtaccggttaggtaaagcaactcacaatttcgcaagaca-3’

12. Primers to tag Warts.

Primer for cloning galK into N-terminal of **wts** (before ATG):

Forward: galK_wtsNterm_F:5'- gtg tgc gga gca ttt ctg tga tat gag tgc taa atg cca cag ggc gaa gca gca gca tcC CTG TTG ACA ATT AAT CAT CGG CA-3'

Reverser: galK_wtsNterm_R:5'-gct tcc gcc gtg tat tta tca ttg ggg cga ccg ccc ctt ttt tcg ccc gct gga tgc atT CAG CAC TGT CCT GCT CCT T-3'

Primer for cloning galK into C-terminal of **wts** (before TAG):

Forward: galK_wtsCterm_F: 5'-cgc ttc ttc gac gac aag cag ccg ccg gat atg acg gac gat cag gcg ccg gtt tac gtc CCT GTT GAC AAT TAA TCA TCG GCA-3'

Reverser: galK_wtsCterm_R:5'-gac taa caa tga ttc ggg ggc ggg gtg ttg gtg ttg ggc aca tgg aga gca tcc att tca TCA GCA CTG TCC TGC TCC TT-3'

Checking primers for wts

645bp(wt)

Wts_Nterm_chkF: 5'- cccgcgccttagttcgttgtagtc-3'

Wts_Nterm_chkR: 5'- gaatggaagatctgtattcaacccattc-3'

423bp

Wts_Cterm_chkF: 5'- gcggctgggcaagagcgtggacgag-3'

Wts_Cterm_chkR: 5'- gccacgcttcctttacaatgcaagccc-3'

To generate Pacman-wts-donor 6-20-2008

wts_donor_LA_F:5'- cgatggcgcgccgctagatagatcgtgttacggctcaa-3'

wts_donor_LA_R: 5'- ccgcgcggatccgaaaagcggagacgcactgccgcgc-3'

wts_donor_RA_F: 5'- cttttcggatccgcgcggcggctctggccaaattgg-3'

wts_donor_RA_R: 5'- cggccttaattaatttttttacgcattaatgttttagcttttag-3'

To generate fusion protein:

Sequence for overlapping region.

ChrySOE5: (w/ ATG; reverse strand; combine with upstream primers): 5'-tat cct cct cgc cct tgc tca cca t 3'

ChrySOE3a: (w/o stop codon; for N-term fusion; sense strand; use with downstream primers): 5'-cggcggcatggacgagctgtacaag-3'

ChrySOE3a: (w/ stop codon; for C-term fusion; sense strand; use with downstream primers): 5'- cggcatggacgagctgtacaagtaa-3'

LA check with MCS_F: 700+36bp

Wts_LACheck_R: 5'-gcgtttcgctcgctcgtttggcgatttgc-3'

RA check with MCS_R: 659+57bp

Wts_RACheck_F: 5'-gtcgagtggcaagcggcagccggaggcc-3'

To make Pacman-mycwts

Overlapping:

wtsN_mycR: 5'- cttcagaaatcagcttttgttccatgatgctgctgcttcgccctgtggc-3'

wtsN_mycF: 5'- ggaacaaaagctgatttctgaagaagacttgcatccagcgggcgaaaaaaggg -3'

To make WtsC-chery

WtsC_chry_R: 5'- ttatcctcctcgcccttgctcaccattcctcctcctccgacgtaaaccggcgcctgatcg-3'

WtsC_Chry_F: 5'- ggcatggacgagctgtacaagtaatgaaatggatgctctccatgtgcccaac-3'

To make WtsC_V5:

WtsC_V5R: 5'- atc gag acc gag gag agg gtt agg gat agg ctt acc tcc tcc tcc tcc gac gta aac cgg cgc ctg atc g-3'

WtsC_V5F: 5'- accctctcctcggtctcgattctacgcgtaccggttgaaatggatgctctccatgtgccc-3'

13. Maps of *fat* genomic rescue constructs.

Genomic rescue construct V5:ft:Flag

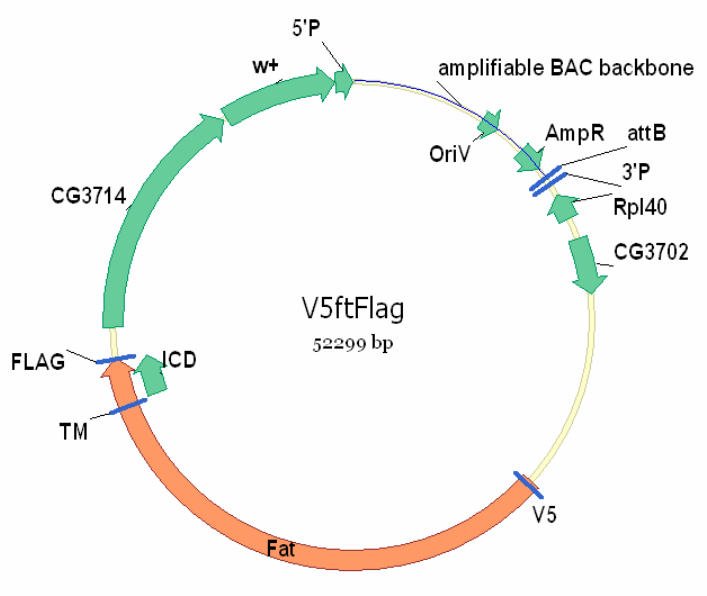

Genomic rescue construct V5:ft:Cherry

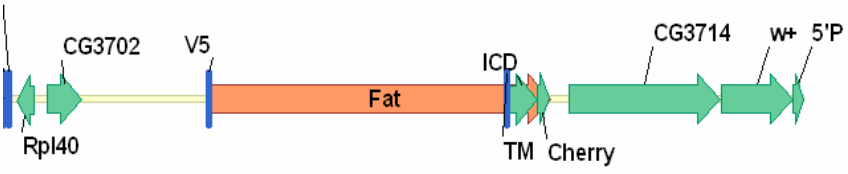

Human ft1-ICD fusion with Drosophila fat signal peptide plus TM

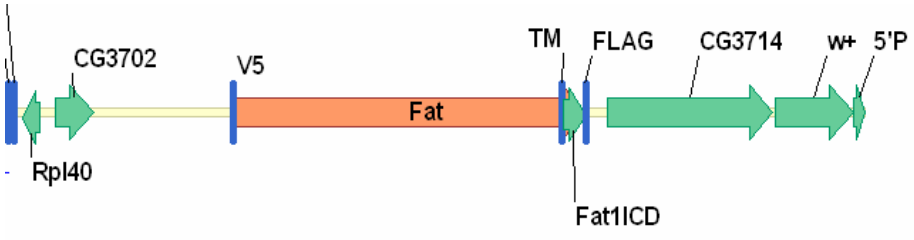

14. Multi-alignment of *Drosophila* Fat-ICD anf human Fat-ICDs.

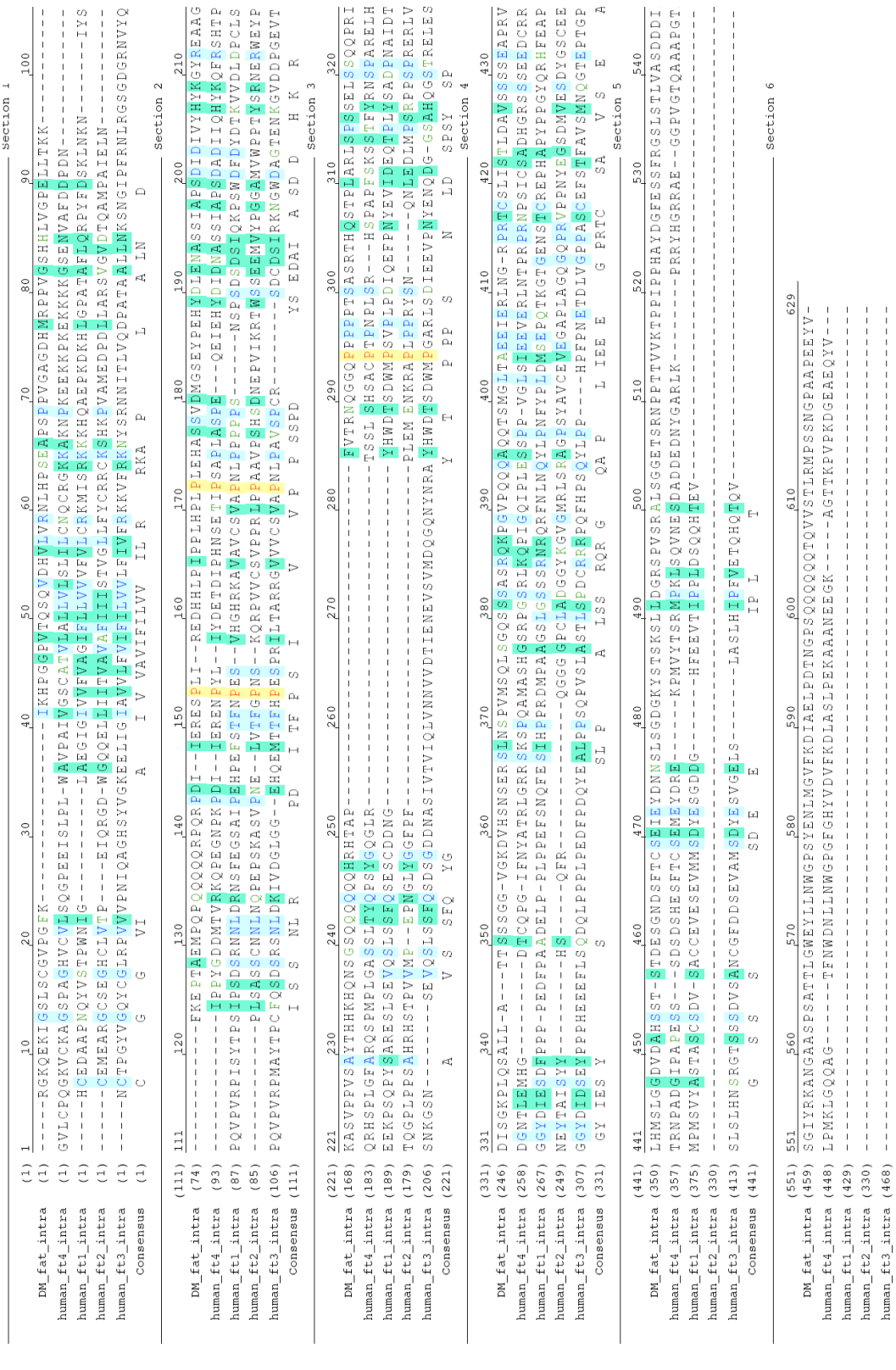

15. Multi-alignment of Fat-ICDs from various species.

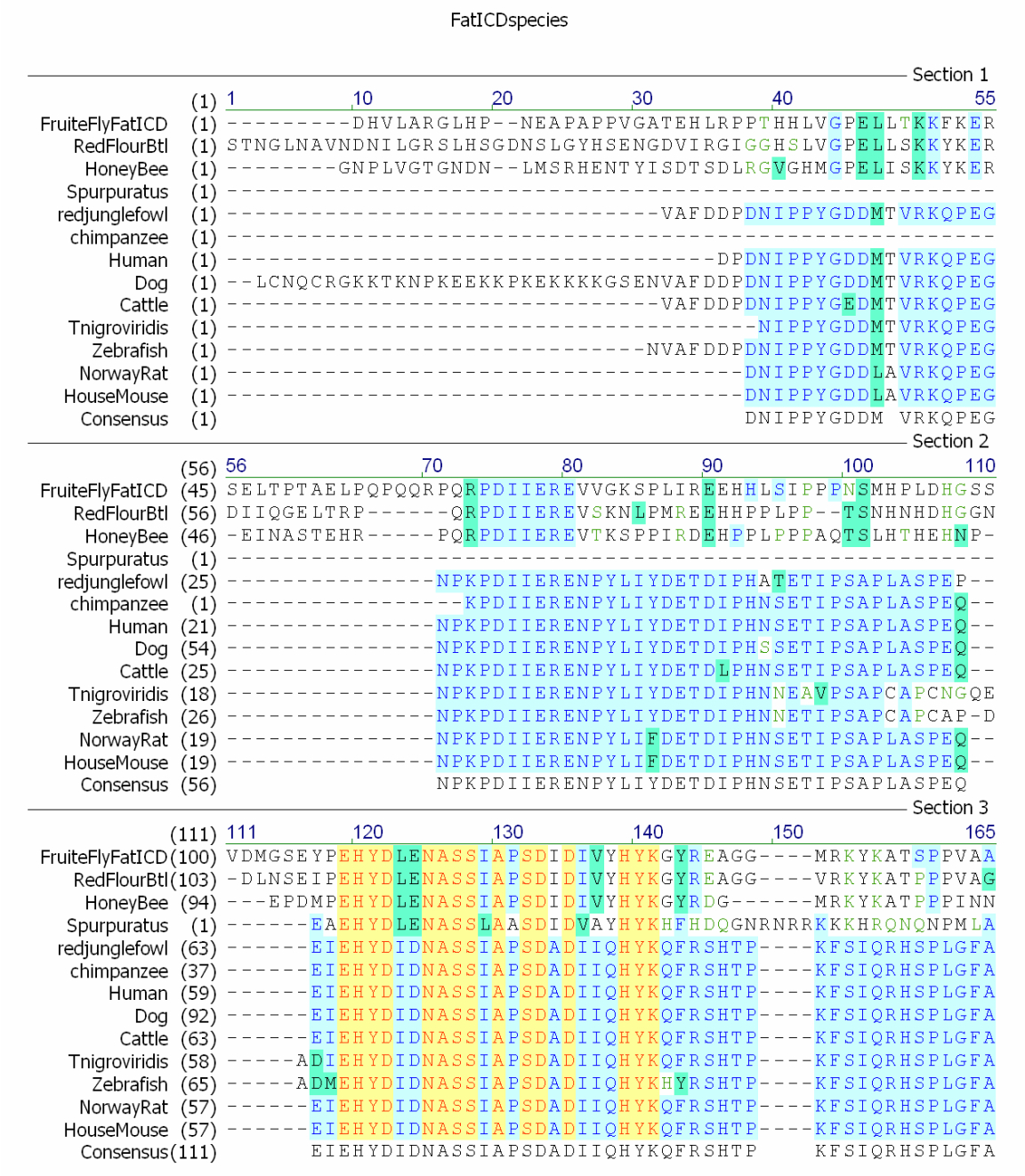

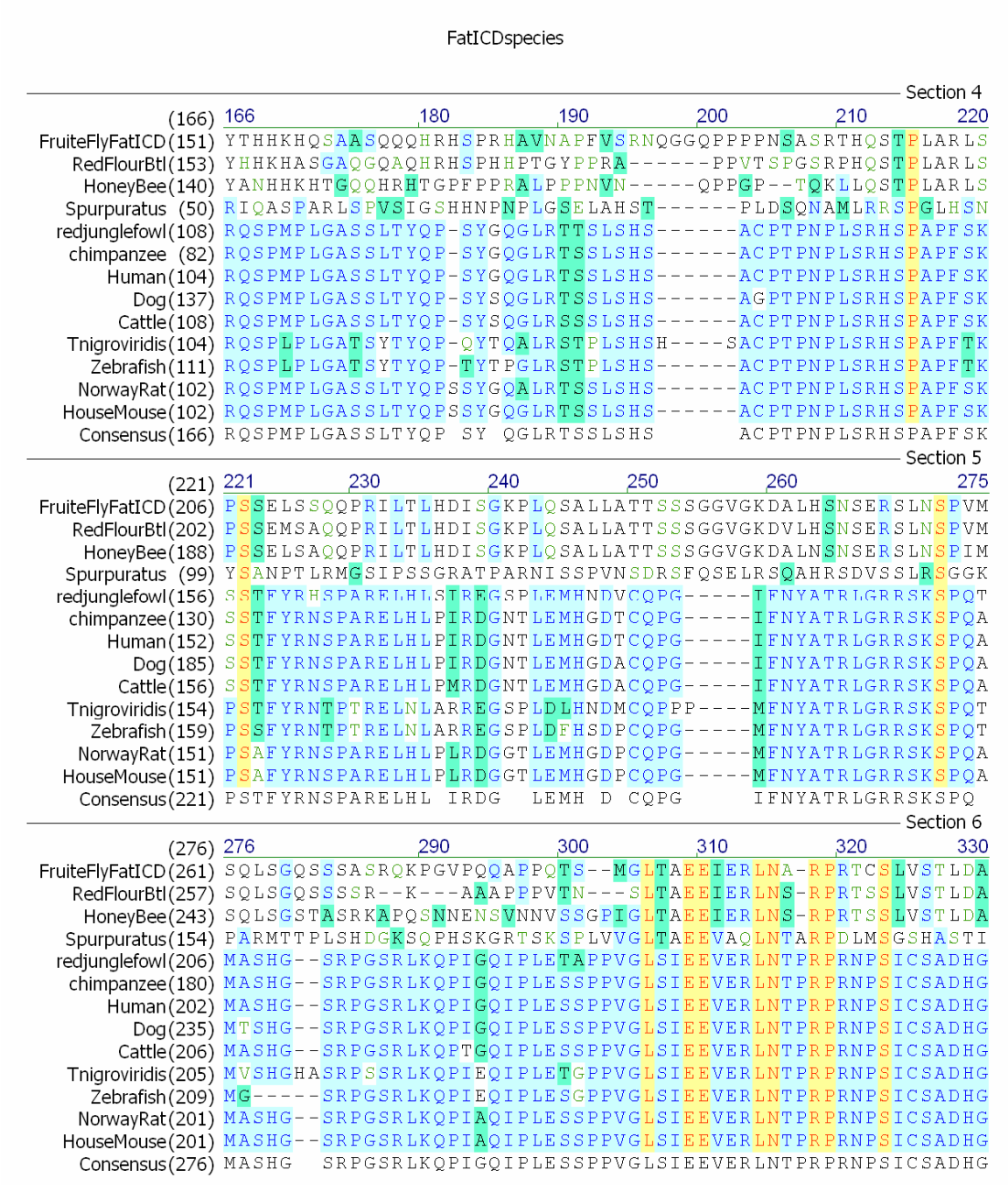
FatICDspecies
Section 4
(166) 166 180 190 200 210 220
FruiteFlyFatICD(151) YTHHKHQSAASQQQHRHSPRHAVNAPFVSRNQGGQPPPPNSASRTHQSTPLARLS
RedFlourBtl(153) YHHKHASGAQGQAQHRHSPHHPTGYPPRA------PPVTSPGSRPHQSTPLARLS
HoneyBee(140) YANHHKHTGQQHRHTGPFPPRALPPPNVN-----QPPGP--TQKLLQSTPLARLS
Spurpuratus (50) RIQASPARLSPVSIGSHHNPNPLGSELAHST------PLDSQNAMLRRSPGLHSN
redjunglefowl(108) RQSPMPLGASSLTYQP-SYGQGLRTTSLSHS------ACPTPNPLSRHSPAPFSK
chimpanzee (82) RQSPMPLGASSLTYQP-SYGQGLRTSSLSHS------ACPTPNPLSRHSPAPFSK
Human(104) RQSPMPLGASSLTYQP-SYGQGLRTSSLSHS------ACPTPNPLSRHSPAPFSK
Dog(137) RQSPMPLGASSLTYQP-SYSQGLRTSSLSHS------AGPTPNPLSRHSPAPFSK
Cattle(108) RQSPMPLGASSLTYQP-SYSQGLRSSSLSHS------ACPTPNPLSRHSPAPFSK
Tnigroviridis(104) RQSPLPLGATSYTYQP-QYTQALRSTPLSHSH----SACPTPNPLSRHSPAPFTK
Zebrafish(111) RQSPLPLGATSYTYQP-TYTPGLRSTPLSHS------ACPTPNPLSRHSPAPFTK
NorwayRat(102) RQSPMPLGASSLTYQPSSYGQALRTSSLSHS------ACPTPNPLSRHSPAPFSK
HouseMouse(102) RQSPMPLGASSLTYQPSSYGQGLRTSSLSHS------ACPTPNPLSRHSPAPFSK
Consensus(166) RQSPMPLGASSLTYQP SY QGLRTSSLSHS ACPTPNPLSRHSPAPFSK
Section 5
(221) 221 230 240 250 260 275
FruiteFlyFatICD(206) PSSELSSQQPRILTLHDISGKPLQSALLATTSSSGGVGKDALHSNSERSLNSPVM
RedFlourBtl(202) PSSEMSAQQPRILTLHDISGKPLQSALLATTSSSGGVGKDVLHSNSERSLNSPVM
HoneyBee(188) PSSELSAQQPRILTLHDISGKPLQSALLATTSSSGGVGKDALNSNSERSLNSPIM
Spurpuratus (99) YSANPTLRMGSIPSSGRATPARNISSPVNSDRSFQSELRSQAHRSDVSSLRSGGK
redjunglefowl(156) SSTFYRHSPARELHLSTRFGSPLEMHNDVCQPG-----TFNYATRLGRRSKSPQT
chimpanzee(130) SSTFYRNSPARELHLPIRDGNTLEMHGDTCQPG-----IFNYATRLGRRSKSPQA
Human(152) SSTFYRNSPARELHLPIRDGNTLEMHGDTCQPG-----IFNYATRLGRRSKSPQA
Dog(185) SSTFYRNSPARELHLPIRDGNTLEMHGDACQPG-----IFNYATRLGRRSKSPQA
Cattle(156) SSTFYRNSPARELHLPMRDGNTLEMHGDACQPG-----IFNYATRLGRRSKSPQA
Tnigroviridis(154) PSTFYRNTPTRELNLARREGSPLDLHNDMCQPPP----MFNYATRLGRRSKSPQT
Zebrafish(159) PSSFYRNTPTRELNLARREGSPLDFHSDPCQPG-----MFNYATRLGRRSKSPQT
NorwayRat(151) PSAFYRNSPARELHLPLRDGGTLEMHGDPCQPG-----MFNYATRLGRRSKSPQA
HouseMouse(151) PSAFYRNSPARELHLPLRDGGTLEMHGDPCQPG-----MFNYATRLGRRSKSPQA
Consensus(221) PSTFYRNSPARELHL IRDG LEMH D CQPG IFNYATRLGRRSKSPQ
Section 6
(276) 276 290 300 310 320 330
FruiteFlyFatICD(261) SQLSGQSSSASRQKPGVPQQAPPQTS--MGLTAEEIERLNA-RPRTCSLVSTLDA
RedFlourBtl(257) SQLSGQSSSSR--K---AAAPPPVTN---SLTAEEIERLNS-RPRTSSLVSTLDA
HoneyBee(243) SQLSGSTASRKAPQSNNENSVNNVSSGPIGLTAEEIERLNS-RPRTSSLVSTLDA
Spurpuratus(154) PARMTTPLSHDGKSQPHSKGRTSKSPLVVGLTAEEVAQLNTARPDLMSGSHASTI
redjunglefowl(206) MASHG--SRPGSRLKQPIGQIPLETAPPVGLSIEEVERLNTPRPRNPSICSADHG
chimpanzee(180) MASHG--SRPGSRLKQPIGQIPLESSPPVGLSIEEVERLNTPRPRNPSICSADHG
Human(202) MASHG--SRPGSRLKQPIGQIPLESSPPVGLSIEEVERLNTPRPRNPSICSADHG
Dog(235) MTSHG--SRPGSRLKQPIGQIPLESSPPVGLSIEEVERLNTPRPRNPSICSADHG
Cattle(206) MASHG--SRPGSRLKQPTGQIPLESSPPVGLSIEEVERLNTPRPRNPSICSADHG
Tnigroviridis(205) MVSHGHASRPSSRLKQPIEQIPLETGPPVGLSIEEVERLNTPRPRNPSICSADHG
Zebrafish(209) MG-----SRPGSRLKQPIEQIPLESGPPVGLSIEEVERLNTPRPRNPSICSADHG
NorwayRat(201) MASHG--SRPGSRLKQPIAQIPLESSPPVGLSIEEVERLNTPRPRNPSICSADHG
HouseMouse(201) MASHG--SRPGSRLKQPIAQIPLESSPPVGLSIEEVERLNTPRPRNPSICSADHG
Consensus(276) MASHG SRPGSRLKQPIGQIPLESSPPVGLSIEEVERLNTPRPRNPSICSADHG

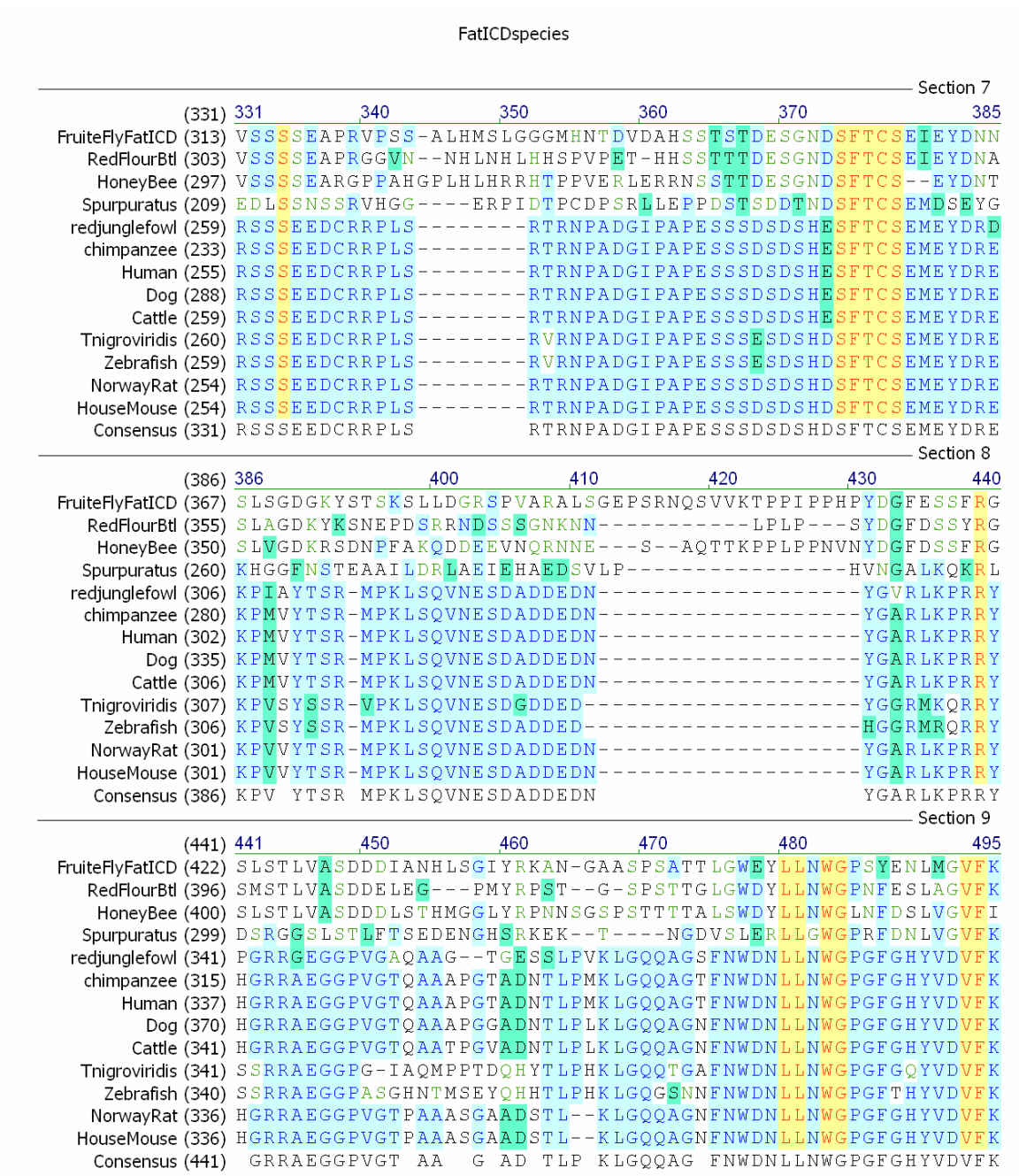
FatICDspecies
Section 7
(331) 331 340 350 360 370 385
FruiteFlyFatICD (313) VSSSSEAPRVPSS-ALHMSLGGGMHNTDVDAHSSTSTDESGNDSFTCSEIEYDNN
RedFlourBtl (303) VSSSSEAPRGGVN--NHLNHLHHSPVPET-HHSSTTTDESGNDSFTCSEIEYDNA
HoneyBee (297) VSSSSEARGPPAHGPLHLHRRHTPPVERLERRNSSTTDESGNDSFTCS--EYDNT
Spurpuratus (209) EDLSSNSSRVHGG----ERPIDTPCDPSRLLEPPDSTSDDTNDSFTCSEMDSEYG
redjunglefowl (259) RSSSEEDCRRPLS--------RTRNPADGIPAPESSSDSDSHESFTCSEMEYDRD
chimpanzee (233) RSSSEEDCRRPLS--------RTRNPADGIPAPESSSDSDSHESFTCSEMEYDRE
Human (255) RSSSEEDCRRPLS--------RTRNPADGIPAPESSSDSDSHESFTCSEMEYDRE
Dog (288) RSSSEEDCRRPLS--------RTRNPADGIPAPESSSDSDSHESFTCSEMEYDRE
Cattle (259) RSSSEEDCRRPLS--------RTRNPADGIPAPESSSDSDSHESFTCSEMEYDRE
Tnigroviridis (260) RSSSEEDCRRPLS--------RVRNPADGIPAPESSSESDSHDSFTCSEMEYDRE
Zebrafish (259) RSSSEEDCRRPLS--------RVRNPADGIPAPESSSESDSHDSFTCSEMEYDRE
NorwayRat (254) RSSSEEDCRRPLS--------RTRNPADGIPAPESSSDSDSHDSFTCSEMEYDRE
HouseMouse (254) RSSSEEDCRRPLS--------RTRNPADGIPAPESSSDSDSHDSFTCSEMEYDRE
Consensus (331) RSSSEEDCRRPLS RTRNPADGIPAPESSSDSDSHDSFTCSEMEYDRE
Section 8
(386) 386 400 410 420 430 440
FruiteFlyFatICD (367) SLSGDGKYSTSKSLLDGRSPVARALSGEPSRNQSVVKTPPIPPHPYDGFESSFRG
RedFlourBtl (355) SLAGDKYKSNEPDSRRNDSSSGNKNN----------LPLP---SYDGFDSSYRG
HoneyBee (350) SLVGDKRSDNPFAKQDDEEVNQRNNE---S--AQTTKPPLPPNVNYDGFDSSFRG
Spurpuratus (260) KHGGFNSTEAAILDRLAEIEHAEDSVLP----------------HVNGALKQKRL
redjunglefowl (306) KPIAYTSR-MPKLSQVNESDADDEDN-------------------YGVRLKPRRY
chimpanzee (280) KPMVYTSR-MPKLSQVNESDADDEDN-------------------YGARLKPRRY
Human (302) KPMVYTSR-MPKLSQVNESDADDEDN-------------------YGARLKPRRY
Dog (335) KPMVYTSR-MPKLSQVNESDADDEDN-------------------YGARLKPRRY
Cattle (306) KPMVYTSR-MPKLSQVNESDADDEDN-------------------YGARLKPRRY
Tnigroviridis (307) KPVSYSSR-VPKLSQVNESDGDDED-------------------YGGRMKQRRY
Zebrafish (306) KPVSYSSR-MPKLSQVNESDADDED-------------------HGGRMRQRRY
NorwayRat (301) KPVVYTSR-MPKLSQVNESDADDEDN-------------------YGARLKPRRY
HouseMouse (301) KPVVYTSR-MPKLSQVNESDADDEDN-------------------YGARLKPRRY
Consensus (386) KPV YTSR MPKLSQVNESDADDEDN YGARLKPRRY
Section 9
(441) 441 450 460 470 480 495
FruiteFlyFatICD (422) SLSTLVASDDDIANHLSGIYRKAN-GAASPSATTLGWEYLLNWGPSYENLMGVFK
RedFlourBtl (396) SMSTLVASDDELEG---PMYRPST--G-SPSTTGLGWDYLLNWGPNFESLAGVFK
HoneyBee (400) SLSTLVASDDDLSTHMGGLYRPNNSGSPSTTTTALSWDYLLNWGLNFDSLVGVFI
Spurpuratus (299) DSRGGSLSTLFTSEDENGHSRKEK--T----NGDVSLERLLGWGPRFDNLVGVFK
redjunglefowl (341) PGRRGEGGPVGAQAAG--TGESSLPVKLGQQAGSFNWDNLLNWGPGFGHYVDVFK
chimpanzee (315) HGRRAEGGPVGTQAAAPGTADNTLPMKLGQQAGTFNWDNLLNWGPGFGHYVDVFK
Human (337) HGRRAEGGPVGTQAAAPGTADNTLPMKLGQQAGTFNWDNLLNWGPGFGHYVDVFK
Dog (370) HGRRAEGGPVGTQAAAPGGADNTLPLKLGQQAGNFNWDNLLNWGPGFGHYVDVFK
Cattle (341) HGRRAEGGPVGTQAATPGVADNTLPLKLGQQAGNFNWDNLLNWGPGFGHYVDVFK
Tnigroviridis (341) SSRRAEGGPG-IAQMPPTDQHYTLPHKLGQQTGAFNWDNLLNWGPGFGQYVDVFK
Zebrafish (340) SSRRAEGGPASGHNTMSEYQHHTLPHKLGQGSNNFNWDNLLNWGPGFTHYVDVFK
NorwayRat (336) HGRRAEGGPVGTPAAASGAADSTL--KLGQQAGNFNWDNLLNWGPGFGHYVDVFK
HouseMouse (336) HGRRAEGGPVGTPAAASGAADSTL--KLGQQAGNFNWDNLLNWGPGFGHYVDVFK
Consensus (441) GRRAEGGPVGT AA G AD TLP KLGQQAG FNWDNLLNWGPGFGHYVDVFK

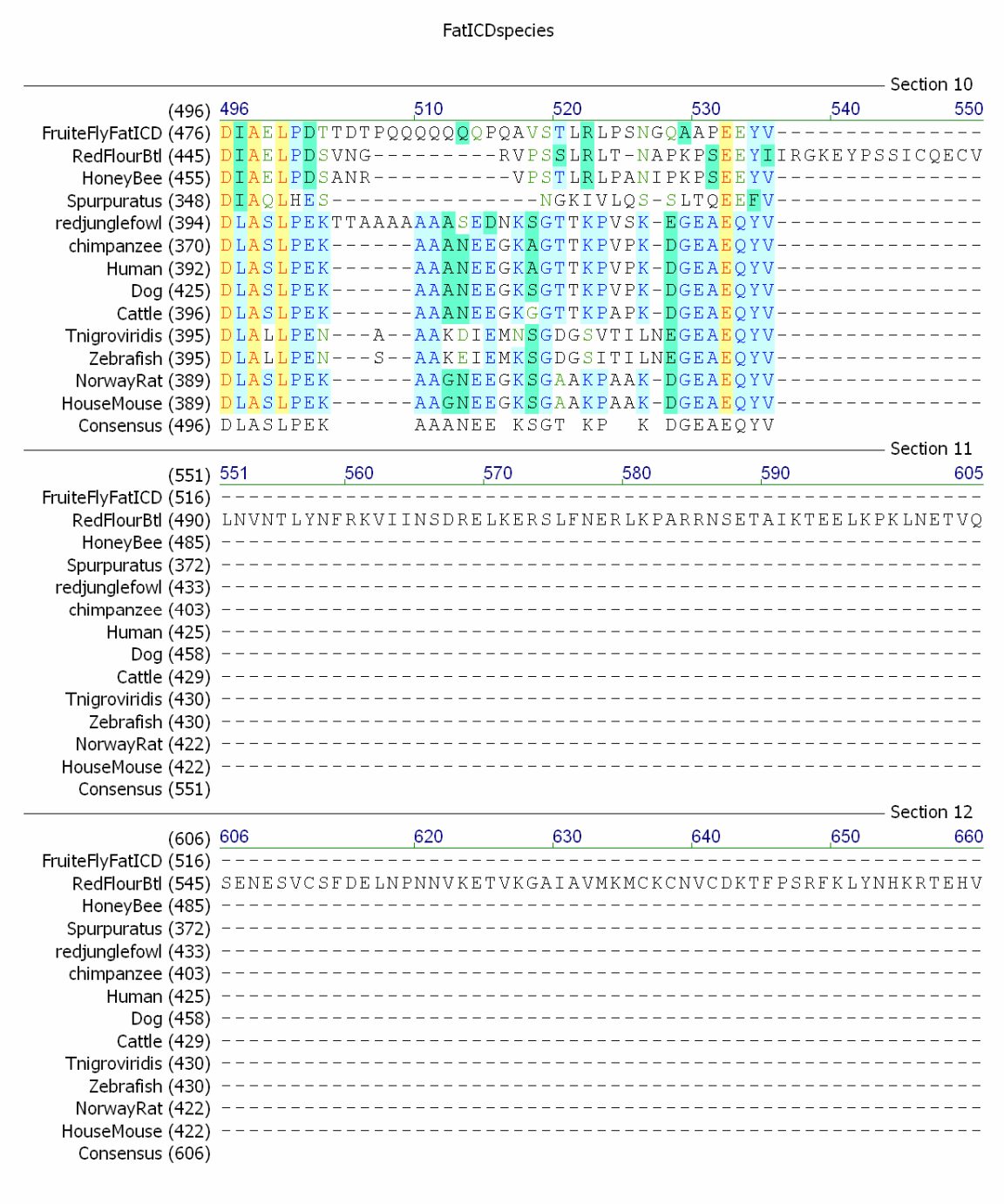

Multi alighment was performed with Vector NTI software package (Invitrogen).

Drosophila pseudoobscura (fruit fly) GA17399-PA (Fat-ICD), accession: EAL34175, aa 4621-5195.

Tribolium castaneum (red flour beetle), accession:XP_971084, aa 4501-5264.

Apis mellifera (honey bee), accession: XP_393497, aa 4561-5044.

Strongylocentrotus purpuratus, similar to Fat4, accession: XP_785601, aa 4441-4811.

Gallus gallus (red jungle fowl), Fat4 homolog, accession, XP_420617, aa 4501- 4932.

Pan troglodytes (chimpanzee), Fat4 homolog, accession, XP_001156257, aa 2821- 3222.

Homo sapiens (human), Fat4, accession, NP_078858, aa 4501-4924

Canis familiaris (dog), Fat4, accession, XP_856760, aa 3121-3577.

Bos taurus (cattle), Fat4, accession, XP_001249786, aa 4501-4928.

Tetraodon nigroviridis, accession, CAG04696,aa 1861-2289.

Danio rerio (zebrafish), Fat4, accession , XP_689394, aa 1751-2179.

Rattus norvegicus (Norway rat), Fat4, accession, XP_227060, aa 4561- 4981.

Mus musculus (house mouse), Fat4, accession, ABB88946, aa 4561-4981.

16. Protein motif prediction of *Drosophila* Fat-ICD.

(http://motif.genome.jp/):

Potential phosphorylation sites for CKI and GSK etc are not listed.

359..381, ARPRtcSLVSTLDAvSSSsEAPR, Receptor tyrosine kinase, class V.

462..471, VKTPPIPPhP, Actin-binding WH2.

395..426, mhnTdvdAhssTstdEsgnD**sfTCs**Eieydnn, Influenza C non-structural protein NS2.

REFERENCES

1. Acar, M. et al. Rumi Is a CAP10 Domain Glycosyltransferase that Modifies Notch and Is Required for Notch Signaling. *Cell* 132, 247-258 (2008).
2. Irvine, K. D. A Notch Sweeter. *Cell* 132, 177-179 (2008).
3. Kidd, T., Bland, K. S. & Goodman, C. S. Slit is the midline repellent for the robo receptor in Drosophila. *Cell* 96, 785-94 (1999).
4. Panin, V. M., Papayannopoulos, V., Wilson, R. & Irvine, K. D. Fringe modulates Notch-ligand interactions. *Nature* 387, 908-12 (1997).
5. Lum, L. et al. Identification of Hedgehog Pathway Components by RNAi in Drosophila Cultured Cells. 10.1126/science.1081403. *Science* 299, 2039-2045 (2003).
6. Kiger, A. et al. A functional genomic analysis of cell morphology using RNA interference. *Journal of Biology* 2, 27 (2003).
7. Boutros, M. et al. Genome-Wide RNAi Analysis of Growth and Viability in Drosophila Cells. 10.1126/science.1091266. *Science* 303, 832-835 (2004).
8. DasGupta, R., Kaykas, A., Moon, R. T. & Perrimon, N. Functional Genomic Analysis of the Wnt-Wingless Signaling Pathway. 10.1126/science.1109374. *Science* 308, 826-833 (2005).
9. Cho, E. & Irvine, K. D. Action of fat, four-jointed, dachsous and dachs in distal-to-proximal wing signaling. *Development* 131, 4489-500 (2004).
10. Mao, Y. et al. Dachs: an unconventional myosin that functions downstream of Fat to regulate growth, affinity and gene expression in Drosophila. *Development* 133, 2539-51 (2006).
11. Cho, E. et al. Delineation of a Fat tumor suppressor pathway. *Nat Genet* 38, 1142-50 (2006).
12. Feng, Y. & Irvine, K. D. Fat and expanded act in parallel to regulate growth through warts. *Proc Natl Acad Sci U S A* 104, 20362-7 (2007).
13. Feng, Y. & Irvine, K. D. Processing and Phosphorylation of the Fat receptor. *Accepted by Proc Natl Acad Sci U S A* (2009).
14. Hao, X. Science in China: 30 Years On. *Cell* 134, 375-377 (2008).
15. Gilbert, S. Developmental Biology. (2006).
16. Xu, T. & Rubin, G. M. Analysis of genetic mosaics in developing and adult Drosophila tissues. *Development* 117, 1223-37 (1993).
17. Perrimon, N. Creating mosaics in Drosophila. *Int J Dev Biol* 42, 243-7 (1998).
18. Lee, T. & Luo, L. Mosaic analysis with a repressible cell marker for studies of gene function in neuronal morphogenesis. *Neuron* 22, 451-61 (1999).
19. Choi, C. M. et al. Conditional Mutagenesis in Drosophila. 10.1126/science.1168275. *Science* 324, 54- (2009).
20. Nusslein-Volhard, C. & Wieschaus, E. Mutations affecting segment number and polarity in Drosophila. 287, 795-801 (1980).
21. Potter, C. J. & Xu, T. Mechanisms of size control. *Curr Opin Genet Dev* 11, 279-86 (2001).
22. Pan, D. Hippo signaling in organ size control. *Genes Dev* 21, 886-97 (2007).
23. Cook, M. & Tyers, M. Size control goes global. *Curr Opin Biotechnol* 18, 341-50 (2007).
24. Zhang, L., Yue, T. & Jiang, J. Hippo signaling pathway and organ size control. *Fly (Austin)* 3 (2009).
25. Reddy, B. V. & Irvine, K. D. The Fat and Warts signaling pathways: new insights into their regulation, mechanism and conservation. *Development* 135, 2827-38 (2008).
26. McClure, K. D. & Schubiger, G. Transdetermination: Drosophila imaginal disc cells exhibit stem cell-like potency. *Int J Biochem Cell Biol* 39, 1105-18 (2007).
27. Hariharan, I. K. & Bilder, D. Regulation of imaginal disc growth by tumor-suppressor genes in Drosophila. *Annu Rev Genet* 40, 335-61 (2006).
28. Johnston, L. A. Regeneration and transdetermination: new tricks from old cells. *Cell* 120, 288-90 (2005).
29. Kauffman, S. A. Control circuits for determination and transdetermination. *Science* 181, 310-8 (1973).

30. Schubiger, G. Regeneration, duplication and transdetermination in fragments of the leg disc of Drosophila melanogaster. *Dev Biol* 26, 277-95 (1971).
31. McClure, K. D. & Schubiger, G. A screen for genes that function in leg disc regeneration in Drosophila melanogaster. *Mech Dev* 125, 67-80 (2008).
32. Sustar, A. & Schubiger, G. A transient cell cycle shift in Drosophila imaginal disc cells precedes multipotency. *Cell* 120, 383-93 (2005).
33. Whittle, J. R. Pattern formation in imaginal discs. *Semin Cell Biol* 1, 241-52 (1990).
34. Irvine, K. D. & Rauskolb, C. BOUNDARIES IN DEVELOPMENT: Formation and Function. *Annual Review of Cell and Developmental Biology* 17, 189 LP - 214 (2001).
35. Klein, T. Wing disc development in the fly: the early stages. *Current Opinion in Genetics & Development* 11, 470-475 (2001).
36. Lawrence, P. A. & Struhl, G. Morphogens, Compartments, and Pattern: Lessons from Drosophila? *Cell* 85, 951-961 (1996).
37. Gibson, M. C. & Schubiger, G. Peripodial cells regulate proliferation and patterning of Drosophila imaginal discs. *Cell* 103, 343-50 (2000).
38. Gibson, M. C. & Schubiger, G. Drosophila peripodial cells, more than meets the eye? *Bioessays* 23, 691-7 (2001).
39. Nusinow, D., Greenberg, L. & Hatini, V. Reciprocal roles for bowl and lines in specifying the peripodial epithelium and the disc proper of the Drosophila wing primordium. *Development* 135, 3031-41 (2008).
40. Stultz, B. G., Lee, H., Ramon, K. & Hursh, D. A. Decapentaplegic head capsule mutations disrupt novel peripodial expression controlling the morphogenesis of the Drosophila ventral head. *Dev Biol* 296, 329-39 (2006).
41. Baena-Lopez, L. A., Pastor-Pareja, J. C. & Resino, J. Wg and Egfr signalling antagonise the development of the peripodial epithelium in Drosophila wing discs. *Development* 130, 6497-506 (2003).
42. Cho, K. O., Chern, J., Izaddoost, S. & Choi, K. W. Novel signaling from the peripodial membrane is essential for eye disc patterning in Drosophila. *Cell* 103, 331-42 (2000).
43. McClure, K. D. & Schubiger, G. Developmental analysis and squamous morphogenesis of the peripodial epithelium in Drosophila imaginal discs. *Development* 132, 5033-42 (2005).
44. Held, L. I., Jr. Imaginal Discs. (2005).
45. Kopan, R. & Ilagan, M. X. G. The Canonical Notch Signaling Pathway: Unfolding the Activation Mechanism. *Cell* 137, 216-233 (2009).
46. Irvine, K. D. & Rauskolb, C. Boundaries in development: formation and function. *Annu Rev Cell Dev Biol* 17, 189-214 (2001).
47. Knust, E. Control of epithelial cell polarity in Drosophila. *Trends Genet* 10, 275-80 (1994).
48. Muller, H. A. Genetic control of epithelial cell polarity: lessons from Drosophila. *Dev Dyn* 218, 52-67 (2000).
49. Tepass, U., Tanentzapf, G., Ward, R. & Fehon, R. Epithelial cell polarity and cell junctions in Drosophila. *Annu Rev Genet* 35, 747-84 (2001).
50. Mlodzik, M. Planar cell polarization: do the same mechanisms regulate Drosophila tissue polarity and vertebrate gastrulation? *Trends Genet* 18, 564-71 (2002).
51. Shin, K., Fogg, V. C. & Margolis, B. Tight Junctions and Cell Polarity. *Annual Review of Cell and Developmental Biology* 22, 207 LP - 235 (2006).
52. Brumby, A. M. & Richardson, H. E. scribble mutants cooperate with oncogenic Ras or Notch to cause neoplastic overgrowth in Drosophila. *Embo J* 22, 5769-79 (2003).
53. Wodarz, A. & Nathke, I. Cell polarity in development and cancer. *Nat Cell Biol* 9, 1016-24 (2007).
54. Wodarz, A. & Nathke, I. Cell polarity in development and cancer. 9, 1016-1024 (2007).
55. Adler, P. N. Planar signaling and morphogenesis in Drosophila. *Dev Cell* 2, 525-35 (2002).
56. Narimatsu, M. et al. Regulation of Planar Cell Polarity by Smurf Ubiquitin Ligases. *Cell* 137, 295-307 (2009).
57. Amonlirdviman, K. et al. Mathematical modeling of planar cell polarity to understand domineering nonautonomy. *Science* 307, 423-6 (2005).
58. Simons, M. & Mlodzik, M. Planar cell polarity signaling: from fly development to human disease. *Annu Rev Genet* 42, 517-40 (2008).

59. Simons, M. & Mlodzik, M. Planar Cell Polarity Signaling: From Fly Development to Human Disease. *Annual Review of Genetics* 42, 517 LP - 540 (2008).
60. Mohr, O. L. Modifications of the sex-ratio through a sex-linked semi-lethal in Drosophila melanogaster. (Besides notes on an autosomal section deficiency). *Studia Mendeliana, Brunn*, 266-287 (1923).
61. Bryant, P. J., Huettner, B., Held, L. I., Ryerse, J. & Szidonya, J. Mutations at the fat locus interfere with cell proliferation control and epithelial morphogenesis in Drosophila. *Developmental Biology* 129, 541-554 (1988).
62. Garoia, F. et al. Cell behaviour of Drosophila fat cadherin mutations in wing development. *Mechanisms of Development* 94, 95-109 (2000).
63. Mahoney, P. A. et al. The fat tumor suppressor gene in Drosophila encodes a novel member of the cadherin gene superfamily. *Cell* 67, 853-68 (1991).
64. Halbleib, J. M. & Nelson, W. J. Cadherins in development: cell adhesion, sorting, and tissue morphogenesis. 10.1101/gad.1486806. *Genes & Development* 20, 3199-3214 (2006).
65. Cadigan, K. M. & Nusse, R. Wnt signaling: a common theme in animal development. *Genes Dev* 11, 3286-305 (1997).
66. Clark, H. F. et al. Dachsous encodes a member of the cadherin superfamily that controls imaginal disc morphogenesis in Drosophila. *Genes Dev* 9, 1530-42 (1995).
67. Matakatsu, H. & Blair, S. S. Interactions between Fat and Dachsous and the regulation of planar cell polarity in the Drosophila wing. *Development* 131, 3785-94 (2004).
68. Charroux, B., Freeman, M., Kerridge, S. & Baonza, A. Atrophin contributes to the negative regulation of epidermal growth factor receptor signaling in Drosophila. *Dev Biol* 291, 278-90 (2006).
69. Fanto, M. et al. The tumor-suppressor and cell adhesion molecule Fat controls planar polarity via physical interactions with Atrophin, a transcriptional co-repressor. *Development* 130, 763-74 (2003).
70. Zhang, S., Xu, L., Lee, J. & Xu, T. Drosophila atrophin homolog functions as a transcriptional corepressor in multiple developmental processes. *Cell* 108, 45-56 (2002).
71. Matakatsu, H. & Blair, S. S. Separating the adhesive and signaling functions of the Fat and Dachsous protocadherins. *Development* 133, 2315-24 (2006).
72. Couso, J., Bishop, S. & Martinez Arias, A. The wingless signalling pathway and the patterning of the wing margin in Drosophila. *Development* 120, 621-636 (1994).
73. Yang, C. H., Axelrod, J. D. & Simon, M. A. Regulation of Frizzled by fat-like cadherins during planar polarity signaling in the Drosophila compound eye. *Cell* 108, 675-88 (2002).
74. Casal, J., Struhl, G. & Lawrence, P. A. Developmental Compartments and Planar Polarity in Drosophila. *Current Biology* 12, 1189-1198 (2002).
75. Clark, H. F. et al. Dachsous encodes a member of the cadherin superfamily that controls imaginal disc morphogenesis in Drosophila. 10.1101/gad.9.12.1530. *Genes & Development* 9, 1530-1542 (1995).
76. Lawrence, P. A., Struhl, G. & Casal, J. Do the protocadherins Fat and Dachsous link up to determine both planar cell polarity and the dimensions of organs? *Nat Cell Biol* 10, 1379-82 (2008).
77. Ma, D., Yang, C.-h., McNeill, H., Simon, M. A. & Axelrod, J. D. Fidelity in planar cell polarity signalling. 421, 543-547 (2003).
78. Waddington, C. H. The genetic control of wing development in Drosophila. *J. Genet.* 41, 75-139 (1940).
79. Villano, J. & Katz, F. four-jointed is required for intermediate growth in the proximal-distal axis in Drosophila. *Development* 121, 2767-2777 (1995).
80. Strutt, H., Mundy, J., Hofstra, K. & Strutt, D. Cleavage and secretion is not required for Four-jointed function in Drosophila patterning. *Development* 131, 881-90 (2004).
81. Brodsky, M. H. & Steller, H. Positional information along the dorsal-ventral axis of the Drosophila eye: graded expression of the four-jointed gene. *Dev Biol* 173, 428-46 (1996).
82. Villano, J. L. & Katz, F. N. four-jointed is required for intermediate growth in the proximal-distal axis in Drosophila. *Development* 121, 2767-77 (1995).
83. Ishikawa, H. O., Takeuchi, H., Haltiwanger, R. S. & Irvine, K. D. Four-jointed is a Golgi kinase that phosphorylates a subset of cadherin domains. *Science* 321, 401-4 (2008).

84. Strutt, H. & Strutt, D. Nonautonomous Planar Polarity Patterning in Drosophila: Dishevelled-Independent Functions of Frizzled. *Developmental Cell* 3, 851-863 (2002).
85. Buckles, G. R., Rauskolb, C., Villano, J. L. & Katz, F. N. Four-jointed interacts with dachs, abelson and enabled and feeds back onto the Notch pathway to affect growth and segmentation in the Drosophila leg. *Development* 128, 3533-42 (2001).
86. Bridges, C. B., Morgan, T.H. Contributions to the genetics of Drosophila melanogaster. II. The second-chromosome group of mutant characters. *Publs Carnegie Instn* 278, 123-304 (1919).
87. Rogulja, D., Rauskolb, C. & Irvine, K. D. Morphogen control of wing growth through the Fat signaling pathway. *Dev Cell* 15, 309-21 (2008).
88. Matakatsu, H. & Blair, S. S. The DHHC palmitoyltransferase approximated regulates Fat signaling and Dachs localization and activity. *Curr Biol* 18, 1390-5 (2008).
89. Morgan, N. S. The myosin superfamily in Drosophila melanogaster. *J Exp Zool* 273, 104-17 (1995).
90. Swank, D. M., Wells, L., Kronert, W. A., Morrill, G. E. & Bernstein, S. I. Determining structure/function relationships for sarcomeric myosin heavy chain by genetic and transgenic manipulation of Drosophila. *Microsc Res Tech* 50, 430-42 (2000).
91. Yamashita, R. A., Sellers, J. R. & Anderson, J. B. Identification and analysis of the myosin superfamily in Drosophila: a database approach. *J Muscle Res Cell Motil* 21, 491-505 (2000).
92. O'Connell, C. B., Tyska, M. J. & Mooseker, M. S. Myosin at work: motor adaptations for a variety of cellular functions. *Biochim Biophys Acta* 1773, 615-30 (2007).
93. Zilian, O. et al. double-time is identical to discs overgrown, which is required for cell survival, proliferation and growth arrest in Drosophila imaginal discs. *Development* 126, 5409-20 (1999).
94. Price, M. A. CKI, there's more than one: casein kinase I family members in Wnt and Hedgehog signaling. *Genes Dev* 20, 399-410 (2006).
95. Strutt, H., Price, M. A. & Strutt, D. Planar polarity is positively regulated by casein kinase Iepsilon in Drosophila. *Curr Biol* 16, 1329-36 (2006).
96. Klein, T. J., Jenny, A., Djiane, A. & Mlodzik, M. CKIepsilon/discs overgrown promotes both Wnt-Fz/beta-catenin and Fz/PCP signaling in Drosophila. *Curr Biol* 16, 1337-43 (2006).
97. Guan, J., Li, H., Rogulja, A., Axelrod, J. D. & Cadigan, K. M. The Drosophila casein kinase Iepsilon/delta Discs overgrown promotes cell survival via activation of DIAP1 expression. *Dev Biol* 303, 16-28 (2007).
98. Zeidler, M. P., Perrimon, N. & Strutt, D. I. Multiple roles for four-jointed in planar polarity and limb patterning. *Dev Biol* 228, 181-96 (2000).
99. Schweisguth, F. Regulation of notch signaling activity. *Curr Biol* 14, R129-38 (2004).
100. Zeidler, M. P., Perrimon, N. & Strutt, D. I. The four-jointed gene is required in the Drosophila eye for ommatidial polarity specification. *Current Biology* 9, 1363-1372 (1999).
101. Zeidler, M. P., Perrimon, N. & Strutt, D. I. Multiple Roles for four-jointed in Planar Polarity and Limb Patterning. *Developmental Biology* 228, 181-196 (2000).
102. Adler, P., Charlton, J. & Liu, J. Mutations in the cadherin superfamily member gene dachsous cause a tissue polarity phenotype by altering frizzled signaling. *Development* 125, 959-968 (1998).
103. Willecke, M., Hamaratoglu, F., Sansores-Garcia, L., Tao, C. & Halder, G. Boundaries of Dachsous Cadherin activity modulate the Hippo signaling pathway to induce cell proliferation. 10.1073/pnas.0805201105. *Proceedings of the National Academy of Sciences* 105, 14897-14902 (2008).
104. Chishti, A. H. et al. The FERM domain: a unique module involved in the linkage of cytoplasmic proteins to the membrane. *Trends Biochem Sci* 23, 281-2 (1998).
105. Sun, C. X., Robb, V. A. & Gutmann, D. H. Protein 4.1 tumor suppressors: getting a FERM grip on growth regulation. *J Cell Sci* 115, 3991-4000 (2002).
106. Boedigheimer, M. & Laughon, A. Expanded: a gene involved in the control of cell proliferation in imaginal discs. *Development* 118, 1291-301 (1993).
107. Mangeat, P., Roy, C. & Martin, M. ERM proteins in cell adhesion and membrane dynamics. *Trends in Cell Biology* 9, 187-192 (1999).
108. McCartney, B., Kulikauskas, R., LaJeunesse, D. & Fehon, R. The neurofibromatosis-2 homologue, Merlin, and the tumor suppressor expanded function together in Drosophila to regulate cell proliferation and differentiation. *Development* 127, 1315-1324 (2000).

109. McCartney, B. M. & Fehon, R. G. Distinct cellular and subcellular patterns of expression imply distinct functions for the Drosophila homologues of moesin and the neurofibromatosis 2 tumor suppressor, merlin. *J Cell Biol* 133, 843-52 (1996).
110. McClatchey, A. I. Merlin and ERM proteins: unappreciated roles in cancer development? *Nat Rev Cancer* 3, 877-83 (2003).
111. Maeda, M., Matsui, T., Imamura, M. & Tsukita, S. Expression level, subcellular distribution and rho-GDI binding affinity of merlin in comparison with Ezrin/Radixin/Moesin proteins. *Oncogene* 18, 4788-97 (1999).
112. Flaiz, C., Ammoun, S., Biebl, A. & Hanemann, C. O. Altered adhesive structures and their relation to RhoGTPase activation in merlin-deficient Schwannoma. *Brain Pathol* 19, 27-38 (2009).
113. Hamaratoglu, F. et al. The tumour-suppressor genes NF2/Merlin and Expanded act through Hippo signalling to regulate cell proliferation and apoptosis. *Nat Cell Biol* 8, 27-36 (2006).
114. Yin, F. & Pan, D. Fat flies expanded the hippo pathway: a matter of size control. *Sci STKE* 2007, pe12 (2007).
115. Wu, S., Huang, J., Dong, J. & Pan, D. hippo Encodes a Ste-20 Family Protein Kinase that Restricts Cell Proliferation and Promotes Apoptosis in Conjunction with salvador and warts. *Cell* 114, 445-456 (2003).
116. Lai, Z.-C. et al. Control of Cell Proliferation and Apoptosis by Mob as Tumor Suppressor, Mats. *Cell* 120, 675-685 (2005).
117. Huang, J., Wu, S., Barrera, J., Matthews, K. & Pan, D. The Hippo signaling pathway coordinately regulates cell proliferation and apoptosis by inactivating Yorkie, the Drosophila Homolog of YAP. *Cell* 122, 421-34 (2005).
118. Oh, H. & Irvine, K. D. In vivo analysis of Yorkie phosphorylation sites. *Oncogene* (2009).
119. Dong, J. et al. Elucidation of a universal size-control mechanism in Drosophila and mammals. *Cell* 130, 1120-33 (2007).
120. Oh, H. & Irvine, K. D. In vivo regulation of Yorkie phosphorylation and localization. *Development* 135, 1081-8 (2008).
121. Wu, S., Liu, Y., Zheng, Y., Dong, J. & Pan, D. The TEAD/TEF Family Protein Scalloped Mediates transcriptional Output of the Hippo Growth-Regulatory Pathway. D*evelopmental Cell* 14, 388-398 (2008).
122. Goulev, Y. et al. SCALLOPED Interacts with YORKIE, the Nuclear Effector of the Hippo Tumor-Suppressor Pathway in Drosophila. C*urrent Biology* 18, 435-441 (2008).
123. Zhang, L. et al. The TEAD/TEF Family of Transcription Factor Scalloped Mediates Hippo Signaling in Organ Size Control. D*evelopmental Cell* 14, 377-387 (2008).
124. Zhao, B. et al. TEAD mediates YAP-dependent gene induction and growth control. 10.1101/gad.1664408. G*enes & Development* 22, 1962-1971 (2008).
125. Nolo, R., Morrison, C. M., Tao, C., Zhang, X. & Halder, G. The bantam MicroRNA Is a Target of the Hippo Tumor-Suppressor Pathway. C*urrent Biology* 16, 1895-1904 (2006).
126. Thompson, B. J. & Cohen, S. M. The Hippo pathway regulates the bantam microRNA to control cell proliferation and apoptosis in Drosophila. C*ell* 126, 767-74 (2006).
127. Rothenberg, M. E. & Jan, Y.-N. Cell biology: The hippo hypothesis. 425, 469-470 (2003).
128. Overholtzer, M. et al. Transforming properties of YAP, a candidate oncogene on the chromosome 11q22 amplicon. P*roc Natl Acad Sci U S A* 103, 12405-10 (2006).
129. Zhao, B. et al. Inactivation of YAP oncoprotein by the Hippo pathway is involved in cell contact inhibition and tissue growth control. G*enes Dev* 21, 2747-61 (2007).
130. Cao, X., Pfaff, S. L. & Gage, F. H. YAP regulates neural progenitor cell number via the TEA domain transcription factor. G*enes Dev* 22, 3320-34 (2008).
131. Hao, Y., Chun, A., Cheung, K., Rashidi, B. & Yang, X. Tumor suppressor LATS1 is a negative regulator of oncogene YAP. J *Biol Chem* 283, 5496-509 (2008).
132. Oka, T., Mazack, V. & Sudol, M. Mst2 and Lats kinases regulate apoptotic function of Yes kinase-associated protein (YAP). J *Biol Chem* 283, 27534-46 (2008).
133. Ota, M. & Sasaki, H. Mammalian Tead proteins regulate cell proliferation and contact inhibition as transcriptional mediators of Hippo signaling. D*evelopment* 135, 4059-69 (2008).
134. Zhang, J., Smolen, G. A. & Haber, D. A. Negative regulation of YAP by LATS1 underscores evolutionary conservation of the Drosophila Hippo pathway. C*ancer Res* 68, 2789-94 (2008).

135. Zhao, B. et al. TEAD mediates YAP-dependent gene induction and growth control. G*enes Dev* 22, 1962-71 (2008).
136. Zhang, H. et al. TEAD transcription factors mediate the function of TAZ in cell growth and epithelial-mesenchymal transition. 10.1074/jbc.M900843200. J. *Biol. Chem.,* M900843200 (2009).
137. Lei, Q. Y. et al. TAZ promotes cell proliferation and epithelial-mesenchymal transition and is inhibited by the hippo pathway. M*ol Cell Biol* 28, 2426-36 (2008).
138. Chan, S. W. et al. Teads mediate nuclear retention of taz to promote oncogenic transformation. 10.1074/jbc.M901568200. J. *Biol. Chem.,* M901568200 (2009).
139. Saucedo, L. J. & Edgar, B. A. Filling out the Hippo pathway. N*at Rev Mol Cell Biol* 8, 613-621 (2007).
140. Katoh, Y. & Katoh, M. Comparative integromics on FAT1, FAT2, FAT3 and FAT4. I*nt J Mol Med* 18, 523-8 (2006).
141. Saburi, S. et al. Loss of Fat4 disrupts PCP signaling and oriented cell division and leads to cystic kidney disease. N*at Genet* 40, 1010-5 (2008).
142. Rock, R., Schrauth, S. & Gessler, M. Expression of mouse dchs1, fjx1, and fat-j suggests conservation of the planar cell polarity pathway identified in Drosophila. D*ev Dyn* 234, 747-55 (2005).
143. St John, M. A. et al. Mice deficient of Lats1 develop soft-tissue sarcomas, ovarian tumours and pituitary dysfunction. N*at Genet* 21, 182-6 (1999).
144. Tao, W. et al. Human homologue of the Drosophila melanogaster lats tumour suppressor modulates CDC2 activity. N*at Genet* 21, 177-81 (1999).
145. Tapon, N. et al. salvador Promotes both cell cycle exit and apoptosis in Drosophila and is mutated in human cancer cell lines. C*ell* 110, 467-78 (2002).
146. Lai, Z. C. et al. Control of cell proliferation and apoptosis by mob as tumor suppressor, mats. C*ell* 120, 675-85 (2005).
147. Hou, R., Liu, L., Anees, S., Hiroyasu, S. & Sibinga, N. E. The Fat1 cadherin integrates vascular smooth muscle cell growth and migration signals. J *Cell Biol* 173, 417-29 (2006).
148. Braun, G. S. et al. Differentially spliced isoforms of FAT1 are asymmetrically distributed within migrating cells. J *Biol Chem* 282, 22823-33 (2007).
149. Kwaepila, N., Burns, G. & Leong, A. S. Immunohistological localisation of human FAT1 (hFAT) protein in 326 breast cancers. Does this adhesion molecule have a role in pathogenesis? P*athology* 38, 125-31 (2006).
150. Matsui, S. et al. Knockdown of Fat2 by siRNA inhibits the migration of human squamous carcinoma cells. J *Dermatol Sci* 51, 207-10 (2008).
151. Nagae, S., Tanoue, T. & Takeichi, M. Temporal and spatial expression profiles of the Fat3 protein, a giant cadherin molecule, during mouse development. D*ev Dyn* 236, 534-43 (2007).
152. Nakaya, K. et al. Identification of homozygous deletions of tumor suppressor gene FAT in oral cancer using CGH-array. O*ncogene* 26, 5300-8 (2007).
153. Chao Qi, Y. T. Z., Liping Hu, Yi-Jun Zhu,. Identification of Fat4 as a candidate tumor suppressor gene in breast cancers. I*nternational Journal of Cancer* 124, 793-798 (2009).
154. dachsous1. h*ttp://www.ncbi.nlm.nih.gov/UniGene/.*
155. dachsous2, Gene Expression Data. *http://www.informatics.jax.org/searches/expression_report.cgi?id=MGI:2685263*.
156. Ashery-Padan, R., Alvarez-Bolado, G., Klamt, B., Gessler, M. & Gruss, P. Fjx1, the murine homologue of the Drosophila four-jointed gene, codes for a putative secreted protein expressed in restricted domains of the developing and adult brain. M*ech Dev* 80, 213-7 (1999).
157. Jarvinen, A. K. et al. High-resolution copy number and gene expression microarray analyses of head and neck squamous cell carcinoma cell lines of tongue and larynx. G*enes Chromosomes Cancer* 47, 500-9 (2008).
158. Trofatter, J. A. et al. A novel moesin-, ezrin-, radixin-like gene is a candidate for the neurofibromatosis 2 tumor suppressor. C*ell* 72, 791-800 (1993).
159. Ruttledge, M. H. et al. Evidence for the complete inactivation of the NF2 gene in the majority of sporadic meningiomas. N*at Genet* 6, 180-4 (1994).
160. FRMD6. *http://www.ncbi.nlm.nih.gov/UniGene/*.

161. Seidel, C. et al. Frequent hypermethylation of MST1 and MST2 in soft tissue sarcoma. M*ol Carcinog* 46, 865-71 (2007).
162. Chiba, S., Ikeda, M., Katsunuma, K., Ohashi, K. & Mizuno, K. MST2- and Furry-Mediated Activation of NDR1 Kinase Is Critical for Precise Alignment of Mitotic Chromosomes. C*urr Biol* (2009).
163. Chan, E. H. et al. The Ste20-like kinase Mst2 activates the human large tumor suppressor kinase Lats1. O*ncogene* 24, 2076-86 (2005).
164. Yoo, N. J. et al. Mutational analysis of salvador gene in human carcinomas. A*pmis* 111, 595-8 (2003).
165. Strazisar, M., Mlakar, V. & Glavac, D. LATS2 tumour specific mutations and down-regulation of the gene in non-small cell carcinoma. L*ung Cancer* (2008).
166. Li, Y. et al. Lats2, a putative tumor suppressor, inhibits G1/S transition. O*ncogene* 22, 4398-405 (2003).
167. Yabuta, N. et al. Lats2 is an essential mitotic regulator required for the coordination of cell division. J *Biol Chem* 282, 19259-71 (2007).
168. Zhao, B., Lei, Q. Y. & Guan, K. L. The Hippo-YAP pathway: new connections between regulation of organ size and cancer. C*urr Opin Cell Biol* 20, 638-46 (2008).
169. Saucedo, L. J. & Edgar, B. A. Filling out the Hippo pathway. N*at Rev Mol Cell Biol* 8, 613-21 (2007).
170. Zeng, Q. & Hong, W. The emerging role of the hippo pathway in cell contact inhibition, organ size control, and cancer development in mammals. C*ancer Cell* 13, 188-92 (2008).
171. Maitra, S., Kulikauskas, R. M., Gavilan, H. & Fehon, R. G. The tumor suppressors Merlin and Expanded function cooperatively to modulate receptor endocytosis and signaling. C*urr Biol* 16, 702-9 (2006).
172. Badouel, C. et al. The FERM-Domain Protein Expanded Regulates Hippo Pathway Activity via Direct Interactions with the Transcriptional Activator Yorkie. D*evelopmental Cell* 16, 411-420 (2009).
173. Xu, T., Wang, W., Zhang, S., Stewart, R. & Yu, W. Identifying tumor suppressors in genetic mosaics: the Drosophila lats gene encodes a putative protein kinase. D*evelopment* 121, 1053-1063 (1995).
174. Zhao, B., Lei, Q.-Y. & Guan, K.-L. Harness the Power: New Insights into the Inhibition of YAP/ Yorkie. D*evelopmental Cell* 16, 321-322 (2009).
175. Silva, E., Tsatskis, Y., Gardano, L., Tapon, N. & McNeill, H. The tumor-suppressor gene fat controls tissue growth upstream of expanded in the hippo signaling pathway. C*urr Biol* 16, 2081-9 (2006).
176. Willecke, M. et al. The fat cadherin acts through the hippo tumor-suppressor pathway to regulate tissue size. C*urr Biol* 16, 2090-100 (2006).
177. Bennett, F. C. & Harvey, K. F. Fat cadherin modulates organ size in Drosophila via the Salvador/Warts/Hippo signaling pathway. C*urr Biol* 16, 2101-10 (2006).
178. Tyler, D. M. & Baker, N. E. Expanded and fat regulate growth and differentiation in the Drosophila eye through multiple signaling pathways. D*evelopmental Biology* 305, 187-201 (2007).
179. Bischof, J., Maeda, R. K., Hediger, M., Karch, F. & Basler, K. An optimized transgenesis system for Drosophila using germ-line-specific phiC31 integrases. P*roc Natl Acad Sci U S A* 104, 3312-7 (2007).
180. Venken, K. J. T., He, Y., Hoskins, R. A. & Bellen, H. J. P[acman]: A BAC Transgenic Platform for Targeted Insertion of Large DNA Fragments in D. melanogaster. 10.1126/science.1134426. S*cience* 314, 1747-1751 (2006).
181. Feng, Y. & Irvine, K. D. Processing and Phosphorylation of the Fat receptor. s*ubmitted* (2009).
182. Nishiyama, Y. et al. A human homolog of Drosophila warts tumor suppressor, h-warts, localized to mitotic apparatus and specifically phosphorylated during mitosis. F*EBS letters* 459, 159-165 (1999).
183. Rogulja, D. & Irvine, K. D. Regulation of cell proliferation by a morphogen gradient. C*ell* 123, 449-61 (2005).
184. Kiecker, C. & Lumsden, A. Compartments and their boundaries in vertebrate brain development. 6, 553-564 (2005).

185. Tanoue, T. & Takeichi, M. New insights into Fat cadherins. J *Cell Sci* 118, 2347-53 (2005).
186. Badouel, C. et al. The FERM-domain protein expanded regulates Hippo pathway activity via direct interactions with the transcriptional activator Yorkie. D*ev Cell* 16, 411-20 (2009).
187. Aoki, K. & Taketo, M. M. Adenomatous polyposis coli (APC): a multi-functional tumor suppressor gene. 10.1242/jcs.03485. J *Cell Sci* 120, 3327-3335 (2007).
188. Cadigan, K. M. & Nusse, R. Wnt signaling: a common theme in animal development. 10.1101/gad.11.24.3286. Gen*es & Development 11*, 3286-3305 (1997).
189. Vidal, M. & Cagan, R. L. Drosophila models for cancer research. Cur*rent Opinion in Genetics & Developmen. Oncogenes and cell proliferation 16*, 10-16 (2006).
190. Watson, K., Justice, R. & Bryant, P. Drosophila in cancer research: the first fifty tumor suppressor genes. J C*ell Sci Suppl. 18*, 19-33 (1994).
191. Pagliarini, R. A. & Xu, T. A Genetic Screen in Drosophila for Metastatic Behavior. 10.1126/science.1088474. Sci*ence 30*2, 1227-1231 (2003).
192. Golic, K. G. & Lindquist, S. The FLP recombinase of yeast catalyzes site-specific recombination in the drosophila genome. Cel*l 59*, 499-509 (1989).
193. Justice, R. W., Zilian, O., Woods, D. F., Noll, M. & Bryant, P. J. The Drosophila tumor suppressor gene warts encodes a homolog of human myotonic dystrophy kinase and is required for the control of cell shape and proliferation. 10.1101/gad.9.5.534. Gen*es & Development 9,* 534-546 (1995).
194. McCartney, B. M., Kulikauskas, R. M., LaJeunesse, D. R. & Fehon, R. G. The neurofibromatosis-2 homologue, Merlin, and the tumor suppressor expanded function together in Drosophila to regulate cell proliferation and differentiation. Dev*elopment 12*7, 1315-24 (2000).
195. Blaumueller, C. M. & Mlodzik, M. The Drosophila tumor suppressor expanded regulates growth, apoptosis, and patterning during development. Mec*h Dev 92*, 251-62 (2000).
196. Rauskolb, C. & Irvine, K. D. Notch-Mediated Segmentation and Growth Control of the Drosophila Leg. Dev*elopmental Biology 21*0, 339-350 (1999).
197. Ding, Q., Dimayuga, E. & Keller, J. N. Proteasome regulation of oxidative stress in aging and age-related diseases of the CNS. Ant*ioxid Redox Signal 8,* 163-72 (2006).
198. Breusing, N. & Grune, T. Regulation of proteasome-mediated protein degradation during oxidative stress and aging. Bio*l Chem 38*9, 203-9 (2008).
199. Hay, B., Wolff, T. & Rubin, G. Expression of baculovirus P35 prevents cell death in Drosophila. Dev*elopment 12*0, 2121-2129 (1994).
200. Lawrence, P. A., Casal, J. & Struhl, G. Cell interactions and planar polarity in the abdominal epidermis of Drosophila. Dev*elopment 13*1, 4651-64 (2004).
201. Lawrence, P. A., Casal, J. & Struhl, G. Cell interactions and planar polarity in the abdominal epidermis of Drosophila. 10.1242/dev.01351. Dev*elopment 13*1, 4651-4664 (2004).
202. Edgar, B. A. From Cell Structure to Transcription: Hippo Forges a New Path. Cel*l 12*4, 267-273 (2006).
203. Boedigheimer, M. J., Nguyen, K. P. & Bryant, P. J. Expanded functions in the apical cell domain to regulate the growth rate of imaginal discs. Dev *Genet 20*, 103-10 (1997).
204. Pellock, B. J., Buff, E., White, K. & Hariharan, I. K. The Drosophila tumor suppressors Expanded and Merlin differentially regulate cell cycle exit, apoptosis, and Wingless signaling. Dev *Biol 30*4, 102-15 (2007).
205. Sukontason, K. et al. Ommatidia of blow fly, house fly, and flesh fly: implication of their vision efficiency. Par*asitology Research 10*3, 123-131 (2008).
206. Tomlinson, A. The molecular basis of pattern formation in the developing compound eye of Drosophila. Sem*in Cell Biol 1,* 229-39 (1990).
207. Jaiswal, M., Agrawal, N. & Sinha, P. Fat and Wingless signaling oppositely regulate epithelial cell-cell adhesion and distal wing development in Drosophila. Dev*elopment 13*3, 925-35 (2006).
208. Lee, T. & Luo, L. Mosaic analysis with a repressible cell marker (MARCM) for Drosophila neural development. Tre*nds Neurosci 24*, 251-4 (2001).
209. Kloss, B. et al. The Drosophila clock gene double-time encodes a protein closely related to human casein kinase Iepsilon. Cel*l 94*, 97-107 (1998).
210. Jia, J. et al. Phosphorylation by double-time/CKIepsilon and CKIalpha targets cubitus interruptus for Slimb/beta-TRCP-mediated proteolytic processing. Dev *Cell 9,* 819-30 (2005).

211. Price, M. A. & Kalderon, D. Proteolysis of the Hedgehog Signaling Effector Cubitus interruptus Requires Phosphorylation by Glycogen Synthase Kinase 3 and Casein Kinase 1. Cel*l 10*8, 823-835 (2002).
212. Ko, H. W., Jiang, J. & Edery, I. Role for Slimb in the degradation of Drosophila Period protein phosphorylated by Doubletime. Nat*ure 42*0, 673-8 (2002).
213. Yanagawa, S. et al. Casein kinase I phosphorylates the Armadillo protein and induces its degradation in Drosophila. Emb*o J 21*, 1733-42 (2002).
214. Nishioka, N. et al. The Hippo Signaling Pathway Components Lats and Yap Pattern Tead4 Activity to Distinguish Mouse Trophectoderm from Inner Cell Mass. Dev*elopmental Cell 16*, 398-410 (2009).
215. Groth, A. C., Fish, M., Nusse, R. & Calos, M. P. Construction of transgenic Drosophila by using the site-specific integrase from phage phiC31. Gen*etics 16*6, 1775-82 (2004).
216. Bateman, J. R., Lee, A. M. & Wu, C. T. Site-specific transformation of Drosophila via phiC31 integrase-mediated cassette exchange. Gen*etics 17*3, 769-77 (2006).
217. Kopan, R. & Cagan, R. Notch on the cutting edge. Tre*nds in Genetics 13*, 465-467 (1997).
218. Usui, T. et al. Flamingo, a Seven-Pass Transmembrane Cadherin, Regulates Planar Cell Polarity under the Control of Frizzled. Cel*l 98*, 585-595 (1999).
219. Simon, M. A. Planar cell polarity in the Drosophila eye is directed by graded Four-jointed and Dachsous expression. Dev*elopment 13*1, 6175-84 (2004).
220. Graves, P. R. & Roach, P. J. Role of COOH-terminal Phosphorylation in the Regulation of Casein Kinase I. 10.1074/jbc.270.37.21689. J. *Biol. Chem. 27*0, 21689-21694 (1995).
221. Price, J. L. et al. double-time is a novel Drosophila clock gene that regulates PERIOD protein accumulation. Cel*l 94*, 83-95 (1998).
222. Preuss, F. et al. Drosophila doubletime mutations which either shorten or lengthen the period of circadian rhythms decrease the protein kinase activity of casein kinase I. Mol *Cell Biol 24*, 886-98 (2004).
223. Kivimäe, S., Saez, L. & Young, M. W. Activating PER Repressor through a DBT-Directed Phosphorylation Switch PLo*S Biology 6,* e183 (2008).
224. Joseph B. Duffy. GAL4 system in *Drosophila*: A fly geneticist's swiss army knife. gen*esis 34*, 1-15 (2002).
225. Rong, Y. S. & Golic, K. G. A Targeted Gene Knockout in Drosophila. Gen*etics 15*7, 1307-1312 (2001).
226. Myers, E. W. et al. A whole-genome assembly of Drosophila. Sci*ence 28*7, 2196-204 (2000).
227. Adams, M. et al. The genome sequence of Drosophila melanogaster. Sci*ence 28*7, 2185 - 2195 (2000).
228. Benos, P. V. et al. From Sequence to Chromosome: The Tip of the X Chromosome of Drosophila melanogaster. 10.1126/science.287.5461.2220. Sci*ence 28*7, 2220-2222 (2000).
229. Hillenmeyer, M. E. et al. The Chemical Genomic Portrait of Yeast: Uncovering a Phenotype for All Genes. 10.1126/science.1150021. Sci*ence 32*0, 362-365 (2008).
230. Zhai, B., Villen, J., Beausoleil, S. A., Mintseris, J. & Gygi, S. P. Phosphoproteome Analysis of Drosophila melanogaster Embryos. doi:10.1021/pr700696a. Jour*nal of Proteome Research 7,* 1675-1682 (2008).
231. Sun, S., Zhao, S. & Wang, Z. Genes of Hippo signaling network act unconventionally in the control of germline proliferation in Drosophila. Dev *Dyn 237*, 270-275 (2007).
232. Polesello, C. & Tapon, N. Salvador-warts-hippo signaling promotes Drosophila posterior follicle cell maturation downstream of notch. Curr *Biol 17,* 1864-70 (2007).
233. Natzle, J. & Vesenka, G. Isolation and organ culture of imaginal tissues. Met*hods Cell Biol 44,* 109-127 (1994).
234. Hironori Takeda, A. K., Makoto Takahashi, Atsushi Yamada, Tohru Koike,. Matrix-assisted laser desorption/ionization time-of-flight mass spectrometry of phosphorylated compounds using a novel phosphate capture molecule. Rapi*d Communications in Mass Spectrometry 17,* 2075-2081 (2003).
235. Kinoshita, E., Kinoshita-Kikuta, E., Takiyama, K. & Koike, T. Phosphate-binding Tag, a New Tool to Visualize Phosphorylated Proteins. 10.1074/mcp.T500024-MCP200. Mol *Cell Proteomics 5,* 749-757 (2006).

236. Eiji Kinoshita, A. Y., Hironori Takeda, Emiko Kinoshita-Kikuta, Tohru Koike,. Novel immobilized zinc(II) affinity chromatography for phosphopeptides and phosphorylated proteins. Jour*nal of Separation Science 28,* 155-162 (2005).
237. Bryant, P. J., Huettner, B., Held, L. I., Jr., Ryerse, J. & Szidonya, J. Mutations at the fat locus interfere with cell proliferation control and epithelial morphogenesis in Drosophila. Dev *Biol 129*, 541-54 (1988).
238. Zecca, M. & Struhl, G. Control of growth and patterning of the Drosophila wing imaginal disc by EGFR-mediated signaling. Deve*lopment 129*, 1369-76 (2002).
239. Wang, S. H., Simcox, A. & Campbell, G. Dual role for Drosophila epidermal growth factor receptor signaling in early wing disc development. Gene*s Dev 14,* 2271-6 (2000).
240. Milan, M. & Cohen, S. M. Temporal regulation of apterous activity during development of the Drosophila wing. Deve*lopment 127*, 3069-78 (2000).
241. Adler, P. N. & Lee, H. Frizzled signaling and cell-cell interactions in planar polarity. Curr *Opin Cell Biol 13,* 635-40 (2001).
242. Shimada, Y., Usui, T., Yanagawa, S., Takeichi, M. & Uemura, T. Asymmetric colocalization of Flamingo, a seven-pass transmembrane cadherin, and Dishevelled in planar cell polarization. Curr *Biol 11,* 859-63 (2001).
243. Nishiyama, Y. et al. A human homolog of Drosophila warts tumor suppressor, h-warts, localized to mitotic apparatus and specifically phosphorylated during mitosis. FEBS *Lett 459*, 159-65 (1999).
244. Emoto, K., Parrish, J. Z., Jan, L. Y. & Jan, Y. N. The tumour suppressor Hippo acts with the NDR kinases in dendritic tiling and maintenance. Natu*re 443*, 210-3 (2006).
245. Parrish, J. Z., Emoto, K., Jan, L. Y. & Jan, Y. N. Polycomb genes interact with the tumor suppressor genes hippo and warts in the maintenance of Drosophila sensory neuron dendrites. Gene*s Dev 21,* 956-72 (2007).
246. Venken, K. J., He, Y., Hoskins, R. A. & Bellen, H. J. P[acman]: a BAC transgenic platform for targeted insertion of large DNA fragments in D. melanogaster. Scie*nce 314*, 1747-51 (2006).
247. Striedinger, K. et al. The neurofibromatosis 2 tumor suppressor gene product, merlin, regulates human meningioma cell growth by signaling through YAP. Neop*lasia 10,* 1204-12 (2008).
248. Bertini, E., Oka, T., Sudol, M., Strano, S. & Blandino, G. YAP: at the crossroad between transformation and tumor suppression. Cell *Cycle 8,* 49-57 (2009).
249. Harvey, K. F., Pfleger, C. M. & Hariharan, I. K. The Drosophila Mst ortholog, hippo, restricts growth and cell proliferation and promotes apoptosis. Cell *114*, 457-67 (2003).
250. Pantalacci, S., Tapon, N. & Leopold, P. The Salvador partner Hippo promotes apoptosis and cell-cycle exit in Drosophila. Nat *Cell Biol 5,* 921-7 (2003).
251. Udan, R. S., Kango-Singh, M., Nolo, R., Tao, C. & Halder, G. Hippo promotes proliferation arrest and apoptosis in the Salvador/Warts pathway. Nat *Cell Biol 5,* 914-20 (2003).
252. Nolo, R., Morrison, C. M., Tao, C., Zhang, X. & Halder, G. The bantam microRNA is a target of the hippo tumor-suppressor pathway. Curr *Biol 16,* 1895-904 (2006).
253. Hipfner, D. R., Weigmann, K. & Cohen, S. M. The bantam gene regulates Drosophila growth. Gene*tics 161*, 1527-37 (2002).
254. Brennecke, J., Hipfner, D. R., Stark, A., Russell, R. B. & Cohen, S. M. bantam encodes a developmentally regulated microRNA that controls cell proliferation and regulates the proapoptotic gene hid in Drosophila. Cell *113*, 25-36 (2003).
255. Baena-Lopez, L. A., RodrÃguez, I. & Baonza, A. The tumor suppressor genes dachsous and fat modulate different signalling pathways by regulating dally and dally-like. 10.1073/pnas.0803747105. Proce*edings of the National Academy of Sciences 105,* 9645-9650 (2008).
256. Lawrence, P. A. Morphogens: how big is the big picture? Nat C*ell Biol 3, E*151-4 (2001).
257. Driever, W. & Nüslein-Volhard, C. The bicoid protein determines position in the Drosophila embryo in a concentration-dependent manner. Cell 5*4, 9*5-104 (1988).
258. Zecca, M., Basler, K. & Struhl, G. Sequential organizing activities of engrailed, hedgehog and decapentaplegic in the Drosophila wing. Develo*pment 121,* 2265-2278 (1995).
259. Rashid, T. et al. Opposing gradients of ephrin-As and EphA7 in the superior colliculus are essential for topographic mapping in the mammalian visual system. Neuron *47, 5*7-69 (2005).

260. Frisen, J. et al. Ephrin-A5 (AL-1/RAGS) is essential for proper retinal axon guidance and topographic mapping in the mammalian visual system. Neuron *20, 2*35-43 (1998).
261. Gurdon, J. B. & Bourillot, P.-Y. Morphogen gradient interpretation. 413, 797-803 (2001).
262. Piddini, E. & Vincent, J.-P. Interpretation of the Wingless Gradient Requires Signaling-Induced Self-Inhibition. Cell 1*36,* 296-307 (2009).
263. Strutt, D. Frizzled signalling and cell polarisation in Drosophila and vertebrates. 10.1242/dev.00695. Develo*pment 130,* 4501-4513 (2003).
264. Usui, T. et al. Flamingo, a seven-pass transmembrane cadherin, regulates planar cell polarity under the control of Frizzled. Cell 9*8, 5*85-95 (1999).
265. Weber, U., Pataki, C., Mihaly, J. & Mlodzik, M. Combinatorial signaling by the Frizzled/PCP and Egfr pathways during planar cell polarity establishment in the Drosophila eye. Dev Bi*ol 316,* 110-23 (2008).
266. Wu, J. & Mlodzik, M. The frizzled extracellular domain is a ligand for Van Gogh/Stbm during nonautonomous planar cell polarity signaling. Dev Ce*ll 15, 4*62-9 (2008).
267. MacDougall, N. et al. Merlin, the Drosophila homologue of neurofibromatosis-2, is specifically required in posterior follicle cells for axis formation in the oocyte. Develo*pment 128,* 665-73 (2001).
268. Sun, S., Zhao, S. & Wang, Z. Genes of Hippo signaling network act unconventionally in the control of germline proliferation in Drosophila. Dev Dy*n 237,* 270-5 (2008).
269. Warming, S., Costantino, N., Court, D. L., Jenkins, N. A. & Copeland, N. G. Simple and highly efficient BAC recombineering using galK selection.10.1093/nar/gni035. Nucl. *Acids Res. 33, e*36- (2005).
270. Milan, M., Diaz-Benjumea, F. J. & Cohen, S. M. Beadex encodes an LMO protein that regulates Apterous LIM-homeodomain activity in Drosophila wing development: a model for LMO oncogene function. Genes *Dev 12, 2*912-20 (1998).
271. Rong, Y. S. & Golic, K. G. Gene Targeting by Homologous Recombination in Drosophila. 10.1126/science.288.5473.2013. Scienc*e 288,* 2013-2018 (2000).
272. Gong, W. J. & Golic, K. G. Ends-out, or replacement, gene targeting in Drosophila. 10.1073/pnas.0535280100. Proceed*ings of the National Academy of Sciences of the United States of America 100,* 2556-2561 (2003).
273. Rubin, G. M. & Spradling, A. C. Genetic transformation of Drosophila with transposable element vectors. Scienc*e 218,* 348-53 (1982).
274. Markstein, M., Pitsouli, C., Villalta, C., Celniker, S. E. & Perrimon, N. Exploiting position effects and the gypsy retrovirus insulator to engineer precisely expressed transgenes. 40, 476-483 (2008).
275. Richa, J. & Lo, C. Introduction of human DNA into mouse eggs by injection of dissected chromosome fragments. 10.1126/science.2749254. Scienc*e 245,* 175-177 (1989).
276. Co, D. et al. Generation of Transgenic Mice and Germline Transmission of a Mammalian Artificial Chromosome Introduced into Embryos by Pronuclear Microinjection. Chromo*some Research 8, 18*3-191 (2000).
277. Eliyahu, H., Barenholz, Y. & Domb, A. Polymers for DNA Delivery. Molecu*les 10, 3*4-64 (2005).
278. Davies, L. A. et al. Enhanced Lung Gene Expression After Aerosol Delivery of Concentrated pDNA/PEI Complexes. 16, 1283-1290 (2008).
279. Kneuer, C. et al. A Nonviral DNA Delivery System Based on Surface Modified Silica-Nanoparticles Can Efficiently Transfect Cells in Vitro. doi:10.1021/bc0000637. Biocon*jugate Chemistry 11, 9*26-932 (2000).
280. Tanoue, T. & Takeichi, M. Mammalian Fat1 cadherin regulates actin dynamics and cell-cell contact. J Cell *Biol 165,* 517-28 (2004).
281. Meignin, C., Alvarez-Garcia, I., Davis, I. & Palacios, I. M. The salvador-warts-hippo pathway is required for epithelial proliferation and axis specification in Drosophila. Curr B*iol 17, 1*871-8 (2007).
282. Riechmann, V. Developmental biology: hippo promotes posterior patterning by preventing proliferation. Curr B*iol 17, R*1006-8 (2007).
283. Rauskolb, C. The establishment of segmentation in the Drosophila leg. Develo*pment 128,* 4511-4521 (2001).

284. de Celis, J., Tyler, D., de Celis, J. & Bray, S. Notch signalling mediates segmentation of the Drosophila leg. Develo*pment 125,* 4617-4626 (1998).
285. Galindo, M. I., Bishop, S. A., Greig, S. & Couso, J. P. Leg Patterning Driven by Proximal-Distal Interactions and EGFR Signaling.10.1126/science.1072311. Scienc*e 297,* 256-259 (2002).
286. Zhu, H. Is anisotropic propagation of polarized molecular distribution the common mechanism of swirling patterns of planar cell polarization? Journa*l of Theoretical Biology 256,* 315-325 (2009).
287. Tree, D. R., Ma, D. & Axelrod, J. D. A three-tiered mechanism for regulation of planar cell polarity. Semin *Cell Dev Biol 13, 2*17-24 (2002).
288. Casal, J., Lawrence, P. A. & Struhl, G. Two separate molecular systems, Dachsous/Fat and Starry night/Frizzled, act independently to confer planar cell polarity. Develo*pment 133,* 4561-72 (2006).
289. Strutt, D. Organ shape: controlling oriented cell division. Curr B*iol 15, R*758-9 (2005).
290. Baena-Lopez, L. A., Baonza, A. & Garcia-Bellido, A. The orientation of cell divisions determines the shape of Drosophila organs. Curr B*iol 15, 1*640-4 (2005).
291. Duffy, J. B. GAL4 system in Drosophila: a fly geneticist's Swiss army knife. Genesi*s 34, 1*-15 (2002).
292. Jensen, J. D., Wong, A. & Aquadro, C. F. Approaches for identifying targets of positive selection. Trends *Genet 23, 5*68-77 (2007).
293. Bourne, H. R., Sanders, D. A. & McCormick, F. The GTPase superfamily: conserved structure and molecular mechanism. 349, 117-127 (1991).
294. Shaner, N. C., Steinbach, P. A. & Tsien, R. Y. A guide to choosing fluorescent proteins. Nat Me*thods 2, 90*5-9 (2005).
295. Irvine, K. D. & Wieschaus, E. fringe, a Boundary-specific signaling molecule, mediates interactions between dorsal and ventral cells during Drosophila wing development. Cell 7*9, 5*95-606 (1994).
296. Moloney, D. J. et al. Fringe is a glycosyltransferase that modifies Notch. Nature *406,* 369-75 (2000).
297. Weihe, U., Milan, M. & Cohen, S. M. Regulation of Apterous activity in Drosophila wing development. Develo*pment 128,* 4615-22 (2001).
298. Milan, M. & Cohen, S. M. Regulation of LIM homeodomain activity in vivo: a tetramer of dLDB and apterous confers activity and capacity for regulation by dLMO. Mol Ce*ll 4, 26*7-73 (1999).
299. Yan, S. J., Gu, Y., Li, W. X. & Fleming, R. J. Multiple signaling pathways and a selector protein sequentially regulate Drosophila wing development. Develo*pment 131,* 285-98 (2004).
300. O'Keefe, D. D., Prober, D. A., Moyle, P. S., Rickoll, W. L. & Edgar, B. A. Egfr/Ras signaling regulates DE-cadherin/Shotgun localization to control vein morphogenesis in the Drosophila wing. Develo*pmental Biology 311,* 25-39 (2007).
301. Shilo, B. Z. Signaling by the Drosophila epidermal growth factor receptor pathway during development. Exp Ce*ll Res 284,* 140-9 (2003).
302. Jiang, H. & Edgar, B. A. EGFR signaling regulates the proliferation of Drosophila adult midgut progenitors.10.1242/dev.026955. Develo*pment 136,* 483-493 (2009).
303. Nishimura, M., Inoue, Y. & Hayashi, S. A wave of EGFR signaling determines cell alignment and intercalation in the Drosophila tracheal placode.10.1242/dev.010397. Develo*pment 134,* 4273-4282 (2007).
304. Foltenyi, K., Greenspan, R. J. & Newport, J. W. Activation of EGFR and ERK by rhomboid signaling regulates the consolidation and maintenance of sleep in Drosophila. 10, 1160-1167 (2007).
305. Tree, D. R. et al. Prickle mediates feedback amplification to generate asymmetric planar cell polarity signaling. Cell 1*09,* 371-81 (2002).
306. Doyle, K., Hogan, J., Lester, M. & Collier, S. The Frizzled Planar Cell Polarity signaling pathway controls Drosophila wing topography. Dev Bi*ol 317,* 354-67 (2008).
307. Phelps, C. B. & Brand, A. H. Ectopic Gene Expression inDrosophilaUsing GAL4 System. Method*s 14, 3*67-379 (1998).

308. Wu, S., Huang, J., Dong, J. & Pan, D. hippo encodes a Ste-20 family protein kinase that restricts cell proliferation and promotes apoptosis in conjunction with salvador and warts. Cell 1*14,* 445-56 (2003).
309. Giepmans, B. N., Adams, S. R., Ellisman, M. H. & Tsien, R. Y. The fluorescent toolbox for assessing protein location and function. Scienc*e 312,* 217-24 (2006).
310. Zhai, B., Villen, J., Beausoleil, S. A., Mintseris, J. & Gygi, S. P. Phosphoproteome analysis of Drosophila melanogaster embryos. J Prot*eome Res 7, 16*75-82 (2008).
311. Heim, R. & Tsien, R. Y. Engineering green fluorescent protein for improved brightness, longer wavelengths and fluorescence resonance energy transfer. Curr B*iol 6, 17*8-82 (1996).

CURRICULUM VITA

YONGQIANG FENG

EDUCATION

2002-2009 Ph.D., RU/UMDNJ Joint Program in Cell and Developmental Biology, Waksman Institute, Rutgers University, New Jersey, U.S.A.

1997-2000 M.S., Biochemistry and Molecular Biology.
The Fourth Military Medical University, Xi'an, China.

1993-1997 B.S., Biology.
College of Life Sciences, Shaanxi Normal University, Xi'an, China.

PUBLICATIONS

Feng, Y., and Irvine, K. D. Processing and Phosphorylation of the Fat receptor. (Accepted by *PNAS*)

Feng, Y., and Irvine, K. D. (2007). Fat and expanded act in parallel to regulate growth through warts. *PNAS 104*, 20362-20367.

*Cho, E., *Feng, Y., Rauskolb, C., Maitra, S., Fehon, R., and Irvine, K. D. (2006). Delineation of a Fat tumor suppressor pathway. Nat Genet *38*, 1142-1150. (* Contributed equally).